UNIVERSITÀ
DEGLI STUDI
DI PADOVA

Head Office: Università degli Studi di Padova

Department of Women's and Children's Health

Ph.D. COURSE IN: DEVELOPMENTAL MEDICINE AND HEALTH PLANNING SCIENCES

CURRICULUM: ONCOHEMATOLOGY, MEDICAL GENETICS, RARE DISEASES AND PREDICTIVE MEDICINE HEALTHCARE PLANNING SCIENCES

XXXVI SERIES

DEVELOPMENT OF MODELS FOR ELUCIDATING THE GENETIC BASIS AND PATHOGENESIS OF MITOCHONDRIAL DISEASES AND RELATED CONDITIONS

Thesis written with the financial contribution of IRP – Istituto di Ricerca Pediatrica Città della Speranza

Coordinator: Prof. Gianni Bisogno
Supervisor: Prof. Leonardo Salviati

Ph.D. student: Marco Marchi

CONTENT

SUMMARY

The yeast *Saccharomyces cerevisiae* is a cheap, time-saving, and versatile tool to study human genetic diseases, since a great number of genes and biological processes are evolutionarily conserved. Moreover, residues where mutations occur in human are often conserved in yeast. Not least, yeast can grow either by mitochondrial-dependent respiration or by ethanol fermentation, thus permitting to study mitochondrial diseases. We utilized this model organism to assess the functional impact of mutations in *STRADA*, *SGPL1*, and *COQ* genes, which are linked to primary CoQ_{10} deficiency, and where our goal was also to explore and enhance our understanding of their involvement in CoQ biosynthesis.

Loss of function in the STRADA gene leads to PMSE syndrome (MIM #611087), a rare neurodevelopmental disorder characterized by drug-resistant epilepsy and severe developmental delays. Treatment with sirolimus has been effective. We employed a yeast model to evaluate the missense variants Ser264Arg in *STRADA* and its complete deletion, underscore the significance of timely molecular diagnosis for these patients and highlight the utility of yeast as a straightforward yet effective tool for validating the pathogenicity of missense variants.

The *SGPL1* gene encodes an enzyme involved in sphingolipid metabolism. Yeast's similarity to the human pathway makes it suitable for studying diseases like SPLIS (MIM # 617575), an autosomal recessive syndrome characterized by steroid-resistant nephrotic syndrome and multisystemic manifestations, resembling CoQ deficiency. Vitamin B6 shows promise in mitigating these diseases. Our study focused on the Gly210Glu mutation, which is situated at the pyridoxal 5'-phosphate (PLP) binding site (active form of vitamin B_6) and revealed a potential role for the yeast gene *GAD1*.

Coenzyme Q (CoQ) biosynthesis involves multiple genes. We investigated *PDSS1*, *PDSS2*, *COQ4*, and *COQ5* in yeast.

In yeast, the COQ1 gene controls the length of the polyprenyl chain and the number of isoprene units in CoQ synthesis. In contrast, humans and mice rely on PDSS1 and PDSS2 subunits to form heterotetramers for CoQ biosynthesis. This study aimed to clarify the roles of polyprenyl diphosphate genes and explore hybridization between human and murine sequences in determining isoprene chain length in *S.cerevisiae*, where the orthologous protein typically forms homodimeric or

homotetrameric structures. We used a yeast model and revealed that both murine *Pdss1* and *Pdss2* effectively complemented the absence of the *coq1* gene in *S.cerevisiae*. Thus, we also validated the pathogenicity of 12 human missense mutations, 7 in *PDSS1* (His78Asn, Glu123Gly, Val239Gly, Gln245His, Gly296Arg, Asp308Glu, Ser370Arg) and 5 in *PDSS2* (Val116Met, His162Arg, Ser382Leu, Ala384Asp, Ile391Thr) genes. Additionally, we investigated mitochondrial import capabilities of murine PDSS1 vs. human PDSS1, revealing the crucial role of the mPDSS1 N-terminal in mitochondrial import in *S.cerevisiae*. Finally, we quantified CoQ levels in hybrid strains using HPLC, confirming that PDSS1 subunit 1 primarily determines the number of isoprene units in the Q-aromatic ring.

COQ4's role in CoQ synthesis remains unclear. We created a yeast model with *coq4* deletion and identified the importance of its metal-binding site, through the mutant Asp164Ala, and its catalytic activity. We expressed wild-type and mutant COQ4 proteins in bacteria for future enzymatic assays.

COQ5 is crucial for CoQ synthesis and interacts with the CoQ-synthome. We confirmed genotype-phenotype correlations using yeast and studied severe and milder patient mutations, as Gly118Ser and Arg123Trp.

Saccharomyces cerevisiae, a simple eukaryotic model, offers a well-annotated genome, rapid generation times, and a versatile toolkit. These attributes position yeast as an optimal model for understanding genes and mutations associated with human diseases.

PART I

The Model Organism *S.cerevisiae*

1 General Introduction

1.1 *Saccharomyces cerevisiae*

The yeast *Saccharomyces cerevisiae* (*S.cerevisiae*) is a eukaryotic, single-celled microorganism belonging to the kingdom *Fungi* and phylum *Ascomycota*. *Saccharomyces* derives from Latinized Greek and means “sugar fungus”, while *cerevisiae* has its origins in many ancient languages (Latin, Gaelic) and means beer.

Humans have cultivated yeast since the dawn of agriculture to make beer, bread, and wine. Nowadays, it is one of the most studied organisms for molecular and cell biology, emerging as a versatile and robust model system for eukaryotic genetics.

In fact, the yeast shows many advantages as a model organism because it is easy and rapid to grow (short generation time of about ninety minutes); it is cheap and simple to manipulate as well, displaying a flexible and rapid DNA transformation system: yeast has a high endogenous rate of homologous recombination, and a variety of extrachromosomal DNA elements can stably transform yeast cells (Burgess et al., 2017). Yeast genes have few introns, intergenic regions are very short, and genetic redundancy in the yeast genome is low: this facilitates the analysis of gene function.

Moreover, the genome of *S.cerevisiae* has been completely sequenced (Smith & Snyder, 2006),making it the first eukaryotic organism whose DNA is completely known.

Conversely, the use of *S.cerevisiae* as a model organism has some limitations. Firstly, because of it is unicellular, it lacks some important features such as the immune system, tissues and organs: yeast cells cannot specialize in different cells (e.g., eyes, muscles, central nervous system), so they are not very suitable for studies related to the differentiation of cells in different organs and tissues.

Additionally, while the human genome contains approximately 20,000 protein-coding genes, the yeast genome consists of around 6,000 genes (Laurent et al., 2016) in 12 megabase pairs of DNA on 16 linear chromosomes in the nucleus. The genome is very compact for a eukaryote: the number and size of genes are relatively small, and the density of genes is relatively high.

S.cerevisiae is also known as the budding yeast, because it divides asymmetrically, and possesses a cell wall in addition to the plasma membrane. The genes and mechanisms involved in many cellular processes are highly conserved across eukaryotic taxa, so studying the yeast teaches us about the fundamental biology of all eukaryotes. Much of what we have learned about cell and molecular biology has come from research on yeast and it remains one of the best eukaryotic models to understand the molecular basis of human diseases.

1.2 The life cycle of *Saccharomyces cerevisiae* and its vegetative cell cycle

The life cycle of the budding yeast alternates between haploid and diploid states. A mother cell buds to produce a genetically identical daughter cell (where copies of each chromosome are separated by mitosis): followed by nuclear cell division, cell wall formation, and finally cell separation. A haploid contains one of each chromosome, whereas when two haploid cells mate and fuse, they yield a diploid cell (containing two of each chromosome). A diploid can grow by budding or, under conditions of nutrient starvation, it can undergo meiosis, where two rounds of cell division generates four haploid spores in a structure called ascus or tetrad. The spores can be isolated and propagated or mated to another one to form a diploid (Fig.1.1).

The cell cycle is composed of 4 distinct phases: G1, S, G2, and M. The morphology of the budding yeast changes through the cell cycle: it is a round, unbudded cell when it is in the G1 phase of the cell cycle. During G1 phase, the cell grows and synthesizes mRNA and protein that are required for DNA synthesis. A small bud emerges from one end of the cell when the cells are in S phase: this is when the chromosomes are duplicated (sister chromatids). The bud grows in the G2 phase, and the nucleus is close to the bud: this is the phase in which the cells are ready to divide. Finally, during mitosis (M phase), chromosomes condense, and sister chromatids separate between the mother cell and the bud, dividing the original cell into two cells. At the end, two G1 cells (mother and daughter) are left with genetically identical nuclei. Yeast cell division lacks the nuclear envelope breakdown and metaphase plate.

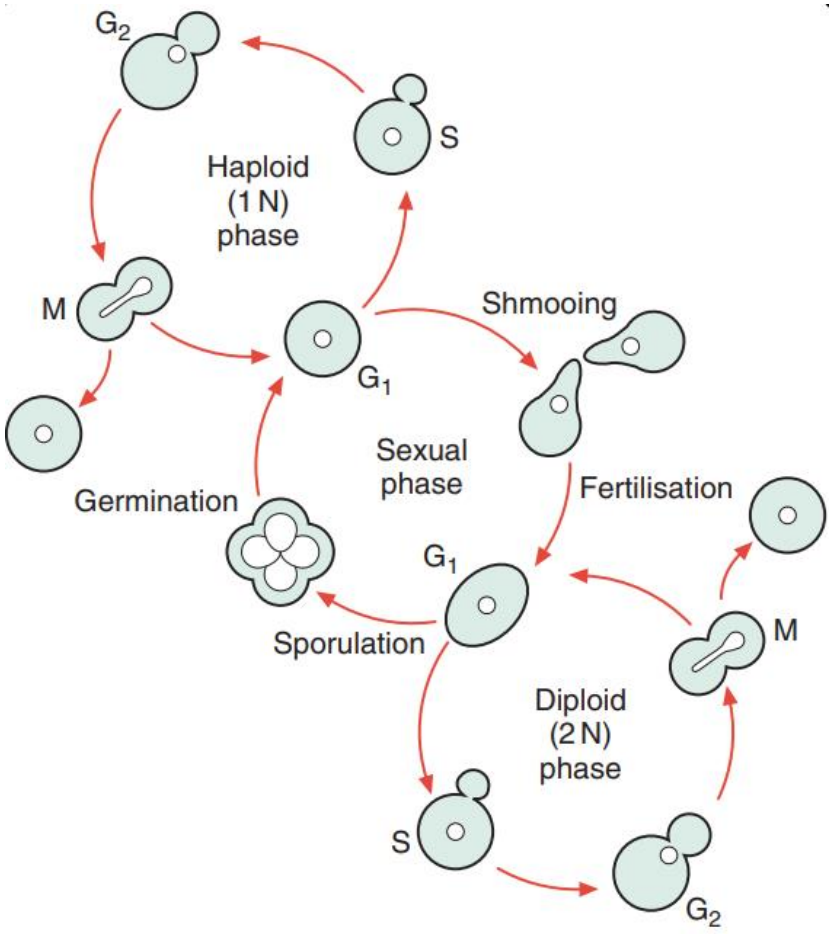

Figure 1.1. The life cycle of *Saccharomyces cerevisiae*. Cells can be grown vegetatively as haploids or diploids. Sporulation is a cellular pathway that is induced by limited nutrients. The output of sporulation is four haploid spores (tetrad) encased in an ascus coat.(Burgess et al., 2017)

1.3 Mating and homothallism

S.cerevisiae has two mating types, termed **a** and **α**. A yeast cell of one mating type produces a pheromone that is detected by a cell of the opposite mating type, stimulating fertilization.

The cells first grow protrusions towards each other in a process called shmooing, then they fuse to form a diploid cell, which is **a**/**α** and cannot mate. The newly formed zygote can divide mitotically to generate diploid colonies or cultures. When a diploid undergoes meiosis to generate four haploid progenies, two will be **a** and two will be **α** (2:2 segregation)

A peculiarity of yeast genetics is the homothallism when a haploid cell switches its mating type between **a** and **α** in alternating mitotic divisions. This allows the yeast to mate with its clonal progeny to form diploids. During G1 (after budding) the mother cell switches, so it and its following daughter

have the opposite mating type to the previous daughter and its budding progeny. The mating type of a haploid cell is determined by whether **a** or **α** information is expressed at the MAT locus on chromosome III. The cell has got the information for both **a** and **α** at two transcriptionally silent loci (HML and HMR) at opposite ends of the chromosome. When a cell switches, DNA encoding the opposite type is copied from the silent locus by homologous recombination, and the old mating type information at MAT is degraded. A DNA double-strand break made by the HO endonuclease at the MAT locus induces this specific recombination event during G1 in mother cells (Fig.1.2). Most laboratory yeast strains are heterothallic, carrying a mutation in the HO endonuclease: this allows researchers to maintain stable haploid cell cultures.

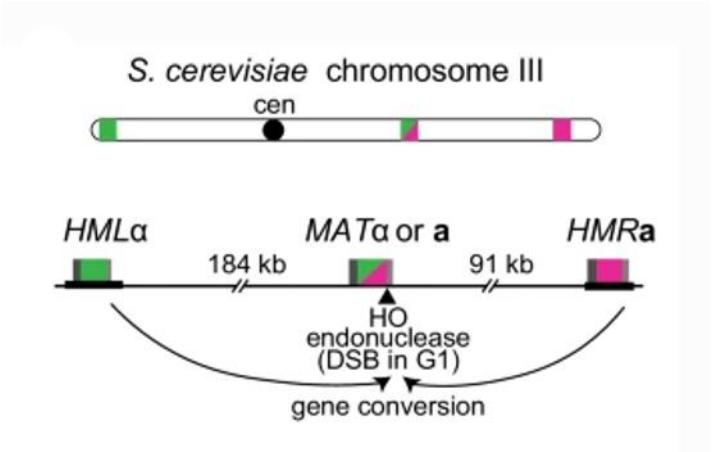

Figure 1.2 In *S. cerevisiae*, the expressed *MAT* locus switches between *MAT***α** and *MAT***a** due to conversions by *HML***α** and *HMR***a**. Silent heterochromatic regions are indicated by thick black lines. Gene conversions are initiated in both cases by a DNA break at the expressed locus followed by strand invasion at one of the silent cassettes (Thon et al., 2019).

1.4 Yeast genome and genetic engineering

The *Saccharomyces cerevisiae* genome, consisting of approximately 12 million base pairs, is remarkably compact and organized into a haploid set of 16 chromosomes. Its most recent annotation in SGD predicts the presence of 6,611 open reading frames (ORFs). In comparison, the human genome is substantially larger, with around 3,054,815,472 base pairs (Nurk et al., 2022), making it more than 200 times larger than the yeast genome. However, the human genome contains only 20,000-25,000 protein-coding genes (Pray, 2008), which is only about three to four times the number of genes found in yeast. This significant difference in gene count can be attributed to the compact nature of the yeast genome, which has few and short introns and rare repetitive sequences, while the human genome comprises numerous non-coding regions.

Interestingly, despite the huge disparity in gene number, about one-third of yeast genes have counterparts in the human genome. Furthermore, the amino acid sequences of comparable proteins in both yeast and humans show an average overlap of 32% (Leslie, 2015). This similarity between yeast and human genes provides a unique opportunity for functional complementation studies. Given the efficiency of homologous recombination in yeast, it is relatively easy to target specific genes for further investigation.

The collaborative effort that led to the complete sequencing of the *Saccharomyces cerevisiae* genome was a remarkable milestone in modern molecular biology. More than 600 scientists from over 100 laboratories around the world participated in this decentralized experiment. Their collective work resulted in the first comprehensive set of genes from a eukaryotic organism. The project involved laboratories from Europe, the United States, Canada, and Japan, making it a truly international effort.

Since its initial release in 1996, the *S. cerevisiae* genome has been regularly updated in the *Saccharomyces* Genome Database, serving as a valuable and continually evolving data resource. This genome sequence has paved the way for ground-breaking research, enabling the study of human genes and mutations in conserved genes associated with inherited diseases through functional complementation studies.

1.5 Yeast metabolism and associated mitochondrial morphology

S. cerevisiae, a facultative anaerobic microorganism, has a remarkable ability to generate ATP through two distinct pathways: oxidative phosphorylation (OXPHOS) and fermentation. The choice between fermentation and respiration is primarily influenced by the types and concentrations of carbon sources available during growth. Glucose, the preferred sugar for yeast in its natural environment, plays a central role in this regulatory process. Under aerobic conditions, even when respiration is possible, *S. cerevisiae* exhibits alcoholic fermentation until the glucose is depleted, a phenomenon known as the *Crabtree effect* or *glucose repression* (Pfeiffer & Morley, 2014).

This regulatory mechanism is achieved primarily through transcriptional control, although mRNA stability, translation, and proteolysis also contribute (Carlson, 1998). Abundant glucose induces the expression of genes encoding glycolytic enzymes, glucose transporters, ribosomal proteins, and other proteins, while repressing many genes involved in the use of alternative carbon sources, gluconeogenesis, the tricarboxylic acid cycle, respiration, and other processes: this is surprising because fermentation has a much lower ATP yield than respiration (2 ATP versus approximately 18 ATP per glucose). The advantage of the Crabtree effect is its impact on competition through heat production and other factors such as higher growth rates at high glucose availability and the minimization of the proteome costs as protein translation parameters, including ribosomal content and efficiency, that are lower (Malina et al., 2021). However, by maintaining a very low glucose concentration in the medium or using non-fermentable carbon sources such as glycerol, ethanol, or acetate, yeast can achieve pure respiratory growth under aerobic conditions.

Metabolic conditions have a profound impact on the morphology of yeast mitochondria. Respiratory growth leads to an abundance of small mitochondria, while fermentative metabolism results in fewer, larger, and more branched mitochondria (Visser et al., 1995). Throughout the cell growth process, *S. cerevisiae* finely regulates the shape, size, and number of its mitochondria (Hermann & Shaw, 1998; Yaffe, 1999).During mid-log phase, yeast cells exhibit "promitochondria," which lack respiratory chain enzyme activity and have limited cytochrome levels. As the cells progress to the late log phase and enter the diauxic shift, mitochondria continue to develop, acquiring the typical

cristae conformation and organizing into a reticulum. When glucose becomes limiting, in the diauxic phase, yeast cells switch metabolism from glycolysis to OXPHOS. The cells then continue to grow in the post-diauxic phase where the mitochondrial reticulum fragments, and the mitochondria become small organelles at the periphery of the cell. Finally, growth stops, and unbudded cells accumulate, indicating entry into the stationary phase (Fig. 1.3).

In summary, S. cerevisiae exhibits a remarkable metabolic flexibility and morphological plasticity in response to carbon source availability, with glucose playing a central role in controlling these dynamic processes. Understanding the intricacies of glucose regulation in yeast opens exciting avenues for exploring cellular metabolism and its implications in various biological contexts.

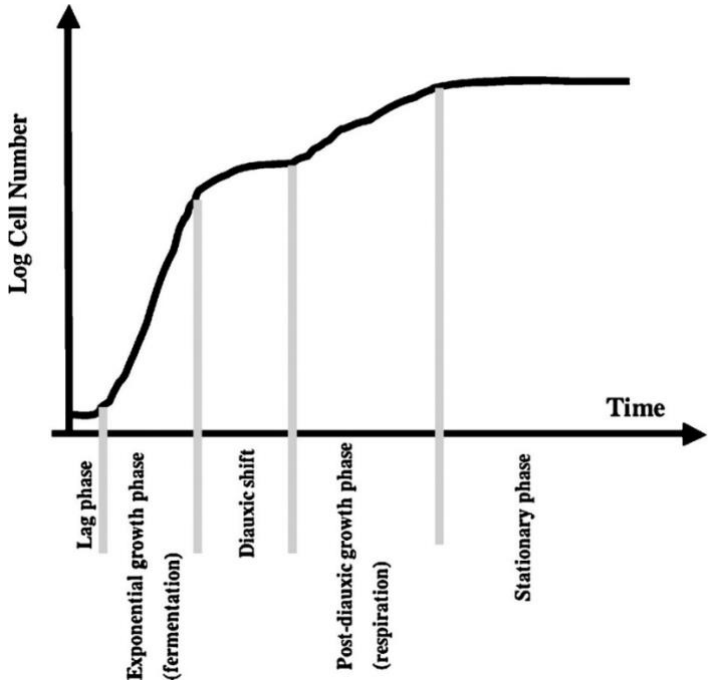

Figure 1.3 Growth phases in the budding yeast, *S. Cerevisiae*. Yeast growth on fermentable carbon sources (such as glucose) is divided into four phases. When cells are inoculated into a fresh medium, they initially undergo a growth delay known as the lag phase. After the lag phase, the yeast cells start a logarithmic growth phase in which the cells use glucose as a carbon source to produce ethanol. This is the phase of fermentation, also known as the prediauxic phase. When glucose becomes rare in the media, the cells begin to use the ethanol available in the media (produced during the fermentative growth) to produce carbon dioxide; this is respiration. This second phase of growth is commonly known as the post-diauxic phase. A stationary phase follows the post-diauxic phase; during which the yeast cells do not divide and growth reaches a plateau.(Matmati & Hannun, 2008)

1.6 *Petite* mutants

Petite yeasts are unable to grow on media containing non-fermentable media (such as glycerol or ethanol), due to the defect in the respiratory chain, but they are viable and able to form small colonies when grown on fermentable carbon sources (e.g.: glucose) (Fig.1.4). The *petite* phenotype can be caused by the absence of mitochondria or mutations in mitochondrial DNA (cytoplasmic *petite* mutants) or by mutations in nuclear genes involved in OXPHOS (nuclear *petite* or *pet* mutants): the colonies appear smaller (*petite* in French, in fact they were first discovered in France more than 50 years ago) because of the inability of such strains to metabolize ethanol produced from glucose. The growth of mutant, but not of wild-type cells, is therefore arrested when the glucose in the medium is exhausted (Tzagoloff & Dieckmann, 1990). The ability of *S.cerevisiae* to be a facultative aerobe allows this organism to be used to study and characterize nuclear genes involved in mitochondrial functions.

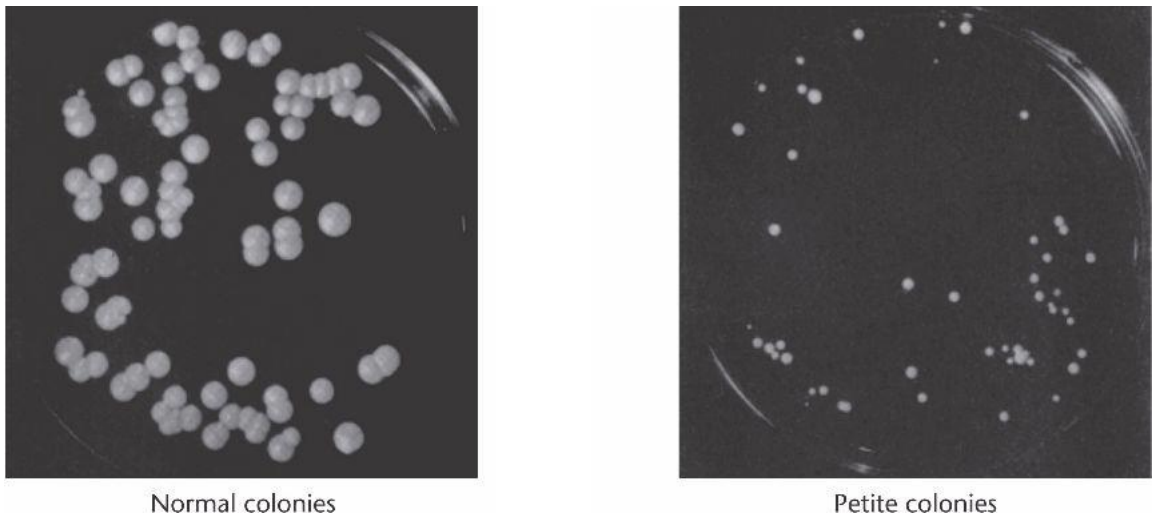

Figure 1.4 The *petite* phenotype on the right, derived from respiratory deficient *S.cerevisiae* yeasts, appears smaller than the normal phenotype of the colonies *wild type* on the left, when cultured on fermentable carbon sources (such as glucose).

1.7 Yeast as a model for mitochondrial diseases

Yeast is a robust model to analyze the genetic defects causing diseases, as a significant proportion of human enzymes have orthologs in yeast (Dolinski & Botstein, 2007). Basically, human mitochondria are more complex than yeast mitochondria, but the degree of functional similarity between them is high.

Mitochondria, the powerhouses of cells, produce energy in the form of adenosine triphosphate (ATP) through oxidative phosphorylation (OXPHOS), and perform essential functions such as lipid and steroid synthesis (Horvath & Daum, 2013),iron-sulfur cluster and heme biosynthesis (Lill et al., 2012), as well as the involvement in intracellular calcium signalling and apoptotic cell death (Vafai & Mootha, 2013; Galluzzi et al., 2012). They have a double-membrane structure and undergo continuous remodelling through fusion and fission (Chen & Chan, 2009; Westermann, 2010).

The first step of the oxidative phosphorylation involves the oxidation of nutrients (Saraste, 1999). Energy is transferred from fuel molecules (such as monosaccharides and fatty acids) to NAD and FAD nucleotides through glycolysis, the Krebs cycle, and β-oxidation. The energized molecules then pass through the electron transport chain (ETC) in the mitochondrial inner membrane (IM) until they reach oxygen. Through the ETC, electrons flow through specific protein complexes (CI, CIII, and CIV), releasing free energy that establishes an electrochemical potential (ΔμH) across the IM, consisting of an electrical gradient (ΔΨ) and a pH gradient. This potential drives ATP synthesis by the F1FO-ATP synthase enzyme (CV) using ADP and Pi. The majority of ATP produced is transported out of mitochondria to supply energy to the rest of the cell (Boekema & Braun, 2007; Dudkina et al., 2011;Winge, 2012; Wittig & Schägger, 2009).

Mitochondrial genomes are remnants of the ancestral prokaryotic genomes, with most genes (>99%) moved in the cell's nucleus during the evolution of eukaryotes (Gray, 2014). Nuclear DNA-encoded mitochondrial proteins are synthesized by cytoplasmic ribosomes and imported into mitochondria (Dolezal et al., 2006; Harbauer et al., 2014; Neupert & Herrmann, 2007); however, maintaining a distinct genetic system in mitochondria is costly, because it requires numerous proteins for several processes (Fox, 2012). The mitochondrial DNA (mtDNA) and its mutations are exclusively inherited

through the maternal lineage, in contrast to the typical mendelian segregation followed by nuclear genes, leading to complicated genomic duplicity (DiMauro, 2004)

Mitochondria contain a 16.5 kb molecule of double-stranded DNA (mtDNA); this encodes 13 core peptide subunits of the OXPHOS system and 24 RNAs that are essential for intra-mitochondrial protein synthesis. (Bandelt et al., 2014).

The total number of mitochondrial proteins, which is currently estimated to be 1,500 (Calvo & Mootha, 2010), are transcribed from genes present in the nucleus, and are translated in the cytosol before being delivered across the mitochondrial membrane. Both these two distinct genetic systems are essential for the functioning of the human mitochondrion.

Throughout evolution, differences have emerged between mtDNA and nuclear DNA. For instance, mtDNA maintains a circular and condensed coding system, and instead of paired chromosomes, there are many independently replicating copies of mtDNA in each cell.

For example, in human cells, the number of mtDNA copies ranges from 100 copies in sperm to hundreds of thousands in an unfertilized oocyte. Mitochondrial DNA repair mechanisms are less efficient than that of nuclear DNA repair due to the high copy number of mtDNA, which buffers against the deleterious effects of stochastic mutation events.

Mutations in mtDNA can affect either all or a fraction of the molecules, leading to either homoplasmy or heteroplasmy. The level of heteroplasmy can vary among cells in the same tissue or organ, from organ to organ, within the same person, or between individuals in the same family. A pathogenic mutation can usually be tolerated at high percentage levels by the cell before it exceeds the biochemical threshold (typically >80%), and a defect in respiratory chain is detected (Fig.1.5).

Heteroplasmy can significantly affect different aspects of genetics related to mitochondrial diseases, since the existence of mutated mtDNA in certain cells or tissues can influence the severity and expression of specific genetic conditions. This phenomenon is particularly relevant in research on mitochondrial diseases and in the field of genetic medicine.

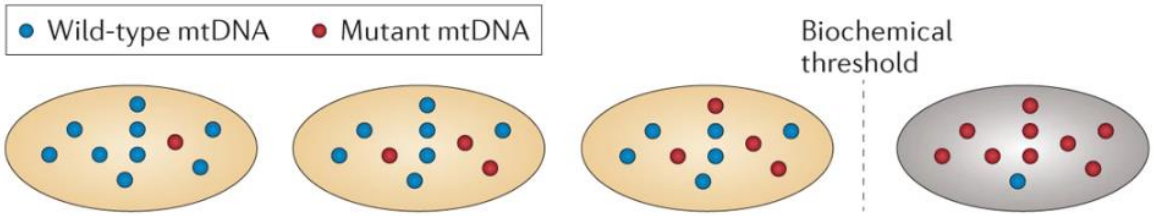

Figure 1.5 Mitochondrial DNA (mtDNA) mutations that have occurred within approximately three human generations are usually heteroplasmic, and the same cell can contain varying proportions of mutated and wild type mtDNA. In case a mutation is pathogenic, the cell can usually tolerate a high proportion this variant before the biochemical threshold is exceeded and a defect in the respiratory chain is detected. Typically, this threshold level is above 80%, suggesting that most mtDNA mutations are either haploinsufficient or recessive (Stewart & Chinnery, 2015)

Mitochondrial dysfunction is associated with various human diseases, which affect at least 1 in 5,000 live human births (Skladal et al., 2003) and with over 150 genetic mitochondrial dysfunction syndromes have been identified (Ernster et al., 1959; Skladal et al., 2003). Mitochondrial pathologies mainly affect high energy-demanding tissues, such as the brain, skeletal muscle, and heart, and appear at various stages of life. These conditions may result in visual and hearing impairment, diabetes, obesity, neurodegenerative and cardiovascular diseases, as well as aging due to the decline in mitochondrial function over time, diabetes, and more (DiMauro & Schon, 2003; Koopman et al., 2013; Vafai & Mootha, 2012; Wallace, 2012; Zeviani & Carelli, 2007)

Despite progress in understanding mitochondrial disorders, effective therapies are lacking (Andreux et al., 2013; Wallace, 2010).While gene therapy may be an option, it is more feasible to consider metabolic or pharmacological treatments (Kerr, 2010, 2013).Various pharmacological agents have been tested, but none have shown conclusive therapeutic benefits. (

Yeast is a valuable model for studying mitochondrial disorders and identifying potential therapies, as recent research has demonstrated. A common strategy for validating the pathogenicity of novel genetic variants is the functional complementation of yeast deletion mutants. Additionally, it is useful to establish correlations between the patient's genotype and the clinical phenotype (Trevisson et al., 2009).Expressing the human gene (whether the wild type or various mutant alleles) in strains deleted for the orthologous gene is an effective approach for observing the consequences on cell growth or other biochemical parameters. The yeast mutants must have a simple assessable phenotype, with an ideal growth defect in selective media, and the heterologous expression of the human gene must

efficiently rescue the growth phenotype. Potentially, it is possible to model the human mutations, particularly those that affect conserved residues, in the yeast gene. The particular life cycle of the S.cerevisiae allows also to study potential lethal mutations by using heterozygous diploid cells, inducing sporulation, and selecting the haploid mutant for further analysis.

In summary, mitochondria play a vital role in cellular energy production and various other functions. Mitochondrial dysfunction is associated with a wide range of human diseases. While treatments are currently lacking, research in yeast allows to characterize the molecular basis and the pathogenic mechanisms of several human mitochondrial disorders, offering promising paths to identify potential therapeutic compounds for these mitochondrial disorders.

1.8 Heterologous genes expression vectors

Yeast vectors are indispensable tools in yeast research: they can be used to introduce heterologous genes into *S.cerevisiae* with a defined copy number. These plasmids, called “shuttle vectors”, can be constructed, manipulated and analysed in both *E.coli* and *S.cerevisiae*. They contain a series of recognition sites for restriction enzymes, known as polylinker or multiple cloning site (MCS).

They have an origin of replication (*ori*) and a selectable marker gene (antibiotic resistance) for their maintenance in bacteria. High or low-copy *ori* sequences are utilized when either high yields are desired or low-copy is beneficial in case the gene products have a bulky effect on the host cell.

In *S.cerevisiae*, plasmids are usually maintained either extrachromosally or by integration into the genome; for selection, they have auxotrophic markers encoding for a metabolic enzyme that complements a corresponding mutation in the host yeast strain: in this way only plasmid-carrying yeast cells can grow in media where the end product of the respective biosynthetic pathway is absent (Gnügge & Rudolf, 2017).

There are also other types of selection markers, defined dominant selectable markers that allow the yeast cells to grow in specific chemical environments. Commonly, these genes encode enzymes that inactivate toxic compounds, such as antibiotics. The most used gene is the KANMX4, which confers resistance to geneticin (Romanos et al., 1992)

There are three types of commonly used yeast shuttle vectors: centromeric, episomal and integrating plasmids.

Episomal vectors contain the 2μ origin of replication, which allows the vector to replicate independently of cell cycle replication. The vector is therefore present in cells in multiple copies (approximately 100 copies per haploid genome) (Murray, 1987), allowing the hyperexpression of the gene of interest. However, the number of copies within different cells is variable, and so is the level of expression of the heterologous gene.

Centromeric vectors contain the yeast ARS (autonomous replication sequences) together with the CEN (centromeric sequences) replication origins. The CEN sequence allows the vector to exist in the cell like an “autonomous chromosome” and to be maintained and passed on to daughter cells during cell division, just as it was part of the yeast genome. This allows the vector to be present in the cell in the same number of copies (1-2 per cell) (Clarke & Carbon, 1980), to achieve a uniform level of expression of the genes.

Integrative vectors allow heterologous genes to be expressed and replicated together with the yeast genome. They take advantage of the ability of yeast to readily undergo homologous recombination. They are also used to replace genes to create deleted strains.

1.9 Promoters for heterologous gene expression

Expression of heterologous genes in *Saccharomyces cerevisiae* is usually achieved using native yeast promoters, as foreign promoters often have limited activity or lead to the production of aberrant mRNA products, unless co-expressed with a compatible RNA polymerase. The most commonly used heterologous promoters include the glycolytic, GAL, and glucose-repressible promoters (Romanos et al., 1992).

Glycolytic promoters, such as ADH1 (alcohol dehydrogenase 1), respond to the presence of glucose in the growth medium, resulting in the induction of gene expression. On the other hand, GAL promoters are strictly regulated by the carbon source provided to the yeast during growth. Galactose induces hyper-expression of the target gene, while glucose completely inhibits gene expression. In

the presence of other carbon sources, such as raffinose, a basal level of gene expression can be achieved. Another well-known glucose-repressible promoter is the promoter of cytochrome c1 (CYC1).

In addition to nutrient-dependent promoters, researchers have also explored the use of promoters that are independent of the nutrients provided. For instance, temperature-sensitive promoters allow gene expression only when yeast cells are grown at a certain temperature.

Regulation of gene expression can also be achieved by the incorporation of tetR activator or repressor sequences that act on tetO promoters. These specific sequences, positioned downstream of the promoter, control gene expression by either inducing or repressing it in the presence of tetracycline (Bellí et al., 1998)

Alternatively, to achieve expression levels comparable to endogenous genes, researchers may choose to use the specific promoter of the yeast gene that needs to be expressed. This approach ensures tight regulation and proper expression of the heterologous gene within the yeast system.

In summary, the choice of a suitable promoter is a critical consideration when expressing heterologous genes in *S. cerevisiae*. The choice of promoter will determine the level of gene expression, regulation, and overall success of the heterologous gene expression system. Researchers must carefully evaluate the available options and their specific requirements to achieve optimal results in their experiments.

PART II

Development of a Functional Yeast Assay for the Validation of Missense *STRADA* Mutations

2.1 Introduction

2.1.1 STRADA gene and mTOR pathway

The STRADA gene on chromosome 17q23.encodes the STE20-related kinase adaptor protein, an upstream inhibitor of the mammalian target of rapamycin complex I (mTORC1) and pivotal regulator of neuronal proliferation, pathfinding, and migration.

The protein has a STE20-like kinase domain but lacks crucial residues necessary for catalytic activity. As a result, it is referred to as a 'pseudokinase' (Baas et al., 2003). Although it shares similarities with other protein kinases and can bind with ATP, it is incapable of phosphorylating substrates.

The protein forms a heterotrimeric complex with serine/threonine kinase 11 (STK11, also known as LKB1) and the scaffolding protein calcium binding protein 39 (CAB39, also known as MO25) (Fig.2.1).

This pseudokinase, in complex with CAB39/MO25, binds to and activates STK11/LKB1: it adopts a closed conformation that is typically observed in active protein kinases and binds STK11//LKB1 as a pseudosubstrate and promoting its conformational change into an active conformation (Zeqiraj et al., 2009).

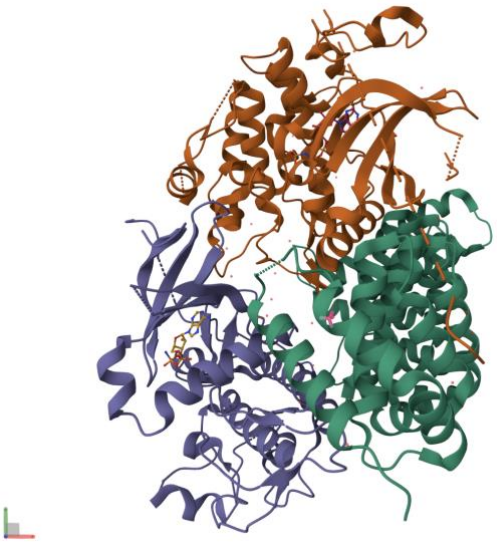

Figure 2.1 Structure of the heterotrimeric LKB1-STRADalpha-MO25alpha complex: LKB1 magenta, STRADA green and MO25 indigo (Zeqiraj et al., 2009)

As a result, STK11 is localized in the cytoplasm rather than the nucleus, where it performs its function: here it is necessary for STK11-induced G1 cell cycle arrest (Tiainen et al., 2002)

When bound to LKB1, STRADA increases its kinase activity. In absence of STRADA, LKB1 has minimal kinase activity, and it cannot phosphorylate AMPK, one of its primary substrates.

The AMP-activated protein kinase (AMPK) cascade is a crucial mechanism for monitoring and adapting cellular energy resources in response to different physiological conditions and metabolic stresses.

This primary signalling pathway converges to regulate the mechanistic target of rapamycin (mTOR). The energy-sensing arm of the pathway responds to low or insufficient ambient cellular ATP levels. The serine/threonine protein kinase STK11 (also known as liver kinase B1, LKB1) phosphorylates AMPK, resulting in TSC2-mediated mTOR inhibition. When ATP levels are repleted, the inhibition of mTOR is relieved due to diminished LKB1 complex activity (Fig.2.2).

mTOR is evolutionarily conserved protein that modulates protein synthesis, cell growth, and cellular autophagy in response to specific intracellular and extracellular signals. Due to its role as a critical signalling node, changes in mTOR activty have been associated with various neurological conditions with diverse phenotypes: including epilepsy, autism, intellectual disability, neurodegenerative disorders, CNS tumours, and hypoxic–ischaemic brain injury.

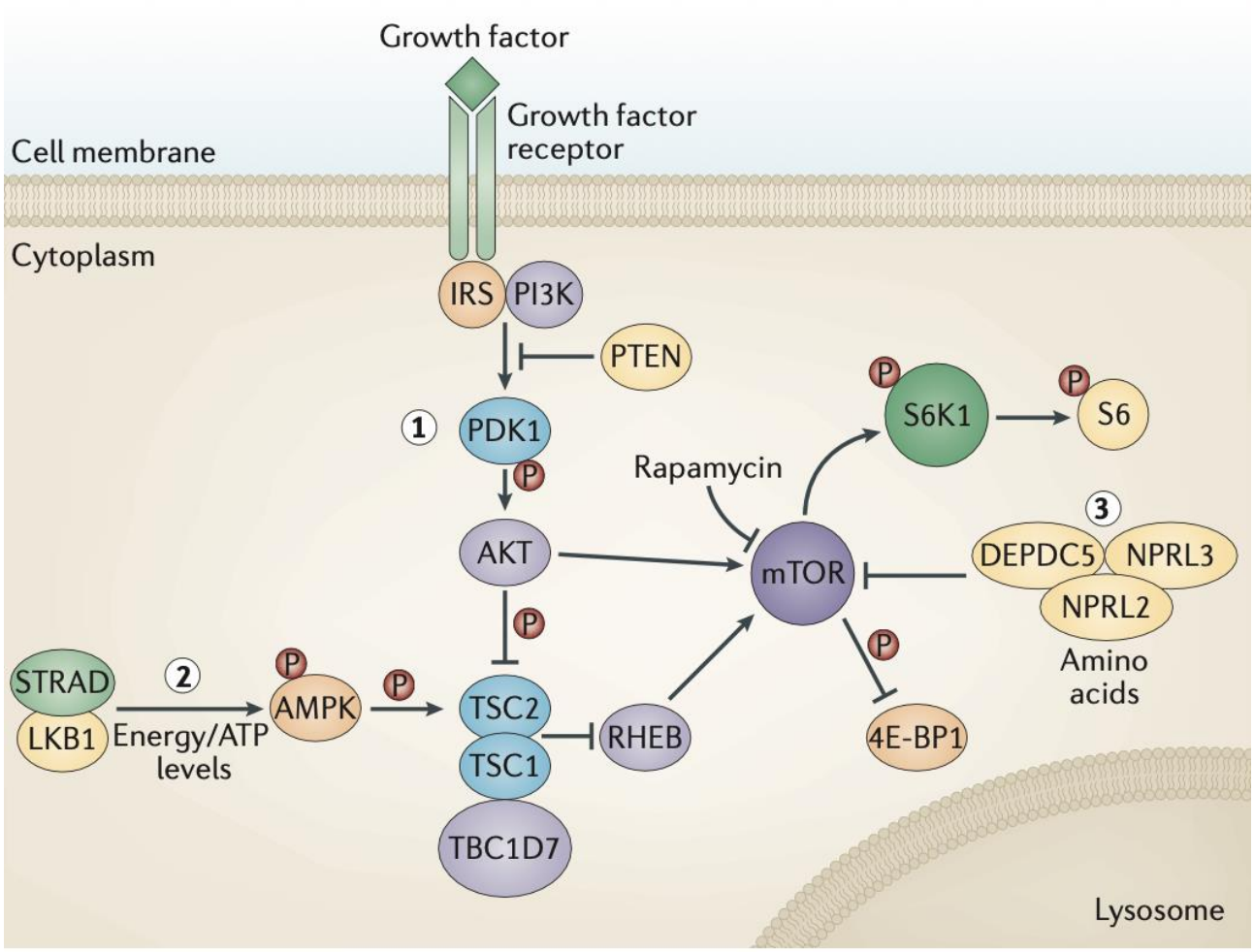

Figure 2.2 The mTOR signalling pathway: the three different primary signalling pathways converge to regulate mechanistic target of rapamycin (mTOR). The growth factor pathway (1), the amino acid sensor (3) and the energy-sensing arm of the pathway (2) responds to low or insufficient ambient cellular ATP. The serine/threonine protein kinase STK11 (also known as liver kinase B1, LKB1) phosphorylates AMPK, which results in TSC2-mediated mTOR inhibition. When ATP levels are repleted, diminished LKB1 complex activity releases inhibition of mTOR. The downstream substrates of mTOR include S6K1, ribosomal S6 (S6), and 4E-BP1, which modulate translation of mRNAs (Crino, 2016).

The *MTOR* gene (chromosome 1p36) encodes the mTOR protein, which is predicted to have a molecular weight of 280 kDa. It can combine with protein binding partners to form two functionally distinct mTOR complexes: mTORC1 and mTORC2 (Baretić & Williams, 2014). In the brain, mTORC1 and mTORC2 regulate different cellular processes in different distinct cell lineages, such as neurons, astrocytes, and neuroglial progenitor cells. mTORC1 specifically functions in relation to neuronal excitability, memory formation, and learning. It has a dynamic subcellular localization and can be found in the cytoplasm, endoplasmic reticulum, and nucleus. An increasing amount of literature indicates that mTORC2 plays a role in maintaining cytoskeletal integrity and regulating cell migration. Up to now, most neurological disorders associated with mTOR signalling have been linked

to mTORC1. STRADA inactivation results in reduced TSC1/TSC2 activity and hyperactivation of the mTOR pathway.

2.1.2 Polyhydramnios, megaencephaly and symptomatic epilepsy (PMSE)

Pretzel syndrome (PMSE) (OMIM #611087) is a complex condition characterized by polyhydramnios, megalencephaly, and symptomatic epilepsy that is associated with loss-of-function mutations in STRADA.

In 2007, Puffenberger and colleagues studied 16 Old Order Mennonite children with PMSE and found that all affected pregnancies experienced complications with polyhydramnios. The majority of pregnancies resulted in premature labor, occurring between 25- and 36-weeks' gestation. Nearly all affected children had macrocephaly, and experienced seizures started between 3 and 7 months of age. The affected children had significant motor and mental development delays. Also, some patients showed additional health issues, including atrial septal defects, congestive heart failure, diabetes insipidus, osmoregulatory defects, and nephrocalcinosis. Tragically, six of the children died between the ages of 7 months and 6 years due to various causes, including status epilepticus, diabetes insipidus-induced hypovolemic shock, and leukemia. The transmission pattern of PMSE in the families described followed the pattern typical for autosomal recessive inheritance (Table 2.1).

Bi et al. (2016) reported a case of a 5-year-old boy from consanguineous Indian parents, sharing similar characteristics of PMSE. During pregnancy, an ultrasound identified excessive amniotic fluid at 12 weeks, and the child was born with difficulty feeding and poor weight gain. The child developed seizures, which began at 3 months of age and were difficult to control. The boy exhibited global developmental delay, severe psychomotor retardation, muscle weakness, low muscle tone and joint laxity. At 5 years old, he continued to be unable to speak, with specific facial features and nephrocalcinosis evident in imaging. Brain scans showed periventricular white matter signal abnormalities, and EEG displayed multifocal epileptiform discharges and generalized background slowing (Table 2.1).

Aerden et al. (2021) reported on a 7-year-old girl with PMSE clinical features. The girl was born prematurely at 36 weeks and 6 days, with polyhydramnios, intrauterine growth retardation, fetal distress, and breech position complications. Seizures began at 5 months of age, leading to a diagnosis of West syndrome with infantile spasms and hypsarrhythmia on EEG at 8 months. Brain imaging revealed hypotrophy of the supratentorial brain, enlargement of the arachnoid space, ventriculomegaly, corpus callosum hypoplasia, and periventricular leukomalacia. At age 7, she suffered from severe developmental delay and psychomotor retardation, with an inability to speak or walk independently. Additional physical manifestations included hypotonia, dyskinesia, hypermobility of lower limb joints, facial abnormalities, and an irregular area of skin resembling cutis verticis gyrata on her cheek. She also had dextrocardia as detected by echocardiogram (Table 2.1).

The studies mentioned above, together with others (Alfares et al., 2017; Alsaif et al., 2020;.; Evers et al., 2017; Nelson et al., 2018; Parker et al., 2013;) provide valuable insights into the clinical presentation and features of PMSE in various populations and contribute to the understanding of this rare and complex syndrome: patients display distinctive craniofacial dysmorphisms, severe developmental delay and infantile-onset drug resistant epilepsy (Table 2.1) and show the constitutive activation of the mammalian target of rapamycin (mTOR) signalling pathway in the brain.

Parker(Parker et al., 2013) and colleague reported in 2013 that the drug sirolimus (also known as rapamycin), which inhibits mTOR, was effective in controlling seizures and improving receptive language in five young individuals with PMSE syndromeFare clic o toccare qui per immettere il testo.without complication. This was based on preclinical studies conducted on mouse progenitor and human fibroblast cells.

The findings demonstrate a mechanistic link between STRADA loss and mTOR hyperactivity in PMSE and suggest that mTOR inhibition may be a potential treatment for PMSE as well as other mTOR-associated neurodevelopmental disorders.

	Puffenberger et al., 2007	Parker et al., 2013	Bi et al., 2016	Evers et al., 2017	Alfares et al., 2017	Nelson et al., 2018	Nelson et al., 2018	Alsaif et al., 2020	Alsaif et al., 2020	Aerden et al., 2021
N. of patients	16	5	1	1*	1°	1	1	1	1	1
Variant	exon 9-13 del	exon 9-13 del	c.842dupA, p.(Asp281fs)	c.891dupC, p.(Cys298Leu fs*11)	c.1101-1G>C	exon 7-9 del	exon 7-9 del	c.682C > T, p.(Arg228*)	c.682C > T, p.(Arg228*)	c.792T>A, p.(Ser264Arg)
Age, Gender	7mo-28 y, NA	8mo-4y 8mo, 3/5 F	5y, M	16y, F	NA	16y, F	13y, F	8y, F	4y, M	7y, F
Country	USA	USA	India	Turkey	Saudi Arabia	NA (Caucasian)	NA (Caucasian)	Yemen	Yemen	NA
Death (cause)	2/16 (SE); 1/16 (hypovolemic shock); 1/16 (leukemia); 2/16 (undetermined)	-	-	-	NA	-	-	-	-	-
Prematurity (GA)	12/16 (mean 31 GA)	NA	-	NA	NA	+ (34^{+4} GA)	-	-	-	+ (36^{+6} GA)
Perinatal complications	NA	NA	SGA, failure to progress	-	NA	-	-	MAS, Oc encephalocele	RDS, PNMD	IUGR, FD, breech position
Polyhydramnios	16/16	NA	+	NA	NA	+	+	+	NA	+
Craniofacial dysmorphisms	16/16	NA	+	+	NA	+	+	+	+	+
Macrocephaly	15/16	NA	-	relative	NA	+	+	-	+	relative
Hypotonia	16/16	NA	+	+	NA	+	+	+	+	+
GI/feeding	+	NA	FTT, drooling	NA	NA	+	gastrostomy	FTT, GERD, drooling	FTT	constipation, ARM
Renal	2/16 NC	NA	NC, bl pyelectasis	NC	NA	NC, NL	NC	-	calyceal dilatation, kidney atrophy, hydronephrosis	-
Cardiac	4/16 atrial septal defect; 1/16 SVT	NA	mesocardia	atrial septal defect	NA	-	-	-	PDA, PFO	dextrocardia
Musculoskeletal	16/16 muscle hypoplasia	NA	large and small joint laxity, muscle hypotrophy	neurogenic kyphoscoliosis	NA	distal phalange hypoplasia, pectus carinatum	NA	joint laxity, finger contractures, scoliosis, muscle hypotrophy	joint laxity, talipes equinovarus, multifocal bone expansion areas, muscle hypotrophy	joint laxity, acetabular dysplasia, coxa valga, equinovarus feet, thumb hypoplasia, pectus carinatum
Endocrine	2/16 DI; 2/16 osmoregulatory defect	NA	NA	NA	NA	hypothyroidism	NA	hirsutism	NA	CPP
Other	1/16 leukemia	NA	-	-	NA	OSAS	OSAS	laryngomalacia	single umbilical artery, hypospadia	cutis gyrata, skin hypopigmentation
Global NDD	16/16	NA	+	+	NA	+	+	+	+	+

ASD/Behavioral	4/16	NA	-	+	NA	+	-	-	-	NA
Communication	NV	NV	NV	NV	NA	NV	NA	NV	NV	NV
Mobility	12/16 wheelchair-bound; 4/16 assistive devices	NA	assistive devices	non-ambulatory	NA	non-ambulatory	NA	non-ambulatory	non-ambulatory	non-ambulatory
Movement disorder	mild chorea	NA	NA	NA	NA	+	NA	NA	NA	dyskinesia
Brain MRI *(age)*	2/4 subependymal dysplasia; 4/4 ventriculomegaly; 2/4 WM anomalies	NA	WM anomalies *(2y10mo)*	cortical malformation, midbrain and posterior fossa anomalies	NA	WM volume loss, mild cbl atrophy, L middle-T gyrus focal encephalomalacia, foramen magnum stenosis *(15y)*	PVLM, Fr and P WM gliosis *(4mo)*	bl mesial T lobe sclerosis, diffuse cerebral atrophy *(4y)*	normal *(2mo)*	supratentorial brain hypotrophy, arachnoid space enlargement, ventriculomegaly, CC hypoplasia, PVLM
Epilepsy	+ (16/16)	4/5	+	+	NA	+	+	+	+	+
Age at onset	3-7mo	3-8mo	3mo	3mo	NA	4mo	4mo	5mo	6mo	5mo
Sz type at onset	FIAS, FBTCS	NA	FBTCS	NA	NA	tonic	focal tonic	BLTC	ES	febrile BLTC
Other sz type	ES (2/16), SE, EPC (1/16)	FIAS, BL-TC, SE	focal, BLTC, ES	NA	NA	focal, ES, BLTC, SE	FIAM, ES, SE	ES	NA	WS, SE
EEG at last FU *(age)*	multifocal IEDs (bl high voltage Fr/T/P/Oc spike/SW), long runs of spikes, rhythmic SW	NA	BGS, multifocal IEDs (R Fr, bl central) *(4y)*	NA	NA	hypsarrhythmia *(6mo)*	BGS, multifocal IEDs (bl T ShW) *(5y)*	BGS, generalized IEDs	hypsarrhythmia	hypsarrhythmia
ASM, *best*	NA (multidrug-resistant)	OXC, PB, LEV, TPM, CBZ	TPM, *ACTH, pyridoxine, biotin, PB, OXC*	*OXC, VPA*	NA	*PB*, ACTH, LEV, LTG, CNZ, VPA, RUF	PB, *ACTH, LTG*, LEV, PER, *VPA*	VPA, ACTH, GVG, PB, CZP, LTG, CBZ, PER, TPM	ACTH, GVG	*PB*, VPA, LEV, GVG, high dose hydrocortisone, *TPM, CZP, BRV*
sirolimus *(age)*	-	*5/5 (3-8 mo)*	-	-	NA	+ *(adolescence)*	+ *(adolescence)*	-	-	-
sirolimus dose (mg/m^2/day)	-	2.5 (1-4.9)	-	-	NA	NA	NA	-	-	-
Avg sirolimus through blood level (ng/ml)	-	8.2	-	-	NA	NA	NA (max 15.1)	-	-	-
sirolimus tolerability	-	+	-	-	NA	+	hypercolesterolemia, hypertriglyceridemia	-	-	-
Seizure control	-	complete	+	+	NA	complete	-	-	partial	partial

		5/5								
Other benefits with sirolimus	-	fewer ASM, improvement in receptive language and social interaction	-	-	NA	improvement in behavior and attention, decrease in somnolence	mild and subjective improvements in alertness	-	-	-

Table 2.1 Clinical, EEG and genetic features of probands and published patients affected by STRADA mutations.

Legend:
ARM: anorectal malformation; ASD: autism spectrum disorder; ASM: anti-seizure medication; avg: average; bl: bilateral; BLTC: bilateral tonic clonic; BRV: brivaracetam; CBZ: carbamazepine; CC: corpus callosum; cbl: cerebellar; CLB: clobazam; CPP: central precocious puberty; CZP: clonazepam; C-P: centro-parietal; del: deletion; DI: diabetes insipidus; dup: duplication; EEG: electroencephalogram; ES: epileptic spasm; F: female; FBTCS: focal to bilateral tonic-clonic seizure; FD: fetal distress; FIAM: focal impaired awareness motor seizure; FIAS: focal impaired awareness seizure; Fr: frontal; fs: frameshift; FTT: failure to thrive; FU: follow-up; Hy: hippocampi; GA: gestational age; GBS: generalized background slowing; GERD: gastroesophageal reflux disease; GI: gastrointestinal; GVG: vigabatrin; IED: interictal epileptiform discharge; int: internal; IUGR: intrauterine growth restriction; L: left; LCS: lacosamide; LEV: levetiracetam; LTG: lamotrigine; LV: lateral ventricle; M: male; MAS: meconium aspiration syndrome; max: maximum; mo: month; MRI: magnetic resonance imaging; NA: not available; NC: nephrocalcinosis; NDD: neurodevelopmental disorder; NL: nephrolithiasis; NV: non-verbal; Oc: occipital; OSAS: obstructive sleep apnea syndrome; OXC: oxcarbazepine; P: parietal; PB: phenobarbital; PDA: patent ductus arteriosus; PER: perampanel; PFO: patent foramen ovale; PHT: phenytoin; PNMD: pneumomediastinum; PVLM: periventricular leukomalacia; R: right; RDS: respiratory distress syndrome; RUF: rufinamide; SE: status epilepticus; SGA: small for gestational age; SVT: supraventricular tachycardia; ShW: sharp wave; SW: slow wave; Sz: seizure; T: temporal; TPM: topiramate; VABAM: vigabatrin-associated brain abnormalities on magnetic resonance imaging; VPA: valproic acid; WM: white matter; WS: West syndrome; y: year.

* = the paper reports an older brother of the patient, who died at 10 years of age during SE. This individual's DNA was not available for sequencing.
° = the paper reports an additional individual affected by PMSE syndrome (no further information available).
^ = a deficiency in complex 1 identified by muscle biopsy was also reported, leading to an initial diagnosis of possible mitochondrial cytopathy.

2.1.3 *SPS1* gene: the yeast homolog for validating missense *STRADA* mutations

The primary sequence of STRADA protein contains the kinase domain (pfam: PF00069) within the 69-379 region, which is structurally conserved in all members of the STE20-related kinase subfamily, including fungi. A BLAST search for sequence similarity in the *Saccharomyces cerevisiae* proteome unveiled the best score (27% identity, 43% similarity) for the protein encoded by yeast *SPS1* gene (Fig.2.3).

The *SPS1* gene encodes for a GCKIII protein kinase (STE20 subfamily), whose functions are required to yeast cells to complete the sporulation process, as reported by several studies (Friesen et al., 1994; Slubowski et al., 2014; Iwamoto et al., 2005).

Additional experimental evidence actually demonstrated that yeast cells carrying either *SPS1* deletion and/or its inactivation were not affected in vegetative growth, but were completely unable to

undergo sporulation: in fact, defects in this gene affect the cell wall biogenesis, which surrounds each of the haploid nuclei generated by the meiotic divisions, resulting in the absence of visible spores (Paulissen et al., 2016; Paulissen & Huang, 2016)

In conclusion, the yeast *S. cerevisiae* was selected as an evaluative model to confirm the pathogenicity of clinical missense STRADA mutations: reproducing them in the *SPS1* gene and observing the impact on sporulation capability.

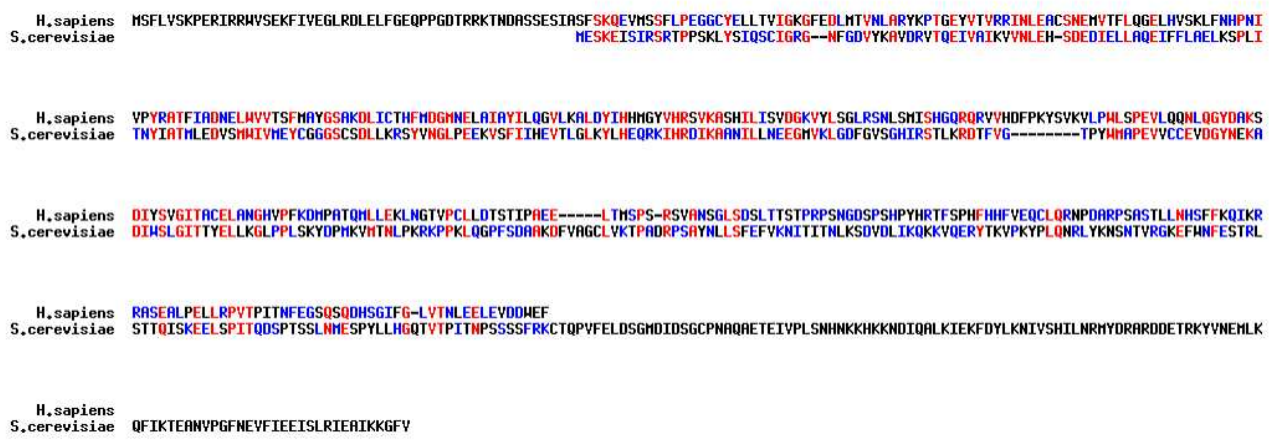

Figure 2.3 Multiple sequence alignment of human STRADA (NP_001003787.1) and yeast Sps1 (QHB07976.1) proteins (Corpet, 1988). Human STRADA and yeast Sps1 protein show 27% identity and 43% similarity.

2.1.4 CRISPR/Cas9 gene editing

Saccharomyces cerevisiae has been widely used as a model organism and metabolic engineering platform in research. Optimizing heterologous product pathways in *S. cerevisiae* requires multiple genetic modifications, which have been found to be time-consuming and labor-intensive.

To overcome this limitation, researchers have looked for novel genetic markers for *S. cerevisiae* and developed recycling strategies for these markers. Recombinase-based methods have been used but can lead to genome instability. Recently, the "delitto perfetto" (Storici & Resnick, 2003) and I-SceI-induced double-stranded breaks (Katz et al., 2014) methods have allowed scarless removal of counter-selectable markers. Nevertheless, replacing target genes with marker cassettes remained a time-consuming process. Alternative methods like meganucleases (Epinat et al., 2003), zinc finger nucleases (ZFNs) (Urnov et al., 2010), and transcription activator-like effector nucleases (TALENs)

(Joung & Sander, 2013)) have been investigated as options for marker-free modifications, but designing and generating new proteins for each genetic modification can be challenging.

Bacteria, throughout their evolution, have developed several systems to degrade foreign DNA such as phages and plasmid DNA. The prokaryotic immune mechanism, known as Clustered Regularly Interspaced Short Palindromic Repeats (CRISPR) and CRISPR-associated (Cas) systems, was discovered in 2007 (Barrangou et al., 2007)

From the 3 types of CRISPR/Cas systems identified so far, the type-II bacterial CRISPR system of Streptococcus pyogenes has been the most extensively studied *in vivo*. During this immune response, the invading DNA is initially cleaved into small fragments and then integrated into the CRISPR locus.

Subsequently, this locus is transcribed into a singular noncoding precursor CRISPR RNA (pre-crRNA), which undergoes additional processing to produce condensed crRNA segments. These crRNA fragments, together with the trans-activating CRISPR RNA (tracrRNA), form a ribonucleoprotein complex with the Cas9 endonuclease. This complex then identifies and cleaves the foreign DNA (Doudna & Charpentier, 2014)

In 2012, Emmanuelle Charpentier and Jennifer Doudna's research team harnessed the Streptococcus pyogenes type II CRISPR system for genome editing. This was achieved by fusing crRNA with tracrRNA, creating a single guide RNA (sgRNA) (Jinek et al., 2012). This sgRNA guides the Cas9 nuclease to specific genomic sites through conventional Watson-Crick base pairing. When a suitable protospacer adjacent motif (PAM), such as NGG, follows the target sequence, Cas9 engages with the target DNA sequence as shown in Fig.2.4 (Deltcheva et al., 2011).

The CRISPR/Cas9 complex induces site-specific double-strand breaks (DSBs), initiating genome editing through two distinct mechanisms. In the absence of a matching DNA template, DSBs are repaired via nonhomologous end joining (NHEJ), an error-prone process that leads to minor insertions or deletions. Conversely, in the presence of an artificial repair template, DSBs undergo homology-directed repair (HDR), enabling the introduction of desired base-pair alterations.

The Cas9-based system uniquely relies on RNA for targeting the Cas9 nuclease, allowing for selective targeting of any genomic locus and the introduction of double-stranded breaks (DSBs).

Since its discovery, Cas9 has been widely used for developing genetic modifications in various organisms, including human pluripotent stem cells (González-Ramos et al., 2013), zebrafish (Hwang et al., 2013), plants (Feng et al., 2013), flies (Gratz et al., 2013), and mice (Hsu et al., 2014)

The CRISPR/Cas9 system was first employed in *S. cerevisiae* in 2013. This was achieved by introducing a plasmid-borne cas9 gene from *S. pyogenes* along with a plasmid containing a guide-RNA (gRNA) targeting the CAN1 gene, which encodes an arginine amino acid transporter localized to the yeast plasma membrane) (Dicarlo et al., 2013). The gRNA guided the Cas9 enzyme to induce a double-strand break at the CAN1 locus, which was repaired using a co-transformed repair fragment with a premature stop codon. As a result of this repair, canavanine-resistant colonies were formed. Recently, it has been demonstrated that the CRISPR/Cas9 system can enable up to three simultaneous gene deletions in yeast (Bao et al., 2015)

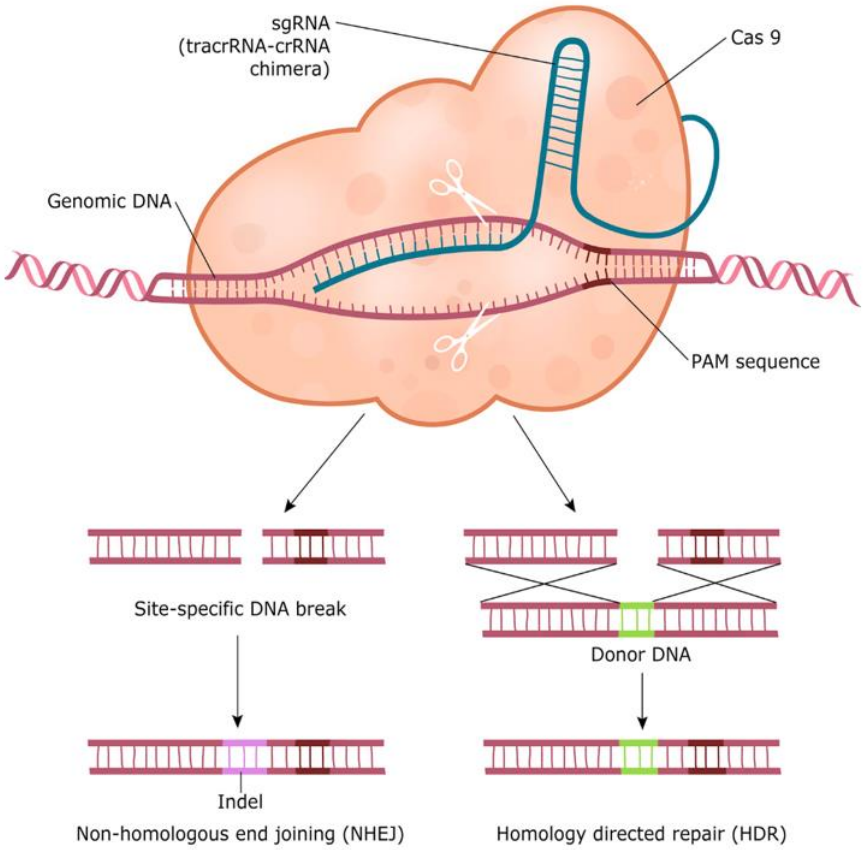

Figure 2.4 Genome editing is achieved through the CRISPR/Cas9 system. The Cas9 recruitment to the target DNA is mediated by a chimeric single-guide RNA (sgRNA). It contains a protospacer recognizing the target sequence followed by protospacer adjacent motif (PAM). Cas9-induced DSBs are repaired either by NHEJ giving rise to insertions or deletions (indel) or by HDR using a synthetic donor DNA template, which enables the introduction of desired sequence changes (Savić & Schwank, 2016).

2.2 Materials and Methods

2.2.1 Patients

Two new patients with PMSE syndrome, affected by missense STRADA mutations, are described: characterizing in detail their electro-clinical phenotype together with genetic features (Table 2.2).

Patient #1 is a 12-year-old Moroccan boy, first child of consanguineous parents with unremarkable family history. He was born at term after a regular pregnancy. Perinatal history and auxological parameters were reported normal. Parents described regular psychomotor development until age 5 months, when he presented with tonic-clonic seizures and psychomotor regression. Initially, he received treatment with valproate and carbamazepine which reduced his seizure frequency and duration. He was evaluated for the first time at age 3.5 years at our center, Clinical Genetics and Epidemiology Unit of the Department of Women's and Children's Health at the University of Padua (Padua, Italy). His physical attributes included macrocephaly and mild dysmorphisms, presenting with a coarse face with a wide forehead, broad nasal root and hypertelorism. Additionally, he had severe developmental delay, absence of speech and eye contact, ataxic-dyskinetic tetraparesis, and oculomotor apraxia. Parents reported episodes of psychomotor agitation and self-aggression and a severe sleep disorder, characterized by awakenings every 1-2 hours with screaming and agitation, which did not respond to chronic treatment with benzodiazepines and antihistamines. He had infrequent (1-2 times per year) focal motor tonic asymmetric seizures and focal-to-bilateral seizures. EEG conducted while the patient was awake revealed diffuse high voltage (up to 220 μV) fast activity (20 Hz), predominantly in the bilateral fronto-central regions and theta-delta (3-5 Hz) activity at the vertex (Fz-Cz) (Fig.2.5, E). Sleep EEGs recorded abundant diffuse fast activity and high-voltage (up to 360 μV) epileptiform discharges appeared over both centro-parietal regions and the vertex (Fig.2.5, F-G). A 24-hour video-EEG confirmed that the sleep disorder was not of epileptic origin.

Brain magnetic resonance imaging (MRI) revealed mild ventriculomegaly characterized by dysmorphic lateral ventricles, diffuse white matter abnormalities, and enlarged perivascular spaces and mild pontine hypoplasia. The patient also exhibited incomplete hippocampi rotation, tortuous internal carotid arteries and frontal bone thickening (Fig.2.5, A-D).

At last follow-up, facial features have become more pronounced and sleep problems were still persistent. Seizures are well controlled with valproate and carbamazepine (Table 2.2).

Patient #2 is a 22-month-old girl, first child of consanguineous parents of Syrian descent. Family history was unremarkable, except for a paternal aunt with epilepsy and migraine. Pregnancy was characterized by gestational diabetes and polyhydramnios. She was born at 36+4 gestational age by vaginal delivery. Birth weight was 2560 g (33rdcentile), length 47 cm (44thcentile) and head circumference 32 cm (28thcentile). She had mild dysmorphic features but no major neurological dysfunction.

At the age of 3 months, she had accelerated growth in head circumference and plagiocephaly. Brain ultrasound was unremarkable.

At the age of 5 months, she presented at our center, Clinical Genetics and Epidemiology Unit of the Department of Women's and Children's Health at the University of Padua (Padua, Italy). with macrocephaly, occipital plagiocephaly and frontal bossing, facial dysmorphisms characterized by a coarse face with broad nasal root, low-set cupped ears with folded helices, epicanthus, hypertelorism, and sparse hair. She had severe global developmental delay with limited eye contact and interaction, axial hypotonia, diffuse muscle hypotrophy, and a movement disorder characterized by dyskinetic limb jerks. In addition, she had a patent foramen ovale, nephrocalcinosis, vascular anomalies (lumbar angioma, radial artery aneurysm with vascular tortuosity), diffuse joint laxity with overlapping toes, and an anteriorly placed anus with chronic constipation.

Epilepsy started at 5 months of age, with focal motor tonic seizures, focal to bilateral seizures and status epilepticus. Seizures, often organized in clusters, were triggered by fever, vaccines, infections, intense crying, and pain.

EEGs revealed poorly organized background activity in wake and sleep, with multifocal epileptic anomalies, predominantly in the temporal regions (Fig.2.5, L-N). Frequent subclinical electrical patterns characterized by sequences of rapid activity of variable duration were also notable (Fig.2.5, M). During sleep, rapid (approximately 10 Hz) bilateral activity of moderate to high voltage (150 mV) was observed, predominantly in the temporal regions.

Brain MRI showed mild ventricular dilatation, significant enlargement of the subarachnoid spaces, moderate frontal lobe hypoplasia and a reduction in the width of the occipital foramen (Fig.2.5, H-J). Multiple antiepileptic drugs were used throughout the clinical course, including levetiracetam, phenytoin, vigabatrin and clobazam, resulting in incomplete seizure control despite polytherapy. Intravenous phenytoin was effective as a rescue treatment in several episodes of status epilepticus. Vigabatrin had to be discontinued due to the appearance of vigabatrin-associated MRI brain abnormalities in the thalami and basal ganglia (Fig.2.5, K). In view of the favourable response to sodium channel blockers, lacosamide was added with good efficacy (Table 2.2).

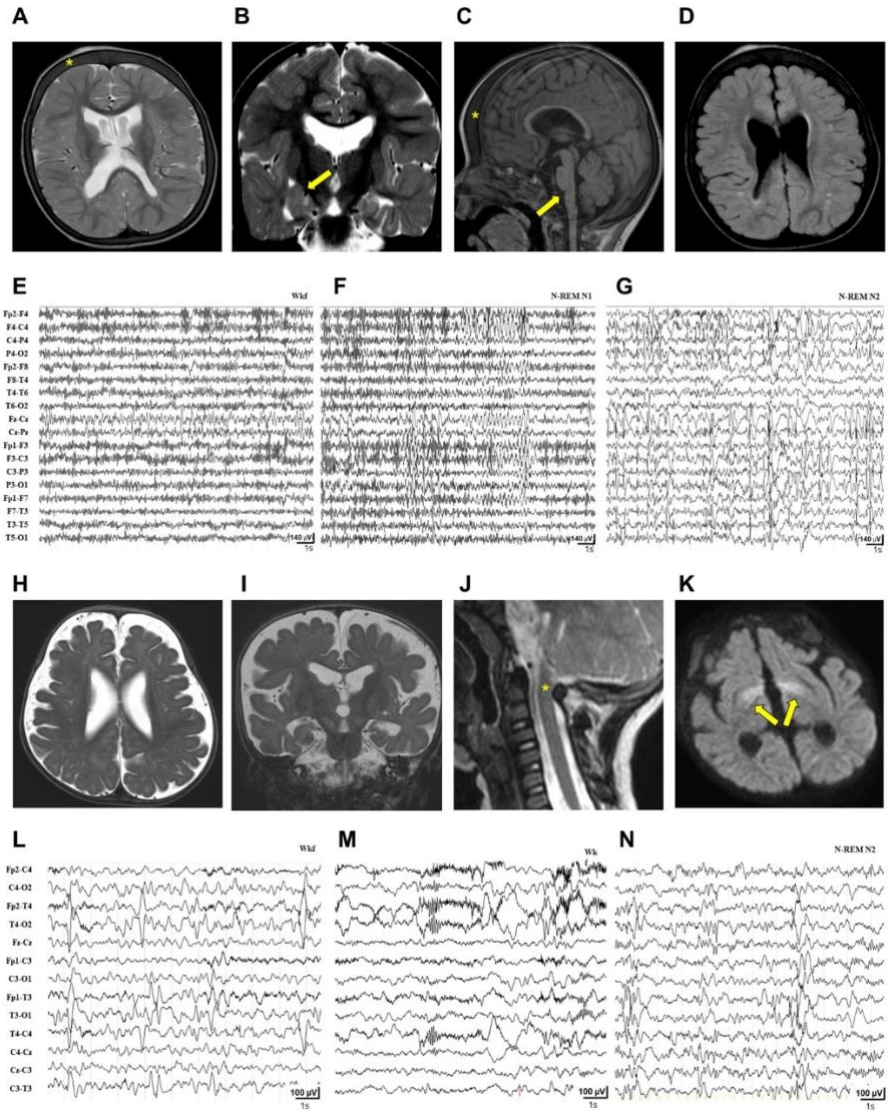

Figure 2.5 Brain MRI of patient 1 at 3 years 7 months of age. A) axial T2W, B) coronal T2W, C) sagittal T1W and D) axial FLAIR sequences showing mild ventriculomegaly, with dysmorphic lateral ventricles and white matter abnormalities (A, B, D), mild pontine hypoplasia (C, arrow) incomplete hippocampal rotation (B, arrow) and calvarial thickening (A, C, star).
EEG of patient #1 at age 10 years during wakefulness (E) showing poor organization of background activity, diffuse high voltage fast activity (20 Hz) and abundant epileptiform discharges, mainly in the vertex region. During an early stage of somnolence (F) high voltage fast activity persists with increase of epileptiform discharges in the frontal regions. During N2 N-REM sleep (G) fast activity recedes, with diffuse epileptic discharges, mainly in the bilateral fronto-central-parietal regions.
Brain MRI of patient 2 at 9 months of age. Axial T2W (H), coronal T2W (I) , sagittal T2W (J) and axial DWI (K) sequences, showing cerebral atrophy, with enlarged periencephalic CSF spaces, mild ventriculomegaly, slight perivascular spaces enlargement (H, I), cervical spine canal stenosis at C1 level (J, star), and Vigabatrin-associated cytotoxic edema of the globus pallidus (K, arrow).
EEG of patient #2 at 5 months of age during wakefulness showing frequent multifocal epileptiform discharges, mainly in the temporal regions (L) and focal patterns of fast activity without clinical correlation (M). During N-REM sleep (N) EEG shows multifocal epileptiform discharges and sequences of beta activity.

Legend:
EEG: electroencephalogram; N-REM: non-rapid eye movement sleep; Pt.: patient; Wkf: wakefulness.
CSF: cerebrospinal fluid; DWI: diffusion weighted; FLAIR: Fluid attenuated inversion recovery; MRI: magnetic resonance imaging; T1W: T1-weighted; T2W: T2-weighted.

	Patient #1	Patient #2
N. of patients	1	1
Variant	c.792T>A, p.(Ser264Arg)	c.891dupC, p.(Cys298Leu fs*11)
Age, Gender	11y, M	2y, F
Country	Morocco	Syria
Death (cause)	-	-
Prematurity (GA)	-	+ (36 GA)
Perinatal complications	-	FD
Polyhydramnios	NA	+
Craniofacial dysmorphisms	+	+
Macrocephaly	+	+
Hypotonia	+	+
GI/feeding	GERD, constipation, FTT	constipation, ARM
Renal	-	NC
Cardiac	-	PFO
Musculoskeletal	distal phalange hypoplasia, muscle hypotrophy	joint laxity, muscle hypotrophy
Endocrine	-	-
Other	sideropenic anemia, sleep disorder	congenital colesteatoma, radial artery aneurysm
Global NDD	+	+
ASD/Behavioral	+	+
Communication	NV	NV
Mobility	non-ambulatory	non-ambulatory
Movement disorder	ataxic-dyskinetic tetraparesis	dyskinesia
Brain MRI (age)	dilatated dysmorphic LV, diffuse WM anomalies, pontine hypoplasia, incomplete Hy rotation, tortuous int carotid artery, Fr bone thickening (3y7mo)	LV dilatation, enlarged subarachnoid spaces, Fr lobe hypoplasia, VABAMs, oc foramen restriction(9mo)
Epilepsy	+	+
Age at onset	5mo	5mo
Sz type at onset	BLTC, febrile TC	FBTCS
Other sz type	focal tonic, FBTCS	focal tonic, SE
EEG at last FU (age)	BGS, diffuse 20-Hz activity, multifocal IEDs (midline, bl T-Oc and C-P ShW) (11y)	multifocal IEDs (R>L bl T), sequences of rapid activity; bl fast activity in sleep (1y)
ASM, best	VPA, CBZ	PHT, LEV, GVG, LCS, CLB
sirolimus (age)	-	+ (7mo)
sirolimus dose (mg/m²/day)	-	1.2
Avg sirolimus through blood level (ng/ml)	-	3.1
sirolimus tolerability	-	+
Seizure control	partial	complete
Other benefits with sirolimus	-	fewer ASMs, improvement in interaction and communication

Table 2.2 Clinical, EEG and genetic features of probands and published patients affected by STRADA mutations.

Legend:
ARM: anorectal malformation; ASM: anti-seizure medication; bl: bilateral; BLTC: bilateral tonic clonic; CBZ: carbamazepine; CLB: clobazam; C-P: centro-parietal; F: female; FBTCS: focal to bilateral tonic-clonic seizure; FD: fetal distress; Fr: frontal; FTT: failure to thrive; Hy: hippocampi; GA: gestational age;; GERD: gastroesophageal reflux disease; GVG: vigabatrin; IED: interictal epileptiform discharge;; L: left; LCS: lacosamide; LEV: levetiracetam; LV: lateral ventricle; M: male;; mo: month; NA: not available; NC: nephrocalcinosis;; NV: non-verbal; Oc: occipital; PFO: patent foramen ovale; PHT: phenytoin; R: rightSE: status epilepticus; ShW: sharp wave; T: temporal; VABAM: vigabatrin-associated brain abnormalities on magnetic resonance imaging; VPA: valproic acid; WM: white mattery: year.

2.2.2 Genetic analyses

All diagnostic procedures were performed after obtaining informed consent from the patients' parents and involved using Array Comparative Genome Hybridization (Array-CGH) and Next-Generation Sequencing (NGS) technologies (specifically, the Illumina TruSight One Sequencing Panel kit and Agilent SureSelect targeted NGS panel). Genomic DNA was extracted from peripheral blood leukocytes.

Array-CGH is a potent molecular technique used to detect and examine genomic copy number variations (CNVs) in high resolution. This methodology enables researchers to identify comprehensively the changes in DNA copy numbers across the genome, thus facilitating the comprehension of genetic alterations associated with different diseases. The basic principle that underlies Array-CGH involves co-hybridization of labelled test DNA and reference DNA onto an array, which contains immobilized DNA fragments that represent the entire genome. Researchers can precisely map CNVs by quantifying the relative fluorescence intensities and pinpointing amplifications or deletions in test DNA compared to the reference (Lucito et al., 2003).

NGS is a breakthrough technology enabling rapid and parallel sequencing of DNA fragments. This technique includes making DNA libraries with unique markers, followed by simultaneous sequencing on solid surfaces. NGS has many advantages, including the ability to process large amounts of data, adaptability to multiple applications, and has improved research in many disciplines, including medicine (Metzker, 2010). NGS advantages include increased productivity, faster analysis, and flexibility for applications such as whole-genome sequencing and variant detection. In precision medicine, NGS swiftly identifies genetic mutations for early disease diagnosis and personalized therapies (Mardis, 2013)

Bioinformatic tools, such as Sift and PolyPhen, were also used to predict whether an amino acid substitution can affect the protein function and structure, based on physical and comparative considerations. Segregation analysis is an important genetic method for tracing the transmission of traits in families. This method examines patterns of inheritance and their compatibility with theoretical

models using genotyping data and family pedigrees. This process helps in providing accurate diagnosis, genetic counseling, and managing diseases.

2.2.3 Sirolimus treatment

Sirolimus represents a precision medicine approach for controlling seizures. A trial was initiated for patient #2 who was 7 months old based on molecular analysis findings, administering sirolimus at 1.2 mg/m²/day. The patient has continued with a consistent treatment regimen (sirolimus, levetiracetam, lacosamide) for 22 months now. The use of sirolimus treatment was not pursued for patient #1.

2.2.4 Strains and media

Bacterial *E.coli* StellaR (HST08) strain (Clontech, genotype: [(F-, endA1, supE44, thi-1, recA1, relA1, gyrA96, phoA, Φ80d lacZΔ M15, Δ(lacZYA-argF) U169, Δ(mrr-hsdRMS-mcrBC), ΔmcrA, λ-] was used as the host for cloning procedures and plasmid propagation. *E. coli* cells were grown at 37°C in liquid or solid (by adding agar 2% (w/v)) Luria-Bertani (LB) medium (Tryptone 1% (w/v), Yeast extract 0.5% (w/v), NaCl 1% (w/v)), containing ampicillin (100 µg/ml) (Sigma-Aldrich) for the selection of transformants. Haploid and diploid *Saccharomyces cerevisiae* W303 strains (genotype: *MATa/MATα {leu2-3,112 trp1-1 can1-100 ura3-1 ade2-1 his3-11,15}*) were used as genetic background to the experiments described. Yeast growth and manipulation were performed as described in Amberg et al., 2005. Yeast strains were transformed using the high-efficiency protocol (PEG/lithium acetate method) according to Gietz & Woods, 2006). Transformed cells were selected on solid YPD medium (20 $g \cdot L^{-1}$ Bacto peptone, 10 $g \cdot L^{-1}$ Bacto yeast extract, 20 $g \cdot L^{-1}$ Glucose, 2% w/v Agar), supplemented with 200 $mg \cdot L^{-1}$ G418 (Geneticin, Sigma-Aldrich) or in Synthetic Minimal media (1.7 $g \cdot L^{-1}$ Yeast nitrogen base without amino acids, 5 $g \cdot L^{-1}$ Ammonium sulfate) containing 20 $g \cdot L^{-1}$ Glucose, without the specific nutrients for selection of transformed yeasts. Yeast plates were finally incubated for 2-3 days at 30°C.

2.2.5 *SPS1* gene mutagenesis in yeast cells

Yeast genetic modifications have been performed by Crispr/Cas9 strategy as described in Mans et al., 2015 with some modifications. Firstly, a DNA cassette for the constitutive expression of Cas9 was introduced into the SalI site of the original pMEL13 plasmid. The cassette was amplified by pMEL15 backbone using the primers indicated in Table 2.3, originating the pMEL13-Cas9 plasmid. Thereafter, it was inserted the specific sequence targeting *SPS1* (i.e., guide), finally generating the gSPS1-pMEL13-Cas9 plasmid. Among the possible targets indicated by the Yeastriction database (Mans et al., 2015*:* https://github.com/hillstub/Yeastriction), we selected the 616-635 sequence of *SPS1*, because of its proximity to nucleotides 604-606, which corresponds to the Ser202 residue that needs to be replaced. All plasmids were constructed using the In-Fusion HD Cloning Kit (Takara-bio). Briefly, PCR products and digested (or PCR-amplified) vectors were spin-column purified using the GenElute™ PCR Clean-Up Kit (Sigma-Aldrich) and subjected to In-Fusion Cloning Procedure following the manufacturer's instruction. All cloning primers (Table 2.3) were designed as suggested by the manufacture's online tool (www.takarabio.com). Plasmids were verified by both restriction digestion and sequencing. Mutant *SPS1* yeast strains were generated by co-transforming W303 cells (haploid and diploid) with 1 mg of gSPS1-pMEL13-Cas9 plasmid together with an excess amount (3-5 mg) of donor dsDNA, necessary to repair the DSB at *SPS1* locus, and restore cell viability. The dsDNAs were generated by annealing two complementary single-stranded oligonucleotides (Table 2.3), by mixing them (1:1), heating to 95°C for 5 min, and cooling down to room temperature. Two dsDNA molecules were used to generate either *SPS1* deletion, or the missense mutation S202R in *SPS1* sequence. Yeast transformants were selected by their ability to grow on YPD+G418 plates after being incubated at 30°C for 2-3 days. Heterozygous diploid W303 strains either for *SPS1* deletion or S202 missense mutation were further generated, by crossing the haploid mutant yeast strains with isogenic wild-type cells of the opposite mating type. In all cases, gene deletion and mutations were confirmed by PCR using specific diagnostic primers (Table 2.3), and finally verified by sequencing of the *SPS1* locus.

2.2.6 Sporulation media and assay

Yeast strains were firstly grown in Glycerol medium (YPG, 20 $g \cdot L^{-1}$ Bacto peptone, 10 $g \cdot L^{-1}$ Bacto yeast extract, 30 $ml \cdot L^{-1}$ Glycerol and 2% w/v Agar) to avoid possible defects in mitochondrial respiration, which is necessary to sporulation process. Cells were induced to sporulate according to the protocols of Paulissen et al. (2016) and Slubowski et al. (2014). Briefly, yeast cells were incubated at 30°C in YPD medium until stationary phase, and after washing, strains were diluted to OD_{600} = 0.1 in a pre-sporulation medium (YPA, 20 $g \cdot L^{-1}$ Bacto peptone, 10 $g \cdot L^{-1}$ Bacto yeast extract, 20 $g \cdot L^{-1}$ Potassium acetate). Then, cells were grown for 16-18 h at 30°C until OD_{600} reached 1.3-1.5, when yeasts were collected, washed, and finally resuspended at OD_{600} = 2.0 in liquid sporulation medium (containing 10 $g \cdot L^{-1}$ Potassium acetate). Cultures were incubated at 30°C and the sporulation efficiency of yeast strains was evaluated after 24, 48 and 72 h, by analyzing (at least) 600 cells for each sample and performing three independent experiments. Samples were counted for refractile spores or refractile spore-like structures using a bright-field microscope, as reported in Paulissen and Huang (2016).

2.2.7 Statistical analysis

Data are reported as mean ± standard error of the mean (SEM), with the number of experimental replicates (n) indicated in the legend.

Primer Name	Sequence 5'-3'	Purpose
Cas9-pMEL For	ATTAAGGGTTGTCGACAGCTCATAG CTTCAAAATGTTTCTACTCC	Cloning Cas9 in pMEL13
Cas9-pMEL Rev	TACGCTGCAGGTCGACCAAATTAAA GCCTTCGAGCGTCCC	
6006 For	GTTTTAGAGCTAGAAATAGCAAGTT AAAATAAGGCTAGTC	Cloning gSPS1 in pMEL13-Cas9
gSPS1-target Rev	TTCTAGCTCTAAAACTTGAGTAACTC ATAGGTGGTGATCATTTATCTTTCAC TGCGGAGA	
SPS1-S202R For	TATAATGAGAAAGCAGATATATGGC GATTGGGTATCACAACATATGAATT ACTCAAGGGCTTACCCCCATTATCT AAATATGATCCTATGAAAGTTATG	dsDNA repair *SPS1* mutation
SPS1-S202R Rev	CATAACTTTCATAGGATCATATTTAG ATAATGGGGGTAAGCCCTTGAGTAA TTCATATGTTGTGATACCCAATCGC CATATATCTGCTTTCTCATTATA	
SPS1-Delta For	TTTTTTACTAGCTAATTCATTTACTA AACAACAAAAGAAAATAGCACAAAA AAAATAGATATATATATATAATGTGT GTATATGCATGAGTTTTTGTTTT	dsDNA repair *SPS1* deletion
SPS1-Delta Rev	AAAACAAAAACTCATGCATATACAC ACATTATATATATATATCTATTTTTTT TGTGCTATTTTCTTTTGTTGTTTAGT AAATGAATTAGCTAGTAAAAAA	
dgSPS1 For	GTTCGGAACAATGCGGCATC	*SPS1* locus diagnosis
dgSPS1 Rev	TGAGACGCATCAATGACGGG	

Table 2.3 Sequences of the oligonucleotides used in this study.

2.3 Results

2.3.1 Genetic studies

Array comparative genomic hybridization (Array-CGH) analysis showed normal results in both patients. Patient #1 was studied using the Illumina TruSight One kit. The analysis focused on homozygous variants with a minor allele frequency (MAF) inferior to 1%. Only three variants were identified (Table 2.4), along with homozygous missense variant of the *STRADA* gene NM_001003787.2:c.792T>A p.(Ser264Arg) (Fig.2.7).The variant has a MAF of 1:113,732 in Europeans and affects a highly conserved residue. Sift and PolyPhen predicted a possible deleterious role for this substitution (Adzhubei et al., 2013; Ng & Henikoff, 2003). Furthermore, segregation analysis showed that both parents were heterozygous carriers. In support of its pathogenicity, the variant was initially identified in a 7-year-old girl exhibiting a phenotype consistent with PMSE (Aerden et al., 2021).

Patient #2 was analyzed using an Agilent SureSelect targeted NGS panel including 275 genes. We detected a previously reported homozygous truncating mutation NM_001003787.2:c.891dupC p.(Cys298Leufs*11)(Evers et al., 2017) (Fig.2.6).

Gene	Mutation	Conditions Associated
STRADA	NM_001003787.2:c.792T>A p.(Ser264Arg)	PMSE
WNK4	NM_032387.4:c.2023C>T p.(Arg675Trp)	Pseudohypoaldosteronism
SCN4A	NM_000334.4:c.908A>G p.(Asn303Ser)	Periodic paralysis and myopathies

Table 2.4 Homozygous variants with MAF<1% identified in patient #1 using the Illumina TruSight One Kit.

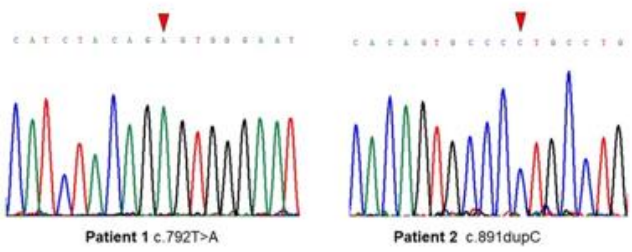

Figure 2.6 Electropherograms of the homozygous mutations found in the patients. Arrowheads indicate the mutant bases.

2.3.2 Validation of the missense mutation

Although the pathogenicity of the truncating mutation found in patient #2 was evident, establishing the role of the missense variant found in patient #1 was more challenging, due to some peculiarities in the patient's phenotype compared to other individuals affected by *STRADA* mutations. Therefore, we used a yeast model to investigate the functional consequences of the p.Ser264Arg variant. The human gene shares significant similarity with the yeast homolog, SPS1. More specifically, amino acid residues 255-282 of STRADA that flank Serine 264 exhibit high similarity to the Sps1p sequence: 11/18 amino acids are identical, including the corresponding Serine at position 202 of Sps1p, as shown in Fig.2.7.

```
            255       264       282
STRADA      GYDAKSDIYSVGITACEL
            ::  : :: : :::  ::
Sps1p       GYNEKADIWSLGITTYEL
            193       202       210
```

Figure 2.7 Sequence alignment between residues 255-282 of the human STRADA protein and the corresponding residues of yeast Sps1p. Identical residues are shown in bold, human Ser264 and yeast Ser202 are underlined.

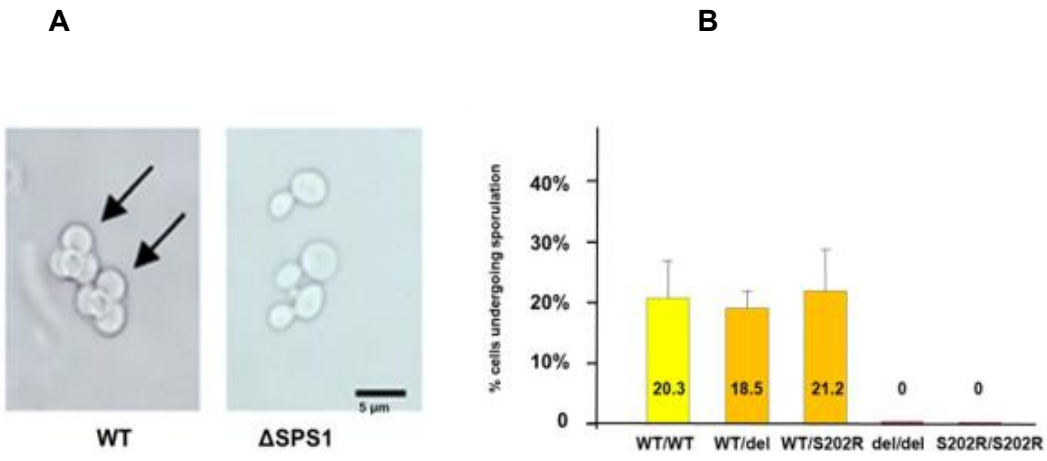

Figure 2.8 A) Representative images of refractile spores (marked with black arrows) visualized using an Olympus Microscope CX41and a 60x-magnification objective (bright-field) in yeast strains carrying wild type (WT) or deleted (ΔSPS1) *SPS1*. Scale bar: 5 µm. B) Sporulation efficiency assay. 72 h after induction of sporulation, we assessed refractile spore formation for yeast diploid cells carrying different *SPS1* allele combinations (del = *SPS1* deletion; S202R: p.Ser202Arg mutation). Data are reported as the mean value ± SEM, n=3 (600 cells were counted in each experiment, see supplementary material).

The *SPS1* gene encodes for a STE20-related protein kinase required to complete the sporulation process (Slubowski et al., 2014). In yeast, sporulation is like meiosis and is the process by which a diploid cell produces 4 haploid daughter cells. Yeast cells lacking *SPS1* do not show any abnormalities in vegetative growth but are unable to undergo sporulation (Fig.2.8 A). Using CRISPR/Cas9 technology we introduced in the genomic DNA of the *SPS1* gene of a haploid W303 yeast strain either the p.Ser202Arg substitution, or the deletion of the entire *SPS1* gene, which mimics the truncating mutations. By mating different mutant strains, we generated diploid yeast strains carrying the different mutations in either homozygous or heterozygous state. Sporulation was normal in the wild type and in the heterozygous strains but was completely abolished in both homozygous mutants (Fig.2.8 B), confirming the pathogenicity of the missense variant.

2.3.3 Sirolimus treatment

Because of the results of the molecular analyses, we started a trial with sirolimus at a dose of 1.2 mg/m^2/day in patient #2 at 7 months of age. The drug was effective and well-tolerated, resulting in prolonged periods of seizure freedom and decreased seizure cluster frequency induced by febrile illnesses. Physical therapists and parents noted improvements in interaction and communication. When the patient was 12 months old, EEGs showed improved organization of background activity during both wakefulness and sleep. However, multifocal epileptic discharges persisted during sleep, and bilateral temporal fast sequences were observed.

At 22 months, the patient's treatment is unchanged (sirolimus, levetiracetam, lacosamide) with overall good seizure control, and sporadic seizure clusters prompted by febrile infections and medication non-adherence. The EEG reveals diffuse and fast sub-continuous activity, predominantly in the posterior regions, accompanied by sporadic multifocal epileptic anomalies. Advances in motor development include independent maintenance of the sitting position, rolling over, reaching for objects, and starting to crawl. Although the patient remains non-verbal, interaction and communication through vocalizations and facial expressions appear slightly improved.

We did not consider employing sirolimus treatment in patient #1 because seizures were well controlled with standard antiseizure therapy.

2.4 Discussion

Yeast has been extensively used as a simple model to validate novel mutations and to establish genotype-phenotype correlations. In this paper, we selected this method because the yeast *SPS1* gene bears significant homology with the human *STRADA* gene, the mutated residue is conserved in the yeast protein, and its inactivation produces a phenotype which is relatively easy to evaluate. Compared to traditional approaches, CRISPR-Cas9 allows to directly mutagenize the yeast genome, avoiding all potential plasmids-related artifacts.

The results were clear: the p.Ser202Arg mutation completely abolished *SPS1* function, suggesting the p.Ser246Arg variant found in patient #1 is indeed pathogenetic. Interestingly, patient #1 presented an uncommon electroclinical phenotype, different from other PMSE patients, with diffuse high amplitude 20 Hz beta activity, affecting predominantly the fronto-central regions. Moreover, he had focal monomorphic seizures, and his epilepsy was well controlled by just two medications, whereas multidrug resistance is a constant feature in other *STRADA* cases. There is currently no clear explanation for the presence of 20 Hz beta activity. We hypothesized that an alteration of the cortex pattern, undetectable by the employed MRI techniques, could be present. Analysis of clinical exome data ruled out mutations in other genes associated with cortical malformations.

On the other hand, the relatively mild epileptic phenotype could be due to the presence of some residual activity of the mutant protein, undetected by our yeast assay. However, the other reported individual carrying the same p.Ser246Arg mutation in the homozygous state (Aerden et al., 2021) displayed a more "classical" PMSE phenotype, suggesting that other factors, probably both genetic and environmental, are involved in modulating the phenotype of *STRADA* patients.

Finally, the favourable response of patient #2 to sirolimus highlights the importance of an early molecular diagnosis, towards a better treatment and quality of life.

The results underlie the importance of a timely molecular diagnosis in these patients and show that yeast is a simple yet effective model to validate the pathogenicity of missense variants.

PART III

Developing a Yeast Model to Validate a Novel *SGPL1* Gene Missense Mutation and Investigate Potential Rescue with B6 Supplementation

3.1 Introduction

3.1.1 Sphingolipids

Sphingolipids are a ubiquitous and diverse category of lipids that were discovered by Thudichum in 1884. He named them after the functional puzzles they presented (McIlwain, 1964). In the 1960s, sphingolipids were acknowledged as standard parts of the plasma membrane, myelin sheath, and plasma and were found to accumulate in patients with sphingolipidoses, storage conditions triggered by innate sphingolipid metabolism problems (Saba, 2019).

Currently, sphingolipids are regarded as crucial and widespread structural elements of cell membranes. Moreover, their metabolites act as signalling molecules in eukaryotic cells. (Hannun & Obeid, 2008). Ongoing discoveries indicate that this trend will continue to rise as our understanding of sphingolipid biology in whole organisms progresses (Gault et al., 2010).

The structure of sphingolipids is based on a long-chain base (LCB) backbone. Sphingosine is the most common LCB found in mammalian cells. Sphingolipids undergo modifications in the LCB anchor through the addition of polar headgroups at C1 position and acylation of the free amino group, which leads to the formation of a wide range of sphingolipid species (Saba, 2019).

Sphingolipids synthesis involves a precisely regulated sequence of enzymatic steps, beginning in the endoplasmic reticulum from non-sphingolipid precursors and ending with the formation of complex higher-order glycosphingolipids within the Golgi apparatus. Although sphingolipid synthesis is a complex process, it can be traced back to a common starting point and ultimately results in a single degradative pathway.

3.1.2 The enzyme SGPL1

The *SGPL1* (also referred to as *SPL*: frequently employed throughout the text to enhance the fluidity, refrain from repetitively using the same term and strive to harmonize images from different sources) gene encodes for a sphingosine-1-phosphate lyase 1 (S1P lyase) of 568 amino acids in length, an

endoplasmic reticulum (ER) enzyme (Fig.3.1) that is ubiquitously expressed in tissues and is essential for the catabolic pathway of sphingolipids in humans.

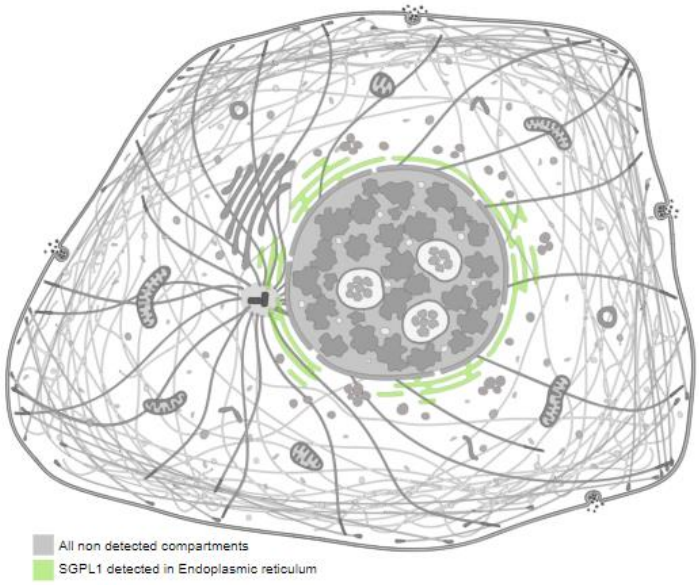

Fig. 3.1 Image showing the cellular localization of the human SGPL1 enzyme in the endoplasmic reticulum (Human Protein Atlas).

Specifically, it binds sphingosine 1-phosphate (S1P) and catalyzes the final and irreversible degradation step in sphingolipid metabolism, forming phosphoethanolamine and the long-chain aldehyde hexadecanal (Fig. 3.2). Both products are further metabolized to carbon dioxide or re-utilized in the synthesis of phospholipids. (Stoffel et al., 1969)

Intracellular levels of S1P are tightly controlled by two other enzymes, the first, sphingosine kinase (SphK), which catalyzes S1P synthesis, and the second, sphingosine-1-phosphate phosphatase (S1Pase), which catabolizes it. Up to this point in the pathway, the enzymatic reactions are reversible. The SPL enzyme is therefore an important regulator of cellular sphingolipid intermediates and sphingosine-1-phosphate (S1P)-mediated signalling. S1P, a bioactive lipid with multiple functions, acts as an intracellular second messenger and as a ligand for a specific group of five G-protein-coupled receptors (S1PR1–5), with crucial roles in development, physiology, and immunology. S1P operates at multiple levels within the steroidogenic pathway, enhancing cortisol biosynthesis (Ozbay et al., 2006). These signalling pathways are involved in several physiological

processes, including angiogenesis, immune cell migration, stem cell specialization, and programmed cell death (Maceyka et al., 2012).

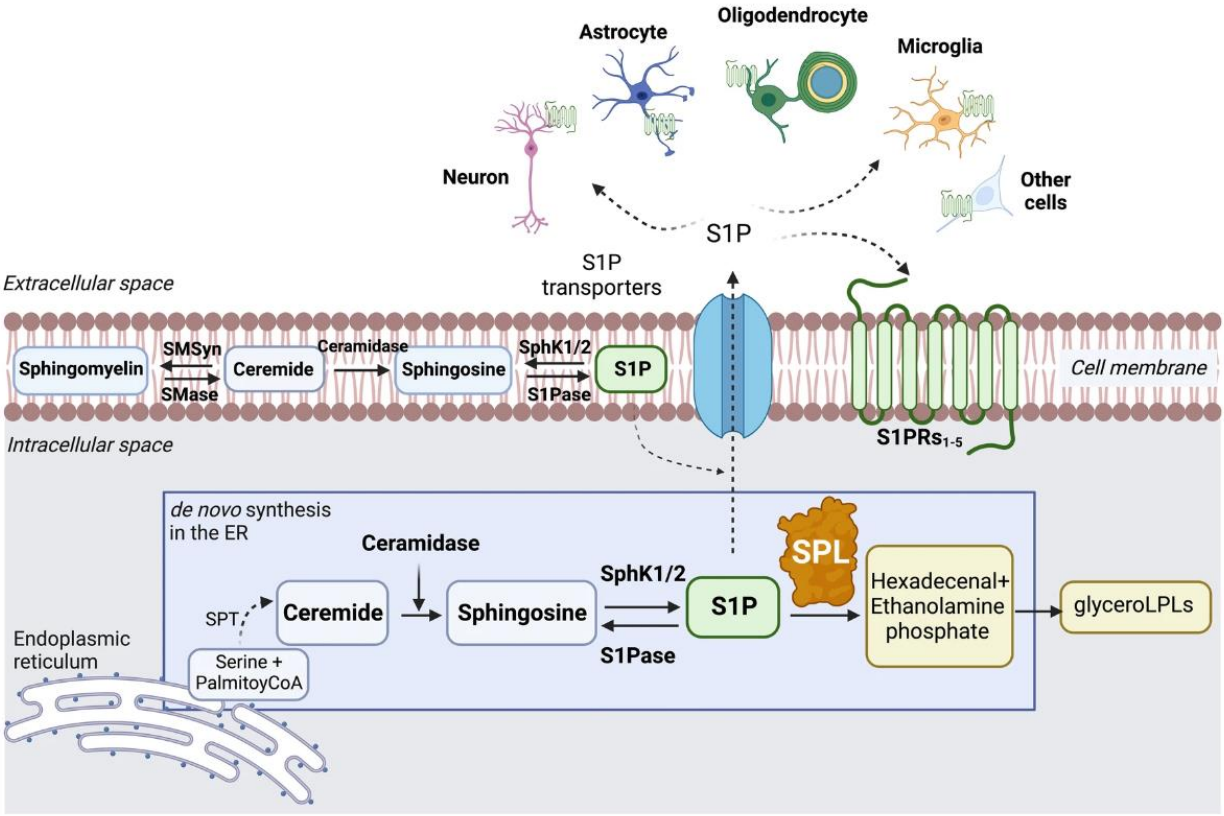

Fig. 3.2 Schematic diagram showing that sphingosine 1-phosphate lyase (SPL) controls sphingosine-1-phosphate (S1P) pools available for both intracellular and extracellular signalling. The S1P can be synthesized in the endoplasmic reticulum (ER, de novo synthesis pathway) and at the plasma membrane (salvage synthesis pathway). Intracellular or plasma membrane ceramide can be subsequently metabolized by ceramidase to generate sphingosine which in turn produces S1P. The level of endogenous S1P is kept under control through equilibrium between its synthesis governed by sphingosine kinases 1 and 2 (SphK1/SphK2), and its degradation by SPL. SPL catalyzes the cleavage of S1P, resulting in the formation of hexadecenal and ethanolamine phosphate, which can subsequently enter the glycerolysophospholipids (glyceroLPLs) synthetic pathway. S1P can also be reverted to sphingosine by sphingosine-1-phosphate phosphatase (S1Pase). Figure prepared in Biorender.com with publication license and shown in “Sphingosine 1-Phosphate Lyase in the Developing and Injured Nervous System: a Dichotomy?” by Xiao (2023).

Typically, S1P is pro-proliferative during normal physiological conditions, and it suppresses the pro-apoptotic actions of ceramide. However, loss of function mutations in SGPL1 lead to a pathological accumulation of S1P, which scientific studies have associated with the induction of apoptosis. (Gennero et al., 2002). Its inactivation causes product depletion and accumulation of upstream sphingolipid intermediates (Fig. 3.3).

Stoffel et al., (1969). demonstrated that the enzyme responsible for the last cleavage reaction of the sphingosine-1-phosphate is highly concentrated in the endoplasmic reticulum (ER) and this finding marks an important milestone in the comprehension of this enzyme: this is currently known to be located in the ER, with a luminal domain at N-terminus, a transmembrane domain and a PLP binding domain that is responsible for catalytic activity (Bourquin et al., 2010).

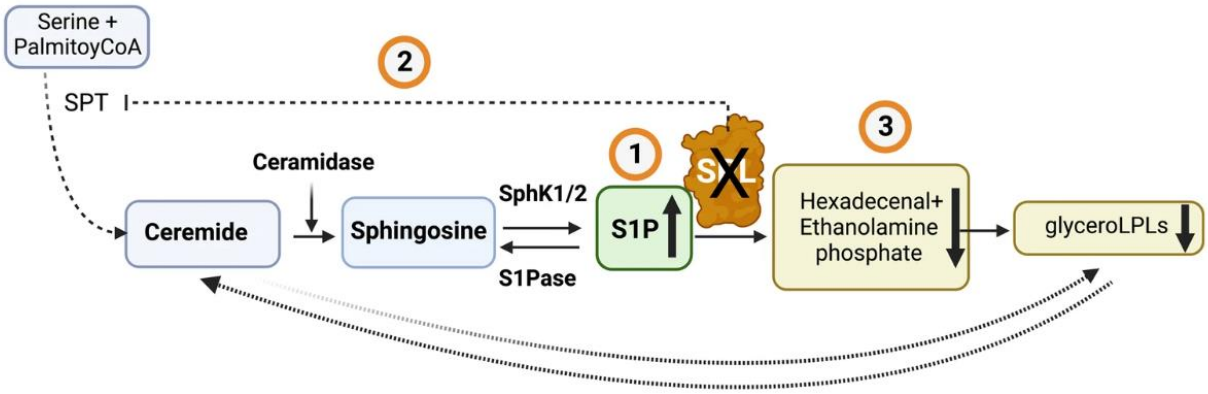

Fig.3.3 Schematic showing the possible consequences of sphingosine-1-phosphate lyase 1 inhibition. The loss of SPL expression or activity results in not only an overall increase in S1P levels but also a potential change in other sphingolipids as well as glycerolysophospholipids (glyceroLPLs). 1. SPL irreversibly degrades S1P hence the loss of SPL typically leads to an increase in S1P levels. 2. The loss of SPL could reduce de novo biosynthesis of sphingolipids via increasing the recycling of sphingoid bases. 3. SPL facilitates hexadecenal and phosphoethanolamine to enter the glyceroLPLs synthetic pathway. Hence, the loss of SPL could indirectly reduce glyceroLPLs. Production. Figure prepared in Biorender.com with publication license and shown in “Sphingosine 1-Phosphate Lyase in the Developing and Injured Nervous System: a Dichotomy?” by Xiao (2023).

SGLP1 belongs to the superfamily of pyridoxal phosphate (PLP)-dependent enzymes, which is one of the active forms of vitamin B6. PLP-dependent enzymes catalyze a wide variety of reaction types and usually have a conserved lysine residue in the active site for PLP binding. In addition to the diversity of reaction specificity, PLP-dependent enzymes are involved in many key cellular processes and metabolism (J. Liang et al., 2019)

The enzyme was crystallized a few years ago and shown to function as a homodimer (Bourquin et al., 2010). The crystal structure of the SGPL1 protein (Fig.3.4) reveals 2 subunits forming a tightly intertwined dimer, with both chains contributing to the catalytic cavity defined by the covalently bound cofactor pyridoxal phosphate (PLP) (Weiler et al., 2014).

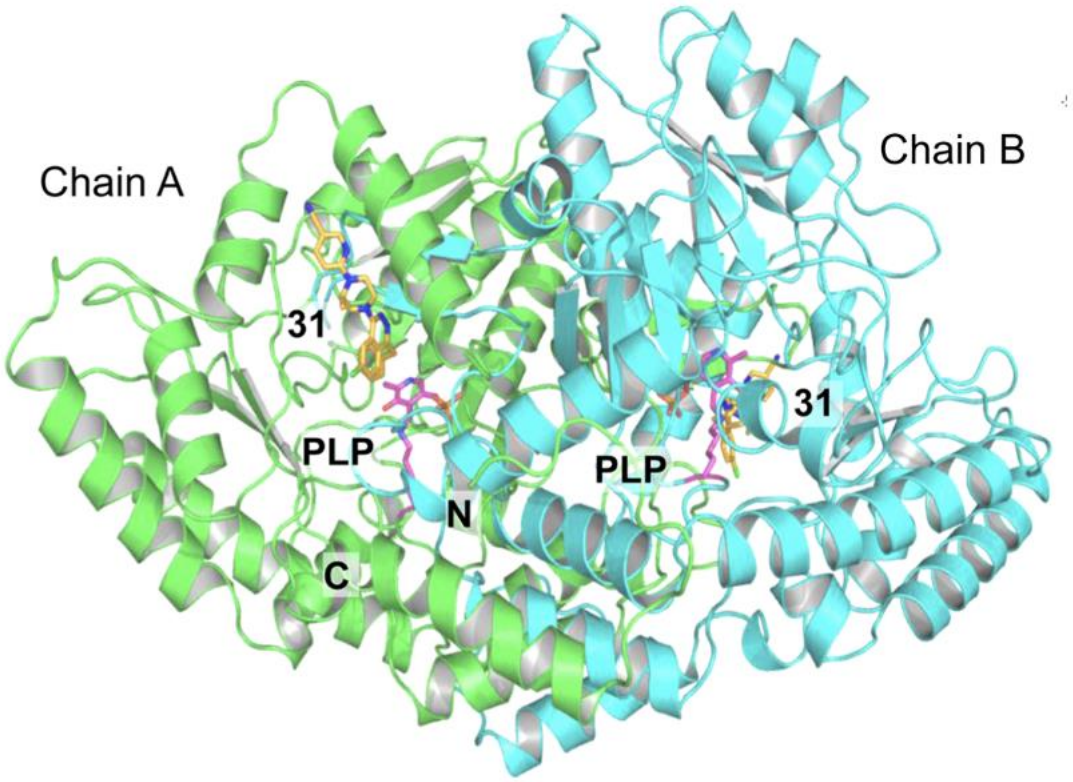

Fig. 3.4 Cartoon representation of SGPL1 crystal with chain A in. green and chain B in blue. The cofactor (PLP) in both chains, together with the covalently bound side chain of K353, is in stick representation (magenta). In this figure, it is also shown a potent and effective inhibitor (31), in stick representation (orange): this class of compounds was found to inhibit the catalytic activity of SPL enzyme by binding to its active site commonly occupied by the cofactor pyridoxal phosphate (Weiler et al., 2014)

3.1.3 Sphingolipid Pathway Evolution: Insights from Yeast Gene *DPL1*

Yeast is an excellent model system for investigating the role of sphingolipids, due to their high similarities to the human sphingolipid pathway (as shown in Fig.3.5) . *LCB4* and its counterpart *LCB5* (Nagiec et al. 1998) encode kinases, which are responsible for the synthesis of two long-chain base phosphates, namely dihydrosphingosine 1-phosphate (DHS1-P) and phytosphingosine 1-phosphate (PS1-P) (Nagiec et al., 1998).

Yeast has two distinct catabolic pathways for LCBPs. The first pathway involves the dephosphorylation of LCBPs back into LCBs, a process carried out by LCBP phosphatases Ysr2p

and Ysr3p (Mao et al., 1997; Qie et al., 1997; Mandala et al., 1998).Alternatively, LCBPs can undergo internal cleavage at the C2-3 bond, initiated by LCBP lyase Dpl1p. This cleavage yields long-chain aldehyde and ethanolamine phosphate (Saba et al., 1997). The hydroxylation of dihydrosphingosine at C4, which generates phytosphingosine, is dependent on the presence of Sur2p (Haak et al., 1997).

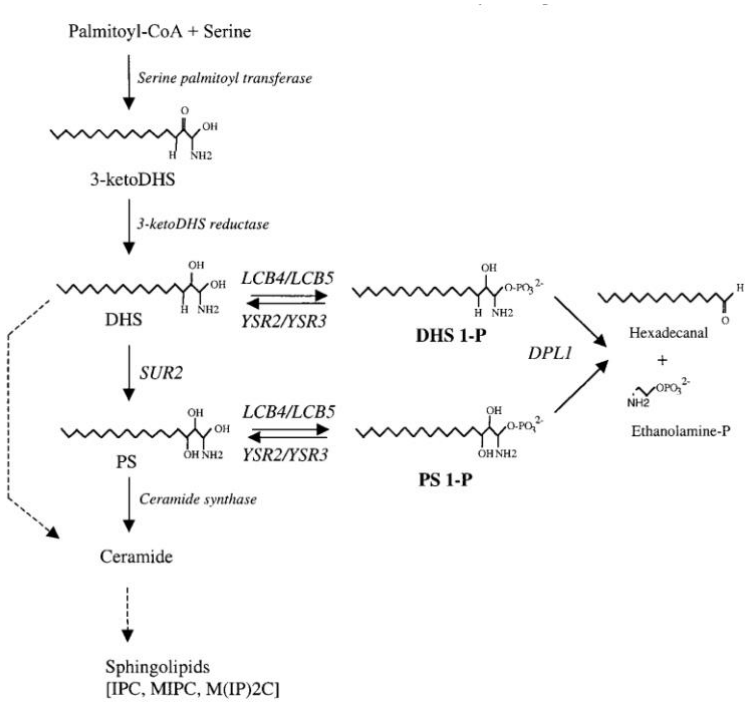

Fig.3.5 The sphingolipid metabolic pathway proposed in *S. cerevisiae*. *DPL1*, also known as *BST1*, encodes an LCBP lyase, as reported by Saba et al. (1997). *YSR2*, also known as *LCB3* and *LBP1*, has been found to encode an LCBP phosphatase according to Mao et al. (1997), Qie et al. (1997), and Mandala et al. (1998). Ysr3/Lbp2/Ykr053c shares 53% amino acid identity with Ysr2/Lcb3/Lbp1. *LCB4* encodes the predominant Lcbp kinase and bears 53% amino acid similarity to Lcb5 (Nagiec et al., 1998). *SUR2*, which was also independently identified as *SYR2*, encodes Lcb hydroxylase (Haak et al. 1997). Yeast contains three different but related sphingolipids: Inositol-phosphorylceramide (IPC), mannoseinositol-P-ceramide (MIPC), and mannose-(inositol-P)2-ceramide [M(IP)2C].

Sphingolipids and their metabolic derivatives elicit a wide variety of eukaryotic cellular responses. Although the stimuli and biological end points differ in each cell type, the role of sphingolipid by-products as second messengers in specific, growth regulatory signal transduction pathways appear to be a universal theme among eukaryotic cells (Saba et al., 1997)

The conservation of sphingolipids throughout evolution allowed the isolation and cloning of the first *SPL* gene, *DPL1*, from *Saccharomyces cerevisiae* (Fig.3.6). Enhanced *DPL1* expression in yeast resulted in resistance to sphingosine, while *DPL1* deletion increased sensitivity to Long Chain Bases (LCBs), including exogenous D-erythro-sphingosine and phytosphingosine. Additionally, deletion led

to the intracellular accumulation of sphingosine 1-phosphate when exposed to external sphingosine (Saba et al., 1997). These findings strongly confirm the common sphingoid base metabolism shared by eukaryotes (Fig. 3.7), suggesting the utility of yeast genetics in discovering new genes involved in sphingolipid signalling and metabolism. The genetic techniques used in yeast accelerated the quick identification of genes related to pathways and their related counterparts in diverse species. Employing genetic manipulation of genes encoding *SPL* in model organisms unveiled the substantial impact of sphingolipid metabolism on developmental processes, physiological functions, and intricate host-pathogen interactions.

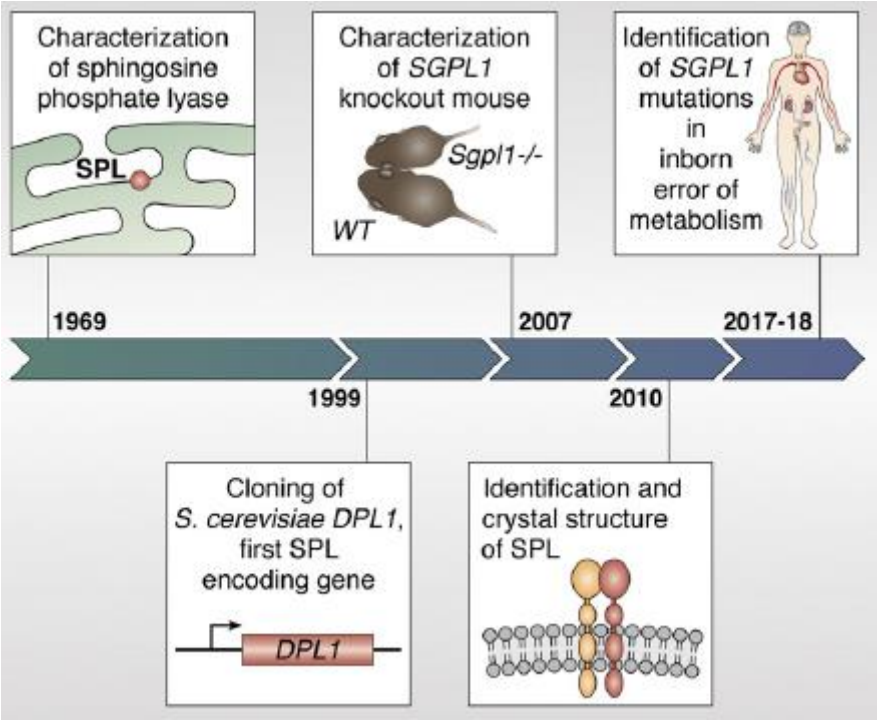

Fig. 3.6 The key milestones associated with the sphingosine-1-phosphate lyase 1 are presented: Stoffel et al. were the first to provide a detailed description of the main features of the SPL enzyme activity in 1969. The initial gene encoding SPL was cloned from budding yeast in 1997. The manipulation of *SPL*-encoding genes in model organisms, such as *SPL1* knock-out mouse models, has demonstrated how sphingolipid metabolism contributes towards the development, physiology and interactions between hosts and pathogens. In 2010, the functional and structural characteristics of the yeast sphingosine-1-phosphate lyase 1 (Dpl1) and its first prokaryotic homolog from *Symbiobacterium thermophilum* were determined. The Dpl1 structure provided a reliable model for *H. sapiens* SPL. Diagnostic genome sequencing identified a novel human syndrome associated with inactivating SGPL1 mutations in 2017-2018. (Saba, 2019)

Furthermore, *Saccharomyces cerevisiae* Δ*dpl1* strain not only exhibited an increase in sensitivity both to Long Chain Bases (LCBs) and calcium, as well as an accumulation of Long Chain Base

Phosphates (LCBPs). Interestingly, this strain demonstrated resilience when experiencing heat shock and nutrient deprivation: this observation suggested that LCBPs may play a protective role (Birchwood et al., 2001; Gottlieb et al., 1999). Therefore, it may be advantageous to aim for the accumulation of LCBPs and the targeting of SPL, because it could lead to favourable results. Nonetheless, a delicate equilibrium exists, beyond which adverse effects manifest. This phenomenon could arise due to the toxicity associated with excessively elevated LCBP levels or precursors in the sphingolipid pathway. Otherwise, this lethality could be a consequence of indirect disruptions in the global regulatory networks that sustain sphingolipid homeostasis.(Saba, 2019).

The orchestration of sphingolipid biosynthesis is meticulously overseen by ORM proteins. These proteins exert control by inhibiting the rate-limiting enzyme of sphingolipid biosynthesis, serine palmitoyltransferase (SPT) (Breslow et al., 2010). Intriguingly, a complete halt in sphingolipid degradation might trigger feedback signals that impede the de novo synthesis of pivotal sphingolipids essential for membrane integrity and organization. The concept of SPL inhibition being a double-edged sword frequently arises in various evolutionary contexts, ranging from yeast to humans.

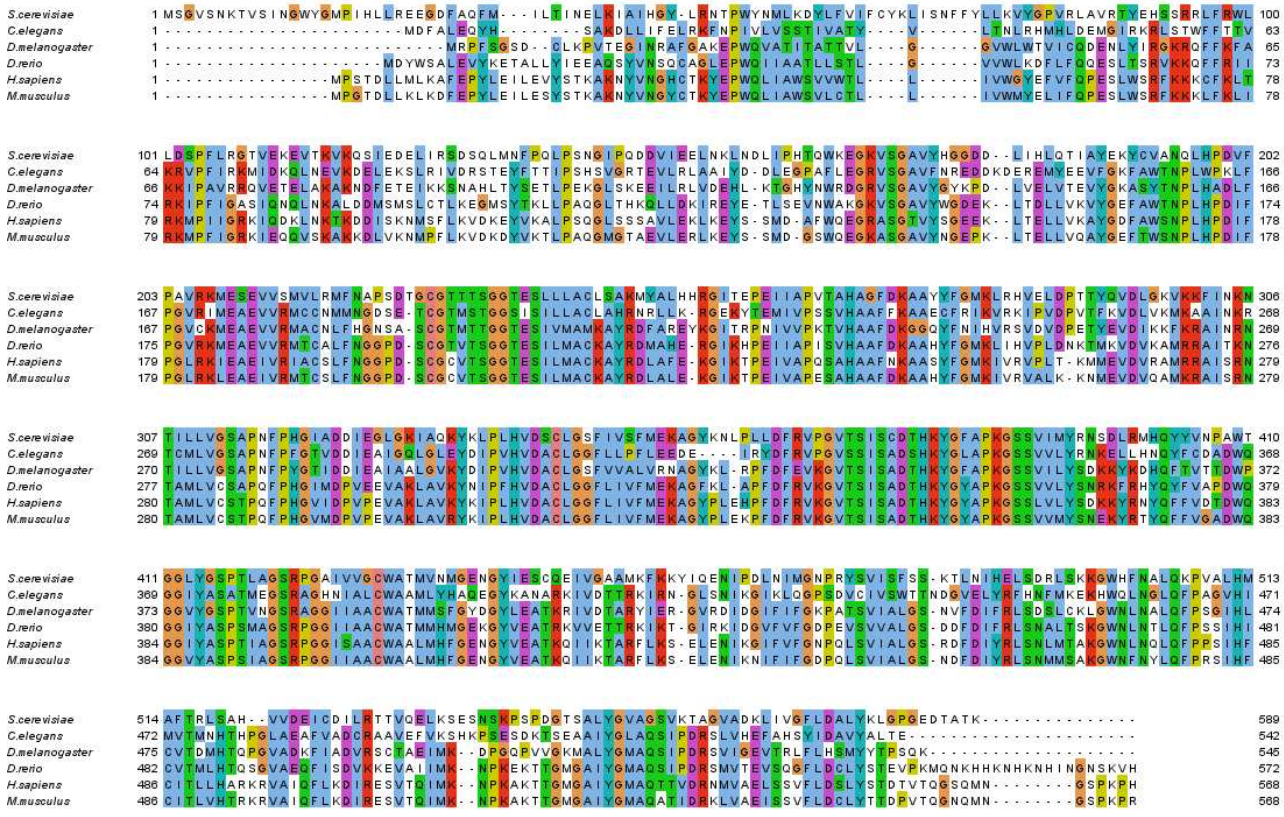

Fig.3.7 Sequence alignment of SPL homologs. Clustal Omega alignment of SPL amino acid sequences of Saccharomyces cerevisiae (QHB07755.1), Caenorhabditis elegans (NP_505372), Drosophila melanogaster (NP_652032.1), Danio rerio (NP_001082938), Homo sapiens (NP_003892.2) and Mus musculus (NP_033189.2).

Legend

Clustal X Default Colouring			
Category	Colour	Residue at position	{ Threshold, Residue group }
Hydrophobic	BLUE	A,I,L,M,F,W,V	{>60%, WLVIMAFCHP}
		C	{>60%, WLVIMAFCHP}
Positive charge	RED	K,R	{>60%,KR}, {>80%, K,R,Q}
Negative charge	MAGENTA	E	{>60%,KR}, {>50%,QE}, {>85%,E,Q,D}
		D	{>60%,KR}, {>85%, K,R,Q}, {>50%,ED}
Polar	GREEN	N	{>50%, N}, {>85%, N,Y}
		Q	{>60%,KR}, {>50%,QE}, {>85%,Q,E,K,R}
		S,T	{>60%, WLVIMAFCHP}, {>50%, TS}, {>85%,S,T}
Cysteines	PINK	C	{>85%, C}
Glycines	ORANGE	G	{>0%, G}
Prolines	YELLOW	P	{>0%, P}
Aromatic	CYAN	H,Y	{>60%, WLVIMAFCHP}, {>85%, W,Y,A,C,P,Q,F,H,I,L,M,V}
Unconserved	WHITE	any / gap	If none of the above criteria are met

Past research shows that restoring growth in *SGPL1*-deficient Δ*dpl1*yeast strains by introducing *SGPL1* gene coding for the wild-type (WT) human protein effectively complements the yeast deletion phenotype (Lovric et al., 2017). Furthermore, previous studies have shown that sphingolipid-induced growth arrest remains consistent in both S. cerevisiae and mammalian cells (Fishbein et al., 1993; Saba et al., 1997).

3.1.4 NPHS14: clinical features and molecular genetics

The NPHS14 (OMIM #617575) condition, also known as SPLIS, is an autosomal recessive syndromic form of steroid-resistant nephrotic syndrome with multisystemic features and closely resembling that caused by CoQ deficiency. Most affected individuals present in infancy or early childhood with progressive renal dysfunction associated with focal segmental glomerulosclerosis (FSGS), resulting in end-stage renal disease within a few years. Some infants may also present with primary adrenal insufficiency. In some cases, patients may present in utero with fetal hydrops, which can lead to fetal demise. Additional features of the disorder can include ichthyosis, acanthosis, adrenal insufficiency, immunodeficiency, and neurologic defects (Lovric et al., 2017; Prasad et al., 2017).

SPLIS mutations were varied and included nonsense mutations, splicing defects, and missense mutations. All were associated with low to undetectable levels of Sphingosine-1-phosphate lyase 1

(SPL) abundance and activity. Mutations were distributed throughout the polypeptide sequence. Cellular findings suggested that many SPLIS missense mutations induce protein instability and rapid clearance due to misfolding, a common defect of inborn errors of metabolism (Bross et al., 1999).

Prasad et al. (2017) identified homozygous loss-of-function mutations in the *SGPL1* gene in 8 patients from 5 distinct families with nephrotic syndrome type 14. These mutations were discovered through whole-exome or Sanger sequencing and were consistently found in families with consanguinity. Cellular expression assays were conducted to investigate two mutations, NM_003901.4:c.664C>T (p.Arg222Trp) and NM_003901.4:c.1633T>C (p.Phe545Leu), which demonstrated decreased protein stability and almost complete absence of enzyme activity, indicating a loss of function.

Similarly, Lovric et al. (2017) identified homozygous or compound heterozygous mutations in the *SGPL1* gene in patients from 7 distinct families with NPHS14, most of which had consanguineous backgrounds. Various mutation types (frameshift, splice site, missense) were detected, all leading to reduced or absent SGPL1 protein and/or enzyme activity. Functional analysis of specific missense mutations, NM_003901.4:c.664C>T (p.Arg222Trp) and NM_003901.4(SGPL1):c.1037G>T (p.Ser346Ile), showed diminished protein levels, enzyme activity, impaired degradation of long-chain sphingoid bases, and altered subcellular localization. Disease-associated variants failed to correct growth defects in yeast or abnormalities in *Drosophila*, Sply mutants, which lack *SGPL1*. Knockdown of *Sgpl1* in rat mesangial cells hindered cell migration, and patient fibroblasts displayed reduced migration compared to controls.

In 2 unrelated male patients with NPHS14, both born to consanguineous parents, Janecke et al. (2017) identified homozygous truncating mutations in the *SGPL1* gene. These mutations, confirmed through whole-exome and Sanger sequencing, co-segregated with the disorder in the respective families. One patient exhibited significantly elevated levels of SGPL1 substrates, S1P, and sphingosine in blood and fibroblasts: suggesting that the underlying pathology in these patients may be due to accumulation of specific sphingolipid intermediates.

Some patients with SPL deficiency (SPLIS) exhibited elevated levels of cholesterol and triglycerides. These increases might result from nephrotic syndrome or directly from the deficiency itself. The

influence of SPL insufficiency was starkly evident in model organisms with *SPL* knockout, revealing the profound consequences of inadequate *SPL* function in humans.

Elevated ceramide levels in mitochondria disrupt the inner mitochondrial membrane, and as the initial and final steps of cortisol production occur there, mitochondrial dysfunction resulting from SPL deficiency could be a significant contributor to disease pathogenesis. (Maharaj et al., 2020)

The fetal and perinatal fatalities among the most gravely afflicted SPLIS patients, coupled with pleiotropic disease symptoms, clearly affirmed the vital role SPL performs in human metabolism.

3.1.5 Strategies for SPLIS treatment and the vitamin B6 supplementation

There are several possible strategies to help SPLIS patients. One approach involves correcting the disease symptoms stemming from abnormal S1P receptor (S1PR) signalling, which may require intervening with S1PRs themselves. An S1PR antagonist approved by the FDA (fingolimod) is available, along with other options that are still under development(Chew et al., 2016).

Another approach might involve substrate reduction in sphingolipidosis treatment (Arenz, 2017). Although the use of sphingosine kinase inhibitors could alleviate S1P-dependent toxicities, it may potentially worsen LCB and ceramide accumulation. Other options that are worth exploring are SPL enzyme replacement through gene therapy, bone marrow transplantation, or enzyme supplementation. It is pertinent to note the considerably favourable impacts that introducing soluble SPL produced in a preclinical model (Huwiler et al., 2011). The correction of mutations in the *SGPL1* gene may require gene editing, while misfolded SPL proteins could be revitalised with the assistance of chaperones. It is important to note that vitamin B6 could assist specific PLP-dependent enzymes, which has significant implications in the scientific context (Lorenz et al., 2014).

Vitamin B6, a group of essential vitamers, is crucial for metabolism and bodily function. Its active form, PLP, participates in over 150 enzymatic reactions, impacting metabolism and immune processes. It maintains normal metabolic and immune functions, especially anti-inflammatory response. Beyond these functions, PLP also acts as a chaperone, helping in the folding of recently formed polypeptides to enhance their enzymatic activity. This property has therapeutic implications

in metabolic diseases like primary hyperoxaluria. At present, there is a deficiency of focused therapies for SPLIS patients. Supplementation of cofactors for B6-responsive *SGPL1* alleles can potentially prevent manifestations of SPLIS, according to Zhao et al. (2020). Vitamin B6 has the potential for mitigating S1P excess and *SPL* deficiency-driven inflammation leading to potential clinical applications (Du et al., 2020). . Chaperone-type drugs could also hold promise. Comparing mouse models demonstrates that even a small amount of SPL activity could prevent severe SPL insufficiency consequences. Hence, modest SPL activity increases via B6 supplementation could have clinical significance. Lymphocyte trafficking sensitivity to S1P gradients indicates potential responsiveness to cofactor supplementation, as observed in lymphocyte count increases (Zhao et al., 2020). The responsiveness of yeast cells *in vivo* indicates their usefulness in establishing genotype-specific responses to B6.

The overall structure, cofactor binding mode, and the active site in general are well conserved between human SGPL1 and Dpl1p (yeast SGPL1 lyase) The use of human SGPL1 is very important as it serves a dual purpose. Firstly, it is crucial in assessing the sphingosine toxicity phenotype, and secondly it is essential for investigating possible responses to vitamin B6 treatment, being a PLP-dependent enzyme.

3.1.6 Exploring *GAD1* gene: an intriguing alternative sphinsogine-1-phosphate lyase?

When George Beadle and Edward Tatum introduced the concept of one gene–one enzyme back in 1941, enzymes were explained using the key and lock model for substrate recognition. In the early stages of molecular biology, proteins and enzymes were viewed as unique, specialised entities with only one specific function. This viewpoint influenced how the functions of biological systems were annotated, resulting in the tendency to ignore any additional roles a protein may have after being assigned a specific function. However, different mechanisms for multifunctionality have been discovered since the 1940s.

Proteins that have multiple functions may affect the development of organisms by enhancing complexity and robustness. Such proteins can broaden the functional range of a limited set of genes

in early life forms and organisms with a reduced genome. Furthermore, multifunctional proteins can promote communication among various biological processes, primarily in organisms with complex metabolic and regulatory networks. The multifunctionality that is hardly noticeable presents a challenge in performing the practical association studies that depend on guilt-by-association, genotype-phenotype mapping, and homology anticipation and notation (Espinosa-Cantú et al., 2020)

The *DPL1 gene* codes for a protein of 589 amino acids in length, which has 23% similarity to *gadA* and *gadB*, two nearly identical *E. coli* genes that encode glutamate decarboxylase. This is a pyridoxal-5'-phosphate-dependent enzyme that catalyzes the conversion of glutamate into the neurotransmitter gamma-amino butyric acid (GABA) (Saba et al., 1997)

Despite weak nucleotide sequence homology between *DPL1* and *gadA/gadB*, analysis of glutamate decarboxylase activity in cytosolic extracts from wild type, *DPL1* overexpression and Δ*dpl1* strains refuted the hypothesis that Dpl1 protein could be the *S. cerevisiae* orthologue of glutamate decarboxylase. (Saba et al., 1997). However, Coleman et al. (2001) proved that *GAD1* (585 aa) was the gene responsible for coding the *S.cerevisiae* glutamate decarboxylase.

Interestingly, querying BLAST with the SGPL1 amino acid sequence reveals, beyond the canonical orthologue Dpl1 (40%) as first result in *S.cerevisiae* organism, also the sequence of the Gad1 (23% identity) was identified: another proof of the strong correlation between these two genes.

SGPL1, Dpl1 and Gad1 are all PLP-dependent enzyme. The crystal structures of the first two enzymes, which are homodimers constituted by two distinct monomers, one of which is predominantly alpha helix, are available. On the other hand, the predicted structure of Gad1 in *S.cerevisiae* shows a monomer constituted by alpha-helix, suggesting a possible conformation in homodimer. In fact, mammalian isoforms of GAD (i.e., GAD67 e GAD65 in humans) have homodimeric structures.

It is worth noting that SGPL1 (*H.sapiens*) and Gad1 (*S.cerevisiae*) enzymes belong to the same superfamily, which suggests a potential correlation between them. Their superfamily is **Aspartate aminotransferase (AAT) superfamily (fold type I) of pyridoxal phosphate (PLP)-dependent enzymes**. When an alpha-amino acid combines with PLP, it forms a compound called a Schiff base or aldimine intermediate that act as the substrate in four types of reactions, namely (1)

transamination (movement of amino groups), (2) racemization (redistribution of enantiomers), (3) decarboxylation (removing COOH groups), and (4) various side-chain reactions that are dependent on the enzyme involved.

Researchers were able to examine the evolution of pyridoxal phosphate (PLP) dependent enzymes over time in depth. This was possible due to the availability of multiple molecular structures. The structural study helped researchers understand the evolutionary relationships among these enzymes. Contrary to expectation, the enzymes' functions-based classification didn't always align with the evolutionary relationships. In other words, the function of these enzymes in living organisms didn't always signify their evolution throughout history. This discovery highlighted that although these enzymes may share similar functions today, their evolutionary paths were often complex and did not always conform to a simple pattern based solely on their functions.

It is possible that the *DPL1* gene has a glutamate decarboxylase function, as Saba et al. (1997) previously performed an experiment with the Δ*dpl1* yeast strain, utilizing the orthologous glutamate decarboxylase within the yeast model. Therefore, it is not so speculative to suggest that a sphingosine-1-phosphate lyase 1 and a glutamate decarboxylase might be linked and replaceable.

It is worth considering the possibility that another enzyme could substitute for a sphingosine-1-phosphate lyase 1 in the Δ*dpl1* yeast strain, particularly if it is demonstrated that the excessive accumulation of intracellular sphingosine-1-phosphate could impair yeast growth (Kim et al., 2000)

To conclude, the transition from a restricted outlook on protein functionality to multifunctionality has completely transformed our comprehension. This expanded perspective enhances our understanding of the roles and interactions of proteins. As research progresses, it is essential to embrace this complexity and the hidden dynamics that control the intricate movements of proteins within cellular system.

3.2 Materials and Methods

3.2.1 Patient and genetic studies

The patient was referred to our center, Clinical Genetics and Epidemiology Unit of the Department of Women's and Children's Health at the University of Padua (Padua, Italy), for molecular analysis. The diagnostic procedures were performed after obtaining informed consent from the patient' parents and involved the use of the Next-Generation Sequencing (NGS) technologies.

The Clinical Exome Sequencing with screening a selection of 6,700 genes, employing the TruSight One Expanded Illumina assay, and a Next-Generation Sequencing panel designed to investigate glomerulopathies.

3.2.2 Molecular Biology

The DNA coding for human sphingosine-1-phosphate lyase 1 (NM_003901) was initially obtained from Origene (RC208705), and it was already included into a mammalian vector (pCMV6-Entry) with C-terminal Myc-DDK Tag (Fig.3.8)

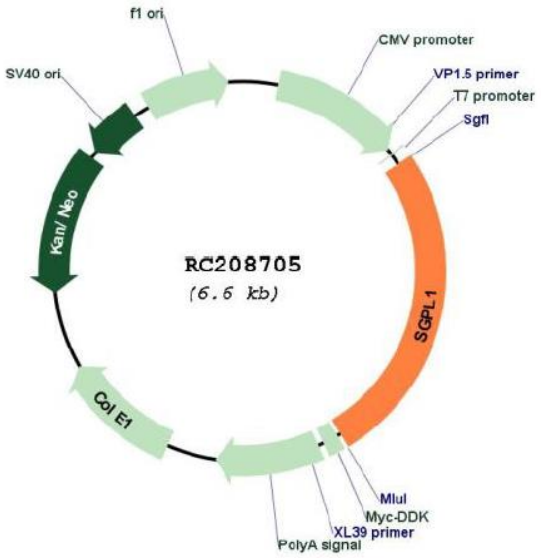

Fig.3.8 The map of the plasmid acquired from Origene with cDNA *SGPL1*.

We amplified the human *SGPL1* gene using coding DNA from Origene and then cloned it downstream of the *CYC1* constitutive promoter into the centromeric pCM189 yeast expression vector (Addgene). The cloning strategy was based on the In-Fusion® HD Cloning (Takara Bio) technique. The amplification of the insert and linearization of the vector through PCR were both carried out using the Phusion® High-Fidelity DNA Polymerase (NEB), following the guidelines provided by the manufacturer. The primers were designed using Takara Bio's specific tool (https://www.takarabio.com/learning-centers/cloning/primer-design-and-other-tools): the first set of primers, with 15 bp extensions complementary to the vector ends, was used to amplify the *SGPL1* cDNA, and the second pair was employed to linearize the pCM189 backbone. Thus, the In-Fusion cloning reaction, based on the homologous recombination, was set up. The correctness and the reading frame of the plasmid were confirmed by direct sequencing.

The plasmid encoding the mutant protein was generated through site-directed mutagenesis by PCR-amplification of the pCM189 *SGPL1* construct with primers carrying the desired mutation, using the QuikChange Lightning Site-Directed Mutagenesis Kit (Agilent) and primers designed using their specific tool (https://www.agilent.com/store/primerDesignProgram.jsp). Mutation was confirmed by Sanger sequencing.

Primer name	**Sequence 5'->3'**	**Purpose**
pCM189 Forward	GAGGGCCGCATCATGTAATTAG	Linearization of the destination vector
pCM189 Reverse	CCCCGAATTGATCCGGTAATTTAG	Linearization of the destination vector
SGPL1 Forward	CGGATCAATTCGGGGATGCCTAGCACAGACCTTCTGATG	Amplification of *SGPL1* cDNA
SGPL1 Reverse	CATGATGCGGCCCTCTTAAACCTTATCGTCGTCATCCTT	Amplification of *SGPL1* cDNA

Table 3.1 Oligonucleotides used for the cloning of SGPL1 cDNA into the yeast expression vector pCM189, as recommended by the In-Fusion® HD Cloning kit.

3.2.3 Yeast strains, media and plasmid transformation

The BY4741 *Δdpl1* strain (*MATa; his3Δ1; leu2Δ0; met15Δ0; ura3Δ0; YDR294c::kanMX4*) was purchased from Euroscarf (Y03653). The BY4741 *Δdpl1/Δgad1* double mutant strain (*MATa; his3Δ1; leu2Δ0; met15Δ0; ura3Δ0; YDR294c::kanMX4; YMR250W:: natMX6*) was generated by disrupting

the endogenous *GAD1* gene by homologous recombination with a nourseothricin (NAT) resistance cassette amplified via PCR from the plasmid pMEL15 (Addgene, #107921), and the inactivation procedure has been described elsewhere (Baudin et al., 1993; M. C. Lorenz et al., 1995). In detail, primers were designed to amplify the NAT cassette from the pMEL15 plasmid, including its promotor and terminator (Table 3.2). These primers contain 45 bp extensions homologous to the upstream and downstream regions of the *GAD1* ORF (locus: *YMR250W*), indicated in capital letters in the table 3.2.

Disruption was confirmed by polymerase chain reaction amplification of genomic DNA from KAN/G418- and NAT-resistant clones, using primers to the yeast genomic sequence a few bases upstream and downstream of the region replaced by the selectable marker (Table 3.2).

Primer name	**Sequence 5'->3'**	**Purpose**
NAT Forward	TTACACGTCGCTCTTAACAATCCAGGCTGAACAAAACAAGGAATAGACATGGAGGCCCAGAATAC	Amplification of *NAT* cassette
NAT Reverse	AGGTACATACATATAGGGGGCGGTATATTGGATGACCTTTTCAACCCGGTAGAGGTGTGGTCAAT	Amplification of *NAT* cassette
Check Forward	AAGAGTTGCATAAGAGCAG	Confirm the *GAD1* gene replacement with the *NAT* cassette
Check Reverse	GTCCAGGCTGAATCCT	Confirm the *GAD1* gene replacement with the *NAT* cassette

Table 3.2 Oligonucleotides used for the amplification of the NAT cassette from the plasmid pMEL15 and the confirmation of the substitution of the *GAD1* gene in *S.cerevisiae* with the selectable marker.

Yeast mutants (single and double deleted) were confirmed using rich medium YPD (1% yeast extract, 2% peptone, 2% dextrose) in combination with selectable markers such as nourseothricin (NAT) and kanamycin (KAN or G418). Yeast were cultured at 30°C in synthetic minimal medium (SM: 0.17% yeast nitrogen base without amino acids, ammonium sulfate and pyridoxine

hydrochloride, 0.5% ammonium sulfate, 2% dextrose, with the addition of 2,3% agar in the solid medium). To select the transformant strains, a synthetic minimal medium with amino acids was used to cover the yeast auxotrophies, excluding uracil (which is carried by the pCM189 vector).

3.2.4 Identification of the toxic PHS concentration

Phytosphingosine (PHS: 4-OH sphinganine) was initially obtained from Sigma (P2795). To investigate its toxicity, it was added to the minimal medium in various concentrations to establish its lethal dose for the yeast strain used in our study. Ethanol was added to the synthetic minimal medium as a carrier vehicle, and it was used as a control. The tested PHS concentrations were: 20, 30, 40, 50, and 60 μM. Ethanol and PHS were added to their respective medium with 0.05% Tergitol (Nonidet P-40, Sigma), to help even distribution of lipids in solid agar. The use of Tergitol did not affect the biological activities of sphingolipid derivatives in liquid culture (Chung et al., 2001).

3.2.5 Testing the effect of B6 supplementation

To test the effect of B6 supplementation, Yeast Nitrogen Base (without amino acids and ammonium sulfate) was acquired from Micropoli (CYN4401). without vitamin B6 specifically for the experiment. The vitamin B6 (pyridoxine hydrochloride) from Sigma (P9755) was used to recover yeast strains exposed to toxic PHS concentration, and it was added directly to the synthetic minimal medium in various concentrations: 20,70,150 μM.

3.5.6 Spot test assay

To analyze growth on solid media, yeast strains were inoculated in glucose-containing selective liquid medium and grown overnight at 30° C. The following day, the culture's concentration was adjusted to OD_{600} = 1 (approximately 10^7 cells/mL) in sterile water, after washings it two times to remove glucose medium, and four serial 10-fold dilutions were performed. For each dilution, 5 μL of the culture was spotted onto two different agar media: one containing PHS (at different

concentrations) and the other containing ethanol. Once the toxic concentration of PHS became evident, the same procedure was carried out on solid media with different B6 supplements. Plates were incubated at 30°C and images were taken 48h, 72h, 96h and 120h after the incubation.

3.5.7 BLAST Analysis

We conducted a BLAST (Basic Local Alignment Search Tool) analysis to evaluate alternative homology and establish the phylogenetic relationships between the human sphingosine-1-phosphate lyase 1 sequence and potential targeted sequences in *S. cerevisiae*. BLAST is a commonly used tool for comparing biological sequences against reference databases to discover important similarities.

3.3 Results

3.3.1 Patient and genetic studies

In the initial phase, Clinical Exome Sequencing was conducted, screening a selected set of 6,700 genes employing the TruSight One Expanded Illumina assay, yielding outcomes that did not exhibit any aberrations. Following this, the implementation of a Next-Generation Sequencing panel, designed specifically for glomerulopathies, led to the identification of two compound heterozygous mutations: NM_003901.4:c.262-24A>G and NM_003901.4:c.629G>A p.(Gly210Glu).

The intronic variant that was identified has already been analyzed in our laboratory, part of the Clinical Genetics and Epidemiology Unit of the Department of Women's and Children's Health at the University of Padua (Padua, Italy). The variant was found to be pathogenic due to its splicing variation (data not published). This was confirmed using the hybrid minigene assay (Forzan et al., 2010), which is a fast and reliable technique for investigating the effects of genetic variations on splicing. The assay has been widely used to functionally characterize variants in numerous genes in literature.

The mutation NM_003901.3:c.629G>A p.(Gly210Glu), which is the primary focus of our investigation, is located at the pyridoxal 5'-phosphate (PLP) binding site. Glycine at position 210 (Fig.3.9), along with 7 other residues within each chain of the homodimer complex, represents the binding site of PLP (Fig.3.10). Currently, there was no evidence in the literature concerning these two mutations, which were not found in the GnomAD database, (consulted on 29th August 2023).

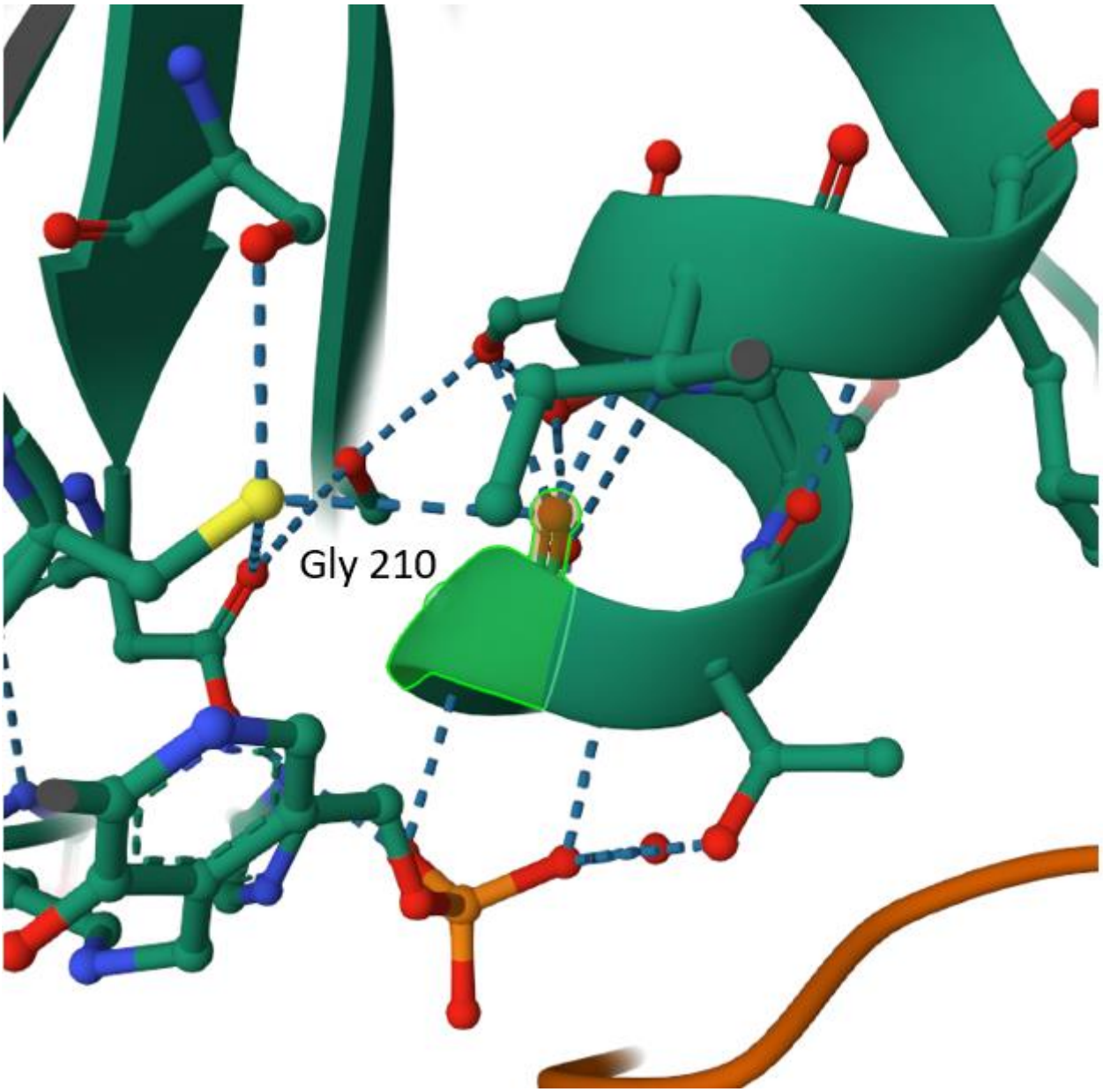

Fig. 3.9 PDB 3D Protein Feature View 4Q6R displays the residue G210 highlighted in bright green and its interactions with the surrounding amino acids within the secondary structure, emphasizing how a single modification can disrupt the overall structure.

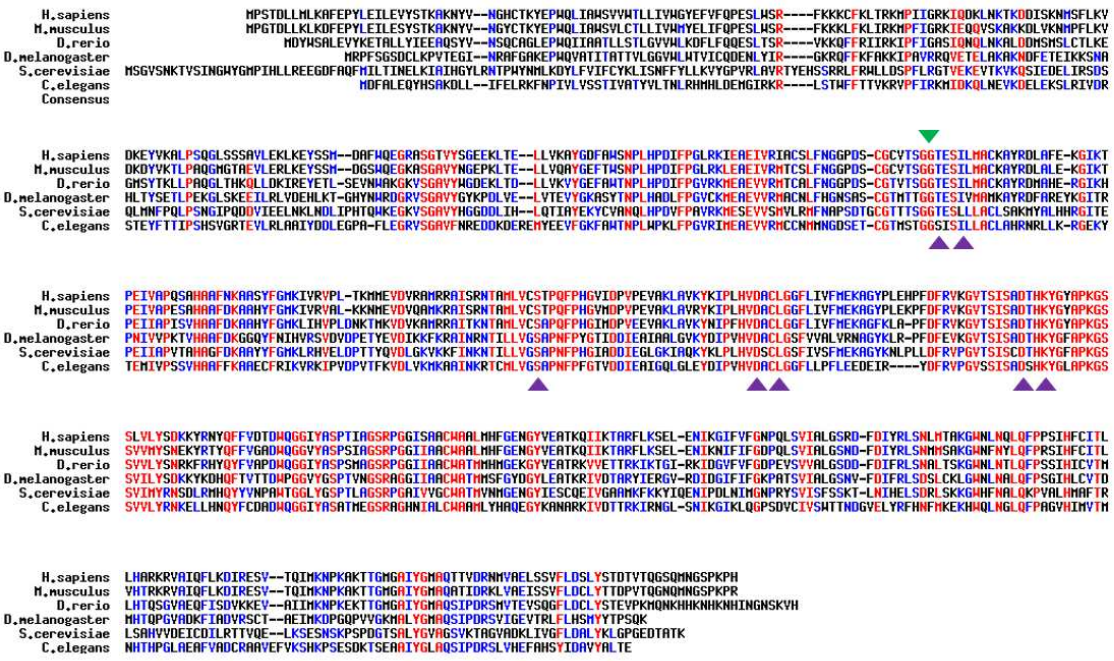

Fig.3.10. Multiple sequence alignment of *Homo sapiens* (NP_003892.2), *Mus musculus* (NP_033189.2), *Danio rerio* (NP_001082938). *Drosophila melanogaster* (NP_652032.1), *Saccharomyces cerevisiae* (QHB07755.1) and *Caenorhabditis elegans* (NP_505372). Identical residues are highlighted in red, while similar ones are shown in blue. The green triangle indicates the high rate of conservation among different species for the amino acid glycine at position 210 of the human protein SGPL1 (NP_003892.2). The glycine located at position 210 together with the other 7 residues, identified by violet triangles, constitute the PLP binding site (Corpet, 1988).

3.3.2 Identification of the toxic PHS concentration

Initially, our aim was to find the lethal concentration of PHS for the BY4741 Δ*dpl1* yeast model used in our study. This was necessary to carry out further investigations. Both the wild type yeast and the Δ*dpl1* strain were genetically transformed with an empty yeast expression vector, pCM189, capable of providing them the necessary autotrophy to grow in a selected synthetic minimal medium. Thus, both strains were spotted on solid plates containing synthetic minimal medium with different concentrations of PHS (20,30,40,50 and 60 μM) and the yeast growth was evaluated (data not shown). The control plates contained equal volumes of ethanol, instead of PHS. Our findings indicate that the optimal toxic PHS concentration for Δ*dpl1*, which has no effect on the wild type strain, is 50 μM, and this data agrees with the previous investigation by Mukhopadhyay et al., (2008)

After this initial PHS toxicity test to validate the lethal concentration for the yeast null mutant compared to the wild type yeast strain, we also investigated the effect of PHS accumulation on the

Δ*dpl1* yeast transformed with the expression vector pCM189 carrying either the human *SGPL1* gene encoding the wild-type protein or the p.Gly210Glu mutant by spot test analysis.

These results showed the growth inhibition induced by the 50 μM PHS on the Δ*dpl1* yeast expressing the mutated hSGPL1 protein, suggesting its pathogenicity, as a similar effect was observed with the complete deletion of the yeast sphingosine-1-phosphate lyase. The results are already evident after 2 and 3 days at 30°C, compared to the control strains which grow without any inhibition, represented by the wild type strain (BY4741 MATa) and the yeast null mutant strain expressing the human sphingosine-1-phosphate lyase 1 wild type (Fig. 3.11).

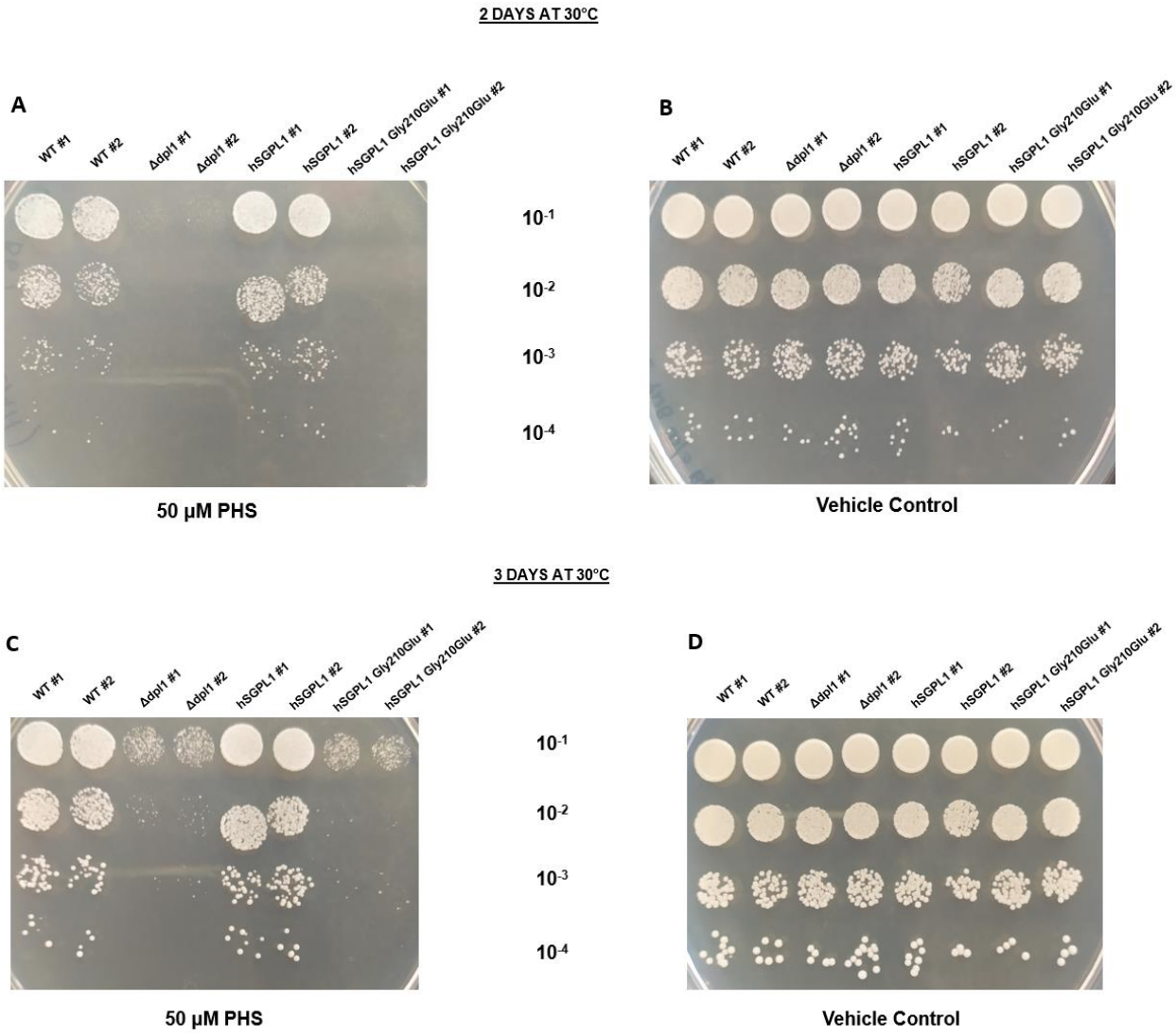

Fig.3.11 Effect of PHS accumulation on the yeast growth on solid synthetic minimal medium by spot test assay at 30°C. The growth of control and mutant yeast strains on solid medium lacking uracil was compared with 50 μM PHS (A, C) or without (B,D), respectively, after 2 and 3 days. The toxic PHS concentration of 50 μM is evident for the yeast null mutant

strain transformed with either empty vector pCM189 or the pCM189 carrying the mutated human *SGPL1* gene. It is important to note that the yeast nitrogen base used for the medium preparation did not already include PLP. Cell cultures were serially diluted and spotted onto the different agar media. Each spot test experiment was conducted in triplicate. Legend: #, followed by an arabic number indicates number of the clone; WT = BY4741 MATa transformed with empty yeast expression vector pCM189; Δ*dpl1* = BY4741 Δ*dpl1* transformed with empty yeast expression vector pCM189*;* hSGPL1 = BY4741 Δ*dpl1* transformed with yeast expression vector pCM189 bearing the hSGPL1 wild type-coding sequence*;* hSGPL1 = BY4741 Δ*dpl1* transformed with yeast expression vector pCM189 hSGPL1 p.Gly210Glu mutant.

3.3.3 Testing the effect of B6 supplementation

Once we had established the lethal concentration of PHS and observed growth inhibition in the yeast *dpl1* null mutant strain, we investigated the effect of vitamin B6 supplementation on the Δ*dpl1* yeast strain transformed with the expression vector pCM189 carrying the SGPL1 p.Gly210Glu mutant coding sequence. Our aim was to determine whether a specific concentration of pyridoxine would promote growth despite the toxic concentration of PHS. In this test we also included the wild type strain (BY4741 MATa), characterized by its own sphingosine-1-phosphate lyase 1 gene (*DPL1*), and the yeast *dpl1* null mutant, with and without the heterologous hSGPL1 protein.

The various concentrations of vitamin B6 were added directly during the preparation of the synthetic medium. No previous studies were available on the correlation between B6 supplementation and a yeast model lacking its sphingosine-1-phosphate lyase 1 gene. Earlier investigations conducted on human fibroblasts found that a B6 concentration of 50 μM was effective (Zhao et al., 2020). It is important to note that all chemical forms of vitamin B6 can easily diffuse through the membranes of most cells. Additionally, it must be taken into consideration that single eukaryotic yeast cells differ from human cells as they have a cell wall surrounding the cell membrane. Therefore, different concentrations of B6 were investigated, building on previous studies that have helped to establish the appropriate order of magnitude for the concentration required.

Our results showed that the B6 concentration required to promote the growth of the Δ*dpl1* yeast strain expressing the hSGPL1 p.Gly210Glu mutant was approximately 20 μM (Fig.3.12) and we identified it as the required therapeutic concentration to counteract the toxic PHS concentration . It is worth noting, however, that this concentration also encouraged the growth of the yeast *dpl1* null mutant.

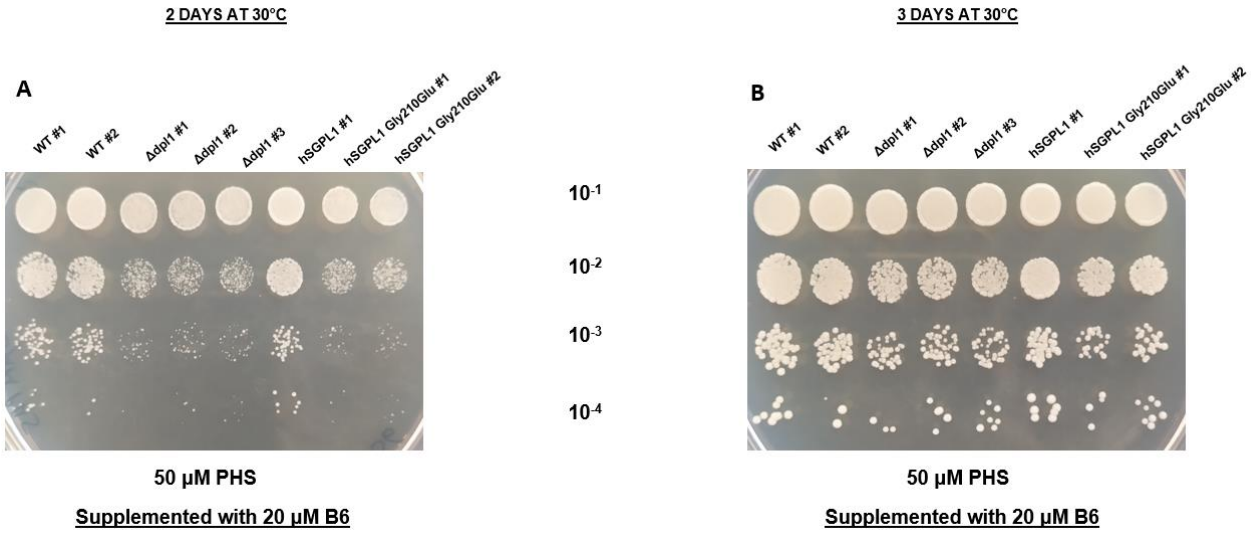

Fig.3.12 Effect of vitamin B6 supplementation on control and mutant yeast strains. The therapeutic effect appears to be set at 20 µM, in fact we observed growth both for the yeast null strain and for the same genetic background expressing the human SGPL1 p.Gly210Glu mutant protein. The analysis was conducted via spot test analysis, where cell cultures were serially diluted and spotted onto the different agar media and incubated at 30°C: solid synthetic minimal medium supplemented with 20 µM B6 and with PHS, after 2 (A) and 3 (B) days. The control medium was the same synthetic minimal medium without PHS and any B6 supplementation, and the growth on the control medium is not shown. Each spot test analysis was conducted in triplicate. Legend: #, followed by an arabic number indicates number of the clone; WT = BY4741 MATa transformed with empty yeast expression vector pCM189; Δ*dpl1* = BY4741 Δ*dpl1* transformed with empty yeast expression vector pCM189*;* hSGPL1 = BY4741 Δ*dpl1* transformed with yeast expression vector pCM189 carrying the h*SGPL1* wild type coding sequence*;* hSGPL1 = BY4741 Δ*dpl1* transformed with yeast expression vector pCM189 hSGPL1 p.Gly210Glu mutant.

Higher B6 concentrations, after 2 and 3 days at 30°C, did not have any improving effect on yeast growth when compared to 20 µM (Fig. 3.13). A concentration of 70 µM generally enhances the growth of the null strain yeast expressing the mutated human enzyme and even that of the simple knockout yeast model (as demonstrated for the B6 concentration of 20 µM). Nevertheless, the results obtained are slightly worse than those obtained with the therapeutic concentration at the same time points. The situation dramatically changes at the highest concentration of 150 µM, where we observed a growth inhibition also in the control strains, represented by the wild type strain (BY4741 MATa) and the Δ*dpl1* yeast expressing the wild type hSGPL1 protein, due to the probably toxic effect of the higher B6 concentration: after 2 days no yeast strain is able to grow and after 3 days only the control strains partially start to grow.

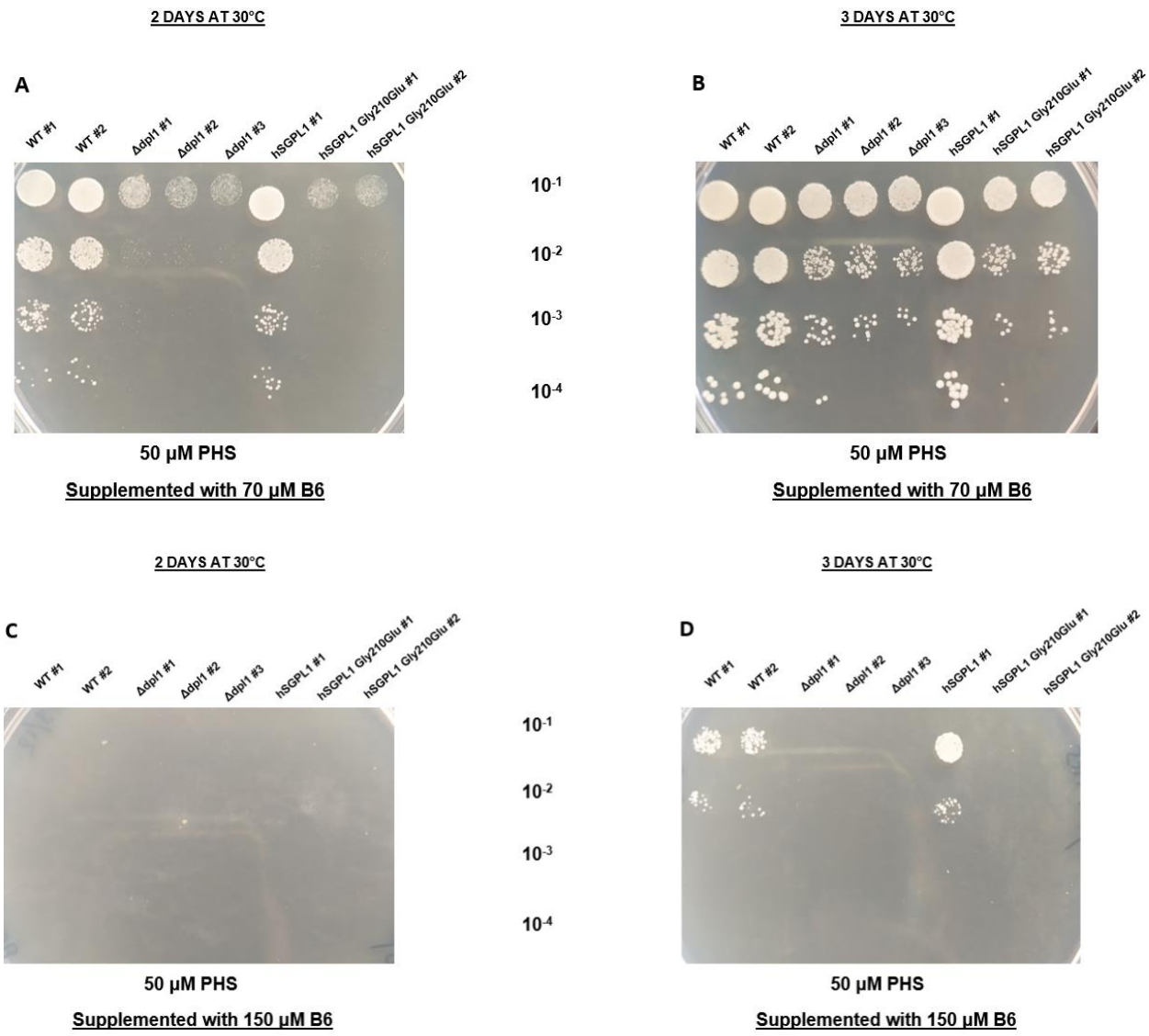

Fig.3.13 Effect of various vitamin B6 concentrations on control and mutant yeast strains. Unlikely from the therapeutic effect of the 20 µM, we observed a different effect on yeast growth. Specifically, an improvement in yeast growth for both the mutant and the null yeast strain was observed at 70 µM: however, this improvement appears to be less effective compared to that found at 20 µM. Conversely, at the highest concentration of 150 µM, our results showed that we have a growth inhibition for all strains: only after 3 days, the control strains (the wild type and the null yeast strain expressing the human SGPL1 wild type protein) partially start to grow. Serial dilutions of cell cultures were performed and then spotted onto distinct solid synthetic minimal media with 50 µM PHS, supplemented with either 70 µM (A, B) or 150 µM (C,D) B6 together, after 2 and 3 days. The control medium was without PHS and any B6 supplementation, and the growth on the control medium is not shown. The study utilized a spot test analysis approach. Each spot test analysis was carried out in triplicate. Legend: #, followed by an arabic number indicates number of the clone; WT = BY4741 MATa transformed with empty yeast expression vector pCM189; Δ*dpl1* = BY4741 Δ*dpl1* transformed with empty yeast expression vector pCM189*;* hSGPL1 = BY4741 Δ*dpl1* transformed with yeast expression vector pCM189 expressing the hSGPL1 wild type protein*;* hSGPL1 = BY4741 Δ*dpl1* transformed with yeast expression vector pCM189 hSGPL1 p.Gly210Glu mutant.

3.3.4 BLAST Analysis and the Gad1 protein

Our results showed that the B6 concentration required to promote the growth of the Δ*dpl1* yeast strain transformed with the expression vector pCM189 carrying the hSGPL1 p.Gly210Glu mutant protein was approximately 20μM. It is worth noting, however, that this concentration also encouraged the growth of the yeast *dpl1* null mutant. This data suggested the possible existence of an alternative mechanism for regulating sphingosine-1-phosphate accumulation in the absence of the orthologous protein responsible for its usual processing. This alternate pathway may also involve a PLP-dependent enzyme, which could explain why vitamin B6 supplementation could also improve the growth of the yeast *dpl1* null mutant.

Thus, we used the human sphingosine-1-phosphate lyase 1 sequence to query BLAST against UniProtKB/Swiss-Prot as the database and Saccharomyces (taxid:4930) as the reference organism. Our findings indicated that, besides the orthologous protein Dpl1, which shares around 40% identity with human SGPL1, there also exists another protein (Gad1). Gad1 displays approximately 23% similarity with human sphingosine-1-phosphate lyase 1 and has a conserved domain that is involved in PLP-catalyzed decarboxylation (Fig. 3.14). Additionally, it belongs to the same superfamily as sphingosine-1-phosphate lyase.

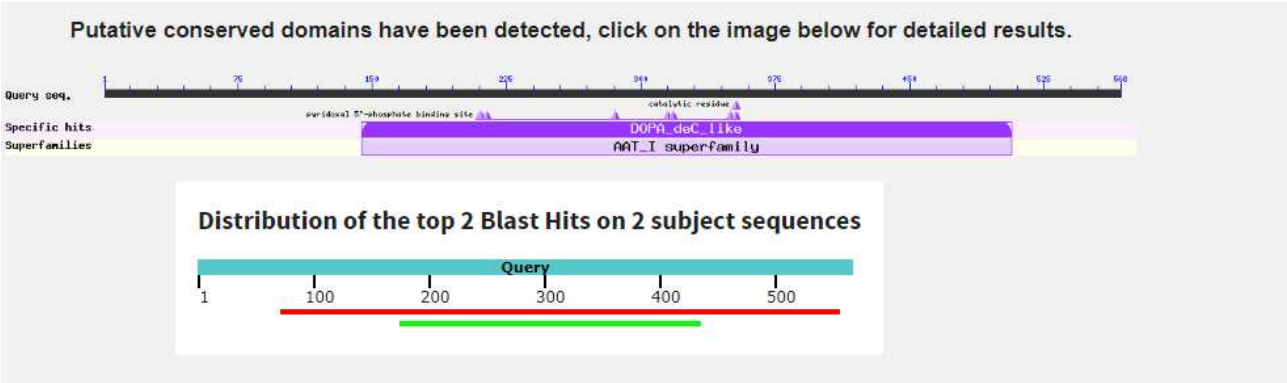

Fig.3.14 Protein BLAST. Querying the hSGPL1 (NP_003892.2) sequence through UniProtKB/Swiss-Prot shows only two results in *S.cerevisiae*: The orthologous Dpl1 (QHB07755.1) and the yeast glutamate decarboxylase (Gad1). The former shares about 40% similarity with human sphingosine-1-phosphate lyase, while the ladder shares about 23%. It is noteworthy that the graphical query cover representation for Dpl1 is 85%, while for Gad1 it is 45%, in comparison to hSGPL1. Additionally, there is conservation of the domain responsible for PLP-dependent decarboxylation.

Gad1 is a PLP-dependent enzyme and belongs to the same superfamily of the sphingosine-1-phosphate lyase 1. Decarboxylases, formally known as carboxy-lyases, are carbon–carbon lyases that remove a carboxyl group from organic compounds. The sphingosine-1-phosphate lyase 1 simply breaks a carbon-carbon single bond in the sphingosine-1-phosphate to obtain hexadecanal and phosphoethanolamine, while the glutamate decarboxylase breaks a carbon-carbon single bond in L-glutamate to remove a carboxyl group and yield GABA and a CO2. Thus, considering the similarity of the chemical reactions they are involved in, it is reasonable to assume that the yeast Gad1 protein plays a role in the processing of sphingosine-1-phosphate to prevent toxic accumulation and ensure yeast survival. For this reason, we generated a double knockout yeast model, which we discovered was still viable, and conducted further tests with B6 supplementation.

3.3.5 PHS toxicity test and B6 supplementation in double knockout yeast

At this point, we conducted a spot test analysis at the toxic concentration of 50 µM PHS. Results showed that this concentration was equally lethal for the Δ*dpl1* Δ*gad1* yeast (Fig.3.15), as it was for the Δ*dpl1* yeast, and this effect was particularly evident after 2 days at 30°C. This data would confirm the pathogenicity of the p.Gly210Glu mutation since the growth inhibition in Δ*dpl1* Δ*gad1* yeast expressing the mutant protein is comparable to that of the double knockout yeast.

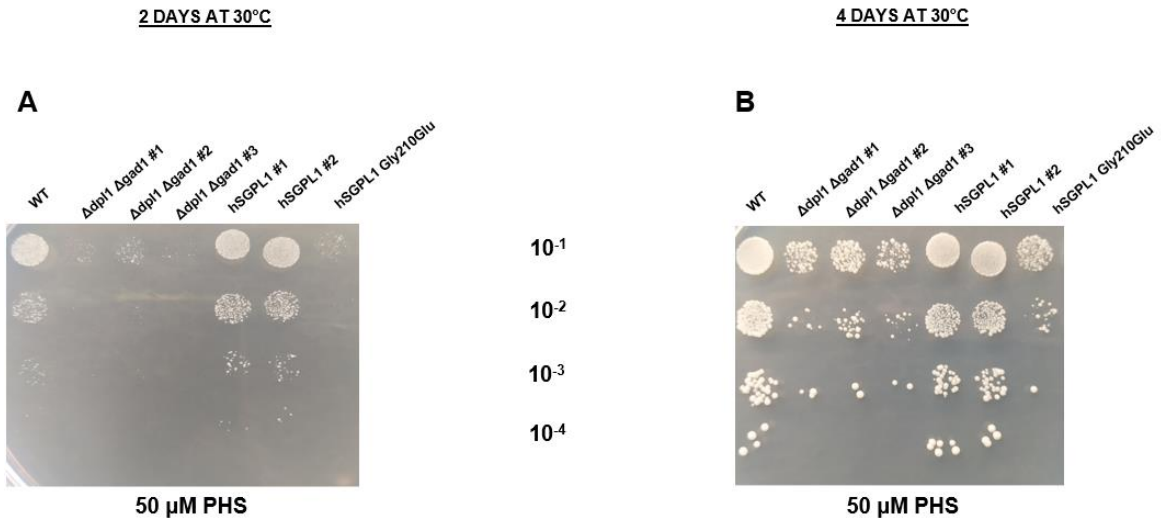

Fig.3.15 Effect of toxic PHS concentration on growth, using the double knockout yeast model, through spot test analysis on solid synthetic minimal medium at 30°C. The growth of control (WT; hSGPL1 wild type) and mutant yeast strains (Δ*dpl1* Δ*gad1*; hSGPL1 Gly210Glu) was compared on solid medium lacking uracil with 50 μM PHS, after 2 (A) and 4 (B) days. The toxic PHS concentration, already validated in the Δ*dpl1* yeast, also seems to have an antiproliferative effect on the growth of the Δ*dpl1* Δ*gad1* yeast and on the same genetic background expressing the mutated protein hSGPL1 p.Gly210Glu, evident mainly after 2 days (A). It is important to note that the yeast nitrogen base used for the medium preparation did not already include PLP. Cell cultures were serially diluted and spotted onto the different agar media. Each spot test experiment was conducted in triplicate. Legend: #, followed by an arabic number indicates number of the clone; WT = BY4741 MATa transformed with empty yeast expression vector pCM189; Δ*dpl1* Δ*gad1* = BY4741 Δ*dpl1* Δ*gad1* transformed with empty yeast expression vector pCM189*;* hSGPL1 = BY4741 Δ*dpl1* Δ*gad1* transformed with yeast vector pCM189 expressing the hSGPL1 wild type*;* hSGPL1 p.Gly210Glu = BY4741 Δ*dpl1* Δ*gad1* transformed with yeast vector pCM189 expressing the hSGPL1 p.Gly210Glu mutant.

Considering these results, we retested the B6 supplementation under the same conditions of the yeast *dpl1* null mutant and it would seem that the double knockout model outperforms the previous one since we did not detect any growth in the yeast with dual gene deletion, unlike the single null mutant strain previously observed.

Among the PLP concentrations tested, we included the B6 concentration (20 μM) that was found to be therapeutic in Δ*dpl1* yeast. Additionally, we tested two other concentrations; one was lower (10 μM) and the other higher (70 μM). Both concentrations were, however, lower than those used in the B6 supplementation of our single knockout yeast model, based on the previous results obtained there (Fig.3.16).

2 DAYS AT 30°C

4 DAYS AT 30°C

A

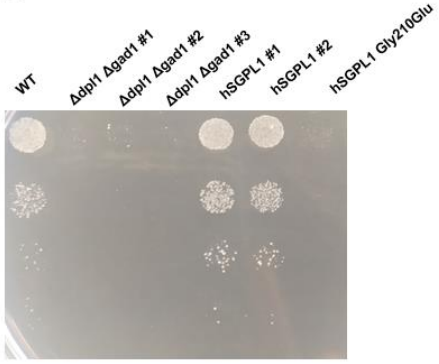

10^{-1}

10^{-2}

10^{-3}

10^{-4}

50 µM PHS

Supplemented with 10 µM B6

B

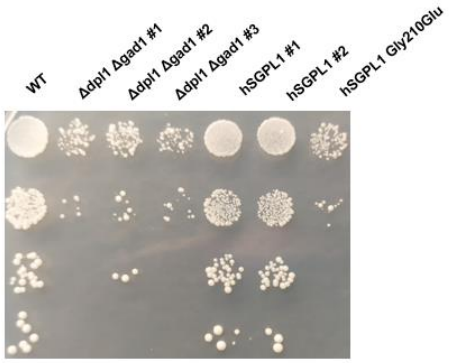

50 µM PHS

Supplemented with 10 µM B6

2 DAYS AT 30°C

4 DAYS AT 30°C

C

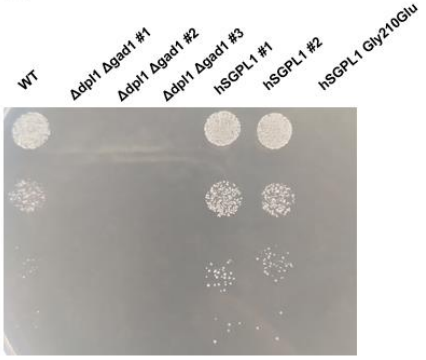

10^{-1}

10^{-2}

10^{-3}

10^{-4}

50 µM PHS

Supplemented with 20 µM B6

D

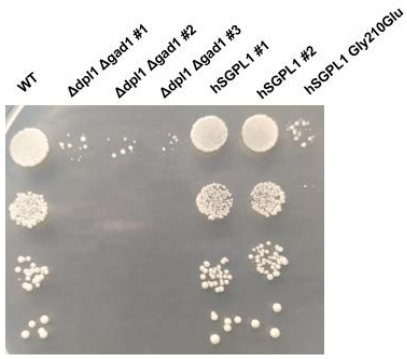

50 µM PHS

Supplemented with 20 µM B6

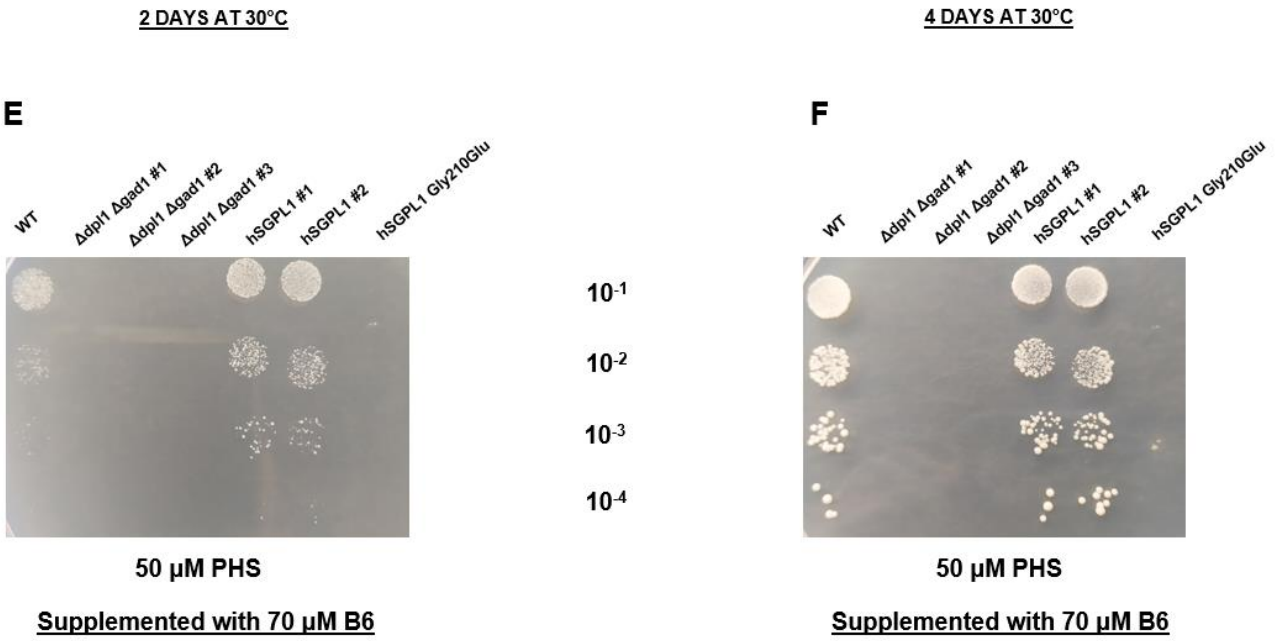

Fig.3.16 Effect of various vitamin B6 concentrations on control and mutant yeast strains, using the double knockout yeast model. Serial dilutions of cell cultures were performed and then spotted onto distinct solid synthetic minimal media, supplemented with 10 µM (A, B), 20 µM (C,D) or 70 µM (E,F) B6 with PHS, respectively after 2 and 4 days.
A, B: The double knockout yeast strain and *Δdpl1 Δgad1* yeast expressing the hSGPL1 p.Gly210Glu mutant showed no growth improvement when exposed to the lowest B6 concentration (10 µM). This was observed after 4 days at 30°C and growth was like that presented in Fig.3.14, in the presence of only 50 µM PHS. **C, D**: Concentration of 20 µM (B6) did not demonstrate any favourable impact on the growth of the double knockout yeast model expressing the human SGPL1 p.Gly210Glu, nor on the basic *Δdpl1 Δgad1* yeast model. Moreover, the situation is worse than with 10 µM B6. **E,F**: Paradoxically, increasing the B6 concentration to 70 µM seems to inhibit the growth of the mutant strains compared to the control strains, represented by the wild type yeast strain and the double knockout yeast strain expressing the human SGPL1 wild type. It is important to note that all the experiments were conducted using a medium without pre-existing pyridoxal-5'-phosphate in the yeast nitrogen base. The control medium did not contain PHS or any B6 supplementation; the growth on the control medium is not shown. The study utilized a spot test analysis approach and each test was carried out in triplicate. . Legend: #, followed by an arabic number indicates number of the clone; WT = BY4741 MATa transformed with empty yeast expression vector pCM189; Δ*dpl1* Δ*gad1* = BY4741 Δ*dpl1* Δ*gad1* transformed with empty yeast expression vector pCM189*;* hSGPL1 = BY4741 Δ*dpl1* Δ*gad1* transformed with yeast expression vector pCM189 hSGPL1 wild type*;* hSGPL1 Gly210Glu = BY4741 Δ*dpl1* Δ*gad1* transformed with yeast expression vector pCM189 hSGPL1 Gly210Glu mutant.

The results displayed that the concentration of 20 µM, which we defined therapeutic based on the proliferative results of B6 supplementation on the growth of the Δ*dpl1* yeast expressing the human SGPL1 p.Gly210Glu, did not show any positive effect on the double knockout yeast model expressing the same human mutant protein. Conversely, it seems to inhibit the growth of both the Δ*dpl1* Δ*gad1* yeast and the same genetic background expressing the mutant protein, compared to the control strains as the wild type and the double knock-out yeast strain expressing the wild type human sphingosine-1-phosphate lyase 1: this inhibitory effect on growth is much more evident with 70 µM.

3.4 Discussion

Yeast showed to be a very effective model to validate the pathogenicity of mutations found in the *SGPL1* gene, due to the conservation of the sphingolipid pathway among eukaryotic organisms. This makes yeast a good model for studying the effects of mutations in the *SGPL1* gene, as the same mutations are likely to have similar effects in yeast and humans. The p.Gly210Glu human mutation found in our patient affects a conserved residue and can be considered a new discovery since it has not yet been recorded in the GnomAD database, consulted on August 30th.

Thus, we decided to express the human sphingosine-1-phosphate aldolase in the yeast null mutant for the orthologous protein (Dpl1). Previous studies have confirmed that the human protein rescued the yeast null mutant in the presence of toxic concentrations of phytosphingosine-1-phosphate (PHS), a sphingosine-1-phosphate (S1P) analogue (Lovric et al., 2017). We chose to evaluate, as phenotype, the growth inhibition in Δ*dpl1* yeast expressing the mutant SGPL1 exposed to toxic concentration of PHS (Kim et al., 2000). While the exact mechanisms behind the antiproliferative effect triggered by intracellular accumulation of sphingolipids remain unclear, it is evident that the inability to degrade toxic long chain bases (LCBs) led to reduced viability and slowed growth.

Since the enzyme is PLP-dependent and the mutation studied is in the PLP binding site, it is expected that the mutation reduces the binding affinity for PLP, with further consequences for its functionality. It is important to note that this deficiency could be compensated by increasing the PLP concentration and, in practice, it is possible to evaluate the rescue of yeast growth by B6 supplementation (Zhao et al., 2020). Recent investigations also suggest an additional role for PLP as a molecular chaperone, improving the folding efficiency of misfolded enzymes (Cellini et al., 2014). It was important to use medium without supplemental vitamin B6 to ensure that the only PLP supplementation could come from our specific enrichment. Vitamins are defined as essential organic molecules that organisms cannot synthesize. In yeast physiology, the use of the term "vitamin" primarily depends on essentiality for humans. However, the genome of *Saccharomyces cerevisiae* contains most of the structural genes that are necessary for synthesizing vitamins, including vitamin B6 (Perli et al., 2020).

First, a titration was conducted which revealed that the Δ*dpl1* yeast exhibited growth inhibition in response to 50 µM concentration of toxic PHS, as compared to the wild type strain (BY4741 MATa). Consequently, through spot test analysis, we show that this toxic concentration of PHS (50 µM) was able to inhibit the growth of both the null mutant yeast strain expressing the empty vector or the human SGPL1 p.Gly210Glu. Conversely, the growth remained normal in the wild type strain and the Δ*dpl1* yeast expressing the wild type human *SGPL1*. These differences became evident after only 2 days of incubation at 30°C in synthetic minimal medium (without vitamin B6) with 50 µM PHS. In the control medium without PHS, we observed growth for all the strains studied. These results, through PHS toxicity test, can confirm the pathogenicity of the p.Gly210Glu mutation, which is comparable to the complete deletion of the gene and suggests a loss-of-function effect. After five days at 30°C (data not shown), also the Δ*dpl1* yeast expressing the mutant SGPL1 and the null mutant yeast started partially to grow: probably the amount of PHS still present in the medium starts to decrease due to its processing by the yeast expressing a functional sphingosine-1-phosphate lyase 1 and due to the porosity of the agar, which allows the molecules to have a certain diffusion rate.

Afterwards, we decided to evaluate the B6 supplementation to assess its potential therapeutic impact on SGPL1 mutation. The mutation on the cofactor binding site involves a residue conserved among eukaryotic species. We expected a reduction in the binding affinity for the active form of vitamin B6, due to a change in the protein structure from a non-polar glycine with an aliphatic group to a polar glutamate with an anion group. Our hypothesis is that supplementing with external PLP might improve the possibilities of retaining it, potentially compensating for the assumed reduced binding capacity.

Interestingly, by testing various B6 concentration, the situation appears to be better as we observed the growth of the yeast null mutant expressing the mutant hSGPL1 after 2 days at 30°C.

Higher B6 concentrations seem to be toxic to all the tested strains, including the wild type and the yeast null mutant expressing the human SGPL1 wild type, particularly at a concentration of 150 µM. This data confirms the importance of finding the right therapeutic concentration of B6. It seems that 20 µM is the most effective B6 concentration to rescue the yeast lacking a functional sphingosine-1-phosphate lyase 1 in the presence of toxic PHS intracellular accumulation.

Curiously, we observed that this proliferative effect of the vitamin B6 is also present in the null mutant yeast strain. This suggest that this beneficial effect could act in a *dpl1*-independent way, inducing us to speculate that there may be an alternative PLP-dependent enzyme able to compensate for the sphingosine-1-phosphate lyase 1 deletion. This alternative mechanism can ensure yeast survival by processing the accumulation of sphingosine-1-phosphate or its analogues. It should not be forgotten that the vitamin B6 may also have a general beneficial effect on yeast growth, due to the many PLP-dependent enzymes present and the several metabolic processes in which it is involved.

Through protein BLAST analysis, our research prioritizes the investigation of the yeast glutamate decarboxylase enzyme (Gad1). This is a PLP-dependent enzyme belonging to the same superfamily as the sphingosine-1-phosphate lyase, sharing 23% similarity with the human SGPL1.

Scientific evidence in literature demonstrates that proteins in biological organisms may have functions beyond their traditional roles. There, it is plausible to consider that a protein that is similar in structure and function, part of the lyase family, and utilizes the same co-factor, could potentially perform the same function as the missing protein, thus preventing yeast growth inhibition.

Based on these observations, we decided to generate a yeast strain with a double deletion of *dpl1* and *gad1*, which was confirmed to be still viable, and repeated the PHS toxicity test and B6 supplementation assay.

After 2 days at 30°C, in presence of 50 µM PHS, we noted growth inhibition for the double null mutant yeast expressing the empty vector as well as the Δ*dpl1* Δ*gad1* expressing the mutant SGPL1 p.Gly210Glu compared to the same strains grown in synthetic minimal medium without PHS (yeast growth on the control medium is not shown). This data is similar to what we already found with single knockout yeast strain.

At this point, we decided to evaluate the B6 supplementation and we tested various PLP concentrations (10,20 and 70 µM). Since previous B6 supplementation showed therapeutic effect with approximately 20 µM, we used concentrations close to this value and maintained as the highest value of the concentration used that of 70µM (that was a middle value in our first B6 supplementation conducted on the single knockout yeast strain).

Generally, it seems that vitamin B6 has not any beneficial effect on double knockout yeast strain and on the same background expressing the mutant SGPL1. Conversely, it appears that for these strains the therapeutic B6 concentration (20 μM) causes a growth inhibition and this effect become more evident with a the highest B6 concentration used (70μM). The double deleted yeast expressing the mutant human protein and the Δ*dpl1* Δ*gad1* yeast showed to be B6 sensitive, compared to the wild type and the double null mutant yeast expressing the wild type human protein. This data aligns with the fact the new model used should not possess any PLP-dependent enzymes able to process the excessive accumulation of sphingosine-1-phosphate (or analogues). Therefore, vitamin B6 cannot improve yeast growth (as it could have on the single knockout yeast) and for this reason could cause a reverse effect.

These final results confirm the pathogenicity of the p.Gly210Glu mutation, because its behaviour mirrors that of the double null mutant yeast strain. Moreover, being the mutation on the PLP binding site and probably causing a significant change in the protein's structure, explains why PLP supplementation has no therapeutic effect, even with increased cofactor concentrations. The double knockout yeast model may be a more reliable model to validate novel mutations pathogenicity, since the B6 supplementation does not have a proliferative effect on the double knockout yeast strain, as it did in the Δ*dpl1* yeast.

Further investigations should be carried out to verify whether a micromolar B6 concentration (less than 10 μM) is able to exert a therapeutic effect on the double knockout yeast model expressing the hSGPL1 p.Gly210Glu. For instance, a cheap and fast disk diffusion analysis could be used to determine a precise B6 concentration able to induce a proliferative effect on the strains under investigation.

Most importantly, it should be assessed whether yeast glutamate decarboxylase can act as sphigosine-1- phosphate lyase 1. This can be accomplished using a simple, fast and cost-effective nonradioactive assay, without relying on expansive mass spectrometric detectors or radioactive substrate To measure SGPL1 activity in yeast cell lysate, alternative substrates can be used, which produce a fluorescent aldehyde that can be analysed by RP-HPLC (Mezzar et al., 2014)

Our double null mutant yeast strain has displayed greater efficacy as a model for investigating novel missense mutations in the *SGPL1* gene. This presents an interesting avenue for further study.

While SGPL1 is widespread across all human tissues, data from the Protein Human Atlas show that glutamate decarboxylases are mainly found in the brain. This implies that our discoveries may have been simpler to accomplish in a single eukaryotic yeast model instead of the human body or specific human cell lines.

Discovering that a protein in yeast has additional functions beyond its known role may offer significant benefits. If this multifunctionality can likewise be found in the human orthologues, it could open up new avenues for disease treatment by identifying fresh targets for therapeutic interventions. Furthermore, this insight increases our understanding of diseases by revealing underlying mechanisms, thus paving the way for more precise treatments. Innovative therapies may arise, taking advantage of proteins' double capacity for both regular and disease-associated functions. Personalised medicine could derive benefits from the comprehension of variant proteins, which in turn enables drug customisation. Additionally, the identification of proteins with dual function may lead to quantifiable biomarkers for early disease diagnosis and monitoring. This discovery may advance fundamental research in molecular biology and genetics, not only in terms of health implications. However, rigorous scientific assessment is crucial to authenticate and efficiently utilise these discoveries.

.

PART IV

Understanding Coenzyme Q and the *COQ* Genes: Insights into Cellular Energy and Genetic Regulation

4.1 General introduction

4.1.1 CoQ: the known cellular roles

Coenzyme Q (CoQ), also known as ubiquinone, is a critical lipid with significant biochemical properties. Although its discovery was made 65 years ago in Madison, WI, USA (Crane et al., 1957) and Liverpool, UK (Morton, 1958), CoQ continues to intrigue researchers because of its multiple involvement in various cellular processes, human diseases, and therapeutic approaches. Recent studies are uncovering unexpected new roles for CoQ. Nonetheless, there are still uncertainties surrounding CoQ, including its biosynthesis, non-canonical functions and transport mechanisms, which hinder our ability to effectively address human diseases caused by CoQ deficiency.

Coenzyme Q (CoQ) has a significant role within the mitochondrial Electron Transport Chain (ETC). It transfers electrons from Oxidative Phosphorylation (OxPhos) complexes I and II to complex III, assisting in the production of the proton motive force which fuels ATP synthesis **(Stefely & Pagliarini, 2017)**. Beyond this central role, CoQ is often unrecognized for its contribution as a co-factor in various enzymatic pathways, such as pyrimidine biosynthesis, proline catabolism, glycolysis, fatty acid oxidation, and sulfide detoxification (Figure 4.1 A). This versatile function provides multiple pathways for electron transport to complex III (Baschiera et al., 2021).

In specific contexts, CoQ's role as a cofactor takes priority. In fact, we know, that mitochondrial complexes I and II donate electrons to ubiquinone (UQ), resulting in the generation of ubiquinol (UQH2) and the regeneration of the NAD+ and FAD cofactors, and complex III oxidizes ubiquinol back to ubiquinone, which also serves as an electron acceptor for dihydroorotate dehydrogenase (DHODH)—an enzyme necessary for de novo pyrimidine synthesis. In this context, for example, particular cancer cells heavily depend on complex III for CoQ regeneration to support the activity of dihydroorotate dehydrogenase (DHODH) and the tricarboxylic acid (TCA) cycle, rather than simply aiding NAD+ regeneration or ATP production (Martínez-Reyes et al., 2020). Moreover, there is an ongoing debate concerning the partitioning of CoQ in mitochondria, as there are two suggested pools with separate functions: one associated with respiratory supercomplexes that receives electrons

from NADH through complex I, and another which diffuses freely within the inner mitochondrial membrane (IMM) and obtains electrons from FAD-dependent enzymes (Lapuente-Brun et al., 2013). Extramitochondrial Coenzyme Q (CoQ) has been associated with the attenuation of ferroptosis, a type of non-apoptotic cell death triggered by iron-driven phospholipid peroxidation (Dixon et al., 2012). This process catalyzes the production of harmful phospholipid hydroperoxides (PLOOHs) from polyunsaturated fatty acids when exposed to oxidative stress from various environmental and metabolic factors. Consequently, this results in the loss of membrane integrity, the occurrence of oxidative damage to large molecules, and ultimately cell death (Jiang et al., 2021). In mammals, the primary defense against ferroptosis is GPX4, a phospholipid hydroperoxide glutathione peroxidase, which counteracts PLOOHs (Yang et al., 2014). Recent research has discovered an alternative mechanism, independent of GPX4, for protecting against ferroptosis, through the involvement of FSP1, an oxidoreductase that reduces extracellular CoQ to its hydroquinone form (CoQH2) on the plasma membrane (PM), which subsequently inhibits the formation of PLOOHs (Bersuker et al., 2019; Doll et al., 2019).

Before the discovery of FSP1, Coenzyme Q (CoQ) was widely accepted as a vital lipophilic antioxidant at the plasma membrane (PM) in both yeast and mammalian systems. The primary oxidoreductases responsible for sustaining a reduced pool of CoQ on the PM are NAD(P)H:quinone oxidoreductase 1 (NQO1) and NADH-cytochrome b5 reductase (Cyb5Red) (Navas et al., 2007)(Fig. 4.1 B). NQO1 functions not only as a catalyst for the two-electron reduction of CoQ, which is an essential part of the PM's redox system, but also acts as a superoxide reductase, producing NAD+ and influencing various signalling enzymes, including HIF1-α, p53, and sirtuins (Ross & Siegel, 2017). Cyb5Red, which exists on both the PM and endoplasmic reticulum (ER), is induced during stressful conditions and facilitates electron transfer from NADH to CoQ, thereby enhancing the protective CoQ antioxidant pool (Bello et al., 2003). While research has primarily explored the antioxidant role of Cyb5Red in the plasma membrane (Villalba et al., 1997), its occurrence in ER membranes suggests its possible involvement in maintaining the CoQ/CoQH2 equilibrium within this organelle. Currently, there is limited knowledge of how CoQ redox state is controlled in organelle

membranes other than the mitochondria and PM, or the consequences of preserving a specific CoQ/CoQH2 proportion in these settings.

CoQ is present in lysosomal membranes and can be reduced through a lysosomal Electron Transport Chain (ETC) (Gille & Nohl, 2000), but the exact proteins involved are still unknown. CoQ deficiency has been linked to abnormal lysosomal acidification (Heaton et al., 2020), although the connection between this phenomenon and the lysosomal ETC is not yet clear.

In addition to its roles in the Electron Transport Chain (ETC), as a cofactor and an antioxidant, Coenzyme Q (CoQ) has been linked with mammalian energy regulation pathways, even though the nature of these connections is frequently not entirely clear. Brown adipose tissue (BAT) can participate in facultative thermogenesis by employing uncoupling proteins (UCPs), which disperse the mitochondrial proton gradient to create heat (Argyropoulos & Harper, 2002). Early studies indicated that CoQ is important for activating proton transport by UCP1 (Echtay et al., 2000) and UCP2/UCP3 (Echtay et al., 2001) in reconstituted liposomes, although these findings have been challenged (Esteves et al., 2004). Recent research on brown adipose tissue (BAT) has demonstrated that the scavenger receptor protein CD36 is vital for CoQ absorption and normal BAT performance. *Cd36*-deficient mice display decreased CoQ levels, impaired nonshivering thermogenesis, and intolerance to cold (Anderson et al., 2015), yet the molecular mechanisms underlying these effects remain unclear.

A rising topic in maintaining CoQ balance is the importance of the proportion between oxidised CoQ and reduced CoQH2 in detecting and demonstrating various metabolic conditions in cells (Murphy & Chouchani, 2022). This proportion has been associated with acute oxygen sensing in mouse chemoreceptor cells, downstream of complex I-derived NADH and ROS (Arias-Mayenco et al., 2018). Similarly, in conditions of hypoxia or impaired ETC in mice, a high CoQH2/CoQ ratio could potentially induce the reversal of complex II, leading to the reduction of fumarate as an alternate electron acceptor (Spinelli et al., 2021). Additional studies are required to examine whether these mechanisms may be connected to the regulation of nucleotide pools or downstream gene expression.

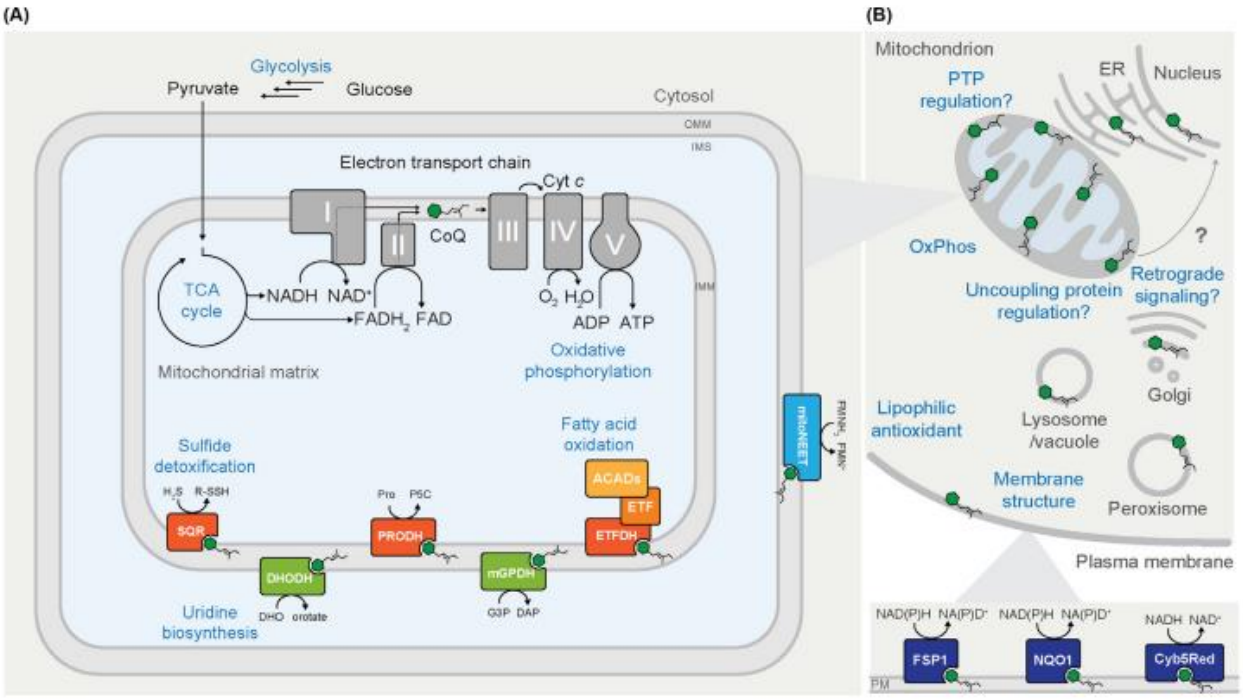

Fig.4.1 Cellular Functions of Coenzyme Q**.** (A) While Coenzyme Q (CoQ) is primarily recognized for its central role in the mitochondrial electron transport chain and oxidative phosphorylation (OxPhos), it also serves as a cofactor for several mitochondrial enzymes. In the core of energy metabolism, the tricarboxylic acid (TCA) cycle provides reducing equivalents that facilitate the reduction of CoQ at OxPhos complexes I and II. Various enzymes involved in processes such as uridine biosynthesis, fatty acid oxidation, and sulfide detoxification, among others, contribute additional pathways for electron entry into complex III of the ETC, ultimately driving ATP synthesis. (B) An overview of the diverse cellular functions of CoQ. CoQ is distributed across nearly all cellular membranes. Some extramitochondrial roles of CoQ are highlighted, including its involvement in modulating membrane dynamics and regulating uncoupling proteins, although many of these roles remain incompletely understood. On the plasma membrane (PM), reduced CoQH2 functions as a lipophilic antioxidant, where it can be oxidized by various oxidoreductases to combat lipid peroxidation and oxidative damage. Abbreviations: DHODH, dihydroorotate dehydrogenase; IMM, inner mitochondrial membrane; IMS, intermembrane space; OMM, outer mitochondrial membrane(Guerra & Pagliarini, 2023)

4.1.2 Coenzyme Q biosynthesis and regulation

CoQ is one of the most hydrophobic molecules in nature, with a long polyisoprenoid lipid tail protected by a redox-active cap. The biosynthesis of CoQ in cells represents a major challenge in cells. Nevertheless, almost all organisms in various domains of life produce CoQ endogenously (Lester & Crane, 1959), with eukaryotes primarily synthesizing it at the IMM (Momose & Rudney, 1972).

Coenzyme Q (CoQ) biosynthesis is a fascinating journey that unfolds in four distinct steps (Fig.4.2). CoQ is synthesized in mitochondria by a set of at least 15 genes (collectively known as *COQ* genes),

originally discovered in yeast and subsequently identified in humans (Doimo et al., 2014; Guerra & Pagliarini, 2023).

In yeast, Coq proteins assemble into a multi-subunit complex called the CoQ-synthome. This complex appears to exist in mammalian cells as well, although the exact composition and structure remain unclear (Desbats, Lunardi, Doimo, Trevisson, & Salviati, 2015).

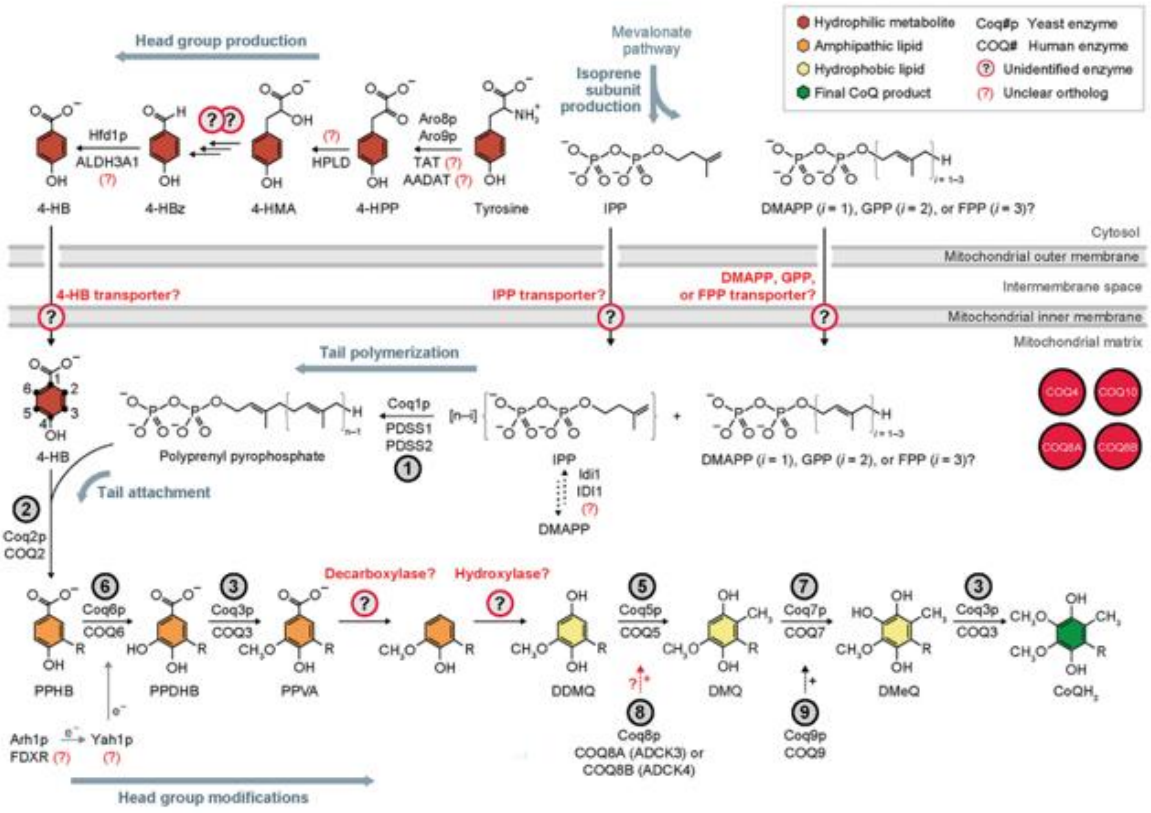

Fig.4-2 The diagram illustrates the principal eukaryotic CoQ biosynthesis pathway, conserved across organisms from *Saccharomyces cerevisiae* to humans. CoQ production starts with the head group precursor 4-HB, derived from tyrosine, and the tail subunit IPP, derived from the mevalonate pathway, both of which are transported into the mitochondrial matrix by unknown mechanisms. Once the tail subunit undergoes polymerization and the head group attaches, CoQ intermediates are subject to successive head group adjustments resulting in the mature CoQ. Biosynthetic enzymes are denoted by the circled number above each arrow. Enzymes and transporters that are unidentified are indicated by circled question marks. Auxiliary proteins with some unclear involvement in CoQ biosynthesis are depicted in red circles. '+' symbol near dashed arrows designates a hypothesized supportive role for the indicated reaction. Abbreviations: 4-HBz, 4-hydroxybenzaldehyde; 4-HMA, 4-hydroxymandelate; 4-HPP, 4-hydroxyphenylpyruvate; AADAT, mitochondrial alpha-aminoadipate aminotransferase; ALDH3A1, aldehyde dehydrogenase 3A1; DDMQ, demethoxy-demethyl-coenzyme Q; DMQ, demethoxy-coenzyme Q; DMeQ, demethyl-coenzyme Q; DMAPP, dimethylallyl pyrophosphate; FDX2 (FDX1L), mitochondrial ferredoxin 2 (ferredoxin 1-like); FDXR, ferredoxin reductase; FPP, farnesyl pyrophosphate; GPP, geranyl pyrophosphate; HPLD, hydroxyphenylpyruvate dioxygenase-like protein; IDI1, isopentenyl-diphosphate delta isomerase 1; IPP, isopentenyl pyrophosphate; PDSS1, prenyl (decaprenyl) diphosphate synthase subunit 1; PPDHB, polyprenyl-

dihydroxybenzoate; PPHB, polyprenyl-hydroxybenzoate; PPVA, polyprenyl-vanillic acid; TAT, tyrosine aminotransferase (Guerra & Pagliarini, 2023).

First, a critical precursor, 4-hydroxybenzoate (4-HB), is formed from tyrosine in mammals, while yeast and bacteria can produce it via the shikimate pathway (Stefely & Pagliarini, 2017). However, the precise stages involved in the tyrosine-to-4-HB pathway have yet to be fully understood, as multiple enzymes may be involved. Recent research has revealed an intermediate, 4-hydroxymandelate (4-HMA), produced from 4-HPP by hydroxyphenylpyruvate dioxygenase-like protein (HPLD), as an intermediate in this pathway (Banh et al., 2021): adding details to the intriguing puzzle pieces of this pathway.

The isoprenoid tail originates from a non-sterol branch of the mevalonate pathway, and it is constructed from isoprene repeats, drawing its building blocks from isopentenyl pyrophosphate (IPP) or dimethylallyl pyrophosphate (DMAPP) subunits (Stefely & Pagliarini, 2017). However, the transportation of 4-HB and isoprene precursors from the cytosol to the mitochondrial matrix remains an unsolved question. Once inside the matrix, the yeast Coq1p, or alternatively, the corresponding human orthologues PDSS1 and PDSS2, are responsible for the assembly of isoprenes into the lipid tail. Its length varies across species and is indicated by a subscripted number that specifies the number of isoprene units in the tail: 10 units in humans (CoQ_{10}), 9 in mice (CoQ_9), 8 in *E.coli* (CoQ_8), and 6 in *S.cerevisiae* (CoQ_6) (Wang & Hekimi, 2016). The Coq1 polypeptide is peripherally associated with the matrix side of the inner mitochondrial membrane; it is not associated with the CoQ-synthome,

Then, Coq2p/COQ2 is required for the attachment of the polyisoprenyl ‘tail’ to the 4-hydroxybenzoate (4HB), which results in the formation of polyprenyl-hydroxybenzoate (PPHB) (Stefely & Pagliarini, 2017). Initially, it was hypothesised that Coq2 might act as an anchor for the CoQ-synthome to the inner mitochondrial membrane; however, there is no evidence linking Coq2 to the other Coq polypeptides that combine to form the complex.

The final steps of CoQ biosynthesis consist of a series of modifications to the PPHB head group. These alterations are carried out by yeast proteins Coq3, Coq5, Coq6, and Coq7, as well as their human counterparts (COQ3, COQ5, COQ6 and COQ7), which are involved in methylation, decarboxylation, hydroxylation of the ubiquinone ring (Stefely & Pagliarini, 2017)(Fig. 4.2). The

specific sequence of reactions that execute the modifications of CoQ's aromatic ring remains uncertain in eukaryotes. Generally accepted models, based on yeast data, suggested that COQ6 catalyzes C5 hydroxylation as the first reaction after the condensation of 4-HB with the polyisoprene tail, followed by the subsequent methylation catalyzed by COQ3 and by the C1 decarboxylation and hydroxylation steps (Ozeir et al., 2011; Stefely & Pagliarini, 2017). However, COQ6 knockout cells, in both human and yeast, accumulate 4-HP, a compound that is decarboxylated and hydroxylated in position C1 of the ring. This suggests that these reactions occur before or independently of C5 hydroxylation, carried out by enzymes that remain unidentified (Acosta Lopez et al., 2019).

Numerous mysteries surround this intricate pathway. One pressing question concerns the identity of the eukaryotic enzyme(s) responsible for catalyzing the decarboxylation and hydroxylation steps of the carbon in position 1 of the aromatic ring of the Q precursor. Additionally, researchers are actively exploring the role of proteins considered to be auxiliary, such as Coq4p/COQ4, Coq8p/COQ8A/COQ8B, Coq9p/COQ9, and Coq10/COQ10A/COQ10B. COQ8, part of the UbiB family of kinase-like proteins, has raised questions about its function. It is necessary for phosphorylating polypeptides Coq3, Coq5, and Coq7. Further, overexpression of Coq8 in certain of the *coq* null strains restores steady-state levels of Coq4, Coq5, Coq7, and Coq9 and stabilizes the formation of the CoQ-synthome. Its human orthologue, ADCK3 (COQ8A), exhibits ATPase activity and possesses a protein-kinase like fold structure as well as adenine nucleotide binding motifs. In contrast, human ADCK4 (COQ8B) functions as an atypical kinase involved in the biosynthesis of coenzyme Q, although its substrate specificity is unclear. Thus, the precise role of Coq8 in supporting CoQ biosynthesis as either a kinase or ATPase remains uncertain.

Similarly, little is known about the function of Coq4 (known as COQ4 in humans), although it appears to play a significant role in complex formation and stability; while Coq9 (COQ9 in humans) polypeptide is essential in both the hydroxylation steps of Coq6 and Coq7, through indirect or supporting roles.

Additionally, while the lipid-binding protein Coq10p is not essential for CoQ biosynthesis, it plays a crucial role in facilitating efficient CoQ synthesis and its utilization in oxidative phosphorylation (Tsui et al., 2019). Human orthologues COQ10A and COQ10B may be interesting targets for studying the

movement of CoQ between the mitochondrial membranes and respiratory complexes due to their hypothesised lipid chaperone function. Coq10 has been proved to be an isolated polypeptide that does not associate with the complex.

Lastly, Coq11 appears to be necessary for de novo CoQ synthesis in yeast, but it has no clear human orthologue. Protein similarity has been found between yeast Coq11 and human NDUFA9, an auxiliary subunit of Complex I in humans important for complex stability. Further studies on their homology are needed to define their functional relationship (Acosta et al., 2016; Awad et al., 2018). Further investigation is needed to illuminate how these proteins considered to be auxiliary contribute to CoQ biosynthesis in yeast and mammalian systems. The journey to understand CoQ biosynthesis continues, with each discovery revealing more layers of this captivating biochemical puzzle.

4.1.3 CoQ biosynthetic complex

The CoQ biosynthetic complex, known as 'complex Q', is a dynamic group of enzymes located on the matrix side of the IMM (Allan et al., 2015; Floyd et al., 2016; He et al., 2014; Hsieh et al., 2007) (Fig.4.3). It works as a 'metabolon' (Srere, 1985), guiding CoQ through sequential metabolic stages via cluster channeling (Pareek et al., 2021). This increases enzyme proximity, optimizes substrate channeling, and prevents the accumulation of toxic CoQ intermediates (Fernández-del-Río et al., 2020). Although essential components such as Coq3-9p/COQ3-9 are known, the complete composition and proportions of enzymes and auxiliary proteins within complex Q are still a mystery. The involvement of both protein and non-protein components such as COQ8A and COQ9 further complicates the picture. CoQ proteins in yeast have shown to depend on each other for stability (Hsieh et al., 2007), suggesting a possible role for CoQ or its intermediates in complex Q formation. Despite recent structural advances obtained from a cryo-electron microscopy study of a human COQ7 and COQ9 complex, the architecture and assembly of complex Q remain enigmatic (Manicki et al., 2022). COQ9, a protein that binds isoprenoid lipids, may act as a lipid presenter, and this complex structure supports the idea of a COQ7:COQ9 tetramer that remodels membranes to extract CoQ lipid intermediates (Manicki et al., 2022). In summary, although progress has been made, many

questions still surround the CoQ biosynthetic complex, making it a fascinating area for future research.

4.1.4 CoQ Uptake, Distribution, and Transport

Coenzyme Q (CoQ) is found in various cellular membranes, but the mechanisms governing its distribution within cells are not yet fully understood. Recent yeast research has unveiled specialized regions called 'CoQ domains,' where enzymes involved in CoQ modification are concentrated (Subramanian et al., 2019). These domains, reliant on essential COQ proteins, can form and break down based on lipid availability(Subramanian et al., 2019). They are closely linked to contact sites between the endoplasmic reticulum (ER) and mitochondria (ERMES). Disruptions in these contact sites can impact CoQ domain formation and result in the accumulation of CoQ intermediates (Subramanian et al., 2019). The proximity of CoQ domains to these contact sites suggests a potential role in coordinating metabolic pathways and distributing mature CoQ within the cell (Fig.4.3).

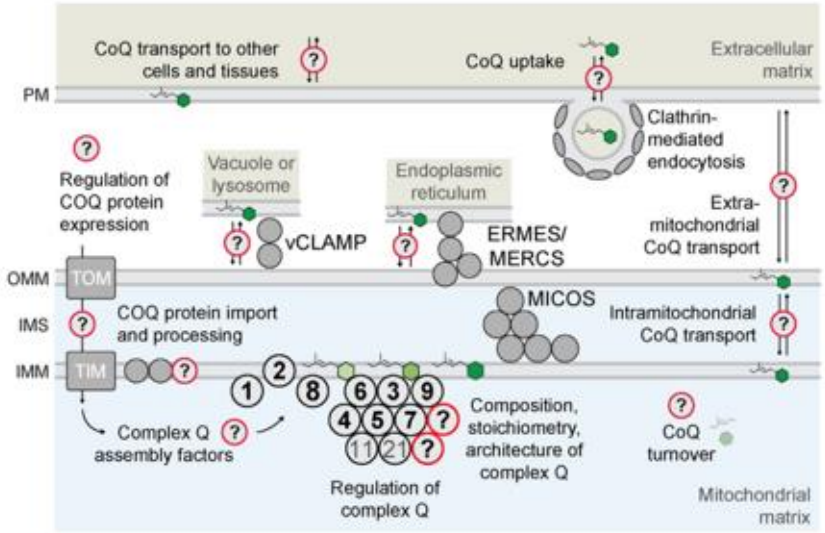

Fig.4.3 Key questions remain about complex Q composition, assembly, and mechanisms governing CoQ transport and distribution. While evidence supports complex Q's existence, its full composition, stoichiometry, and assembly regulation remain unclear. COQ genes are nuclear-encoded, but factors governing their expression and protein processing for mitochondrial import via TIM (translocase of the inner mitochondrial membrane) and TOM (translocase of the outer mitochondrial membrane) complexes pose many queries. Complex Q's proximity to MICOS (mitochondrial contact site and cristae organization system) and ERMES (ER-mitochondria encounter structure) suggests potential roles in CoQ precursor import or mature CoQ export. Studies with exogenous CoQ imply clathrin-mediated endocytosis machinery involvement in CoQ assimilation (Guerra & Pagliarini, 2023).

CoQ is highly hydrophobic and embedded in lipid bilayers, making it unlikely to move freely through the aqueous cellular environment without specific protein machinery. Studies suggest that newly synthesized CoQ is first localized to mitochondria, then to mitochondria-associated membranes, the ER, and finally to the plasma membrane (Fernández-Ayala et al., 2005). The endomembrane system, including the ER-Golgi transport, may be involved in this distribution process (Fig.4.4). However, the specific proteins responsible for bidirectional CoQ trafficking remain unknown. Mitochondrial contact sites between organelles, known for their role in phospholipid trafficking, might also contribute to CoQ distribution (Dimmer & Rapaport, 2017; Rampelt et al., 2017).

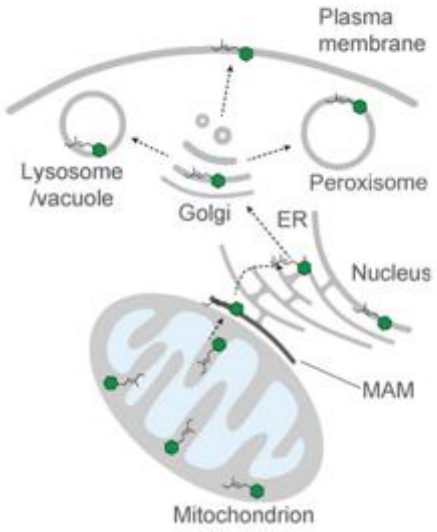

Fig.4.4 Representation of a hypothetical CoQ transport route within the cell. After being synthesized at the inner mitochondrial membrane (IMM), CoQ travels through mitochondria-associated membranes (MAMs) en route to the endoplasmic reticulum (ER). At the ER, CoQ interfaces with the endomembrane system and undergoes packaging within the Golgi apparatus for broad distribution to various organelles and cellular membranes (Guerra & Pagliarini, 2023).
Insights from Exogenous CoQ Uptake Studies:

Understanding how cells assimilate exogenous CoQ is crucial, especially for addressing mitochondrial dysfunction caused by CoQ deficiencies. Yeast studies have identified factors within the endocytic pathway and clathrin-mediated endocytosis that participate in CoQ uptake (Fernández-del-Río et al., 2020). Human clinical trials have also associated specific gene polymorphisms with increased serum CoQ levels in response to CoQ supplementation (Takahashi

et al., 2021, 2022). Further research is necessary to explore the roles of these genes and mechanisms in facilitating CoQ uptake.

A genetic screen in yeast has identified two inner mitochondrial membrane (IMM) proteins, Cqd1p and Cqd2p, as key players in CoQ distribution (Kemmerer et al., 2021). These proteins seem to work reciprocally, with Cqd1p promoting CoQ accumulation in mitochondria and Cqd2p favoring its presence at the plasma membrane. Both proteins belong to the UbiB family and require ATPase activity for CoQ distribution (Kemmerer et al., 2021). This suggests that their ATPase activity may be involved in extracting CoQ from the IMM for transport. Notably, CoQ transport out of mitochondria can occur independently of Cqd1/2p and remains unaffected by the deletion of genes related to various cellular processes, indicating potential redundancy, or overlapping functions in CoQ distribution (Kemmerer et al., 2021).

4.1.5 Primary CoQ_{10} deficiency and treatments

Primary CoQ_{10} deficiency is an inherited disease affecting the mitochondrial respiratory chain (DiMauro et al., 2013). It results from low levels of CoQ_{10} in cells or tissues due to pathogenic biallelic variants (homozygous or compound heterozygous) in one of the ten genes involved in its biosynthesis: *PDSS1*, *PDSS2*, *COQ2*, *COQ4*, *COQ5*, *COQ6*, *COQ7*, *COQ8A*, *COQ8B*, and *COQ9*. This condition can cause a wide range of symptoms (Table 4.1), with onset occurring from birth to adulthood (Berardo & Quinzii, 2020).: from fatal multisystem disease to isolated steroid-resistant nephrotic syndrome or isolated central nervous system disease (Desbats et al., 2015). Genotype-phenotype correlations illustrates how mutations in different COQ genes can impact various organs. The reasons for these diverse effects remain unclear but may involve differences in tissue-specific gene expression levels and mitochondrial DNA pools. In contrast, secondary CoQ_{10} deficiencies are caused by pathogenic variants in genes not directly related to CoQ_{10} biosynthesis (Trevisson et al., 2011). These variants affect other mitochondrial or non-mitochondrial processes that reduce CoQ_{10} levels in tissues, possibly by adaptive mechanisms(Alcázar-Fabra et al., 2021). Some causes of

secondary CoQ_{10} deficiency are defects in the respiratory chain. Molecular genetic testing is the only way to distinguish primary CoQ_{10} deficiency from secondary CoQ_{10} deficiency.

Gene[1]	Clinical Features					
	Kidneys	Heart	Eyes	Hearing	Neurologic	Muscles
COQ2	SRNS	HCM	Retinopathy, optic atrophy	SNHL	Encephalopathy[2] , seizures, other[3]	Myopathy
COQ4		Heart failure, HCM	Retinopathy		Encephalopathy, seizures, other[4]	Myopathy
COQ5[5]			Retinopathy			
COQ6	SRNS[6]			SNHL	Encephalopathy, seizures	
COQ7					Encephalopathy, ID, peripheral neuropathy	Muscle weakness
COQ8A					Encephalopathy, cerebellar ataxia (SCAR9)[7], dystonia, spasticity, seizures	Exercise intolerance
COQ8B	SRNS[6]				ID, seizures	
COQ9	Tubulopathy	HCM			Encephalopathy	Myopathy
PDSS1	SRNS		Retinopathy, optic atrophy		Encephalopathy, peripheral neuropathy, ataxia	
PDSS2	SRNS		Retinopathy	SNHL	Leigh syndrome, ataxia	

Table 4.1 Primary coenzyme Q10 deficiency: genes and associated clinical features.
HCM = hypertrophic cardiomyopathy; ID = intellectual disability; SNHL = sensorineural hearing loss; SRNS = steroid-resistant nephrotic syndrome; 1. Genes are listed in alphanumeric order 2. Encephalopathy comprises a wide spectrum of brain involvement with different clinical and neuroradiologic features, often not further explained by the reporting authors; 3. Adult-onset multisystem atrophy-like phenotype (Desbats et al., 2016); 4. Severe hypotonia, respiratory insufficiency, cerebellar hypoplasia, slowly progressive neurologic deterioration, spasticity, and intellectual disability; 5. The link between COQ5 pathogenic variants and ataxia still needs confirmation.; 6. Because individuals with COQ6- and COQ8B-related CoQ10 deficiency were ascertained by the presence of SRNS, the authors cannot exclude the possibility that biallelic pathogenic variants in these two genes could also cause a broader phenotype. 7. COQ8A-related CoQ10 deficiency is also referred to as autosomal recessive spinocerebellar ataxia 9 or SCAR9 (OMIM 612016). From “Primary Coenzyme Q19 Deficiency Overview” in GeneReviews, Salviati et al., last update on: June 8, 2023

Primary CoQ_{10} deficiency is a rare condition, affecting fewer than 1 in 2,000 individuals according to European criteria. However, it is likely underdiagnosed. Traditionally, diagnosing CoQ_{10} deficiency relied on biochemical tests and later genetic analysis in consanguineous families. Nowadays, Next Generation Sequencing (NGS) is the preferred method for genetic screening and diagnosis of this diverse disorder (Alcázar-Fabra et al., 2021).

Prognostic information for primary CoQ_{10} deficiency is limited due to the rarity of cases. It is a progressive disorder, and the prognosis varies depending on the specific gene involved and the severity of the deficiency. Severe multisystem cases often lead to early mortality, while individuals with later-onset disease may respond better to treatment and experience improved outcomes (Ashraf et al., 2013; Heeringa et al., 2011; Montini et al., 2008)

The pathogenesis of CoQ_{10} deficiencies is not well understood but is believed to result from oxidative stress, mitochondrial dysfunction, and defects in energy production. Other factors such as genetics, epigenetics, compensation mechanisms, maternal effects, and environmental factors may also contribute (Alcázar-Fabra et al., 2021).

Since CoQ_{10} deficiency often leads to irreversible tissue damage, prompt treatment is crucial. The primary treatment for CoQ10 deficiency is high-dose oral CoQ10 supplementation, which has shown some success in patients with mutations in *PDSS2* (Desbats et al., 2015), *COQ2* (Montini et al., 2008), *COQ4* (Salviati et al., 2012), *COQ6* (Heeringa et al., 2011), and *COQ8B* (Ashraf et al., 2013). However, the response varies considerably according to the genetic defect and disease severity, and treatment failure is common because of the limited CoQ_{10} bioavailability.

To improve CoQ therapies, innovative tools such as novel delivery methods and water-soluble CoQ precursors are being explored. In the first case, scientists are investigating various strategies to enhance CoQ uptake. These approaches include mitochondria-targeting compounds like triphenylphosphonium (TPP) and the encapsulation of CoQ in liposomes, nanoparticles, micelles, and nanoemulsions. While TPP-based compounds like MitoQ exhibit antioxidant properties with clinical applications, they may not fully restore CoQ's electron transport chain (ETC) function due to impaired membrane integration. Emerging methods involve encapsulating CoQ in mitochondria-targeted liposomes, designed to fuse directly with mitochondrial membranes. Another promising approach involves micellization with caspofungin (CF), enhancing CoQ's water solubility and cellular uptake.

In the second case, water-soluble CoQ precursors like 2,4-dihydroxybenzoate (DHB) and vanillic acid have also been explored as potential treatments to overcome bioavailability issues (Acosta Lopez et al., 2019; Freyer et al., 2015; Luna-Sánchez et al., 2015). These analogs can bypass specific enzymatic defects in the CoQ biosynthetic pathway and promote proper cellular distribution of CoQ. They have shown promise in restoring CoQ levels in human cell cultures and extending lifespan in mouse models.

Beyond supplementation, researchers are developing small-molecule modulators to influence the CoQ pathway. Various inhibitors, such as 4-nitrobenzoate, clioquinol, and zoledronic acid, have been

developed to study CoQ's role in aging-related disorders. Coq8p and COQ8A are key targets for chemical modulation, with recent selective inhibitors. CoQ limitation can increase lifespan in some organisms (*C.elegans* and *M.musculus*), while inhibiting CoQ biosynthesis may have anticancer applications. Additionally, 2-propylphenol activates COQ8A's ATPase activity. These probes expand our toolkit for CoQ pathway modulation and offer insights into auxiliary protein functions, aiding future therapeutic development (Guerra & Pagliarini, 2023).

These innovative tools offer new avenues for understanding and potentially treating CoQ-related disorders by enhancing bioavailability and manipulating CoQ's biological pathways.

In brief, primary CoQ10 deficiency is a rare and complex disorder with a wide range of symptoms and genetic causes. Early diagnosis and treatment with high-dose oral CoQ_{10} supplementation offer the best chance for improved outcomes, but responses can vary significantly among individuals. Further research is needed to better understand and treat this condition.

The extraordinary biochemical properties of CoQ are at the core of cellular bioenergetics, biosynthesis and homeostasis. Recent studies suggest even more roles for this versatile cofactor. It is vital to fully understand the intricacies of CoQ synthesis and transport, despite the challenges that have hindered progress for over six decades. Overcoming impediments such as hydrophobicity barriers and enzyme redundancy requires innovative tools and approaches. It is necessary to highlight the diverse and often unrecognised cellular functions of CoQ, while emphasising the urgent need to fill existing knowledge gaps. Our intention is to catalyse renewed efforts in CoQ biology and therapeutic progress.

PART IV.A

Unravelling the Role of Human *COQ4* gene in CoQ Biosynthesis

4.A.1 Introduction

4.A.1.1 *COQ4* function and mitochondrial disorders associated with *COQ4* mutations

Among the genes implicated in primary CoQ_{10} deficiency, *COQ4* (MIM 612898) emerges as a relatively recently identified player whose precise function remains largely elusive. Located on chromosome 9q34.11, COQ4 encodes a ubiquitously expressed 265-amino acid (aa) COQ4 protein (isoform 1), primarily localized within the matrix side of the mitochondrial inner membrane (Casarin et al., 2008). Based on evidence from a yeast model, it was initially hypothesised that COQ4 plays a critical role in stabilising a multi-heteromeric complex containing several CoQ10 biosynthetic enzymes, rather than acting as a catalytic enzyme (Marbois et al., 2009).

The human COQ4 protein was proved to be ubiquitously expressed, but at high levels in liver, lung and pancreas. A second group of transcripts, located within intron 1 of the gene, encodes a 241 aa protein lacking the mitochondrial targeting sequence (isoform 2). The functional significance of this second isoform is unknown. Human COQ4 isoform 1 efficiently restores both glycerol growth and CoQ content in a *COQ4* null yeast strain, whereas isoform 2 cannot (Casarin et al., 2008).

The *COQ4* gene was first identified and characterized in *S.cerevisiae* in 2001, where it was shown to encode a protein of 335 amino acids that associates with the matrix face of the inner mitochondrial membrane (Belogrudov et al., 2001). The yeast protein shares 39% identity and 55% similarity with the human protein.

COQ4 is one of the most common causes of CoQ deficiency in humans (Hughes et al., 2017) and mutations in this gene are associated with a variety of clinical pictures ranging from fatal neonatal multisystem disorders to childhood-onset cerebellar ataxia, or isolated retinitis pigmentosa. The first documented case of a patient with a COQ4 variant associated with primary CoQ_{10} deficiency was reported in the literature by Salviati et al (2012). In their study, they described the case of a young boy suffering from a severe encephalomyopathic disorder. This boy carried a *de novo* heterozygous

3.9 Mb deletion affecting at least 80 genes, including COQ4. Consequently, haploinsufficiency of COQ4 was identified as the underlying cause of CoQ_{10} deficiency in this patient (Salviati et al., 2012). The CoQ_{10} supplementation led to a stable improvement in the clinical picture, suggesting that the deficiency played a role in the clinical phenotype. It is worth noting that although this patient had a milder CoQ_{10} deficiency compared to other patients carrying recessive mutations in COQ genes, the presence of one functional COQ4 allele was still observed. COQ4 represents an exception because heterozygosity for mutations in other COQ genes does not affect CoQ_{10} levels (Salviati, et al., 2012). Taken together, these data provide further support to the notion that COQ4 has a critical function within the CoQ_{10} biosynthetic complex.

In 2015, Brea-Calvo et al. and Chung et al. both confirmed the association between *COQ4* variants and primary CoQ_{10} deficiency. Their research unveiled that COQ4 variants are inherited in an autosomal recessive manner (Brea-Calvo et al., 2015; W. K. Chung et al., 2015). This discovery led to the classification of primary CoQ_{10} deficiency caused by COQ4 variants as "primary CoQ_{10} deficiency-7" or COQ10D7. As clinical whole exome sequencing (WES) increasingly gained popularity, more COQ10D7 patients emerged worldwide, displaying diverse phenotypes, and carrying causative variants, either in homozygosity or compound-heterozygosity.

For instance, Brea-Calvo et al. (2015) identified two siblings with had a homozygous p.Arg145Gly mutation. They exhibited symptoms such as hypotonia, bradycardia, and respiratory insufficiency, and unfortunately, both siblings passed away shortly after birth. Another patient with the p.Arg141* and p.Arg240Cys mutations also faced a severe fate, passing away due to respiratory and heart failure within a day of birth. In separate cases, W. K. Chung et al. (2015) found two unrelated Ashkenazi Jewish girls with COQ10D7 who were homozygous for the c.718C-T transition in the COQ4 gene, resulting in an Arg240Cys substitution. Tragically, both patients also died during early infancy.

In another case, two sisters with mutations p. Leu52Ser and p. Thr174del were diagnosed with cerebellar hypoplasia but did not exhibit any cardiac abnormalities. Unfortunately, they passed away shortly after birth due to epileptic encephalopathy and multiorgan failure. Finally, a patient who was homozygous for the p. Pro64Ser mutation experienced a gradually worsening motor condition and

cerebellar atrophy at the age of 18. All available specimens from the affected individuals exhibited lower levels of Coenzyme Q and frequently demonstrated diminished activities in electron transport chain (ETC) complexes. Therefore, COQ4 mutations were discovered to be responsible for early-onset mitochondrial diseases, which are marked by different clinical manifestations and linked to CoQ_{10} deficiency (Brea-Calvo et al., 2015).

As the use of next-generation sequencing expanded, numerous other COQ4 recessive mutations causing CoQ_{10} deficiency were discovered, leading to conditions such as severe neonatal encephalomyopathy (Chung et al., 2015), infantile cardiomyopathy and encephalopathy (Sondheimer et al., 2017), or childhood-onset spinocerebellar ataxia and stroke-like episodes (Bosch et al., 2018). Subsequently, additional COQ4 homozygous mutant patients were reported; some of these patients presented with classical neonatal-onset encephalo-cardiomyopathy, while others exhibited infantile-onset illnesses with a broader range of clinical manifestations (Yu et al., 2019).

More recently, in collaboration with Santorelli's group (IRCCS Stella Maris Foundation, Calambrone, PI), Mero et al. (2021) expanded our understanding of COQ4-related diseases. They identified a total of nine *COQ4* biallelic missense mutations, some in homozygosity and others in compound heterozygosity. Notably, some of these mutations had never been reported before, such as p.Gly95Asp, p.Arg102His, p.Arg141Gln, p.Ala153Val, and p.Pro193Ser, while others had been previously described (p.Pro64Ser, p.Arg145Gly, p.Trp184Arg, p.Arg240Cys) (Brea-Calvo et al., 2015; W. K. Chung et al., 2015; Yu et al., 2019).

4.A.1.2 Unlocking the enigma of *COQ4*

As previously stated, COQ4 has been proposed to be involved in Coenzyme Q (CoQ) synthesis in yeast and human cells (Casarin et al., 2008; Salviati et al., 2012) through the stabilization of the COQ synthome (Marbois et al., 2009). However, the specific function of COQ4 in the CoQ synthesis process remains a challenge.

Marbois et al. (2009) conducted research indicating that the amino acid sequence of Coq4p defines a unique polypeptide family (COG 5031.1- pfam05019) with very limited secondary sequence

homology to other protein families. It is interesting to note that a homologue of Coq4p is present in the genomes of various eukaryotic organisms, as well as in specific species of alpha, beta, delta, and gamma proteobacteria, as well as cyanobacteria. Some of these prokaryotic species, however, are not known to contain CoQ (Collins & Jones, 1981).

Upon aligning the amino acid sequence of yeast Coq4p with prokaryotic homologues, researchers identified a highly conserved putative zinc ligand motif HDxxH-(x)11-E (Fig. 4.5). This motif is similar to those found in catalytic zinc ligand domains (Auld, 2001; Vallee & Auld, 1989, 1993) and shares structural similarities with the thermolysin family of proteases (Marbois et al., 2009).

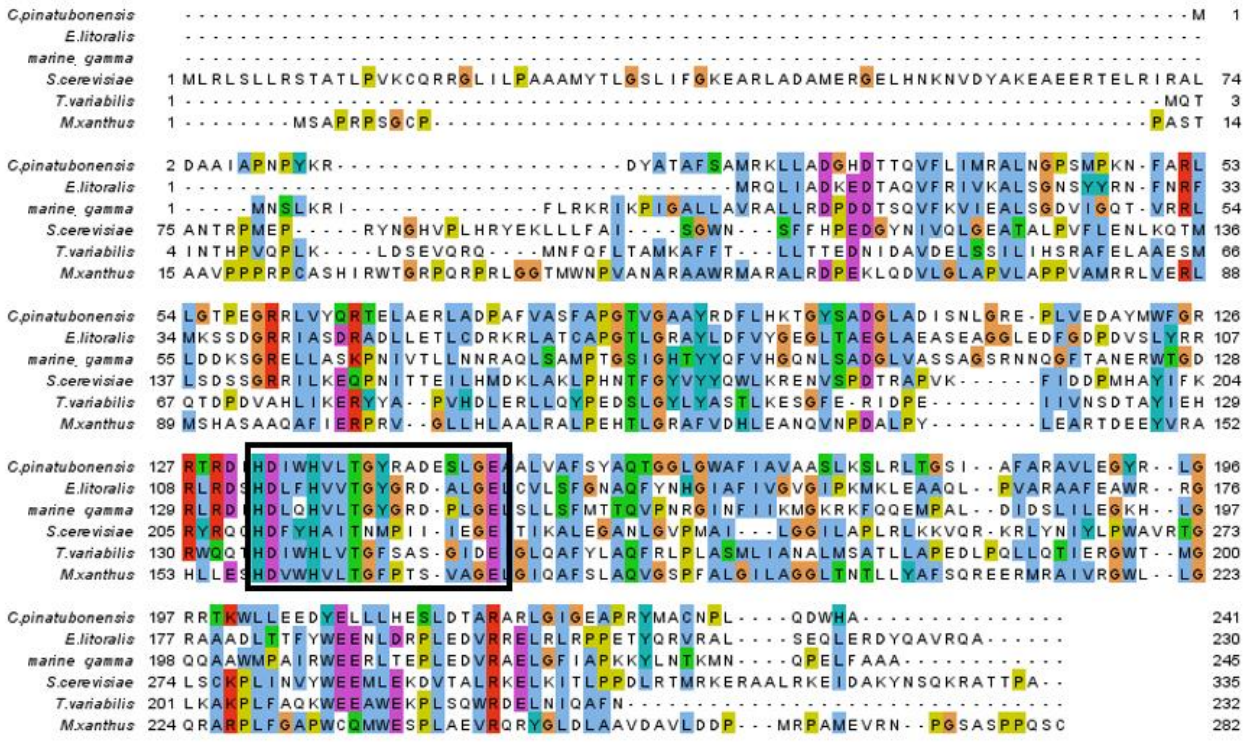

Fig. 4.5 The Coq4p sequence displays a conserved catalytic zinc ligand motif, which is also present in prokaryotic species. A search of current prokaryotic databases reveals Coq4p homologs in various bacterial classes, such as alpha, beta, delta, and gamma proteobacteria, as well as representatives in cyanobacteria. These homologs are classified as members of COG 5031.1 (pfam05019).The protein sequences, shown from top to bottom, are associated with the following gene bank identifiers: AAZ64280 (*C.pinatubonensis*), WP_011415896 (*E.litoralis*), EAW40764 (*marine gamma*), O13525 (*S.cerevisiae*), ABA20718 (*T.variabilis*) and WP_011551234 (*M.xanthus*). The potential location for a catalytic zinc ligand motif is indicated by the boxed residues. The alignment was based on Marbois et al.'s publication (2009) and performed using Clustal O. The alignment has been updated during the writing of this work in September 2023.

Legend

Clustal X Default Colouring			
Category	Colour	Residue at position	{ Threshold, Residue group }
Hydrophobic	BLUE	A,I,L,M,F,W,V	{>60%, WLVIMAFCHP}
		C	{>60%, WLVIMAFCHP}
Positive charge	RED	K,R	{>60%,KR}, {>80%, K,R,Q}
Negative charge	MAGENTA	E	{>60%,KR}, {>50%,QE}, {>85%,E,Q,D}
		D	{>60%,KR}, {>85%, K,R,Q}, {>50%,ED}
Polar	GREEN	N	{>50%, N}, {>85%, N,Y}
		Q	{>60%,KR}, {>50%,QE}, {>85%,Q,E,K,R}
		S,T	{>60%, WLVIMAFCHP}, {>50%, TS}, {>85%,S,T}
Cysteines	PINK	C	{>85%, C}
Glycines	ORANGE	G	{>0%, G}
Prolines	YELLOW	P	{>0%, P}
Aromatic	CYAN	H,Y	{>60%, WLVIMAFCHP}, {>85%, W,Y,A,C,P,Q,F,H,I,L,M,V}
Unconserved	WHITE	any / gap	If none of the above criteria are met

Furthermore, it should be noted that the structure of hCOQ4 remains elusive, although a homologous protein from *Nostoc sp. PCC 7120* (a cyanobacteria species), denoted as Alr8543, had its structure deposited in the PDB a few years ago. When aligning hCOQ4 with Alr8543 and analyzing the hCOQ4 model structure (Fig. 4.6 A, B) based on the cyanobacterial homologue (PDB ID: 6E12), it becomes clear that these two proteins share a 20% homology (Kawamukai, 2016). While this homology is not particularly high, it is significant because certain key residues are conserved (Fig. 4.6 C). In addition, prior investigations in our laboratory have shown that the far UV CD spectrum of recombinant hCOQ4 exhibits a comparable alpha helix content of approximately 60%.

Apart from the metal coordinating pocket, the COQ4 structure, based on its homologue in *Nostoc* (6E12), contains a tunnel surrounded by hydrophobic residues. This tunnel appears to be well-suited for accommodating the isoprene side-chain of the coenzyme Q precursor, enabling the aromatic ring to fit tightly into the active site pocket (Fig. 4.6 A, B).

A

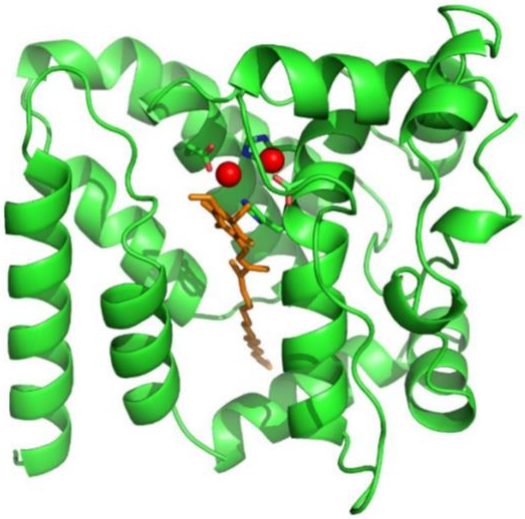

B

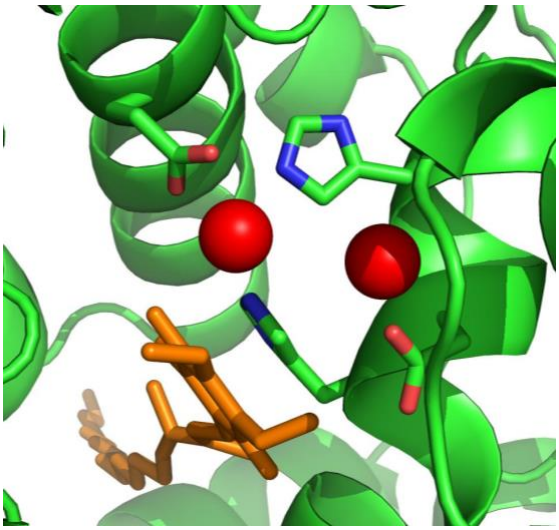

C

```
Q8YJY7_NOSS1 ------------------------------------MIETITQS-QETAIL--
ESFLEL 20
COQ4_HUMAN
MATLLRPVLRRLCGLPGLQRPAAEMPLRARSDGAGPLYSHHLPTSPLQKGLLAAGSAAMA 60
                                                          . :  *  :..:*
*

Q8YJY7_NOSS1 VKSPYGN--FASIGKLSHVLNDPDTLQKVVAVLSLTPQGKQAFEDRPMLG--
KIDLEQLH 76
COQ4_HUMAN   LYNPYRHDMVAVLGE----
TTGHRTLKVLRDQMRRDPEGAQILQERPRISTSTLDLGKLQ 116
              : .** :  .* :*:     ..  **: :   :   *:* * :::** :.
.:** :*:

Q8YJY7_NOSS1 QLPNYTLGYMYADHMIRNQLTPPPV---
NENVNHPFMFLAAHLGETHDIWHVVTGCDTDK 133
COQ4_HUMAN
SLPEGSLGREYLRFLDVNRVSPDTRAPTRFVDDEELAYVIQRYREVHDMLHTLLGMPTNI 176
             .**: :**  *  .:  *:::*      .   :. : ::  :  *.**: *.:
*  *:

Q8YJY7_NOSS1 PGEVKLEAFYTAQLI-PDRLFLALLAKNLLKTAMYEVELCEQILDGLTQGW--
MMGKRAK 190
COQ4_HUMAN   LGEIVVKWFEAVQTGLPMCILGAFFGPIRLGAQSL------
QVLVSELIPWAVQNGRRAP 230
              **: :: * :.*   *  :: *::.   * :         *:* .    *
*:**

Q8YJY7_NOSS1 PLFGIEWNKLWETPLEELQTSLNIVPI-------- 217
COQ4_HUMAN   CVLNLYYERRWEQSLRALREELGITAPPMHVQGLA 265
              ::.: ::: **  *. *: .*.*.
```

Figure 4.6 A) This model depicts the structure of human CoQ4, derived from the PDB coordinates of Nostoc sp. Q8YJY7 (PDB ID: 6E12), with the potential substrate displayed in orange. The red spheres represent the presence of divalent metal ions. B) This close-up view shows the coordination site (HDxxHx(11)E) where two divalent metal ions are located. C) The multiple sequence alignment of human CoQ4 and Nostoc sp. Q8YJY7 is shown here using CLUSTAL O (1.2.4). The green background highlights the regions of the Q8YJY7 sequence characterized by alpha-helical secondary structure.

Our previous investigations, conducted consistently in our laboratory (data not published), have revealed that when recombinant hCOQ4 is treated with a zinc chloride solution, it can effectively retain two zinc ions within its protein structure. In contrast, hCOQ4 mutants at the HDxxH site, namely Asp164Ala and His163Ala-His167Ala, lose both zinc ions. Importantly, despite this loss of zinc ions, these mutants maintain their structural integrity as evidenced by a comparison of their CD

spectra (data not published). This observation strongly suggests that the two zinc ions bind to the same site within the protein, which may play a critical role in its enzymatic activity.

In summary, considering that COQ4 proteins possess a conserved H-D-x(2)-H-(x)11-E motif (Marbois et al., 2009), which is likely involved in the binding and coordination of two metal ions, and based on our structural modelling of hCOQ4 using the Nostoc punctiforme Q8YJY7 structure, it is plausible to classify COQ4 as a member of the 'Binuclear Metallo Hydroxylases' group (Mitić et al., 2006; Schenk et al., 2012). This classification leads us to hypothesize that COQ4 may indeed possess enzymatic activity involved in CoQ synthesis, opening the door to comprehensive investigations aimed at characterizing its function.

We chose to validate the effect of the metal-binding active site mutation p.Asp164Ala in *S. cerevisiae* using a functional complementation strategy. Yeast has demonstrated its effectiveness as a valuable model system for assessing the impact of proteins resulting from various mutated COQ genes. As previously mentioned, many human COQ genes have yeast counterparts, and *S. cerevisiae* has proven to be a simple and powerful model for studying CoQ biosynthesis in human cells.

4.A.2 Materials and Methods

4.A.2.1 Molecular biology

S. cerevisiae COQ4 gene was amplified from genomic DNA of a W303 MATa strain, using Phusion® High-Fidelity DNA Polymerase (NEB). The coding sequence of human *COQ4* was also amplified using the same enzyme from human cDNA. Additionally, the yMTShCOQ4 hybrid gene was created through sequential PCR as previously described(Nguyen et al., 2014). The PCR products were cloned into the pCR8/GW/TOPO® TA entry vector (Invitrogen), using the manufacturer's protocol. The products were moved to the pCM189 yeast expression vector through site-specific recombination, employing the Gateway® LR Clonase® II enzyme mix (Invitrogen). pCM189-RfA was cloned from the Ready Frame A (RfA) cassette into the Multiple Cloning Site of the pCM189 yeast expression vector (Invitrogen), using The Gateway® Vector Conversion System manual (Invitrogen). The plasmid encoding the mutated protein p.Asp164Ala was created by site-directed mutagenesis via PCR-amplification of the pCM189-yMTShCOQ4 construct utilizing primers containing the desired mutation. The QuikChange Lightning Site-Directed Mutagenesis Kit (Agilent) was used for this purpose. Prof. Fabien Pierrel (Université Grenoble Alpes) kindly provided the pRS423-yCOQ8 plasmid.

For the expression of the human COQ4 protein in *E.coli*, we started from the human COQ4 cDNA previously cloned into the expression vector pET21a (ThermoFisher Scientific). The vector contained a N-terminal polyhistidine sequence (His tag) and an enterokinase recognition site (EK site) instead of the mitochondrial targeting sequence of the hCOQ4. The plasmid pET30a GBFusion1 was purchased from Addgene (# 133438) with the aim of introducing GB1 tag (instead of the His tag) into our protein to enhance its expression by improving protein solubility. Based on the In-Fusion® HD Cloning Kit and following the manufacturer's instructions, we amplified the GB1 tag using specific primers from the plasmid pET30a GBFusion1. Then, we cloned it at the N-terminal of the hCOQ4 coding sequence after linearizing the plasmid pET21a hCOQ4 using another set of specific primers.

The plasmid encoding the mutant protein p.Asp164Ala was generated by site-directed mutagenesis. This involved PCR-amplification of the pET21a GB1 *hCOQ4* construct, using a set of primers that carry the desired mutation and the QuikChange Lightning Site-Directed Mutagenesis Kit.

The correctness of all constructs was confirmed by direct sequencing. The oligonucleotides sequences used in this study are listed in Table 4.2.

Primer name	**Sequence 5'->3'**	**Purpose**
yCOQ4_inatt_ Kana_F	ATGTTGAGGTTATCTTTACTGAGATCAACAGCTACTTTGCCAGTGCAGCTGAAGCTTCGTACGC	KO of yeast *coq4* with a kanamycin-resistance cassette
yCOQ4_inatt_Kana_R	TCATGCTGGAGTCGTGGCTCGTTTCTGTGAGTTGTATTTTGCGTCGCATAGGCCACTAGTGGATCTG	KO of yeast *coq4* with a kanamycin-resistance cassette
yCOQ4_F	AGTTGCGGTTTGTGGAAAAG	Amplification of *COQ4* gene from yeast genomic DNA
yCOQ4_R	TCTAACTTCATGGGCGAGAGA	Amplification of *COQ4* gene from yeast genomic DNA
hCOQ4_F	ATGGCGACTCTGCTGCGC	Amplification of *COQ4* gene from human cDNA
hCOQ4_R	TCAGGCCAAGCCCTGGAC	Amplification of *COQ4* gene from human cDNA
yCOQ4_R_hybrid	TTCTGCAGCGGGGAGGTGGGGAGGCCGTTGTACCGAGGTTCCA	Amplification of y*COQ4* MTS (together with yCOQ4_F) to clone it in the hybrid gene
hCOQ4_F_hybrid	TGGAACCTCGGTACAACGGCCTCCCCACCTCCCCGCTGCAGAA	Amplification of functional domain of h*COQ4* (together with hCOQ4_R) to clone it in the hybrid gene
hCOQ4_D164A_F	CGGGAGGTGCACGCCATGCTTCACACC	Mutagenesis
hCOQ4_D164A_R	GGTGTGAAGCATGGCGTGCACCTCCCG	Mutagenesis

GB1_F	ACTTTAAGAAGGAGATATACATATGCAGTACAAAC	Amplification of the GB1 tag to clone it in the pET21a h*COQ4*
GB1_R	GTCGTCGTCATCAATGGATCCTTCGGTAACGGTG	Amplification of the GB1 tag to clone it in the pET21a h*COQ4*
pET21a hCOQ4_F	ATTGATGACGACGACAAGGCG	Linearization of the plasmid pET21a h*COQ4* for the cloning with the GB1 tag
pET21a hCOQ4_R	ATGTATATCTCCTTCTTAAAGTTAAAC	Linearization of the plasmid pET21a h*COQ4* for the cloning with the GB1 tag

Table 4.2 Sequences of all oligonucleotides used in this study.

4.A.2.2 Yeast strains, media and plasmid transformation

The W303 *Δcoq4* strain (MATa; ade2-1; his3-1_15; leu2-3_112; trp1-1; ura3-1 YDR204W::kanMX4) was created through the homologous recombination-mediated disruption of the endogenous gene using a kanamycin-resistance cassette. The procedure for inactivation has been described in detail elsewhere (Vetro, et al., 2017). Yeast strains were grown in rich medium (YPD) or synthetic minimal (SM) medium at 30 °C. YPD (1% yeast extract, 2% peptone, 2% dextrose) was used for routine maintenance of the wild type strain. Synthetic minimal medium (0.17% yeast nitrogen base without amino acids, 0.5% ammonium sulfate, 2% carbon source), supplemented with amino acids to cover yeast auxotrophies except uracil (and histidine when yCOQ8 was overexpressed) was used to select transformant strains (Fig. 4.7). YPGly medium (1% yeast extract, 2% peptone and 3% glycerol) was used to perform functional complementation assays. Growth media components were purchased from Difco. Yeast DNA transformations were performed using the polyethylene glycol-lithium acetate method as previously described (Gietz & Woods, 2006).

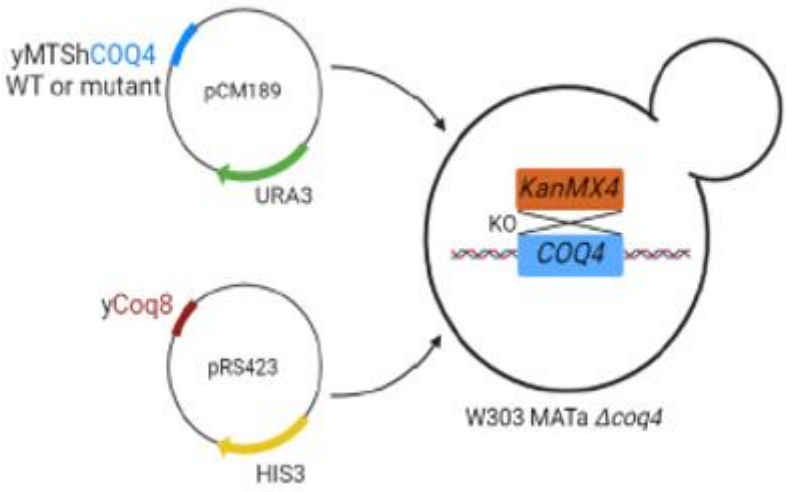

Fig.4.7 Representation of the working model used in this study to obtain a functional yeast-based assay to validate putative hCOQ4 mutations. Image sourced from the PhD Thesis of Cristina Calderan and generated using BioRender (BioRender.com)

4.A.2.3 Functional complementation spot test assay

For testing the ability of the different wt and mutant COQ4 proteins to rescue respiratory growth in *coq4*-deleted yeast, the different yeast strains were inoculated in glucose-containing selective liquid medium and grown for 2 days and 2 nights at 30°C.

The concentration of each culture was then adjusted to OD_{600} = 1 (approximately 10^7 cells/mL) in sterile water, after two washes in water to remove glucose medium, and four serial 10-fold dilutions were performed. For each of these dilutions, 5µL were spotted onto YPD, SM Glu (with proper amino acid selection), and YPGly, plate media. Plates were incubated at 30°C and images were taken 5 days after incubation.

4.A.2.4 Expression and purification of WT and mutant of human CoQ4

The human WT COQ4 and its mutant form expressions are induced by the addition of 1mM isopropyl-1-thio-β-D-galactopyranoside to *E. coli* BL21 (DE3) cell cultures. The cells are then incubated for 4 hours at 30 °C, following by harvesting through centrifugation (20 minutes at 4000

rpm, at 4 °C). The collected cells are suspended in a lysis buffer containing Na_2PO_4 (20 mM), NaCl (50 mM), and DTT (1 mM) with a pH of 7.8. Subsequently, the cells are lysed through sonication. The following centrifugation (30 min at 18000 rpm, 4°C) enables the separation of the soluble (supernatant) from the insoluble fraction (pellet). Due to the low solubility of the hCOQ4 protein, the inclusion bodies in the insoluble fraction are solubilized O/N at room temperature in the lysis buffer (Tris 20 mM, NaCl 50mM, DTT 1mM, pH 8.0) with the addition of 1% sarcosyl. After centrifugation, the solubilized protein is isolated on a Q (quaternary ammonium) Sepharose High Performance strong anion exchange chromatography column (Hi-Trap Q HP, 1 ml, Sigma Aldrich) using an AKTA-FPLC, loading buffer (Tris 20 mM, NaCl 50mM, DTT 1mM and 0.1% sarcosyl) and elution buffer (Tris 20 mM, NaCl 1M, DTT 1mM and 0.1% sarcosyl). The purity and molecular weight of the eluate fractions (resolved by SDS-PAGE) are checked by Western blot and Coomassie staining.

4.A.2.5 SDS-PAGE sample preparation

The eluate fractions are denatured by resuspending them in Laemmli loading buffer (Laemmli, 1970) and reducing them with dithiothreitol (DTT) before being loading them onto a Sodium Dodecyl Sulphate-Polyacrylamide Gel Electrophoresis (SDS-PAGE). This process enables the proteins to be separate according to their molecular weight. Afterward, the samples are heated at 95°C for 5 minutes and then centrifuged at 12,000 rpm for 7 minutes.

4.A.2.6 Analysis of protein expression

Each protein fraction is separated using the Mini-PROTEAN® Tetra Handcast System (BioRad) with 10% Tris-Glycine SDS-PAGE. The Prestained Protein SHARPMASS™ VI (Euroclone) is used for the protein ladder. The Western blot is performed using the polyclonal rabbit anti-COQ4 primary antibody (ab126295, Abcam) diluted 1:500 (incubated overnight at 4°C), and the Horseradish Peroxidase-conjugated goat anti-rabbit secondary antibody diluted 1:6,000. The enhanced chemiluminescence technique, following the guidelines provided by Amersham (GE Healthcare Biosciences), is used to visualize the specific band for the protein of interest.

4.A.2.7 Coomassie Blue staining

Proteins resolved by SDS-PAGE are also stained with Coomassie Blue. Following sodium dodecyl sulfate–polyacrylamide gel electrophoresis (SDS-PAGE), the gel is placed in a loosely covered container with 100 mL of ultrapure water. It is microwaved at high power (950 to 1,100 watts) for 1 minute or until the solution is almost boiling. The gel is shaken on an orbital shaker for 1 minute, and the water is discarded. This procedure is repeated two more times. After the final washing step, 20 mL of SimplyBlue SafeStain (Thermo Fisher Scientific) was added to the gel and microwaved on high power for approximately one minute or until the solution was on the point of boiling. The gel was subsequently agitated on an orbital shaker for five minutes. Following this, it was rinsed in 100 mL ultrapure water for ten minutes while being shaken. Finally, it underwent incubation in 20 mL 20% NaCl for a minimum of five minute.

4.A.3 Results

4.A.3.1 Effects of the p.Asp164Ala mutation on the metal-binding site of human COQ4 protein through a yeast model

Previous experiments (data not shown), conducted in our laboratory, found that the human COQ4 protein could not rescue the respiratory defect of the yeast Δ*coq4*-null strain, nor could it restore its CoQ biosynthesis or respiration. It is evident that only the yeast Coq4 protein can successfully complement our yeast model. We suspected that the human protein was not imported into the yeast mitochondria. To test this, we created a hybrid gene, yMTSh*COQ4*, that combines the mitochondrial targeting sequence of the yeast Coq4 protein (amino acids 1–86) with the conserved C-terminal domain of the human COQ4 protein (amino acids 42–265). We cloned this gene into the yeast expression vector pCM189 and co-transformed it into the Δ*coq4*-null strain, along with a plasmid that overexpresses the yeast Coq8 protein from the high-copy pRS423 vector. The yeast Coq8 protein is a putative regulatory kinase that enhances the levels and assembly of several Coq proteins and complex (He et al., 2014; Awad et al., 2018). We found that overexpression of Coq8 enabled the hybrid yMTSh*COQ4* gene to partially restore the growth of the Δ*coq4*-null strain on respiratory medium.

To study the effect of the hCOQ4 p.Asp164Ala mutation, which affects the metal-binding active site of the human COQ4 protein, we used the yeast model described above. We evaluated the functionality of the mutant protein by analyzing the mitochondrial respiration of the yeast cells on non-fermentable medium. We hypothesized that this mutation would impair the protein function and affect the CoQ biosynthesis pathway. The results confirmed our hypothesis: the Coq4 null mutant yeast expressing the mutant hCOQ4 protein showed no growth on non-fermentable medium (Fig. 4.8), unlike the control strains. The control strains were the Δ*coq4*-null strain expressing the hybrid yMTSh*COQ4* gene, which could grow on non-fermentable carbon source, and the Δ*coq4*-null strain transformed with empty vectors, which could not rescue the respiratory phenotype. These findings

indicate that the hCOQ4 p.Asp164Ala mutation is a severe missense mutation that disrupts the metal-binding site of the human COQ4 protein, which is essential for its function.

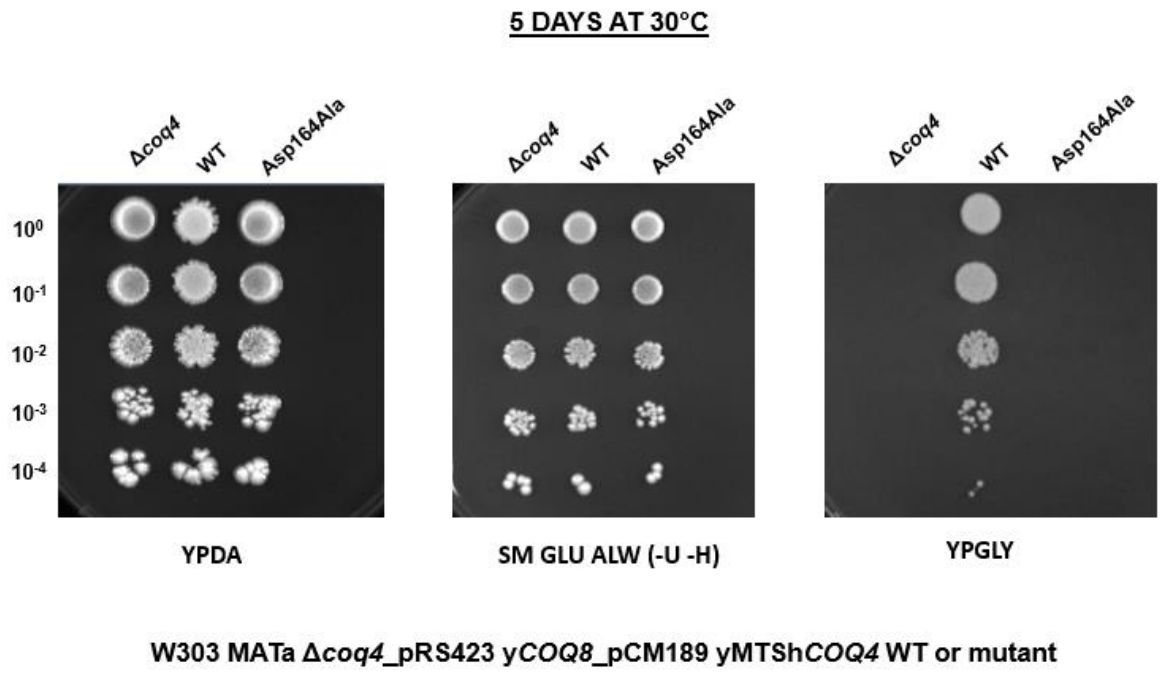

Figure 4.8 Functional complementation assay of yMTSh*COQ4* wt or mutant protein p.Asp164Ala co-expressed with yCoq8 in *Δcoq4* yeast strain. The hCOQ4 mutation in the metal-binding active site totally impaired the ability of the wt yMTSh*COQ4* hybrid protein to compensate for the absence of endogenous yCoq4. The analysis was conducted via spot test, where cell cultures were serially diluted and spotted onto the different agar media and incubated at 30°C. After 5 days, we observed the following, from left to right: rich medium (YPD) for the growth of all strains, synthetic minimal medium (except uracil and histidine, which were supplied by the plasmids used for co-transformation) for the growth of transformants, and YPGly medium to test yeast respiration. Each spot test analysis was repeated three times.

Yeast strains were grown in rich medium (YPD) or synthetic minimal (SM) medium at 30 °C. YPD (1% yeast extract, 2% peptone, 2% dextrose) was used for routine maintenance of the wild type strain. Synthetic minimal medium (0.17% yeast nitrogen base without amino acids, 0.5% ammonium sulfate, 2% carbon source), supplemented with amino acids to cover yeast auxotrophies except uracil (and histidine when yCOQ8 was overexpressed) was used to select transformant strains (Fig. 4.7). YPGly medium.

4.A.3.2 Expression and purification of human COQ4 wild type and p.Asp164Ala mutant protein

To further investigate the function and activity of the human COQ4 protein, we decided to express and purify both the wild type and mutant p.Asp164Ala forms in bacteria. First, the human COQ4 coding sequence was cloned into a specific bacterial expression vector (pET21a) having an N-terminal immunoglobulin binding domain of protein G (GB1), a tag that enhances protein solubility. The cloning process followed the *In-Fusion kit (Takara)* instructions. Sequence was confirmed by Sanger. The mutagenesis of the human construct, thus obtained, allowed the generation of the vector bearing the sequence coding for the hCOQ4 metal-binding active site p.Asp164ala mutant. The transformation was performed using a specific type of chemically competent bacterial cells, known as BL21, commonly used in research to produce recombinant proteins.

In our first approach, we tried to induce protein expression by growing bacteria at low temperature (16°C). This was performed with the aim to improve the solubility of the expressed proteins, thereby enhancing the efficiency of subsequent protein purification efforts. The results indicated that our protocol yielded relatively low concentrations of our protein in the soluble fraction (Fig. 4.9 A), hence suggesting low efficacy of our protocol. The attached tag on our protein, GB1, is a domain derived from protein G, known for its ability to bind to the Fc domain (constant region) of IgG. Using this domain, we developed a series of various strategies to purify our protein (data not shown). Unfortunately, none of the tested methods were effective because the hCOQ4 expressed in the total soluble fraction (with a low-temperature protein expression protocol) was not so particularly high. Considering this, we decided to change our strategy to a classical approach based on protein expression at a high temperature of 30°C. As a result, a higher proportion of the desired proteins

ended up in inclusion bodies, which were then further solubilized in the presence of a specific anionic detergent, sarcosyl. Communication with Fiorella Tonello (CNR, Italy) revealed that hCOQ4 may be solubilized using this specific detergent at a concentration of 1%. Inclusion bodies are protein aggregates that bacteria can produce during the process of expressing recombinant proteins. These bodies form when recombinant proteins are overexpressed or accumulated excessively within host cells and this can occur for various reasons, including rapid protein production at favourable temperatures such as 30°C. Typically, inclusion bodies are insoluble and inactive, and they can interfere with the production of recombinant proteins. They are often found in the cytoplasm of *E.coli* and require isolation, solubilization and purification to recover the functional protein from these aggregates.

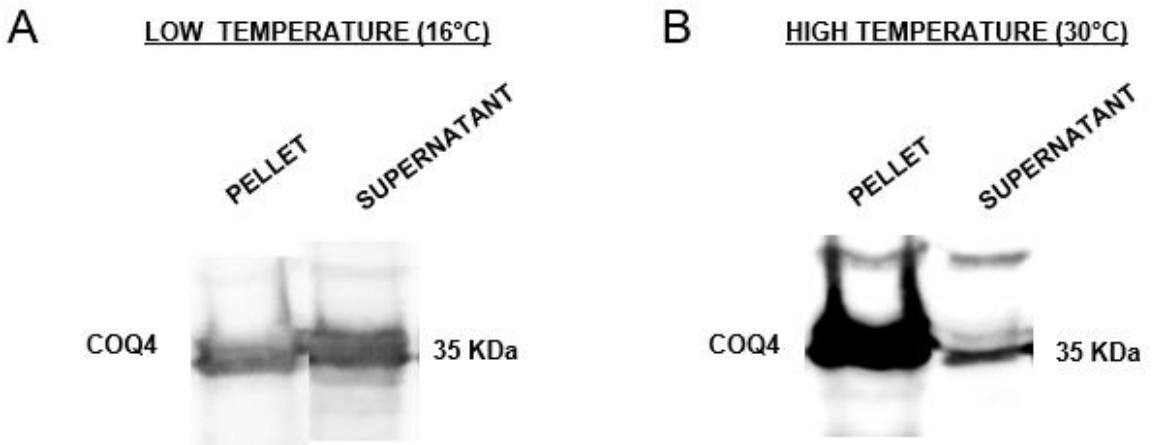

Fig.4.9 Differences in COQ4 protein expression levels resulting from two different methods of growing BL21 cells were analyzed via Western blot. A) Method involved the growth of cells at a low temperature (16°C) , while B) required a high temperature (30°C). After growth, cells were collected by centrifugation, sonicated, and then centrifuged again to separate the insoluble pellet from the soluble fraction (supernatant). Samples were analyzed using SDS-PAGE followed by Coomassie staining (data not shown) and Western blotting, whose results are provided here. Our protocol (A) revealed that the COQ4 protein expression in growing bacteria cells at low temperature was not particularly high in the soluble fraction.

We purified the human COQ4 wild type and mutant protein by AKTA-FPLC (Fast Protein Liquid Chromatography), a technique that separates proteins based on their physicochemical properties, specifically employing ion exchange chromatography. In our procedure, we utilized a Q Sepharose column, which is a type of anion exchange column capable of binding negatively charged proteins under low pH conditions and eluting them at high pH.

To begin, the solubilized protein was loaded onto the Q Sepharose column using a buffer with low pH and a low salt concentration. Subsequently, the column was washed with the same buffer to remove any unbound or weakly bound proteins. The bound protein was then eluted using a buffer with a high pH and salt concentration, disrupting the electrostatic interactions between the protein and the column. The eluted protein was collected in multiple fractions, which were subsequently analyzed using SDS-PAGE and immunoblotting to identify and quantify the COQ4 protein.

The chromatograms presented in Figure 4.10 illustrate the outcome of chromatography runs for both the wild-type protein (A) and the metal-binding active site mutant p.Asp164Ala (D). We assessed the purity and determined the molecular weight of the hCOQ4 wild-type and mutant proteins in the eluate fractions. This assessment involved resolving the proteins on SDS-PAGE, followed by Coomassie staining (B for the wild type hCOQ4 and E for the p.Asp164Ala mutation) and Western blotting (C for the wild type and F for the mutant protein).

Our next steps involve the development of an enzymatic assay to evaluate the *in vitro* functionality of the hCOQ4 protein.

A

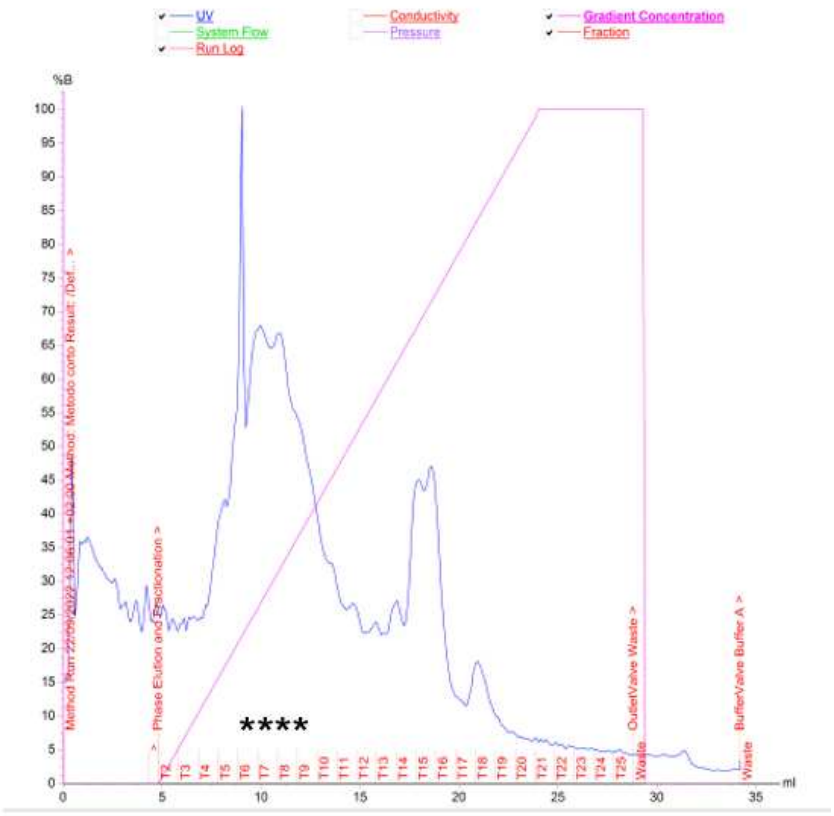
UV
System Flow
Run Log
Conductivity
Pressure
Gradient Concentration
Fraction
%B
ml
****

B

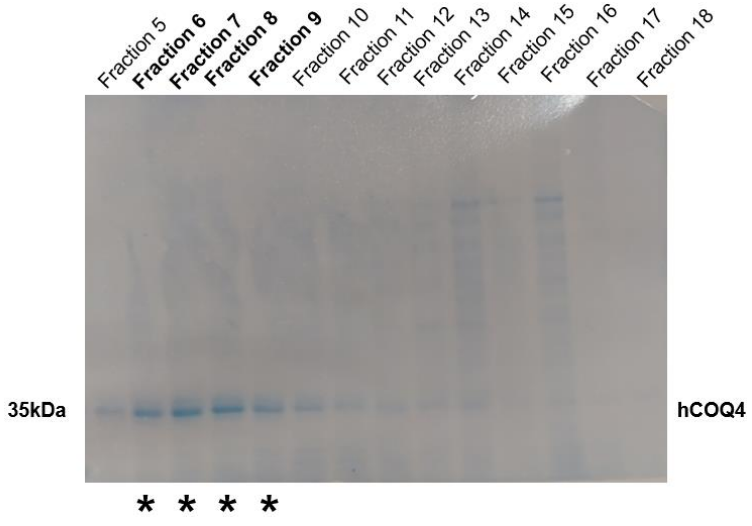
Fraction 5
Fraction 6
Fraction 7
Fraction 8
Fraction 9
Fraction 10
Fraction 11
Fraction 12
Fraction 13
Fraction 14
Fraction 15
Fraction 16
Fraction 17
Fraction 18
35kDa
hCOQ4
* * * *

C

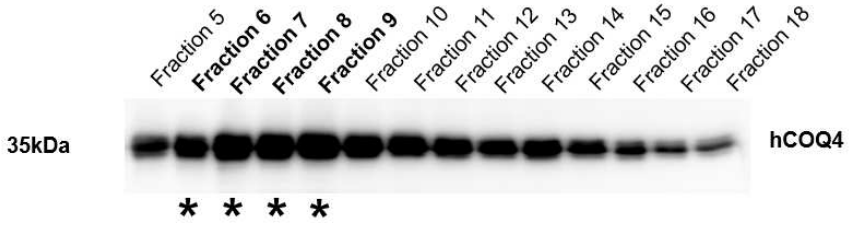
Fraction 5
Fraction 6
Fraction 7
Fraction 8
Fraction 9
Fraction 10
Fraction 11
Fraction 12
Fraction 13
Fraction 14
Fraction 15
Fraction 16
Fraction 17
Fraction 18
35kDa
hCOQ4
* * * *

D

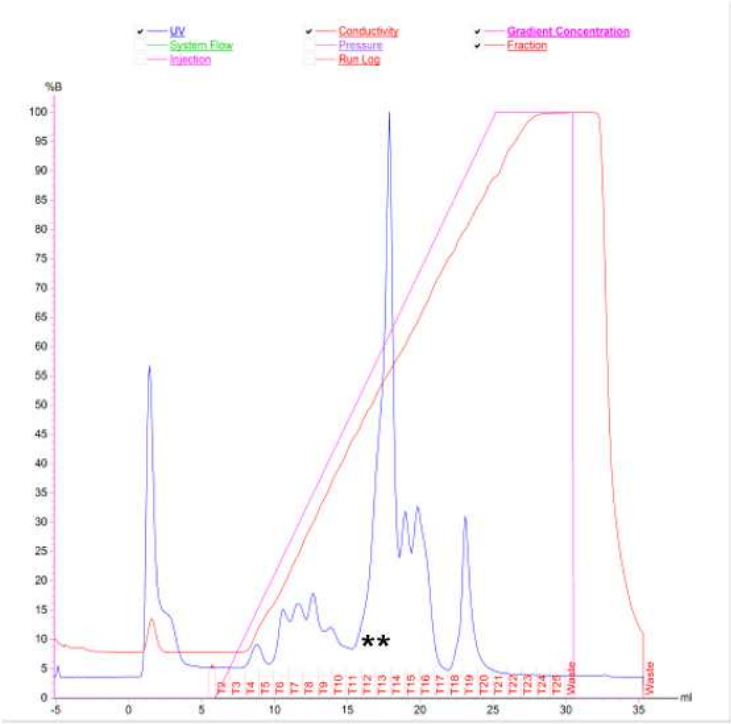
UV
System Flow
Injection
Conductivity
Pressure
Run Log
Gradient Concentration
Fraction
%B
**
ml

E

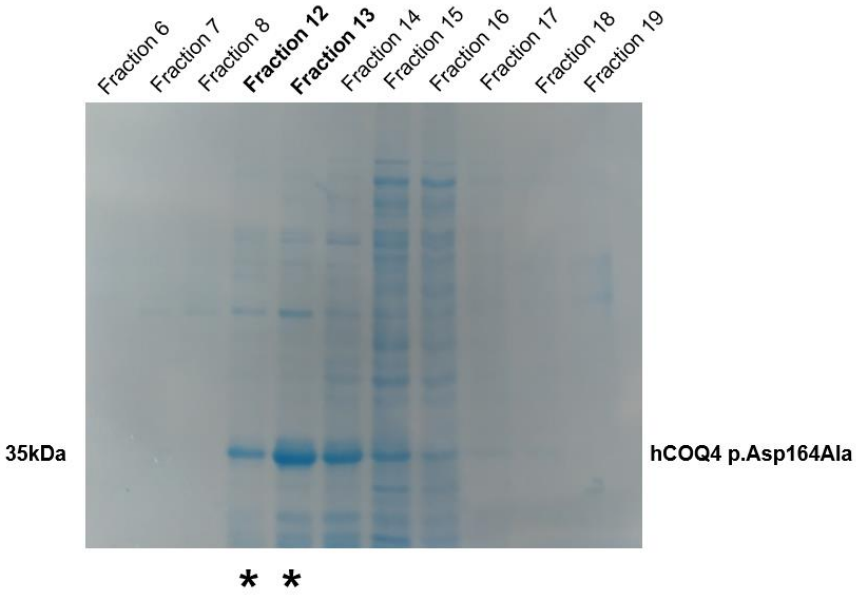
Fraction 6
Fraction 7
Fraction 8
Fraction 12
Fraction 13
Fraction 14
Fraction 15
Fraction 16
Fraction 17
Fraction 18
Fraction 19
35kDa
hCOQ4 p.Asp164Ala
* *

F


Fraction 6
Fraction 7
Fraction 8
Fraction 12
Fraction 13
Fraction 14
Fraction 15
Fraction 16
Fraction 17
Fraction 18
Fraction 19
35kDa
hCOQ4 p.Asp164Ala
* *

Fig. 4.10 Chromatograms obtained by AKTA-FPLC and further analysis through Coomassie and Western blotting of both the human COQ4 wild-type and mutant p.Asp164Ala proteins. The chromatogram plots the detector signal, indicating component concentration relative to eluent volume. Specifically, we presented the chromatograms obtained for the hCOQ4 wild-type (A) and the mutant protein (D). To assess the presence and purity of the hCOQ4 wild type protein, we employed Western blot analysis (B) and Coomassie staining (C) on the eluted fractions. The results confirmed that the fractions 6, 7, 8, and 9 contained the highest amounts of the protein, which had a molecular weight of approximately 35kDa, along with a GB1 N-terminal tag. Similarly, we conducted the same analyses for the hCOQ4 p.Asp164Ala mutant protein. Our findings indicated that fractions 12 and 13 contained the highest protein concentrations, as illustrated by Coomassie staining (E) and Western blotting (F).

4.A.4. Discussion

Nowadays, various aspects of the Q biosynthesis pathway remain incomplete, particularly the complexities of decarboxylation and methylation of the carbon at position 1 within the benzoquinone group of the Q precursor. Initially, it was postulated that Coq4 might serve a structural role in stabilizing the multimeric complex of the CoQ synthome. However, subsequent evidence emerged, suggesting that COQ4 actively participates in Q biosynthesis. This supposition gained strength due to the alignment of Coq4 proteins found in both prokaryotic and eukaryotic species, leading to the identification of a shared catalytic metal-binding site domain. Moreover, these earlier findings were substantiated by the crystal structure analysis of a homologous protein discovered in *Nostoc Punctiforme*. Additionally, recent investigations highlighted the significance of the H-D-x(2)-H-(x)11-E domain, responsible for binding and coordinating two metal ions. The absence of these ions results in the protein maintaining its structure, revealing a potential catalytic role of this domain.

The conservation of the Q biosynthetic pathway between yeast and humans allows us to study the p.Asp164Ala mutation in the metal-binding domain by evaluating the respiratory phenotype of our null-strain yeast model expressing the mutant protein through a classical spot test analysis. The crucial role of this amino acid in protein functionality is evident from the complete growth inhibition of our mutant on a glycerol medium, mirroring the findings in the Δ*coq4* yeast model. This provides proof that the loss of the capability to bind and coordinate metal ions, essential for protein functionality, most likely results in a non-functional protein that impairs Q production, subsequently affecting mitochondrial respiration and causing growth inhibition on non-fermentable carbon sources.

It should be noted that demonstrating the *in vitro* activity of hCOQ4 can further substantiate our hypothesis, although the expression and purification of the protein are not always straightforward and can often be challenging. Indeed, our efforts to obtain human COQ4 wild type and mutant p.Asp164Ala proteins have been intensive. Initially, we aimed to reduce the probability of our protein ending up in inclusion bodies, leading us to employ a protocol inducing expression at a low temperature (16°C). While this temperature helped minimize the protein's presence in inclusion bodies, the quantity of solubilized protein obtained was insufficient for purification.

Inclusion bodies are insoluble protein aggregates formed inside host cells, such as bacteria, during the expression of recombinant proteins. These aggregates are often inactive and challenging to purify, making their minimization crucial during protein expression. Thus, we initially worked at 16°C and incorporated a N-terminal tag (GB1 tag) to enhance protein solubility. Typically, higher temperatures during protein expression increase the likelihood of proteins entering inclusion bodies, as rapid bacterial growth can lead to protein overexpression without proper solubilization factors or correct protein folding.

After discovering that low-temperature expression failed to solubilize enough protein for further study, we switched to a standard protocol with expression at 30°C. To address our protein's insolubility, we used sarcosyl, a specific anionic detergent that had previously been demonstrated to keep hCOQ4 in solution (Fiorella Tonello, personal communication).

Ultimately, through Ion Exchange FPLC, we efficiently purified both hCOQ4 wild type and mutant p.Asp164Ala proteins. However, the presence of the N-terminal GB1 tag, as well as the inclusion of 1% sarcosyl, may potentially interfere with attempts to demonstrate *in vitro* activity. The GB1 tag may be removed, as it was placed in proximity to an enterokinase recognition site, which could affect protein function and folding. Furthermore, prior successful redox reactions have been conducted in the presence of low-concentration detergents (Kido et al., 2010), instilling confidence in the use of solubilized protein obtained from inclusion bodies with the addition of 1% sarcosyl in the elution buffer for this purpose.

Starting for the purified protein, demonstrating *in vitro* activity can be time-consuming, as the specific reaction type, metal ions required for binding and coordination, potential co-factors (NADH, NADPH, $FADH_2$… etc.), and substrate (Q precursors) need to be identified and tested at appropriate concentrations. Currently, commercially available molecules closely resembling the Q precursor are limited to 4-hydroxybenzoate (4-HB) and vanillic acid, although they lack the lipid tail that could enhance *in vitro* reaction efficiency (Lu et al., 2013). Collaborations with the Pharmacy Department at our University may facilitate the synthesis of a compound similar to 4-HB or vanillic acid with a minimal isoprene chain of either 3 or 4units, similar to the synthesis of CoQ_{10} described by (Mu et al., 2011). This could help to demonstrate a potential catalytic activity due to the presence of a

hydrophobic tunnel next to the putative active site. However, the hydrophobicity of polyprenylated substrates complicates their use in *in vitro* assays with aqueous buffers.

Several techniques, such as atomic absorption studies to determine the most effective metal for protein binding, cryo-electron microscopy for visualizing protein structure, and crystallization to obtain the crystal structure of the protein, could offer beneficial insights. Various methods exist for measuring *in vitro* activity in chemical reactions, including spectrophotometry that monitors absorbance or light transmission at specific wavelengths, colourimetric sensors that react to product formation or pH changes, and alternative techniques.

Another possibility to consider is that conducting the *in vitro* reaction may not be straightforward, especially for COQ proteins. It might be necessary to co-express our COQ4 with other COQ proteins and attempt to recreate a mitochondrial-like environment, similar to the approach undertaken by Reidenbach et al. in 2018, who utilized lysosomes for this purpose. Moreover, since COQ4 is associated with the inner mitochondrial membrane (Marbois et al., 2005), the presence of lipids could also be critical for enzymatic activity.

In conclusion, demonstrating a protein's activity *in vitro* is often a complex task due to the various factors that can affect the process. Achieving optimal conditions may require a significant amount of time and effort. Therefore, it is essential not to disregard the possibility of employing alternative organisms for conducting *in vivo* functional assays, such as human or bacterial cells.

Future research is essential for the development of innovative therapeutic strategies, particularly for patients who typically have a limited response to oral CoQ supplementation. This is particularly important as COQ4 mutations are one of the most common causes of primary coenzyme Q deficiency. Understanding the exact function of COQ4 is therefore of critical importance.

PART IV.B

Unlocking the Role of Polyprenyl Diphosphate Synthase in Coenzyme Q Biosynthesis

4.B.1 Introduction

4.B.1.1 Polyprenyl diphosphate synthase

Ubiquinone, a vital compound, exhibits a distinct structural feature consisting of a benzoquinone core fused with an isoprenoid side-chain. The length of this isoprenoid side-chain is remarkably species-specific, serving as a unique identifier for each species. To illustrate this variation, *S. cerevisiae* boasts a six-unit isoprene side-chain, *Candida utilis* extends to seven units, while *E.coli* possesses eight units. In contrast, mice and *Arabidopsis thaliana* exhibit nine units, and *Schizosaccharomyces pombe* and humans impressively have ten units (Kawamukai, 2009; Okada et al., 2004; Saiki et al., 2005; Zhu et al., 1997).

In the biological realm, each organism predominantly synthesizes a specific type of ubiquinone. However, it's worth noting that minor variations are occasionally observed (Saiki et al., 2005). The precise length of the CoQ side chain is governed with exquisite precision by the trans-polyprenyl diphosphate synthase enzymes (Okada et al., 1996, 1998).

Interestingly, previous research has demonstrated that the lengths of UQ side-chains can be manipulated through genetic engineering. For instance, *E.coli*, which typically produces UQ-8, can be induced to generate UQ-7, UQ-9, or UQ-10 by introducing heptaprenyl, solanesyl, or decaprenyldiphosphate synthase genes from *Haemophilus influenzae*, *Rhodobacter capsulatus*, or *Gluconobacter suboxydans*, respectively (Okada et al., 1998; Okada, Kamiya, et al., 1997; Okada, Minehira, et al., 1997; Park et al., 2005).

Similarly, in the case of *S.cerevisiae* COQ1 disruptants, expressing various poly-PDS genes from different organisms can yield provider-type UQs, spanning from UQ-5 to UQ-10 (Okada et al., 1998). These discoveries underscore the intriguing potential for modifying ubiquinone characteristics by introducing trans-polyprenyl diphosphate synthase genes from different organisms. Remarkably, this genetic manipulation results in the production of the same type of ubiquinone observed in the source organisms. Moreover, these experiments suggest that harboring a distinct ubiquinone type, ranging from Q6 to Q10, does not exert a significant impact on the viability of *S.cerevisiae* or *E.coli*.

However, recent research has revealed that various ubiquinones indeed exhibit type-specific biological effects. For instance, when exogenous Q7 was introduced, it was not as effective as Q9 in restoring the growth of the *C.elegans clk-1* mutant (Jonassen et al., 2003).

Long-chain trans-poly-PDSs can be categorized into two distinct groups based on their ability to generate isoprenoid chains: short-chain (C10–C25) and long-chain (C30–C50) variants. Short-chain poly-PDSs, represented by enzymes such as farnesyl diphosphate (FPP) synthase and geranylgeranyl diphosphate (GGPP) synthase, initiate the condensation process by combining isopentenyl diphosphate (IPP) molecules (C5) to form dimethylallyl diphosphate (DMAPP) (C5). This DMAPP compound serves as the initial building block for further condensation of multiple IPP units, resulting in the synthesis of isoprenoids containing up to C25 units. In contrast, long-chain poly-PDSs facilitate the ongoing condensation of IPP, leading to the production of compounds with isoprenoid chain lengths exceeding hexaprenyl diphosphate (C30)(P. H. Liang et al., 2002) (Fig. 4.11).

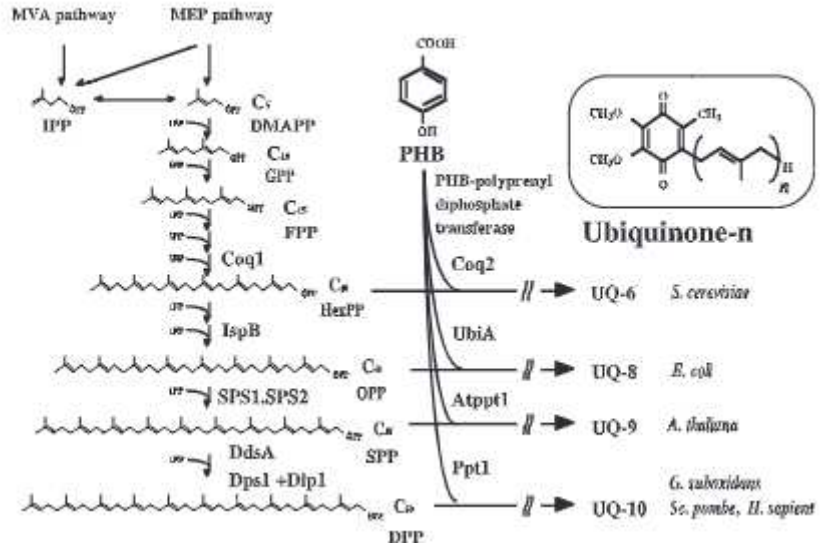

Fig. 4.11 The isoprenoid side-chain of ubiquinone (UQ) is synthesized through a multi-step process. It begins with dimethylallyl diphosphate (DMAPP), a C5 unit compound, which acts as the initial precursor for the condensation of several units of isopentenyldiphosphate (IPP). Isoprenoids containing more than C25 units are typically utilized in the synthesis of the side-chain of UQ. Several enzymes, namely Coq1, IspB, SPS1 (or SPS2), and the Dps1–Dlp1 complex, function as hexaprenyl (HexPP), octaprenyl (OPP), nonaprenyl, and decaprenyl (DPP) diphosphate synthases, respectively. These enzymes are responsible for producing the isoprenoid side-chains of UQ-6, UQ-8, UQ-9, and UQ-10, respectively. Additionally, PHB-polyprenyldiphosphate synthase is involved in the condensation of PHB and prenyl diphosphate in this process. Key precursors include methylerythritolphosphate (MEP) and mevalonic acid (MVA) (Zhang et al., 2008).

4.B.1.2 Structural Insights into PDS Proteins

Sequence analyses have unveiled the existence of seven conserved regions, denoted as domains I through VII, as well as two aspartate-rich motifs, DDXXD, within all-*trans*-type poly-PDSs (Koyama, 1999) (Fig. 4.12). These motifs function as binding sites for substrates and are dependent on the essential cofactor Mg2+ for enzyme activity (Koyama, 1999). Notably, the first DDXXD motif is responsible for binding with FPP, while the second motif is dedicated to binding the individual IPP block unit (Marrero et al., 1992; Song & Poulter, 1994).

However, in poly-PDSs characterized as heteromeric protein complexes, subunit 2 lacks the characteristic aspartate-rich motifs in domains II and VI (Saiki et al., 2003; Saiki et al., 2005). The first reported crystal structure of a trans-prenyltransferase belongs to avian farnesyl diphosphate synthase (FPPS), existing as a homodimer (Tarshis et al., 1994). As illustrated in Fig. 4.13, this 2.6-Å-resolution structure encompasses 13 α-helices, with ten of them surrounding the central cavity. Within this deep cleft, forming the substrate-binding pocket, lie two conserved DDxxD sequences. Short-chain poly-PDS proteins have been extensively studied, and their three-dimensional crystal structures have been elucidated (Tarshis et al., 1994). However, despite ongoing investigations into long-chain synthases and the resolution of their three-dimensional crystal structures (Guo et al., 2004; Sun et al., 2005), the analysis of heteromeric forms of these long-chain enzymes remains limited. To date, long-chain PDSs have been characterized in several organisms, including *E.coli* (Kainou et al., 2001), *R.capsulatus* (Okada, Minehira, et al., 1997), *Bacillus subtilis* (Koike-Takeshita et al., 1995), *S.cerevisiae* (Ashby & Edwards, 1990), *S.pombe* (Saiki et al., 2003), *A.thaliana* (Suzuki & Rothstein, 1997), *Mus musculus*, and *Homo sapiens* (Saiki et al., 2005).

Long-chain PDSs can be classified into homodimeric (e.g., octa-PDS IspB in *E.coli*), heterodimeric (e.g., GerC1 and GerC3 in *B.subtilis*), and heterotetrameric types [e.g., deca-PDSs Dps1 and D-less polyprenyl diphosphate synthase (Dlp1) in *S.pombe*] based on their component patterns.

A

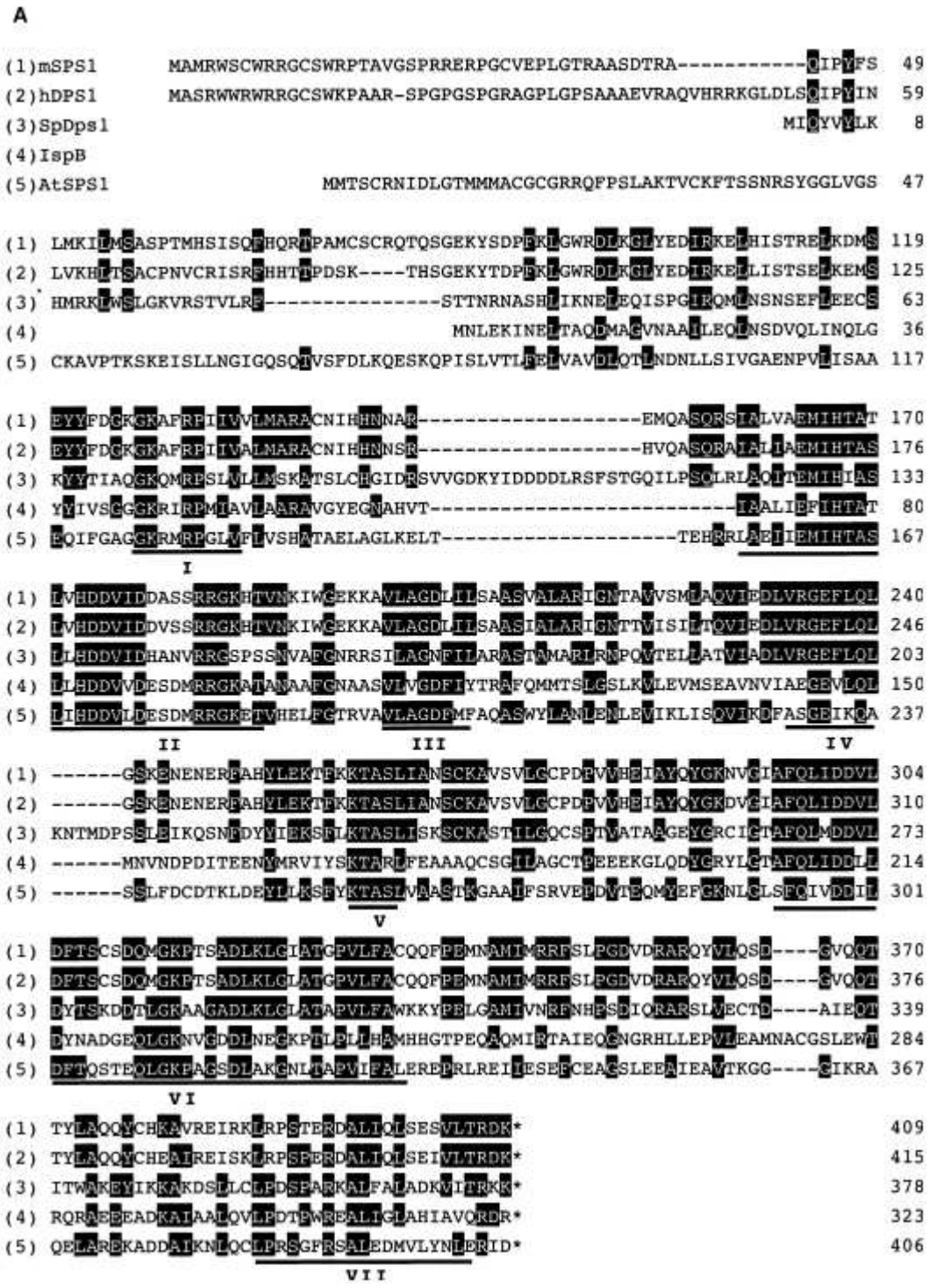
(1)mSPS1 MAMRWSCWRRGCSWRPTAVGSPRRERPGCVEPLGTRAASDTRA 49
(2)hDPS1 MASRWWRWRRGCSWKPAAR-SPGPGSPGRAGPLGPSAAAEVRAQVHRRKGLDLS 59
(3)SpDps1 MI 8
(4)IspB
(5)AtSPS1 MMTSCRNIDLGTMMMACGCGRRQFPSLAKTVCKFTSSNRSYGGLVGS 47
(1) 119
(2) 125
(3) 63
(4) 36
(5) 117
(1) 170
(2) 176
(3) 133
(4) 80
(5) 167
I
(1) 240
(2) 246
(3) 203
(4) 150
(5) 237
II
III
IV
(1) 304
(2) 310
(3) 273
(4) 214
(5) 301
V
(1) 370
(2) 376
(3) 339
(4) 284
(5) 367
VI
(1) 409
(2) 415
(3) 378
(4) 323
(5) 406
VII

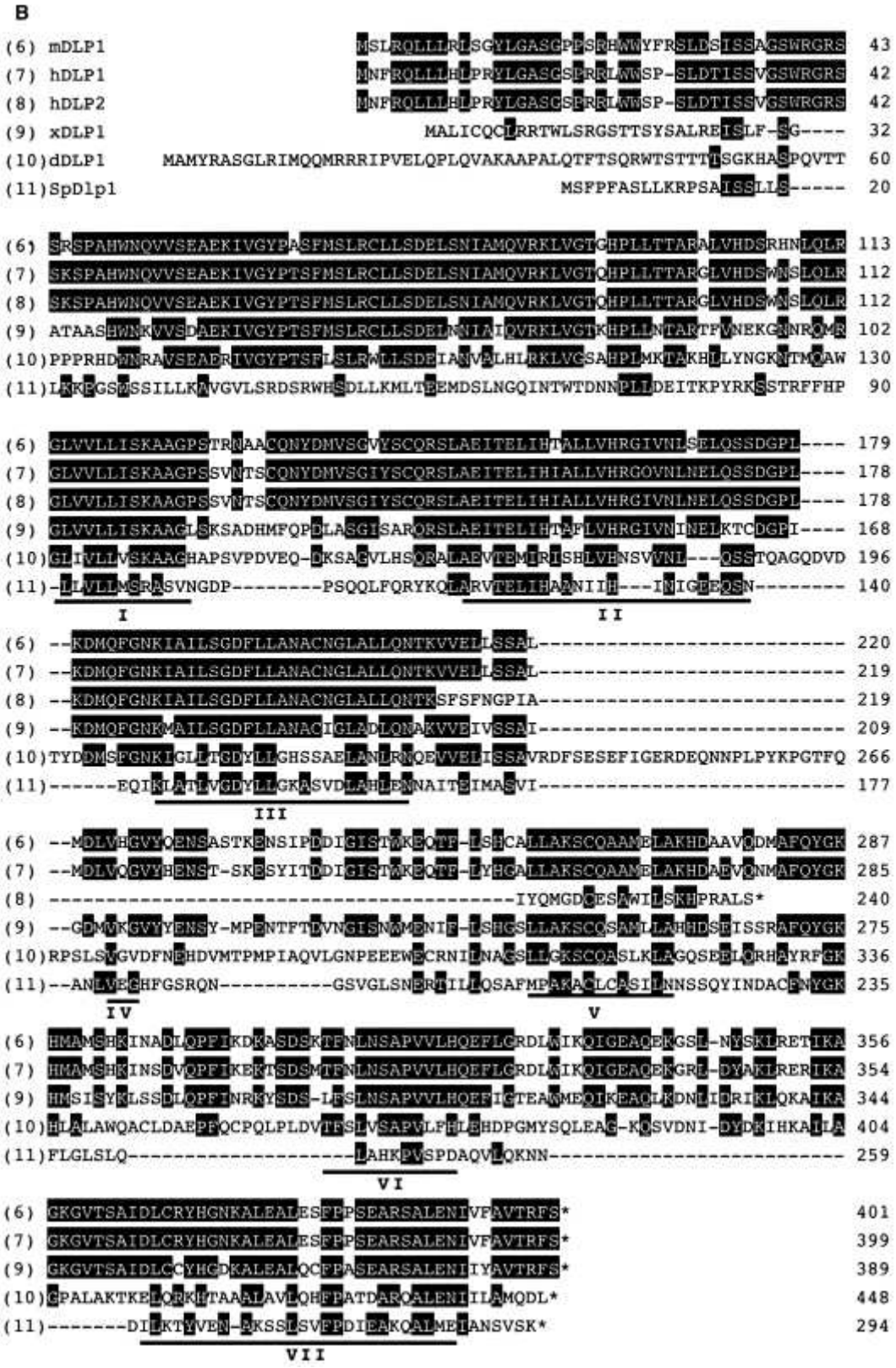
B
(6) mDLP1
(7) hDLP1
(8) hDLP2
(9) xDLP1
(10)dDLP1
(11)SpDlp1
I
II
III
IV
V
VI
VII

Fig. 4.12 (A) The alignment displays the amino acid sequences of known long-chain-producing trans-prenyl diphosphate synthases. (B) The alignment showcases the amino acid sequences of a partner protein present in the long-chain trans-prenyl diphosphate synthases of certain organisms. Residues that are conserved in more than three sequences are enclosed within boxes. Conserved regions (I–VII) are indicated with underlines. While the characteristic aspartate rich DDXXD motifs in regions II and VI were present in (A), they were absent in (B). Amino acid residue positions are indicated on the right. The numbered entries correspond to the following components: (1) One of the two components of solanesyl diphosphate synthase in the mouse, encoded by *mSps1* (NCBI Accession no. AB210841). (2) One of the two components of decaprenyl diphosphate synthase in humans, encoded by *hDPS1* (accession no. AB210838). (3) One of the two components of decaprenyl diphosphate synthase in *S.pombe*, encoded by *SpDps1* (accession no. D84311). (4) The octaprenyl diphosphate synthase in *E.coli* encoded by *ispB* (accession no. U18997). (5) The solanesyl diphosphate synthase in *A.thaliana* encoded by *AtSPS1* (accession no. AB188497). (6) The other component of solanesyl diphosphate synthase in the mouse, the *SpDlp1* homolog *mDLP1* (accession no. AB210840). (7) The other component of decaprenyl diphosphate synthase in humans, the *SpDlp1* homolog *hDLP1* (accession no. AB210839). (8) A splicing variant of *hDLP1*, *hDLP2* (accession no. AI742294). (9) The *Xenopus SpDlp1* homolog *xDLP1* (Accession no. BC082488). (10) The *Drosophila SpDlp1* homolog *dDLP1* (accession no. AY05159). (11) The *S.pombe SpDlp1* gene (accession no. AB118853) (Saiki et al., 2005).

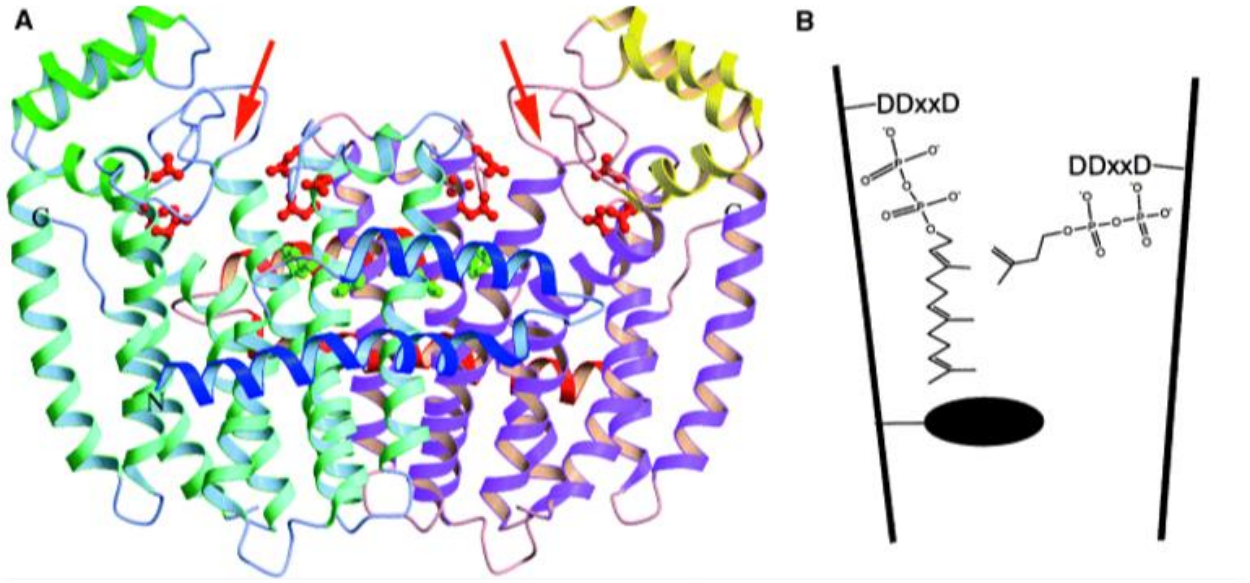

Fig.4.13 A) The crystal structure of trans-type FPPS is depicted in a ribbon diagram format. A dimeric arrangement is formed by two identical subunits, creating a four-layer helix bundle. The N-terminal α helical hairpins within the outer layers are color-coded in blue and red to represent the two individual subunits, while the eight helices in the inner layers are depicted in cyan and magenta. Two smaller peripheral domains are highlighted in green and yellow. Active sites are marked with red arrows, where the aspartate side chains of the two DDxxD motifs within each subunit are also shown in red. The phenylalanine side chains of F112 and F113, crucial for regulating product length, are displayed in green. B) The 5th amino acid (depicted as a filled black circle) before the first DDxxD motif in the sequence is situated adjacent to the tail of FPP. A bulky amino acid at this position has the capacity to obstruct further elongation of the product chain, serving as a mechanism for controlling the length of the product chain (P. H. Liang et al., 2002).

4.B.1.3 Solanesyl and decaprenyl diphosphate synthases in mice and humans

Solanesyl and deca-PDSs from mice and humans were identified as heterotetrameric types (Saiki et al., 2005). Similarly, in *S.pombe*, the decaprenyl diphosphate synthase exhibits a heterotetrameric structure comprising two proteins, SpDps1 (*S.pombe* decaprenyl diphosphate synthase) and SpDlp1 (*S.pombe* D-less polyprenyl diphosphate synthase) (Saiki et al., 2003).

In the case of murine enzymes, a solanesyl diphosphate synthase consists of two essential components: mouse solanesyl diphosphate synthase (mSPS1 or mPDSS1) and mouse D-less polyprenyl pyrophosphate synthase (mDLP1 or mPDSS2). Conversely, the human enzyme is a decaprenyl diphosphate synthase composed of human decaprenyl diphosphate synthase (hDPS1 or hPDSS1) and human D-less polyprenyl diphosphate synthase (hDLP1 or hPDSS2). It's noteworthy that mSPS1 and hDPS1 retain all the conserved regions observed in homodimeric prenyl diphosphate synthases and SpDps1, while mDLP1 and hDLP1 are homologous to SpDlp1.

Saiki et al. (2005) stated that the hPDSS1 gene maps to chromosome 10p12.1, and the hPDSS2 to chromosome 6q21. The predicted 415-amino acid hPDSS1 shares 82% identity with its mouse orthologous, mPDSS1, and contains the 7 conserved domains and DDxxD motifs typical of trans-prenyl diphosphate synthases. The predicted 399-amino acid hPDSS2 shares 88% identity with its mouse homolog, mPDSS2, and contains the 7 conserved domains typically found in trans-prenyl diphosphate synthases, but it lacks DDxxD motifs.

While mSPS1 and hDPS1 have demonstrated the capability to establish functional complexes with SpDlp1 in *S.pombe,* it is noteworthy that mDLP1 and hDLP1 exhibit an inability to form functional complexes with SpDps1, as observed in a study by Saiki et al. (2005).

In a separate investigation conducted by Mollet et al. (2007), the growth of a mutant strain on glycerol-rich medium was successfully restored through the introduction of the yeast *COQ1* gene. However, it is essential to highlight that neither wild-type nor mutant human *PDSS1* cDNAs could achieve the same complementation, thereby underscoring the inability of human prenyl diphosphate synthase to complement the yeast Δ*coq1*-null mutation (Mollet et al., 2007).

Furthermore, in budding yeast, it was found that SpDps1 failed to function effectively as a component alongside Coq1 (Zhang et al., 2008).

Notably, there is emerging evidence suggesting that both mSPS1 and hDPS1 may have a stronger role in influencing the isoprenoid chain length of ubiquinone in *E.coli* (Saiki et al., 2005). However, it is imperative to replicate these observations within eukaryotic systems to ascertain their broader applicability.

4.B.1.4 Characterizing *COQ1*: Hexaprenyl Diphosphate Synthase in Yeast

The polyprenyl diphosphate synthase in *S.cerevisiae* is represented by Coq1*,* hexaprenyl diphosphate synthase (HPS)*,* an enzyme responsible for the producing of the isoprenoid tail (Kawamukai, 2009).

The *COQ1* gene encoding a hexa-PDS consists of 473 amino acids. Similar to several other long-chain PDSs, it is possible to describe seven highly conserved regions including the first aspartate-rich motif (FARM) in domains II and the second aspartate-rich motif (SARM) in domain VI, that are considered to be the binding site for the substrate (M. Zhang et al., 2008).

The protein Coq1 was observed to be associated with the matrix side of the inner mitochondrial membrane (Gin & Clarke, 2005). This localization aligns with various pieces of evidence pointing to the existence of a specific sequence termed the mitochondrial targeting sequence (MTS). The MTS plays a crucial role in directing the translated protein to this subcellular compartment (Ashby & Edwards, 1990). Importantly, this signal is not essential for the protein's functionality; typically, it is removed after the protein's entry into the organelle, allowing the enzyme to undergo proper folding (Yen et al., 2020).

The mitochondrial targeting signal of Coq1 was empirically delineated for the purpose of rescuing a *Coq1*-deficient yeast strain. The objective was to substitute the missing gene with the *E.coli* homolog, *IspB*. However, the sole utilization of the bacterial sequence proved ineffective in this regard. Notably, the only construct that successfully reinstated respiration in the Δ*coq1* yeast encompassed a specific segment from the N-terminal region of Coq1, encompassing 53 amino acids. This segment

was fused with the *IspB* gene and placed under the control of the *coq1* gene's promoter (Okada et al., 1996). This fragment from the *coq1* gene appeared to be indispensable for facilitating the translocation of the IspB enzyme into the mitochondria, as evidenced by the production of CoQ_8 in addition to the native CoQ_6 (Okada et al., 1996). It is worth noting that the same genetically modified yeast strain, when grown on fermentable carbon sources, did not generate CoQ_8. Collectively, these outcomes underscore the potential for functional complementation of yeast deficiencies with proteins from diverse species and underscore the species-specific nature of the polyprenyl synthase product (Okada et al., 1996).

In previous studies, it was demonstrated that Coq1 in *E.coli* functions as a hexa-PDS, similar to its role in *S.cerevisiae*. However, a surprising revelation came from *S.pombe*, where Coq1 cannot operate independently but forms a heteromer with *S.pombe* Dps1, resulting in deca-PDS activity. This heterotetrameric enzyme arises from the interaction between Coq1 and Dps1 originating from different species or origins within *S.pombe*. This unexpected discovery sheds light on the evolutionary transition of long-chain trans-PDSs from homomeric to heteromeric forms (M. Zhang et al., 2008).

It is plausible that a heteromeric version of PDS first emerged in *S.pombe* or in ancestral organisms, eventually evolving into the form observed in humans. The functional artificial heteromeric PDSs, comprising Coq1 and Dps1 or IspB and Dps1 (Cui et al., 2010; Zhang et al., 2008), lend support to the hypothesis that the heteromeric form originated from the homomeric version. Notably, the primary structures of the core components of heteromer-type enzymes closely resemble those of their homomeric counterparts. These findings raise intriguing questions regarding the evolutionary reasons behind the development of heteromer-type enzymes in specific species, including mice and humans.

4.B.1.5 CoQ_{10} deficiency arising from *PDSS1* and *PDSS2* mutations

CoQ_{10} deficiency results in a syndrome characterized by neurological symptoms, including impairments in vision and hearing, sometimes accompanied by cardiac and kidney issues (Quinzii et al., 2008). Among these symptoms, the visual system appears to be particularly affected in cases involving the early stages of CoQ_{10} synthesis, such as in *PDSS1*, *PDSS2*, or *COQ2* deficiency (Mollet et al., 2007; Salviati et al., 2012).

PDSS1 deficiency is a rare, clinically diverse disorder that should be considered when diagnosing individuals with optic atrophy and sensorineural deafness. Sensorineural deafness typically precedes optic atrophy in PDSS1 deficiency. It's worth noting that CoQ_{10} synthesis defects are treatable conditions and should be included in the list of potential diagnoses for optic atrophy and sensorineural deafness, despite their rarity (Nardecchia et al., 2021).

Rötig et al. (2000) identified patients with a coenzyme Q10 deficiency affecting multiple tissues. These patients exhibited significantly low levels of decaprenyl-diphosphate within cell extracts, indicating a deficiency in *trans*-prenyltransferase (TPT) activity. However, no mutations were found in the TPT cDNA. Messenger RNA levels were also notably low in normal fibroblasts and lymphoblastoid cell lines, making it challenging to compare them with CoQ_{10}-deficient cells. Rotig et al. (2000) proposed that the disease-causing mutation might exist either in a different region of the TPT gene or in another gene responsible for regulating TPT activity.

Mollet et al. (2007) reported a consanguineous Moroccan family in which two siblings exhibited COQ10 deficiency-2 (COQ10D2; # 614651). This condition presented as a multisystem disorder characterized by early-onset deafness, optic atrophy, mild mental retardation, peripheral neuropathy, obesity, livedo reticularis, and cardiac valvulopathy. Enzyme analysis revealed reduced quinone-dependent oxidative phosphorylation activity, and COQ_{10} deficiency was confirmed by the restoration of oxidative phosphorylation activity upon quinone addition. Through homozygosity mapping and candidate gene analysis, a homozygous mutation in the PDSS1 gene, NM_014317.5(PDSS1):c.924T>G (p.Asp308Glu), was identified. Introduction of a corresponding mutation into yeast Coq1 resulted in impaired growth on respiratory medium. In the case of a female

infant with COQ10D2, Vasta et al. (2012) identified compound heterozygous missense mutations in the PDSS1 gene, NM_014317.5(PDSS1):c.661C>T (p.Arg221Ter) and NM_014317.5(PDSS1):c.1108A>C (p.Ser370Arg), through sequencing a panel of genes associated with mitochondrial function.

Two Egyptian sisters, born to consanguineous parents, presented with COQ10D2, and Nardecchia et al. (2021) identified a homozygous missense mutation in the PDSS1 gene, NM_014317.5(PDSS1):c.735G>T (p.Gln245His), using whole-exome sequencing. This mutation segregated with the disorder within the family.

In a case of COQ10D2 in a boy, (Bellusci et al., 2021) detected compound heterozygosity involving a missense, NM_014317.5(PDSS1):c.716T>G (p.Val239Gly), and a nonsense, NM_014317.5(PDSS1):c.1183C>T (p.Arg395Ter), mutation in the PDSS1 gene.

In an infant with primary coenzyme Q10 deficiency-3 (COQ10D3; # 614652) leading to fatal encephalomyopathy and nephrotic syndrome, López et al. (2006) identified compound heterozygosity for two mutations in the *PDSS2* gene. One mutation was a c.964C>T transition, resulting in NP_065114.3(PDSS2):p.Gln322Ter substitution, and it was inherited from the unaffected father. The second mutation was a c.1145C>T transition, resulting in a NP_065114.3(PDSS2):p.Ser382Leu with the substitution in the seventh conserved domain, and it was inherited from the unaffected mother.

Biochemical assays using radiolabeled substrates indicated a severe defect in decaprenyl diphosphate synthase in the patient's fibroblasts. Coenzyme Q_{10} (CoQ_{10}) is a crucial lipophilic molecule responsible for transferring electrons from mitochondrial respiratory chain complexes I and II to complex III, and the *PDSS2* gene encodes a subunit of the initial enzyme in the coenzyme Q10 biosynthetic pathway.

Furthermore, Peng et al. (2008) discovered that *Pdss2* knockout in mice led to embryonic lethality, with no homozygous embryos surviving beyond embryonic day 10.5. When *Pdss2* knockout was specifically targeted to renal glomerular podocytes, it resulted in nephrotic syndrome but did not affect coenzyme Q levels in whole kidney homogenates, likely due to the limited number of kidney cells affected. However, when *Pdss2* knockout was directed at hepatocytes, it caused coenzyme Q

depletion in whole liver homogenates, impaired mitochondrial respiratory chain function, and disrupted fundamental metabolic processes.

4.B.1.6 Exploring PDS Enzyme Subunits in Coenzyme Q Biosynthesis

The roles of the human and murine polyprenyl diphosphate synthases subunits remain relatively undefined, posing unresolved questions regarding CoQ biosynthesis and species-specific mechanisms. While it is widely accepted that the PDS enzyme plays a role in determining the ubiquinone's side chain length, it remains unclear if there is functional differentiation between the two subunits in species where the enzyme comprises distinct subunits. Specifically, which of the two proteins is responsible for determining the number of isoprenoid units remains an open question.

Yeast serves as an ideal model organism for this purpose, allowing us to express heterologous polyprenyl diphosphate synthase subunits and define their specific functions. Moreover, previous experiments have shown that another type of CoQ is sufficient to restore growth on glycerol plates, indicating the significance of the quinone ring over the side chain for ubiquinone's function (Okada et al., 1998). Furthermore, experiments in *E.coli* have revealed that heterologous combinations of full-length *mPdss1-hPDSS2* and *hPDSS1-mPdss2* can collaborate to produce ubiquinone (Saiki et al., 2005).

In our investigation, we utilize a yeast model system to elucidate which subunit, among the solanesyl and decaprenyl diphosphate synthases found in mice and humans, predominantly influences the elongation of the side chain of the ubiquinone precursor. Functional complementation tests are the initial experiments to investigate these interactions between enzyme subunits and explore the mechanism of chain length determination.

4.B.2 Materials and Methods

4.B.2.1 Molecular Cloning

4.B.2.1.1 Cloning into yeast expression vector: *hPDSS1*, *hPDSS2*, *mPdss1* and *mPdss2*

The *mPdss1* (NM_019501.4) coding sequence, derived from Mouse Embryonic Fibroblasts (MEFs), was amplified using High-Fidelity Phusion DNA polymerase (NEB) and specific primers, *mPdss*1-24F and *mPdss*1+1257R, following the manufacturer's instructions. The resulting sample was then extracted and purified using the Qiagen Extraction Gel Kit. Subsequently, we performed the TOPO-TA cloning reaction according to the manufacturer's protocol, which involved adding A overhangs to the product obtained from the *mPdss1* PCR gel extraction and then cloning it into pCRIITOPO (Invitrogen). The sequence was confirmed through Sanger sequencing.

For *hPDSS2,* NM_020381.4 (already contained in a pAAV2 CMV lentiviral vector in our laboratory) and *mPdss1*, amplification was carried out using AmpliTaq Gold DNA polymerase (Thermo Fisher) with specific primers that included the BamHI and NotI restriction sites: *mPdss1*/*hPDSS2*_BamHI FOR, *mPdss1*_HA_NotI REV, or *hPDSS2*_NotI REV, which also contained the HA tag sequence at the 3' end in the case of *mPdss1*. Subsequently, the PCR product and the pCM184 and pCM189 vectors underwent double digestion with the BamHI and NotI restriction enzymes. Following the manufacturer's instructions, after ligation and bacterial transformation, positive colonies were selected, and Sanger sequencing confirmed the correctness of the sequence.

For the *hPDSS1* (NM_014317.5) coding sequence, cloning was performed in pCM189 using the In-Fusion® HD Kit (Takara). First, the gene was amplified from a human cDNA clone obtained from Origene, using a specific set of primers designed with the manufacturer's online tool, including BamHI and NotI restriction sites. The reverse primer also included the HA sequence at the 3' end: *hPDSS1* FOR and *hPDSS1* REV. The PCR product was purified and gel-extracted using the Qiagen Extraction Gel Kit. The destination vector, pCM189, was linearized through double enzyme

restriction with BamHI and NotI and then extracted using the Qiagen Extraction Gel Kit. The In-Fusion reaction was performed, and the resulting product was used to transform chemical bacterial cells, followed by the selection of positive colonies. Sanger sequencing was conducted to verify the correct sequence of the insert in the vector.

The coding sequence of *mPdss2* (NM_027772.2) was cloned into the pCM184 yeast expression vector using the In-Fusion kit (Takara) and following the manufacturer's instructions. The *mPdss2* cDNA was amplified using Phusion polymerase (NEB), starting from the pAAV2 CMV lentiviral vector already present in our laboratory, with the primers *mPdss2* FOR and REV, following the manufacturer's instructions. The destination vector, pCM184, was linearized through PCR using the primers pCM184 FOR and pCM184 REV. The two products were then cloned together using the In-Fusion reaction. Positive colonies were selected, and the sequence was confirmed through Sanger sequencing. All the sequences used in this study are listed in Table 4.3, while primers used for cloning *hPDSS1*, *hPDSS2*, *mPdss1*, and *mPdss2* into yeast expression vectors pCM189 and pCM184 are listed in Table 4.4.

Gene name	Reference nucleotide sequence	Reference protein sequence
yCOQ1	Z35872.1	CAA84939.1
hPDSS1	NM_014317.5	NP_055132.2
hPDSS2	NM_020381.4	NP_065114.3
mPdss1	NM_019501.4	NP_062374.2
mPdss2	NM_027772.2	NP_082048.2

Table 4.3 List of reference sequences used in our study.

Primer name	Sequence 5'->3'	Purpose
mPdss1+1257R	AGCTGCCAGAAAGAAGAGGA	Amplification of *mPdss1* from cDNA for cloning in pCRIITOPO
mPdss1-24F	CGCCGCGACTTTCAGACTT	Amplification of *mPdss1* from cDNA for cloning in pRIITOPO

*hPDSS2*_BamHI FOR	CTCTCGGATCCACCCTTCCAGACTCAAACCA	Amplification of *hPDSS2* with BamHI restriction site for cloning in pCM184
*hPDSS2*_NotI REV	CTCTGCGGCCGCCGCTCCCAATCAACCTCATT	Amplification of *hPDSS2* with NotI from for cloning in pCM184
mPdss1_BamHI FOR	CTCTCGGATCCCGCCGCGACTTTCAGACTTG	Amplification of *mPdss1* with BamHI restriction site from pCRIITOPO for cloning in pCM189
*mPdss1*_HA_NotI REV	CTCTGCGGCCGCTCAAGCGTAATCTGGAACATC GTATGGGTATTTATCTCTGGTGA	Amplification of *mPdss1* with NotI from pCRIITOPO for cloning in pCM189
hPDSS1 FOR	TCAATTCGGGGGATCAGACTCCGACCATGGCCTC	Amplification of *hPDSS1* with BamHI from cDNA for cloning in pCM189
hPDSS1 REV	CCTGCAGGGCCCTAGCGGCCTCAAGCGTAATCT GGAACATCGTATGGGTATTTATCTCTTGTGAGTACAATTTCT	Amplification of *hPDSS1* with NotI from cDNA for cloning in pCM189
pCM184 FOR	CGCTAGGGCCCTGCAGGAG	Linearization of the pCM184 vector for cloning *mPdss2*.
pCM184 REV	GGCCTGTTTAAACGGATCCCCC	Linearization of the pCM184 vector for cloning *mPdss2*.
mPdss2 FOR	CCGTTTAAACAGGCCATGAGCCTCCGGCAGCTG	Amplification of *mPdss2* from pAAV2 CMV for cloning in pCM184
mPdss2 REV	TGCAGGGCCCTAGCGTCAAGAAAATCTGGTCACAGCAAAC	Amplification of *mPdss2* from pAAV2 CMV for cloning in pCM184

Table 4.4 Oligonucleotides used in this study to clone human/murine *PDS* subunit 1 genes into pCM189 and human/murine *PDS* subunit 2 genes into pCM184, respectively.

4.B.2.1.2 Design of Hybrid *PDS* Subunit 1 Genes

Hybrid *PDS* subunit 1 genes (hybrids 1, 2, 3, 4, and 5) were constructed by combining N-terminal mPDSS1 regions of varying lengths with their corresponding C-terminal hPDSS1 regions. A different approach was taken for Hybrid 6, which was designed by merging the yMTS (53aa) segment, previously identified by Okada et al. (1996), with the complete hPDSS1 protein without any removal of segments. The strategy adopted for the design of the hybrid PDS subunit 1 protein is detailed in Figure 4.14 and Table 4.5.

Conversely, for Hybrid 7, we employed a reverse strategy by combining a specific N-terminal hPDSS1 amino acid region with the corresponding C-terminal mPDSS1 protein region. All cloning procedures were carried out using the In-Fusion® HD Cloning Kit (Takara) in accordance with the

manufacturer's instructions, along with specific primers designed using the company's online tool, which are listed in Table 4.6.

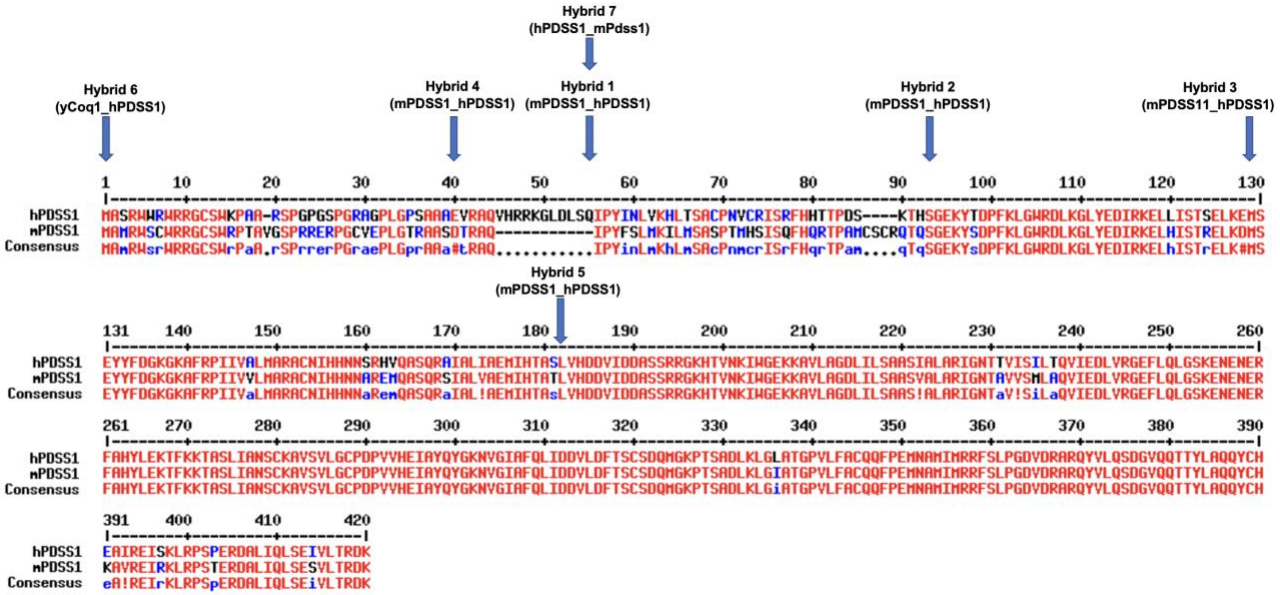

Figure 4.14. Multiple sequence alignment of human PDSS1 (NP_055132.2) and murine PDSS1 (NP_062374.2) proteins (Corpet, 1988), illustrating the strategy employed for the design of hybrid PDS subunit 1 proteins.

Hybrid name	N-terminal PDS subunit 1 sequence	C-terminal PDS subunit 1 sequence
Hybrid 1	mPDSS1 1-44 aa	hPDSS1 55-415 aa
Hybrid 2	mPDSS1 1-82 aa	hPDSS1 89-415 aa
Hybrid 3	mPDSS1 1-118 aa	hPDSS1 125-415aa
Hybrid 4	mPDSS1 1-40	hPDSS1 40-415 aa
Hybrid 5	mPDSS1 1-171	hPDSS1 178-415 aa
Hybrid 6	yCoq1: 1-53 aa	hPDSS1 1-415 aa
Hybrid 7	hPDSS1 1-54 aa	mPDSS1 45-409 aa

Table 4.5 Design of the hybrid PDS subunit 1 proteins.

Primer name	Sequence 5'->3'	Purpose
hPDSS1 Hybrid 1 FOR	ATACCCTATATTAATCTTGTGAAGC	Linearization of the pCM189-h*PDSS1* vector at a specific hPDSS1 C-terminal region for Hybrid 1 design.

hPDSS1 Hybrid 2 FOR	GGTGAAAAATACACCGATCCTTTC	Linearization of the pCM189-h*PDSS1* vector at a specific hPDSS1 C-terminal region for Hybrid 2 design.
hPDSS1 Hybrid 1,2,3,4,5,6 REV	GGTCGGAGTCTGATCCCCC	Linearization of the pCM189-h*PDSS1* vector at a specific hPDSS1 C-terminal region for Hybrid 1, 2,3,4,5,6 design
mPdss1 Hybrid 1,2,3,4,5 FOR	GATCAGACTCCGACCATGGCTATGCGCTGGTCGT	Amplification from the pCM189-m*Pdss1* vector of a specific mPDSS1 N-terminal region for Hybrid 1,2,3,4,5 design.
mPdss1 Hybrid 1 REV	ATTAATATAGGGTATCTGCGCGCGGGTGTCCGA	Amplification from the pCM189-*mPdss1* vector of a specific mPDSS1 N-terminal region for Hybrid 1 design.
mPdss1 Hybrid 2 REV	GGTGTATTTTTCACCACTCTGAGTTTGACGACAACTGC	Amplification from the pCM189-*mPdss1* vector of a specific mPDSS1 N-terminal region for Hybrid 2 design.
hPDSS1 Hybrid 3 FOR	TCTGAGTACTACTTTGATGGGAAAG	Linearization of the pCM189-h*PDSS1* vector at a specific hPDSS1 C-terminal region for Hybrid 3 design.
mPdss1 Hybrid 3 REV	AAAGTAGTACTCAGACATGTCCTTTAGTTCTCTGGTGG	Amplification from the pCM189-m*Pdss1* vector of a specific mPDSS1 N-terminal region for Hybrid 3 design.
hPDSS1 Hybrid 4 FOR	GTCCGCGCGCAGGTTCATAG	Linearization of the pCM189-h*PDSS1* vector at a specific hPDSS1 C-terminal region for Hybrid 4 design.
mPdss1 Hybrid 4 REV	AACCTGCGCGCGGACGTCCGAGGCGGCACGTGT	Amplification from the pCM189-m*Pdss1* vector of a specific mPDSS1 N-terminal region for Hybrid 4 design.
hPDSS1 Hybrid 5 FOR	GTTCACGATGACGTTATTGACG	Linearization of the pCM189-h*PDSS1* vector at a specific hPDSS1 C-terminal region for Hybrid 5 design.
mPdss1 Hybrid 5 REV	AACGTCATCGTGAACCAGAGTAGCAGTGTGGATCATTTC	Amplification from the pCM189-m*Pdss1* vector of a specific mPDSS1 N-terminal region for Hybrid 5 design.
hPDSS1 Hybrid 6 FOR	ATGGCCTCGCGCTGGTGG	Linearization of the pCM189-h*PDSS1* vector at a specific hPDSS1 C-terminal region for Hybrid 6 design.

yCOQ1 Hybrid 6 FOR	GATCAGACTCCGACCATGTTTCAAAGGTCTGGCGCTG	Amplification from the pCM188-y*COQ1* vector of a specific mPDSS1 N-terminal region for Hybrid 6 design.
yCOQ1 Hybrid 6 REV	CCAGCGCGAGGCCATCATCTCCTTCGAGACTAATGATATG	Amplification from the pCM188-y*COQ1* vector of a specific mPDSS1 N-terminal region for Hybrid 6 design.
mPdss1 Hybrid 7 FOR	ATACCCTATTTTAGTCTTATGAAG	Linearization of the pCM189-m*Pdss1* vector at a specific mPDSS1 C-terminal region for Hybrid 7 design.
mPdss1 Hybrid 7 REV	GGTTCAAGTCTGAAAGTCG	Linearization of the pCM189-m*Pdss1* vector at a specific mPDSS1 C-terminal region for Hybrid 7 design.
hPDSS1 Hybrid 7 FOR	TTTCAGACTTGAACCATGGCCTCGCGCTGGTGG	Amplification from the pCM189-h*PDSS1* vector of a specific hPDSS1 N-terminal region for Hybrid 7 design
hPDSS1 Hybrid 7 REV	ACTAAAATAGGGTATCTGAGACAAGTCAAGTCCCTTCCG	Amplification from the pCM189-h*PDSS1* vector of a specific hPDSS1 N-terminal region for Hybrid 7 design

Table 4.6. Oligonucleotides used in this study for the cloning of hybrid *PDS* subunit 1 genes.

4.B.2.1.3 Mutagenesis of Murine *Pds* Subunits 1 and 2 Genes

All mutations within the coding sequences of *mPdss1* and *mPdss2* were introduced via site-directed mutagenesis utilizing the QuikChange Lightning kit (Agilent), with specific primers designed using the company's online tool. The accuracy of all constructs was verified through direct sequencing. The sequences of the oligonucleotides used in this study are provided in Table 4.7.

Primer name	Sequence 5'->3'	Purpose
His68Asn FOR	CTATGCATAGTATATCACAGTTTAATCAAAGGACACCAGCAATGTG	His68Asn mutagenesis in pCM189 *mPdss1*
His68Asn REV	CACATTGCTGGTGTCCTTTGATTAAACTGTGATATACTATGCATAG	His68Asn mutagenesis in pCM189 *mPdss1*

Asp117Gly FOR	CCACCAGAGAACTAAAGGGCATGTCCGAATACTACTT	Asp117Gly mutagenesis in pCM189 *mPdss1*
Asp117Gly REV	AAGTAGTATTCGGACATGCCCTTTAGTTCTCTGGTGG	Asp117Gly mutagenesis in pCM189 *mPdss1*
Lys191Glu FOR	CAAGTTCTCGAAGAGGAAAACATACAGTTAATGAGATCTGGGGTGAGAAAAA	Lys191Glu mutagenesis in pCM189 *mPdss1*
Lys191Glu REV	TTTTTCTCACCCCAGATCTCATTAACTGTATGTTTTCCTCTTCGAGAACTTG	Lys191Glu mutagenesis in pCM189 *mPdss1*
Val233Gly FOR	CCAAGTTATTGAAGATTTGGGGCGTGGTGAATTTCTTCAGC	Val233Gly mutagenesis in pCM189 *mPdss1*
Val233Gly REV	GCTGAAGAAATTCACCACGCCCCAAATCTTCAATAACTTGG	Val233Gly mutagenesis in pCM189 *mPdss1*
Gln239His FOR	GTGCGTGGTGAATTTCTTCATCTAGGGTCAAAAGAAAATG	Gln239His mutagenesis in pCM189 *mPdss1*
Gln239His REV	CATTTTCTTTTGACCCTAGATGAAGAAATTCACCACGCAC	Gln239His mutagenesis in pCM189 *mPdss1*
Gly290Arg FOR	GGTGCATGAGATAGCCTATCAGTATAGGAAAAATGTTGG	Gly290Arg mutagenesis in pCM189 *mPdss1*
Gly290Arg REV	CCAACATTTTTCCTATACTGATAGGCTATCTCATGCACC	Gly290Arg mutagenesis in pCM189 *mPdss1*
Asp302Glu FOR	GCTTTTCAGCTCATAGATGAGGTATTGGATTTCACCTCATG	Asp302Glu mutagenesis in pCM189 *mPdss1*
Asp302Glu REV	CATGAGGTGAAATCCAATACCTCATCTATGAGCTGAAAAGC	Asp302Glu mutagenesis in pCM189 *mPdss1*

Ser364Arg FOR	CGACAGTATGTATTACAGAGGGATGGCGTGCAGCAAA	Ser364Arg mutagenesis in pCM189 *mPdss1*
Ser364Arg REV	TTTGCTGCACGCCATCCCTCTGTAATACATACTGTCG	Ser364Arg mutagenesis in pCM189 *mPdss1*
Val117Met FOR	GATATGAGGAGCATGACCAGGCCCCGC	Val117Met mutagenesis in pCM184 *mPdss2*
Val117Met REV	GCGGGGCCTGGTCATGCTCCTCATATC	Val117Met mutagenesis in pCM184 *mPdss2*
His163Arg FOR	ACTGCTCTCCTGGTGCGTCGTGGGATAGTAAAC	His163Arg mutagenesis in pCM184 *mPdss2*
His163Arg REV	GTTTACTATCCCACGACGCACCAGGAGAGCAGT	His163Arg mutagenesis in pCM184 *mPdss2*
Ser384Leu FOR	TGGAGAGCTTCCCTCCCTTAGAGGCCAGA	Ser384Leu mutagenesis in pCM184 *mPdss2*
Ser384Leu REV	TCTGGCCTCTAAGGGAGGGAAGCTCTCCA	Ser384Leu mutagenesis in pCM184 *mPdss2*
Ala386Asp FOR	CCCTCCCTCAGAGGACAGATCGGCTTTAG	Ala386Asp mutagenesis in pCM184 *mPdss2*
Ala386Asp REV	CTAAAGCCGATCTGTCCTCTGAGGGAGGG	Ala386Asp mutagenesis in pCM184 *mPdss2*
Ile393Thr FOR	GGCCAGATCGGCTTTAGAAAACACTGTGTTTGCTGT	Ile393Thr mutagenesis in pCM184 *mPdss2*
Ile393Thr REV	ACAGCAAACACAGTGTTTTCTAAAGCCGATCTGGCC	Ile393Thr mutagenesis in pCM184 *mPdss2*

Table 4.7 List of the oligonucleotides used for the site-direct mutagenesis of *mPdss1* and mPdss2 genes.

4.B.2.2 Yeast strains, media, and plasmid transformation

The W303 *Δcoq1* strain (MATa; ade2-1; his3-1_15; leu2-3_112; trp1-1; ura3-1 YBR003W::kanMX4) was derived from a yeast strain originally obtained from Euroscarf (BY4741 *Δcoq1*) (MATa; his3Δ1; leu2Δ0; met15Δ0; ura3Δ0 YBR003w::kanMX4) and further modified in Prof. Leonardo Salviati's laboratory. The *KanMX4* cassette, required for *coq1* locus inactivation, was amplified from the genomic DNA of the BY4741 *Δcoq1* strain. The amplification was performed using standard rapid glass-bead lysis and phenol-chloroform extraction methods as previously described (Trevisson et al., 2009). PCR amplification of the *KanMX4* cassette was carried out with the *Kan* Amp FOR and REV primers. Subsequently, the resulting amplicon was used to transform the W303 yeast strain, achieving *coq1* locus inactivation through homologous recombination (HR). The inactivation procedure has been extensively documented elsewhere (Vetro et al., 2017).

Confirmation of *coq1* inactivation in the W303 yeast strain was achieved through genomic DNA extraction, PCR, and electrophoresis on agarose gel using a different set of primers, *Kan* Check FOR and REV, designed further upstream and downstream from those used for the *KanMX4* cassette amplification. A graphical representation of the *coq1* inactivation process is provided in Figure 4.15, and the list of oligonucleotides used for *KanMX4* cassette amplification and verification is presented in Table 4.8.

Yeast strains were cultured in either rich medium (YPD) or synthetic minimal medium (SM) at 30 °C. YPD (1% yeast extract, 2% peptone, 2% dextrose) was utilized for routine maintenance of the wild-type strain. Synthetic minimal medium (0.17% yeast nitrogen base without amino acids, 0.5% ammonium sulfate, 2% carbon source), supplemented with amino acids to compensate for yeast auxotrophies, except for uracil (pCM188 and pCM189 plasmid complementing yeast uracil autotrophy) and tryptophan (pCM184 plasmid complementing yeast tryptophan autotrophy), was employed for selecting transformant strains. YPGly medium (1% yeast extract, 2% peptone, and 3% glycerol) was used for functional complementation assays. All growth media components were sourced from Difco. Yeast DNA transformations were carried out using the polyethylene glycol-lithium acetate method, as previously described (Gietz & Woods, 2006).

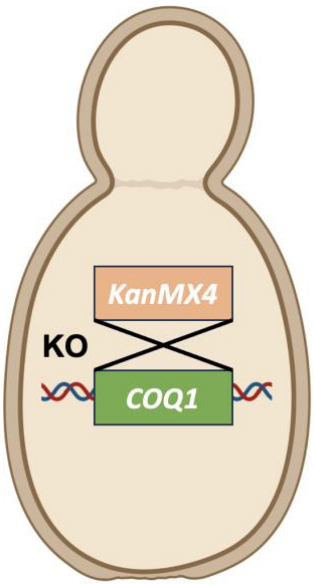

Fig.4.15 Representation of the working model used in this study to obtain a functional yeast-with the inactivation of *coq1* gene by the insertion of the *KanMX4* Cassette. This image was created using BioRender (BioRender.com).

Primer name	Sequence 5'->3'	Purpose
Kan Amp FOR	TGACCAGGTATACCACTATC	Amplification of *KanMX4* cassette from pFA6 with complementary regions for homologous recombination with *Coq1* locus and its inactivation
Kan Amp REV	CCACCAGCCTGATCCTTAATG	Amplification of *KanMX4* cassette from pFA6 with complementary regions for homologous recombination with *Coq1* locus and its inactivation
Kan Check FOR	TCTAGCGAATCTCCTGTTCC	Amplification of *Coq1* locus for checking for *KanMX4* module
Kan Check REV	TACAGACTATCCTATTTGC	Amplification of *Coq1* locus for checking for *KanMX4* module

Table 4.8 List of oligonucleotides used for the amplification of the *KanMX4* Cassette e and its control.

4.B.2.3 Functional complementation spot test assay

To assess the functional capacity of heterologous combinations of polyprenyl diphosphate synthases, we employed wild-type murine, human, and hybrid sequences, as well as mutant murine sequences, in rescuing respiratory growth in yeast strains lacking the *coq1* gene. The yeast strains were initially inoculated into selective liquid medium containing glucose and cultivated at 30°C for 48 hours. The concentration of each culture was then adjusted to OD_{600} = 1 (approximately 10^7 cells/mL) in sterile water, after two washes in water to remove glucose medium, and four serial 10-fold dilutions were performed. For each of these dilutions, 5µL were spotted onto YPD, SM Glu (with proper amino

acid selection), and YPGly, plate media. Plates were incubated at 30°C and images were taken up to 8 days after incubation.

4.B.2.4 HPLC and Analysis of the Quinone Content

This analysis was performed in the laboratory of Fabien Pierrel, in collaboration with the University of Grenoble Alpes and the CNRS (Grenoble, France) and following what it is reported by (Ozeir et al., 2015).

Cultures were grown in synthetic minimal medium, supplemented with the necessary amino acids to cover yeast auxotrophies, except for uracil and tryptophan. They were cultivated until reaching an OD_{600} of 1 and then chilled on ice for 30 minutes. Subsequently, cells were harvested via centrifugation, washed once with ice-cold water, and their wet weight was determined in pre-weighed Eppendorf tubes before being frozen at -20°C. For lipid extraction, glass beads (100 µl), 50 µl of KCl (0.15 m), a Q4 solution (4 µm in methanol, 2 µl/mg of wet weight), and 0.6 ml of methanol were added to cell pellets (10–30 mg wet weight) and the tubes were vortexed for 10 min. The cultures were cultivated in synthetic minimal medium, supplemented with amino acids to cover yeast auxotrophies, excluding uracil and tryptophan, until they reached OD_{600}=1 and then were placed on ice for 30 min, then the cells were collected by centrifugation, washed once with ice-cold water, and their wet weight was determined in pre-weighted Eppendorf tubes before freezing at −20 °C. For lipid extraction, glass beads (100 µl), 50 µl of KCl (0.15 m), a Q4 solution (4 µm in methanol, 2 µl/mg of wet weight), and 0.6 ml of methanol were added to cell pellets (10–30 mg wet weight) and the tubes were vortexed for 10 min. Neutral lipids were extracted by adding 0.4 ml of petroleum ether (40–60 °C boiling range) and by vortexing for 3 min. The phases were separated by centrifugation (3 min, 1000 × g at room temperature). The upper petroleum ether layer was transferred to a fresh tube. Petroleum ether (0.4 ml) was added to the glass beads and methanol-containing tube, and the extraction was repeated once more. The petroleum ether layers were combined and dried under argon. The lipids were resuspended in 100 µl of methanol, and aliquots were analyzed by reversed-phase high-pressure liquid chromatography (HPLC) on a Dionex U3000 system equipped with a C18

column (Betabasic-18, 5 µm, 4.6 × 150 mm, Thermo Scientific) at a flow rate of 1 ml/min with a mobile phase composed of 75% (98% (v/v) methanol, 2% (v/v) 1 m ammonium acetate), 5% isopropyl alcohol, and 20% acetonitrile. Hydroquinones present in injected samples were oxidized with a precolumn 5020 guard cell set in oxidizing mode (E, +600 mV). Electrochemical detection (ECD) was performed with a Coulochem III (ESA) equipped with a 5011A analytical cell (E1, −550 mV; E2, 550 mV). The standard Q4 solution was injected in the same conditions to generate a standard curve that was used to correct for sample loss during the organic extraction (on the basis of the recovery of the Q4 internal standard) and to quantify Q6. When mass spectrometry (MS) detection was needed, the flow was split after the diode array detector with an adjustable split valve (Analytical Scientific Instruments) to allow simultaneous EC (60% of the flow) and MS (40% of the flow) detections. MS detection was achieved with an MSQ Plus spectrometer (Thermo) used in positive mode with electrospray ionization. The probe temperature was 450 °C and the cone voltage was 80 V. Because of the precolumn guard cell, the following compounds were detected by single ion monitoring in their oxidized state: 4-AP6 (M + H+), m/z 515.9–516.9, 7–9 min, scan time 0.2 s; 13C6-4-AP6 (M + H+), m/z 521.9–522.9, 7–9 min, scan time 0.2 s; IDMQ6 (M + H+), m/z 559.9–560.9, 9.5–14 min, scan time 0.2 s; 13C6-IDMQ6 (M + H+), m/z 565.9–566.9, 9.5–14 min, scan time 0.2 s; DMQ6 (M + NH4+), m/z 577.9–578.9, 7–12 min, scan time 0.6 s; 13C6-DMQ6 (M + NH4+), m/z 583.9–584.9, 7–12 min, scan time 0.6 s; Q6 (M + NH4+), m/z 607.9–608.9, 9–11.5 min, scan time 0.2 s. MS spectra were also recorded between m/z 500 and 700 or 450 and 650 with a scan time of 0.4 s.

4.B.3 Results

4.B.3.1 Functional Complementation of Murine-Human *PDS* Genes

We conducted a spot test analysis using our *Δcoq1* yeast model strain to assess the potential of heterologous combinations of human and murine *PDS* genes to rescue the respiratory phenotype in our null-yeast strain when grown on non-fermentable medium. Our control groups included co-transformations of *Δcoq1* with pCM188 *yCOQ1* and pCM184 empty, which clearly complemented the inactivation of the *Coq1* locus. Additionally, we co-transformed our yeast model with pCM189 and pCM184, both of which were empty and, as a result, incapable of growth on glycerol medium
Our findings revealed that only two combinations demonstrated the capacity to enable yeast growth on respiratory medium: *mPdss1* paired with *mPdss2*, and *mPdss1* paired with *hPDSS2* (Fig.4.16)**.** This indicates that only the mPDSS1 protein effectively enters the mitochondria. Consequently, this discovery paved the way to further investigations aimed at identifying the N-terminal murine sequence responsible for mitochondrial import and conducting potential complementation studies using murine sequences to examine human mutations pathogenicity.

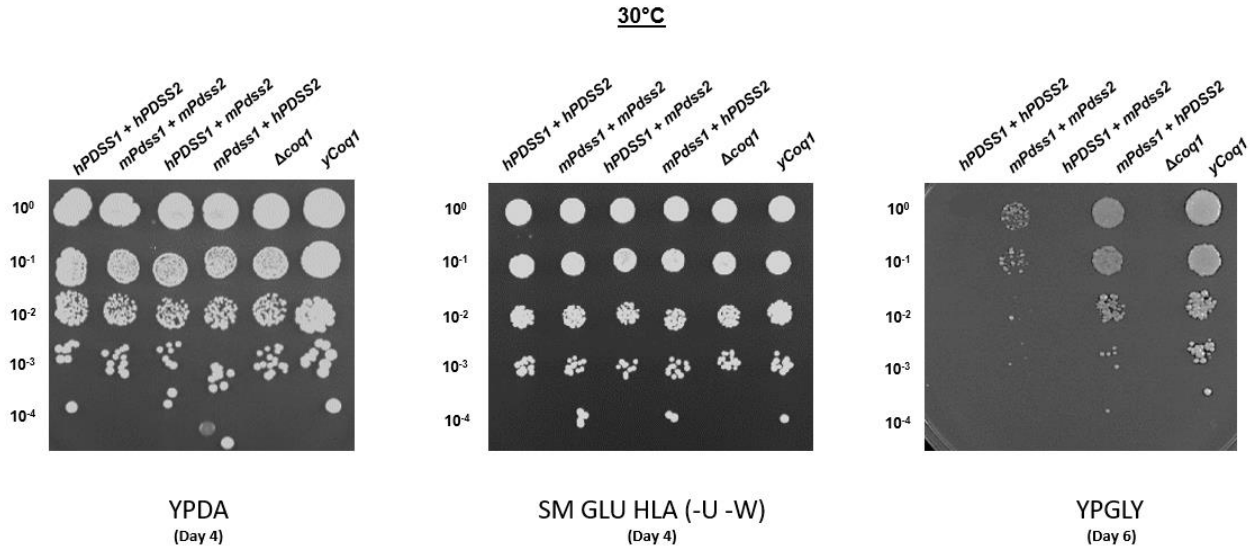

W303 MATa Δ*coq1*_pCM189 *hPDSS1/ mPdss1* _pCM184 *hPDSS2/mPdss2*

Figure 4.16 Functional complementation assays were performed by pairing heterologous combinations of human and murine *PDS* genes. Only combinations that were able to completely rescue the respiratory phenotype in our yeast model included the murine solanesyl diphosphate synthase and the combination of mouse PDS subunit 1 with human PDS subunit 2. The analysis was conducted using a spot test, where cell cultures were serially diluted and spotted onto various agar media, followed by incubation at 30°C. After 6 days, we specifically examined the results on YPGly medium to assess yeast respiration. Additionally, tests were conducted on rich medium (YPD) to evaluate the growth of all strains and on synthetic minimal medium (excluding uracil and tryptophan, which were provided by the plasmids used for co-transformation) to assess the growth of transformants. Images from these two tests were captured after 4 days. Each spot test analysis was replicated three times.

4.B.3.2 Functional Complementation of Murine-Human *PDS* Hybrid Genes

To uncover the murine targeting sequence responsible for yeast mitochondrial import, we decided to design a series of hybrid constructs. These hybrids combined varying lengths of the N-terminal regions of murine PDS subunit 1 with their corresponding C-terminal regions from human PDS subunit 1. This approach was employed for hybrids numbered 1 through 5.

Hybrid 6, designed as a control, featured the yeast mitochondrial targeting sequence (MTS) previously identified by Okada et al., (1996). This MTS comprised the initial 53 amino acids of the *yCOQ1* gene and was seamlessly integrated at the N-terminus of the *hPDSS1* coding sequence, without any excision.

Additionally, we conceived hybrid 7 with the hypothesis that the murine MTS might not be located in the N-terminal region but potentially within the C-terminal region of the mPDSS1 protein. Consequently, hybrid 7 was generated by merging the N-terminal portion of human PDS subunit 1 (1-54 aa) with the C-terminal segment of murine PDS subunit 1 (45-509 aa).

All of these hybrid proteins were co-expressed with the human PDS subunit 2 in order to assess whether the hypothetical murine mitochondrial targeting sequence (MTS) could restore decaprenyl diphosphate synthase functionality within the mitochondria of the yeast null-strain model, allowing it to thrive on non-fermentable medium.

Notably, we made a significant discovery: Hybrid 5 was the only hybrid capable of rescuing the respiratory deficiency observed in the *Δcoq1* yeast strain (Fig. 4.17, 1). This hybrid was carefully constructed by combining the N-terminal portion of the mPDSS1 protein, comprising the initial 171 amino acids, with the corresponding C-terminal segment of the hPDSS1 protein (amino acids 178-

415), as visually depicted in Figure 4.14. This compelling finding strongly suggests that the key component of the murine MTS likely resides within the N-terminal domain of the mPDSS1 protein, specifically within the span of amino acids 119 to 171.

Supporting this hypothesis, Hybrid 3, featuring only the N-terminal region of mPDSS1 spanning amino acids 1-118, displayed no growth on respiratory medium (Fig. 4.17). Additionally, Hybrid 7, which also exhibited no growth on a non-fermentable carbon source, provided evidence that the putative MTS could not be confined solely to the region of amino acids ranging from 45 to 409 within the mPDSS1 protein.

Collectively, these results confirm that the presumed murine MTS may require the entire N-terminal region of mPDSS1, spanning from amino acids 1 to 171, but it could potentially be shorter possibly extending from the first amino acid of the mPDSS1 protein to the second one within the 119-171 region. This indicates that the N-terminal region spanning amino acids 1 to 171 represents the maximum potential length of the putative mitochondrial targeting sequence. Furthermore, Hybrid 6 facilitated the entry of the hPDSS1 protein into yeast mitochondria, as evidenced by the growth of the null-strain model expressing decaprenyl diphosphate synthase with the yeast MTS fused to human PDS subunit 1, as depicted in Figure 4.17 (2).

Lastly, we assessed Hybrids 5 and 6 in conjunction with murine PDS subunit 2 and observed their ability to complement the *Δcoq1* yeast model, shown in Fig.4.17 (3), albeit with slightly weaker growth compared to their human counterparts. This aligns with the notion that subunits of the same species tend to exhibit more robust compatibility than heterologous subunits.

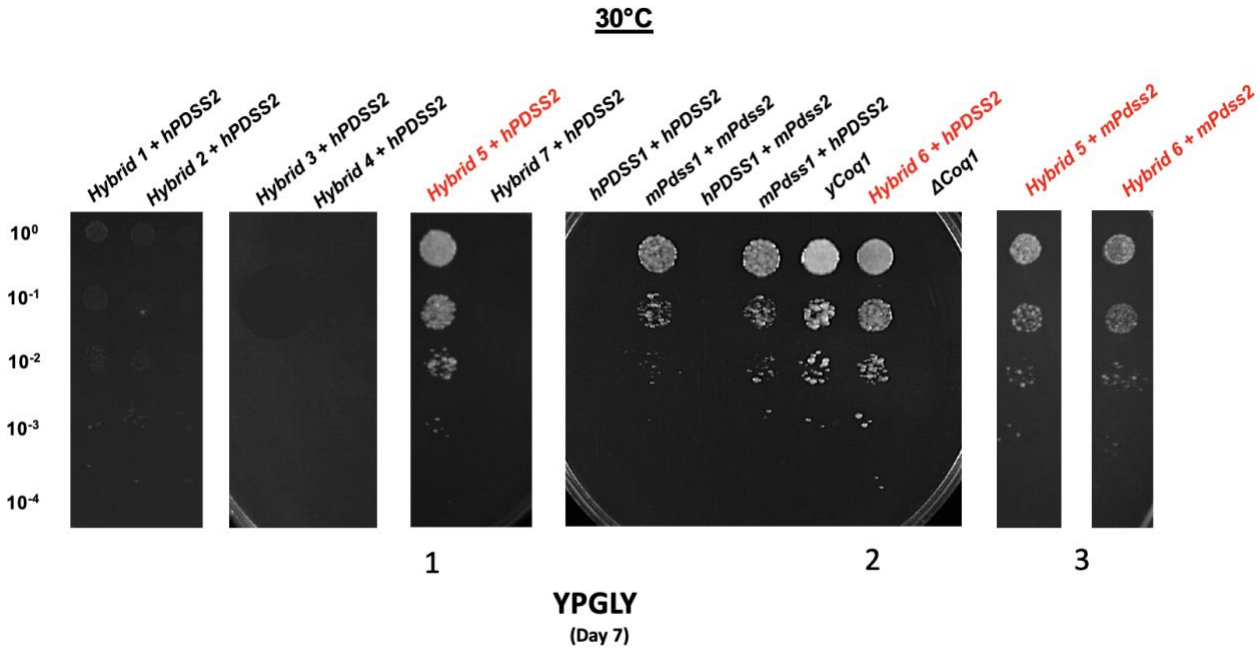

Fig.4.17 Functional complementation assays by pairing various combinations of hybrid PDS subunit 1 genes with human or murine PDS subunit 2 genes. Here are the key findings:1) Hybrid 5 demonstrated the ability to fully rescue the respiratory deficiency in our *Δcoq1* yeast model, allowing for the mitochondrial import of the human decaprenyl diphosphate synthase. This suggests that the primary component of the murine MTS likely resides within the amino acid range of 119 to 171. However, it appears that the N-terminal region of mPDSS1, extending from amino acid 1 to one within the 119-171 region, may also be required. 2) Hybrid 6, in combination with the human PDSS2 protein, effectively complemented the null-strain yeast model, providing further confirmation that the yeast MTS functioned properly in a heterotetrametric enzyme as well. Hybrid 5 and Hybrid 6 successfully rescued the respiratory phenotype even in the presence of murine PDSS2 protein. However, their yeast growth appeared weaker compared to those with their human subunit 2 counterparts. The analysis was conducted using a spot test, involving serial dilution of cell cultures spotted onto various agar media and incubated at 30°C. After 7 days, we specifically assessed the results on YPGly medium to evaluate yeast respiration. Additionally, tests were performed on rich medium (YPD) to assess the growth of all strains and on synthetic minimal medium (excluding uracil and tryptophan, which were provided by the plasmids used for co-transformation) to evaluate the growth of transformants. Images from these two tests are not provided. Each spot test analysis was replicated three times.

4.B.3.3 HPLC and Analysis Q Content

Q content analysis was conducted in collaboration with Fabien Pierrel from the University of Grenoble Alpes and CNRS (Grenoble, France). The Q was extracted and measured from strains expressing various combinations of murine and human *PDS* genes, as well as hybrid PDS subunit 1 proteins paired with either human or murine PDS subunit 2 proteins. These combinations successfully rescued the respiratory phenotype of the *Δcoq1* yeast model. The aim was to identify the type of ubiquinone (Q) produced in each case.

Surprisingly, as illustrated in Figure 4.18, it appears that the type of Q produced may be influenced by the specific PDS subunit 1 expressed. This observation underscores the significant role of the primary subunit of polyprenyl diphosphate synthase in determining the length of the isoprene chain in the ubiquinone molecule.

The results revealed that the null-strain yeast model successfully restored Q6 synthesis, while it remained entirely absent in the *Δcoq1* yeast strain. Notably, the wild-type strain (W303 MATa) exhibited the highest recorded Q6 value (72.88 pmoles/mg cells; data not shown).

Interestingly, the expression of murine solanesyl diphosphate synthase in our yeast model led to the production of Q_9, the same type of Q typically found in mice (Fig. 4.18). Remarkably, even when murine PDS subunit 1 was co-expressed with human PDS subunit 1, Q_9 was predominant, further emphasizing the pivotal role of PDS subunit 1 in determining the length of the ubiquinone side chain. Hybrid 5, when paired with human PDS subunit 2, exhibited a combination of Q_9 and Q_{10}, with Q_{10} levels nearly double those of Q_9. Conversely, when paired with murine PDS subunit 2, Hybrid 5 produced only Q_9. This variation may be attributed to the design of Hybrid 5, which combines an extended N-terminal mPDSS1 region with the C-terminal hPDSS2 region, as well as the presence of mPDSS2, potentially favoring Q_9 production.

Hybrid 6 facilitated the entry of human PDS subunit 1 into yeast mitochondria, enabling the assembly of human decaprenyl diphosphate synthase. This predominantly resulted in Q_{10} production, with a minor quantity of Q_9. When combined with murine PDS subunit 2, Hybrid 6 also primarily produced Q_{10}, albeit in slightly lower quantities compared to its combination with human PDS subunit 2. In this case as well, a small quantity of Q_9 was produced.

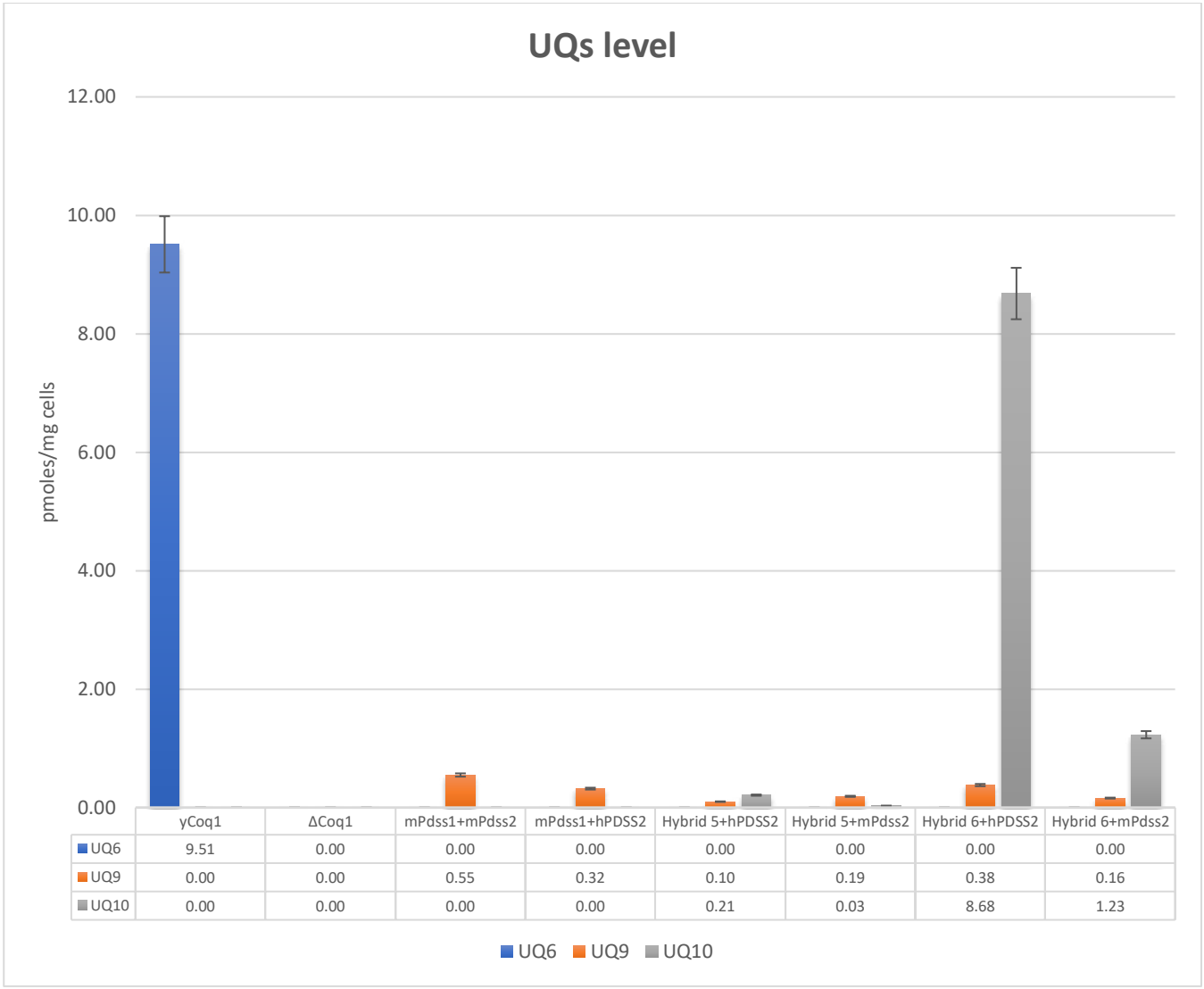

	yCoq1	ΔCoq1	mPdss1+mPdss2	mPdss1+hPDSS2	Hybrid 5+hPDSS2	Hybrid 5+mPdss2	Hybrid 6+hPDSS2	Hybrid 6+mPdss2
UQ6	9.51	0.00	0.00	0.00	0.00	0.00	0.00	0.00
UQ9	0.00	0.00	0.55	0.32	0.10	0.19	0.38	0.16
UQ10	0.00	0.00	0.00	0.00	0.21	0.03	8.68	1.23

Fig.4.18 Analysis of Q content was conducted on respiring strains co-expressing various combinations of murine and human PDS genes, as well as hybrid PDS subunit 1 genes in conjunction with either human or murine PDS subunit 2 genes. Surprisingly, it became evident that the type of Q produced may be influenced by the specific PDS subunit 1 that is expressed. This observation underscores the significant role of the primary subunit of polyprenyl diphosphate synthase in determining the length of the isoprene chain within the ubiquinone molecule. Each value was determined based on the assessment of four independent colonies for every strain.

4.B.3.4 Patients

The previous study involving the complementation of *Δcoq1* using heterologous combinations of human and murine *PDS* genes demonstrated the potential utility of murine sequences as a model for studying human mutations affecting conserved residues and assessing their pathogenicity based on growth on respiratory medium.

This approach represents the simplest and most elegant method for investigating human mutations, especially considering that human *PDS* genes alone cannot rescue the respiratory phenotype of the yeast strain lacking the *Coq1* gene. The use of hybrid PDS subunit 1 proteins (Hybrid 5 and 6) in combination with human PDS subunit 2 may not be as advantageous in this context. This is because it introduces a mixture of sequences from different species (yeast model with a combination of mouse and human genes) in a single experiment, potentially introducing artifacts. Additionally, mutations located in the N-terminal region of the human PDS subunit 1 protein may be affected by the presence of the additional yeast MTS, which could potentially alter their true effects.

Considering this, we examined a total of 8 mutations identified in the *hPDSS1* gene and 5 mutations in the *hPDSS2* gene (Table 4.9). Among these mutations, ten have been previously documented in published references. Additionally, one mutation, denoted as the murine protein alteration p.(Val117Met), is unique to the kd mouse model. The second mutation, p.(Ile393Thr), was discovered in combination with a nonsense mutation in a pediatric patient who underwent molecular analysis at a facility collaborating with our institution, the Clinical and Epidemiological Genetics Unit at the University Hospital of Padua.

Human Gene name	Protein Human Change	Protein Mouse Change	Phenotype	Zigosity	Reference
hPDSS1	p.(His78Asn)	p.(His68Asn)	Late onset retinitis pigmentosa, hearing impairment.	Compound heterozygous with missense p.(Gly296Arg)	Jurkute et al., 2022
hPDSS1	p.(Glu123Gly)	p.(Asp117Gly)	Late onset retinitis pigmentosa, hearing impairment.	Compound heterozygous with a nonsense mutation	Jurkute et al., 2022
hPDSS1	p.(Val239Gly)	p.(Val233Gly)	5 months old, mitochondrial encephalopathy, pulmonary hypertension, livedo reticularis, chronic distal phalangeal involvement, 3-methyl-glutaconic aciduria, and tricarboxylic aciduria. Child passed away at the age of 3 years	Compound heterozygous with a nonsense mutation	Bellusci et al., 2021
hPDSS1	p.(Gln245His)	p.(Gln239His)	2 siblings. 14 years old: deafness, optic atrophy, mild intellectual disability, muscular weakness, valvulopathy. 6 years old: optic atrophy.	Homozygous	Nardecchia et al., 2020
hPDSS1	p.(Gly296Arg)	p.(Gly290Arg)	Late onset retinitis pigmentosa, hearing impairment.	Compound heterozygous with missense p.(His78Asn)	Jurkute et al., 2022
hPDSS1	p.(Asp308Glu)	p.(Asp302Glu)	Early-onset deafness, encephalo-neuropathy, obesity, livedo reticularis, valvulopathy.	Homozigous	Mollet et al., 2007
hPDSS1	p.(Ser370Arg)	p.(Ser364Arg)	Died 16 months old. Developmental delay, nephrotic syndrome, perventricular and brainstem white matter lesions.	Compound heterozygous with a nonsense mutation	Vasta el al., 2012
hPDSS2	p.(Val116Met)	p.(Val117Met)	Present in kd mouse model: resulting in isolated steroid-resistant nephrotic syndrome.	Homozygous	This work
hPDSS2	p.(His162Arg)	p.(His163Arg)	Neonatal-onset nephrotic syndrome, encephalomyopathy, deafness, retinitis pigmentosa, and hypertrophic cardiomyopathy. Died at 8 months of age.	Compound Heterozygous with a large deletion	Iványi et al., 2018
hPDSS2	p.(Ser382Leu)	p.(Ser384Leu)	Neonatal-onset phenotype in compound heterozygosity with a nonsense mutation: encephalopathy, nephrotic syndrome Died at 8 months of age. Pediatric-onset phenotype in homozygosity: steroid-resistant nephrotic syndrome	Compound heterozygous with a nonsense mutation or in homozygous	Lopez et al., 2006; Sadowski et al., 2015
hPDSS2	p.(Ala384Asp)	p.(Ala386Asp)	Variant of Uncertain Significance (VUS): Mutation not yet	Homozygous	Sadowski et al., 2015

			characterized in the literature.		
hPDSS2	p.(Ile391Thr)	p.(Ile393Thr)	Patient displays a mild pediatric-onset phenotype that emerges at around one year of age: nephrotic syndrome and mild encephalopathy	Compound heterozygous with a nonsense mutation	This work

Table 4.9 Patients mutations along with a mutation, p.(Val117Met) in *mPdss2* which was exclusively identified in a mouse model.

4.B.3.5 Analyzing Human Mutations Through Murine Sequences

Analyzing yeast strains expressing mPDSS1 mutants in combination with wild type mPDSS2 protein reveals that the respiratory phenotype reliably characterizes the pathogenicity of the examined human mutations. It's important to note that this method may not be sensitive enough to detect minor growth reductions. The murine p.(His68Asn) mutation exhibited robust growth on a non-fermentable carbon source, resembling the mild human phenotype, as shown in Table 4.8. This similarity can be explained by the fact that in humans, this mutation is compound heterozygous with Gly296Arg, which becomes murine Gly290Arg. Both mutations rescued the respiratory phenotype, aligning with the late-onset retinitis pigmentosa and hearing impairment observed in humans.

The human Glu123Gly, corresponding to murine Asp117Gly due to the similarity between Glu and Asp, demonstrated a complete rescue of yeast respiration impairment. The mild human phenotype, characterized by late-onset retinitis pigmentosa and hearing impairment, may be attributed to the presence of a single functional gene copy, as it is in compound heterozygous with a nonsense mutation.

The human Val239Gly (murine Val233Gly) displayed partial growth on respiratory medium, consistent with the severe phenotype observed in patients (Table 4.9). This human mutation was found in a compound heterozygous state with a nonsense mutation.

The human homozygous Gln245His mutation (murine Gln239His) resulted in a complete yeast growth impairment, reflecting the multiple complications observed in two siblings.

The human Asp308Glu and Ser370Arg mutations, corresponding to murine Asp302Glu and Ser364Arg, showed no growth on respiratory medium, mirroring the human phenotype. The first

mutation was found in a homozygous state and exhibited a complex clinical picture (Table 4.9). The second mutation was compound heterozygous with a nonsense mutation and its severity is confirmed by the clinical presentation of the patient who passed away prematurely.

A) ***mPdss1*** **mutations**

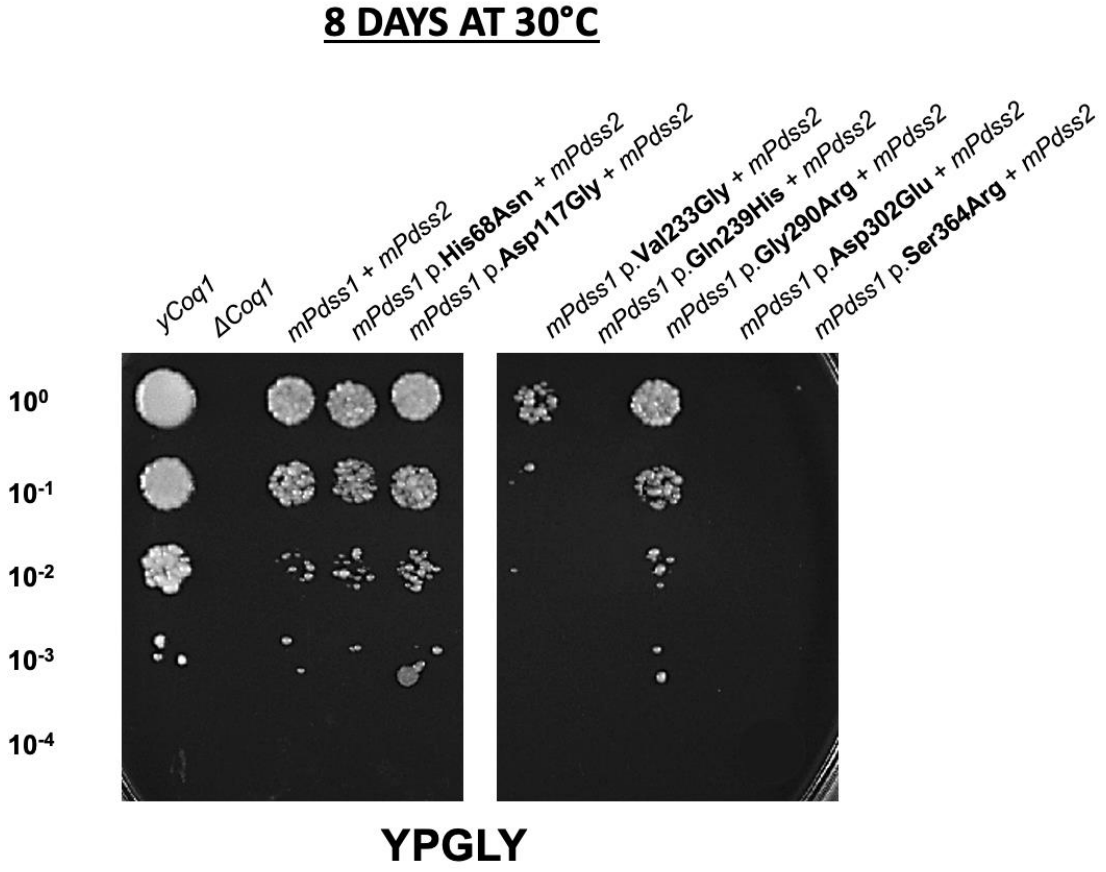

W303 MATa Δ*coq1*_pCM189 *mPdss1* mutant _pCM184 *mPdss2* wild type

B) ***mPdss2*** **mutations**

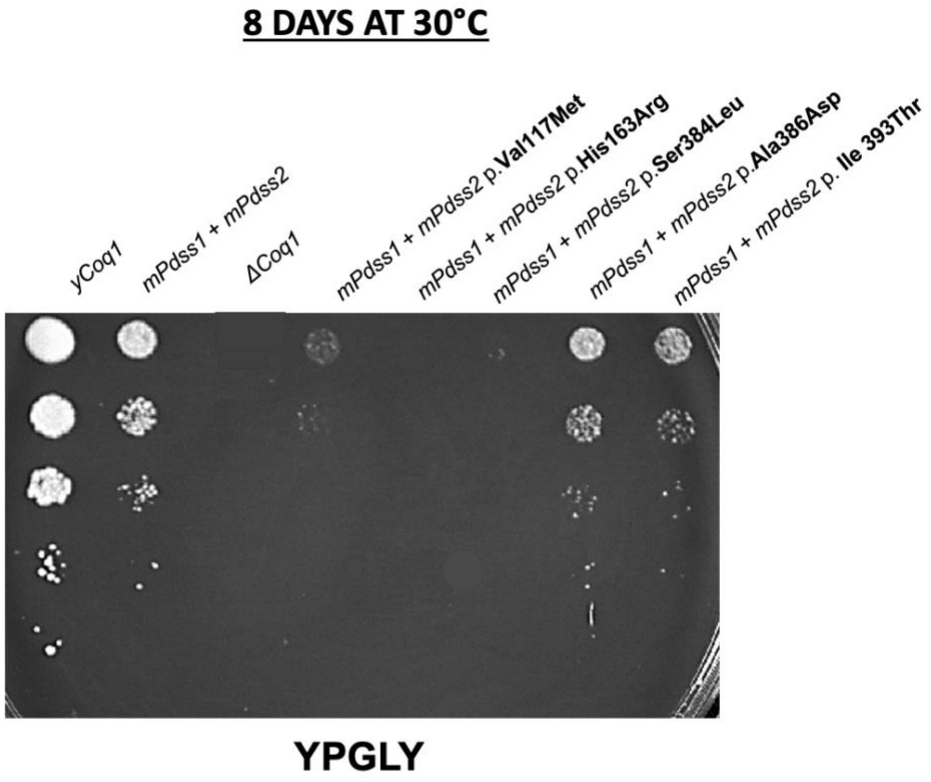

Figure 4.19 Functional complementation assays by pairing mutant mPDSS1 with wild-type mPDSS2 (A) and wild-type mPDSS1 with mutant mPDSS2 proteins (B). Some of these mutations completely compromised the ability of the murine solanesyl diphosphate synthase to compensate for the absence of endogenous yCoq1. The analysis was carried out using a spot test, where cell cultures were serially diluted and spotted onto various agar media, followed by incubation at 30°C. After 8 days, we observed the results specifically on YPGly medium to assess yeast respiration. Additionally, tests were conducted on rich medium (YPD) to assess the growth of all strains and on synthetic minimal medium (except for uracil and tryptophan, which were supplied by the plasmids used for co-transformation) to evaluate the growth of transformants; however, the data from these tests are not presented. Each spot test analysis was replicated three times.

The same analysis was performed using the identical yeast model to assess the respiratory capacity of strains expressing solanesyl diphosphate synthase with murine subunit 2 mutants. The slightly growth observed in the murine Ser384Leu mutant (Figure 4.19) aligns with the severe human phenotype associated with the Ser382Leu mutation (Table 4.9), which was found either in conjunction with a nonsense mutation (Lopez at al., 2006) or in homozygous state (Sadowki et al., 2015). The symptoms identified in compound heterozygosity with a nonsense mutation showed neonatal-onset encephalopathy, nephrotic syndrome leading to a premature death. Instead, we

identified mild symptoms with pediatric-onset phenotype (after the first year of life) in homozygosity: steroid-resistant nephrotic syndrome.

The murine Ala386Asp mutation, which corresponds to the human homozygous mutation Ala384Asp, led to the restoration of the respiratory phenotype. The pathogenicity of this mutation is still a subject of debate in the literature. It seems to resemble a variant of uncertain significance (VUS), and the growth observed in the yeast model expressing the murine mutation would further support its non-pathogenic nature.

The homozygous murine Val117Met mutation, which is specific to the kd mouse model, resulted in isolated steroid-resistant nephrotic syndrome. These mild symptoms are consistent with the partial yeast growth observed when a non-fermentable carbon source was used.

The compound heterozygous condition involving the human Ile391Thr (corresponding to the murine Ile393Thr) in combination with a nonsense mutation resulted in a clinical presentation characterized by early onset nephrotic syndrome and mild encephalopathy at approximately one year of age. This clinical presentation aligns with the growth observed in yeast expressing the murine Ile393Thr on a respiratory medium.

4.B.4 Discussion

Exploring the intriguing factors that determine the organization of polyprenyl diphosphate synthase (PDS) into either heteromeric enzymes or homomeric structures across various organisms, regardless of their evolutionary status, continues to captivate scientific curiosity. The presence of these enzymes in higher eukaryotes alone does not seem to dictate their structural arrangements. For instance, the presence of heteromeric structures in organisms like *S.pombe*, mice, and humans challenges this notion. This enigma leaves us with several unanswered questions that demand extensive research. Understanding why evolution has led to the structuring of these subunits into pairs or even trios, as observed in *A.thaliana*, remains an intriguing path of exploration.

Makoto Kawamukai's research, carried out in the 1990s and early 2000s, aimed to understand the function of *PDS* genes by studying various model organisms. He focused on examining how polyprenyl diphosphate synthase (PDS) is structured and organized in different organisms, without being influenced by their place in the evolutionary hierarchy. His discoveries showed that PDS enzymes can form either heterotetrameric, homodimeric or heterodimeric structures, and this pattern doesn't depend on how complex the organism is in terms of evolution. This variability appears to be governed by intrinsic factors specific to each organism, as the membrane lipid composition or the affinity for binding proteins (Kawamukai, 2018).

Our aim was to utilize a straightforward eukaryotic organism like *S.cerevisiae*, evolutionarily closer to humans than *S.pombe*, to express the solanesyl and decaprenyl diphosphate synthases from mammals. This approach enabled us to investigate which of the two *PDS* genes played a pivotal role in determining the length of the ubiquinone (Q) precursor's side chain.

Our initial findings revealed a fascinating discovery – the ability to reconstruct a functional enzyme with a heteromeric structure using either both murine PDS proteins or a heterologous combination of murine subunit 1 and human subunit 2 proteins within an *in vivo* yeast model, even in the absence of the yeast's native PDS gene. This led to full restoration of respiratory function and emphasized the conservation of these essential genes in eukaryotes. Interestingly, *S.cerevisiae* typically exhibits both homodimeric and homotetrameric structures for heptaprenyl diphosphate synthase (Zhang et

al., 2008). This novel approach provided a powerful tool for characterizing the pathogenicity of human mutations by modeling them on conserved residues of the murine *PDS* coding sequence and studying their impact on the respiratory phenotype. This method may not be sufficiently sensitive to characterize the minor reductions in yeast growth induced by mutations associated with varying degrees of phenotypic severity. Detecting subtle variations that might be challenging to observe on solid medium alone can be achieved by using liquid media containing glycerol.

The same outcome was observed when hybridizing the human PDS subunit 1 protein with yeast or mouse mitochondrial targeting sequences (MTS) to facilitate entry into yeast mitochondria, in combination with either human or murine PDS subunit 2 protein. These results demonstrated that, regardless of their species of origin, homologous proteins retained their catalytic and functional domains to perform their activities even in foreign species.

The analysis of the Q content yielded strong evidence suggesting that the *PDS* subunit 1 gene plays a pivotal role in determining the isoprene chain length in the Q precursor. This aligns with earlier studies on crystal structures conducted in the early 2000s, which indicated that polyprenyl diphosphate synthase subunit 1 likely possesses a more catalytic function, while subunit 2 has a more structural role, as it lacks aspartate-rich domains. Additionally, the HPLC data corroborated earlier studies conducted by Saki et al. (2005), demonstrating a significant influence of the origin of the heterologous PDS on the length of the isoprene chain in the produced Q in the model organism. To fully comprehend the HPLC analysis results, it's important to note that Hybrid 6 contains the complete *hPDSS1* gene, including the yMTS region upstream, without any regions removed. Conversely, Hybrid 5 is a hybridization of PDS subunit 1, where the first 171 amino acids originate from mPDSS1, followed by the subsequent 237 amino acids from hPDSS1. Consequently, it's reasonable to assume that we introduced some putative regions beyond the murine MTS. This includes domain I and a part of domain II, both of which are among the conserved regions of *PDS* subunit 1 genes. Domain II contains specific amino acids that play a role in determining the side chain length, as documented by.Saiki et al., 2008.

Our insights into the design of these hybrid strains may explain why the strain expressing Hybrid 6 in conjunction with its natural counterpart (hPDSS2), can produce a significantly higher concentration of UQ_{10} compared to that of Hybrid 5 together with human PDS subunit 2.

In general, when we expected a favorable environment for UQ_{10} production due to the presence of hPDSS1 with its distinctive (murine/yeast) mitochondrial targeting sequence (as seen in Hybrid 5 together with h*PDSS2*, Hybrid 6 along with h*PDSS2,* but also in Hybrid 6 with m*Pdss2*), traces of UQ_9 were still observed. This phenomenon could potentially be attributed to the fact that decaprenyl diphosphate synthase primarily generates UQ_{10} in larger quantities but also produces UQ_9 in smaller amounts. This phenomenon might be attributed to its potential inefficiency in *S.cerevisiae*, similar to what was observed in *E.coli* when expressing the *S.pombe* orthologous *PDS* genes, as reported by Saiki et al. in 2005, where both UQ_9 and UQ_{10} were detected.

Notably, Hybrid 5 together with m*Pdss2* appears to exclusively produce UQ_9. This observation might be a consequence of the dual nature (murine/human) of Hybrid 5, resulting from its hybrid design, and its combination with the murine counterpart, which appears to favor UQ_9 production.

In general, while HPLC was mainly employed as a semi-quantitative method, the measured Q levels are significantly lower compared to the wild type, represented by W303 MATa. The highest recorded values were for UQ_6 produced by the yeast model expressing the yCoq1 protein and UQ_{10} obtained through the combination of Hybrid 6 with h*PDSS2*. However, these levels are still notably lower than the quantity produced by the wild type. Nevertheless, the Q levels proved to be adequate for inducing growth recovery, indicating that wild-type cells typically contain a surplus of ubiquinone beyond what is necessary for basic cell metabolism (Saiki et al., 2005).

Moreover, biochemical analysis of mitochondrial respiratory complexes can provide additional insights into mitochondrial respiration. Western blot analysis focusing on the protein expression levels of heterologous, hybrid, and mutant subunits can offer a comprehensive view of mitochondrial activity across all the strains we generated. This multifaceted approach will enable us to gain a deeper understanding of polyprenyl diphosphate synthase dynamics and its implications in various cellular processes.

The observation that the type of Q produced may be influenced by the specific PDS subunit 1 that is expressed is significant because it suggests that the composition of the Q pool can be manipulated by expressing different *PDS* subunit 1 genes. This could have implications for the treatment of diseases that are associated with Q deficiency, such as Parkinson's disease and Friedreich's ataxia.

PART IV.C

Exploring Genotype-Phenotype Correlation of Human *COQ5* Gene Mutations Through Functional Yeast Study

4.C.1 Introduction

4.C.1.1 *COQ5* gene

As widely discussed in the general introduction (Part IV of the presented thesis) CoQ consists of a polyisoprenoid "tail" that anchors it to the lipid membrane and a benzoquinone "head" responsible for shuttling electrons from Complexes I and II to Complex III in the mitochondrial respiratory chain (Bentinger et al., 2010; Crane et al., 1957).

In yeast, multiple genes are essential for Q_6 biosynthesis, some of which encode proteins located in the mitochondrial inner membrane, forming a multi-subunit complex referred to as the CoQ-synthome (He et al., 2014). The absence or deficiency of any of these genes results in the inability to produce Q_6, making growth on a medium with a non-fermentable carbon source unachievable. Each Coq polypeptide's presence is crucial for assembling the Coq polypeptide complex and ensuring the proper function of individual enzymes (Hsieh et al., 2007). Overexpression of *COQ8*, encoding a putative regulatory kinase, has been demonstrated to restore steady-state levels of several Coq polypeptides (Xie et al., 2012)and the assembly of the high molecular mass CoQ-synthome (He et al., 2014). *COQ* genes exhibit a high degree of conservation throughout evolution, and various human *COQ* genes have successfully complemented their corresponding yeast coq null mutants (Salviati et al., 2005; Wang & Hekimi, 2013).

Coq5 plays a crucial role in catalyzing the sole C-methylation step involved in Q_6 synthesis in yeast (Barkovich et al., 1997). It is the sole C-methyltransferase enzyme known to participate in Q_6 synthesis, catalyzing the methylation of demethyl-demethoxy-Q_6H2 (DDMQ6H2) to form demethoxy-Q_6H2 (DMQ_6H2) (Fig.4.20). Coq5, along with several other COQ gene products, is part of the CoQ-synthome, a high molecular mass complex peripherally associated with the mitochondrial inner membrane in yeast (He et al., 2014).

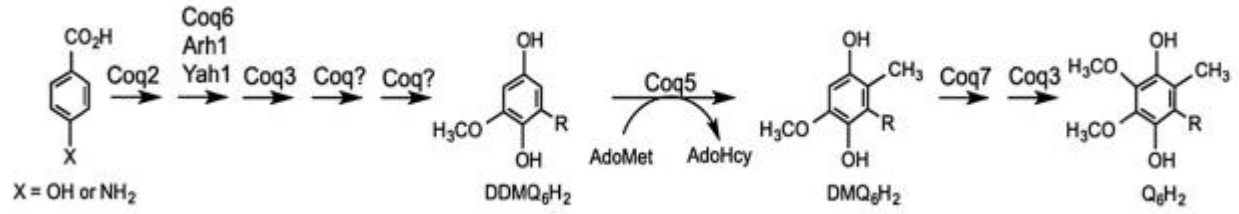

Fig. 4.20. Biosynthesis of Q in *S.cerevisiae* and the amino acid alignment of COQ5 homologs are depicted. (A) The benzoquinone head group of Q is derived from either the 4HB or pABA aromatic ring precursor, prenylated by Coq2, and subsequently modified by Coq polypeptides to generate the Q_6 intermediate known as demethyl-demethoxy-hydroquinone ($DDMQ_6H2$). Coq5 facilitates the transfer of a methyl group from AdoMet to the C2 position of the hydroquinone ring, resulting in the formation of demethoxy-Q_6 (DMQ_6H2). This compound is further converted into the fully substituted Q_6H2 (Nguyen et al., 2014).

4.C.1.2 Identification of the *COQ5* gene

Nguyen and collaborators (2014) confirmed that the human COQ5 protein is localized to the mitochondrial matrix and peripherally associated with the inner membrane. Additionally, they demonstrated that hCOQ5 physically interacts with hCOQ4, indicating the presence of a COQ multi-enzyme complex in human cells.

Nguyen et al. (2014) identified the human *COQ5* gene (h*COQ5*) cDNA sequence through a screening of the Expressed Sequence Tag (EST) database, using the tBLASTn algorithm. The yeast protein sequence served as the query for this search, and this approach was inspired by Sacconi et al., (2005). The h*COQ5* gene, located on chromosome 12q24.31, spans a length of 26 kb and consists of seven exons. The open reading frame encompasses 981 nucleotides, predicting a 327-amino-acid protein. This protein includes a putative mitochondrial targeting sequence and shares 45% identity and 60% similarity with the yeast protein, excluding the targeting region. Figure 4.20 illustrates the amino acid alignment of COQ5 from various species, highlighting the conservation of its catalytic domains. Notably, human *COQ5* RNA levels were higher in liver, lung, placenta, and skeletal muscle, mirroring the expression pattern of *COQ6* (Heeringa et al., 2011), whereas other *COQ* genes exhibited different tissue-specific expression patterns.

It was also identified a potential second transcript encoding a truncated form of COQ5 through an EST database search. Such non-functional protein transcripts have been reported for other *COQ*

genes, and their functional significance remains unclear, but they could potentially play a regulatory role (Nguyen et al., 2014).

4.C.1.3 *COQ5* genetic characterization

Nguyen et al. (2014) discovered that although human *COQ5* shares significant similarity with its yeast counterpart, it couldn't rescue yeast mutants lacking *coq5,* as evidenced by their inability to grow on non-fermentable carbon sources and the absence of Q_6. Only under specific conditions, such as when yeast coq5 mutants had stable but catalytically inactive Coq5 polypeptides or were over-expressing *COQ8*, did human *COQ5* rescue yeast growth. Nguyen et al. (2014) discovered that human COQ5 could indeed compensate for Coq5 deficiency in *S.cerevisiae*, but this was only effective when the human mitochondrial leader sequence was substituted with that of yeast and when other yeast Coq polypeptides were stabilized through the overexpression of Coq8.These conditions permit the stabilization of the CoQ-synthome, which is required for Q_6 biosynthesis in yeast. These findings suggest that *COQ5* orthologs can serve as functional C-methyltransferases and restore Q biosynthesis in yeast *coq5* mutants when other yeast Coq polypeptides are retained. This underscores the functional similarity between yeast and human Q biosynthetic pathways. And this finding carries important implications for the diagnosis and treatment of Q_{10} deficiencies in patients. (Nguyen et al., 2014).

Interestingly, human *COQ5* expression was shown to complement a *S.pombe* Δ*coq5* mutant for growth on a nonfermentable carbon source (Hayashi et al., 2014). Unlike the S.cerevisiae Δ*coq5* mutant, the *S.pombe* Δ*coq5* mutant contained peaks tentatively identified as late-stage Q-intermediates, indicating differences in the phenotypes of these yeast mutants. However, human *COQ* homologs were able to rescue *S.pombe coq* deletion mutants, except for Coq9 (Hayashi et al., 2014). These results suggest that yeast growth on nonfermentable carbon sources can be restored with very low levels of Q, typically less than 0.2% of normal Q levels (Heeringa et al., 2011; Xie et al., 2011).

The yeast Coq5 polypeptide forms a dimer, with amino acid residues at the dimer interface domain identified (Dai et al., 2014). These residues are not as highly conserved among Coq5 homologs as the active-site residues that interact with S-adenosyl-L-methionine (Fig. 4.21). The interaction of the yeast Coq5 dimer with the yeast CoQ-synthome is speculated to enhance the catalytic efficiency of C-methylation. In contrast, heterologous COQ5 polypeptides may not interact as effectively or at all with the yeast CoQ-synthome. It was found that both human COQ5 and yeast Coq5 could be detected at a high molecular mass in specific conditions, but this interaction wasn't observed in normal, wild-type yeast cells. This suggests that the interaction between COQ5 and the CoQ-synthome may not be necessary for its function (Nguyen et al., 2014).

In summary, while the physical interaction between human COQ5 and the yeast CoQ-synthome may not be essential for partial Q_6 rescue, the CoQ-synthome likely needs to provide human COQ5 with its substrate $DDMQ_6H2$. This may be achieved with human COQ5 peripherally associated with the complex. The lower Q_6 content and the presence of Q_6-intermediates indicate either inefficient or weak interaction with the Coq complex. Nguyen end collaborators (2014) suggest that human and *E.coli* Coq5 homologs, when expressed in yeast, retain C-methyltransferase function but rescue yeast *coq5* mutants only when the other yeast Coq polypeptides are retained.

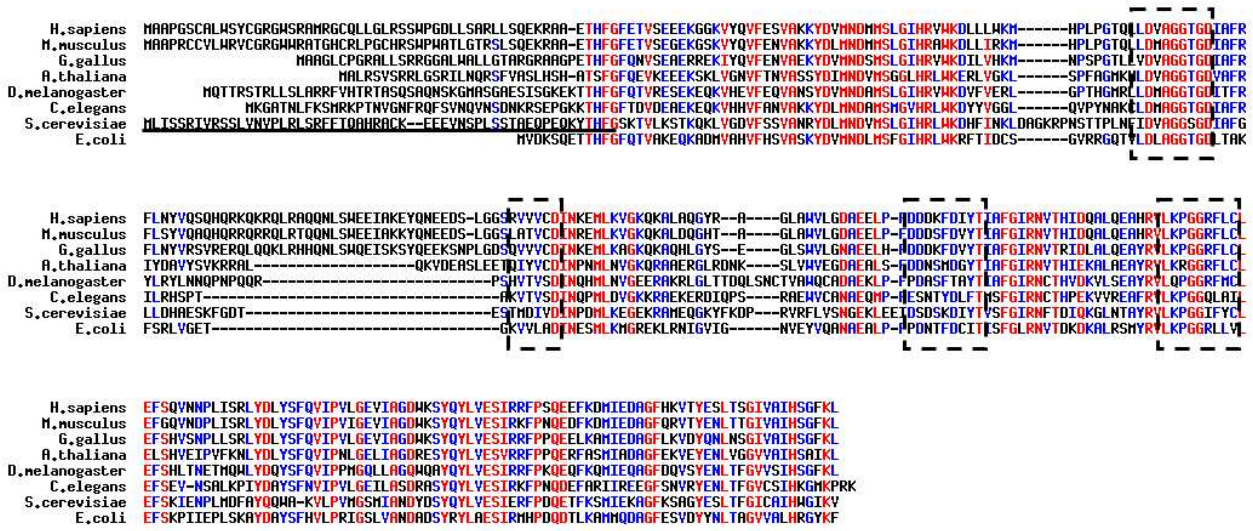

Fig.4.21 Amino acid alignments of COQ5 homologs were generated by MultAlin. In red are highly conserved residues, in blue, moderately conserved residues. Methyltransferase motifs (T. C. Petrossian & Clarke, 2011; T. Petrossian & Clarke, 2009), are designated by the dashed-line boxes. The aligned sequences include

Homo sapiens COQ5 (NP_115690.3), *Mus musculus* Coq5 (NP_080780.1), *Gallus gallus* COQ5 (NP_001006194.1), *Drosophila melanogaster* (NP_572865.1), *Arabidopsis thaliana* (AED96882.1), *Caenorhabditis elegans* COQ5 (P34666.2), *Saccharomyces cerevisiae* Coq5 (KZV08728.1), and *Escherichia coli* UbiE (CAD6023038.1). The yeast DNA segment encoding the amino terminal 54 residues (underlined) replaced the corresponding segment of human *COQ5* DNA to generate the hybrid yeast/human gene.

4.C.1.4 COQ_{10} deficiency caused by *COQ5* mutations

In a study by (Malicdan et al., 2018), sisters from unrelated Iraqi-Jewish parents were diagnosed with coenzyme Q_{10} deficiency-9 (COQ10D9; 619028). Genetic analysis revealed a homozygous duplication spanning 9,590 base pairs in the *COQ5* gene (chr12:120,940,098-120,949,687, GRCh37). This duplication, confirmed by Sanger sequencing, was identified as the causative mutation and co-segregated with the disorder within the family.

The duplicated region encompassed the final four exons of the *COQ5* gene but did not disrupt the open reading frame. It was situated approximately 1 kilobase beyond the DNA sequence encoding the 3-prime untranslated region. Patients exhibited significantly reduced levels of COQ5 mRNA and protein in their fibroblasts, leukocytes, and skeletal muscle tissue compared to control subjects. Furthermore, cultured fibroblasts from one patient demonstrated impaired mitochondrial complex II+III activity and abnormal oxygen consumption, indicating a detrimental impact on mitochondrial respiration. This homozygous duplication was absent in 92 healthy individuals of the same ethnic background. However, three heterozygous carriers were identified, resulting in a minor allele frequency of approximately 1.5%.

4.C.2 Materials and methods

4.C.2.1 Molecular cloning

In this study, we utilized plasmids that were previously employed in the research conducted by Nguyen et al. (2014). The human *COQ5* gene was amplified from cDNA derived from human skin fibroblasts (Casarin et al., 2008) using primers COQ5F and COQ5-1077R. Subsequently, the PCR products were cloned into the pCRII TOPO vector (Invitrogen) as well as the high-copy pYES2.1V5His yeast expression vectors (Invitrogen). The *COQ5* insert from pCRIITOPO-COQ5 was further inserted into the centromeric pCM189 vector (Euroscarf)(Garí et al., 1997).

The yeast *COQ5* (yCOQ5) gene was obtained by amplifying it from genomic DNA extracted from a wild-type BY4741 strain using standard protocols (Trevisson et al., 2009), and then cloned into the same vectors. Amplification primers employed for this purpose were yCOQ5F and yCOQ5R.

To create the hybrid yeast-human *COQ5* (yh*COQ5*) gene, a 5' segment of y*COQ5* corresponding to the mitochondrial targeting region (encoding amino acids 1–54; using primers yCOQ5F and hybridCOQ5R) was combined with the 3' segment of the human *COQ5* (encoding amino acids 56–327; with primers hybridCOQ5F and COQ5-1037R). This fusion was achieved through a sequential PCR protocol (Paret et al., 1999).

To create plasmids encoding mutated proteins Gly118Ser and Arg123Trp, site-directed mutagenesis was performed via PCR amplification of the pCM189-yMTSh*COQ5* construct using primers containing the desired mutations. The QuikChange Lightning Site-Directed Mutagenesis Kit (Agilent) was employed for this purpose. Finally, the pRS423-y*COQ8* plasmid was kindly provided by Prof. Fabien Pierrel (Université Grenoble Alpes). The correctness of all constructed plasmids was verified through direct sequencing. The sequences of the oligonucleotides used in this study are listed in Table 4.10.

Primer name	Sequence 5'->3'	Purpose
COQ5F	CTCGACTACCAAGATGGCGG	Amplification of *hCOQ5* coding region
COQ5-1077R	GATGCTCTGCTGCTGTCTCA	Amplification of *hCOQ5* coding region
yCOQ5F	ACAGATCGCAGCAAGAAAGA	Amplification of *yCOQ5* coding region
yCOQ5R	GGCTATCACATGGCACAGG	Amplification of *yCOQ5* coding region
hybridCOQ5F	GAAGTATACGCATTTTGGTTTTGAGACTGTGTCGGAAG	Generation of hybrid gene
hybridCOQ5R	CTTCCGACACAGTCTCAAAACCAAAATGCGTATACTTC	Generation of hybrid gene
COQ5-1037R	TTCCAGGCTTTCAACAGGA	Generation of hybrid gene
hCOQ5 Gly118Ser FOR	TGTTGCTGGAGGCACAAGTGACATTGCATTCCG	Mutagenesis of yMTS*hCOQ5* to generate the mutation Gly118Ser
hCOQ5 Gly118Ser REV	CGGAATGCAATGTCACTTGTGCCTCCAGCAACA	Mutagenesis of yMTS*hCOQ5* to generate the mutation Gly118Ser
hCOQ5 Arg123Trp FOR	GCACAGGTGACATTGCATTCTGGTTCCTTAATTATGTTCAG	Mutagenesis of yMTS*hCOQ5* to generate the mutation Arg123Trp
hCOQ5 Arg123Trp REV	CTGAACATAATTAAGGAACCAGAATGCAATGTCACCTGTGC	Mutagenesis of yMTS*hCOQ5* to generate the mutation Arg123Trp

Table 4.10 List of the oligonucleotides used in this study.

4.C.2.2 Yeast strains, media and plasmid transformation

The BY4741 *Δcoq5* strain (MATa; his3Δ1; leu2Δ0; met15Δ0; ura3Δ0; YML110c::kanMX4) was acquired directly from Euroscarf. Yeast strains were grown in rich medium (YPD) or synthetic minimal (SM) medium at 30 °C. YPD (1% yeast extract, 2% peptone, 2% dextrose) was used for routine maintenance of the wild type strain. Synthetic minimal medium (0.17% yeast nitrogen base without amino acids, 0.5% ammonium sulfate, 2% carbon source), supplemented with amino acids to cover yeast auxotrophies except uracil (and histidine when y*COQ8* was overexpressed) was used

to select transformant strains. YPGly medium (1% yeast extract, 2% peptone and 3% glycerol) was used to perform functional complementation assays. Growth media components were purchased from Difco. Yeast DNA transformations were performed using the polyethylene glycol-lithium acetate method as previously described (Gietz & Woods, 2006). Figure 4.22 provides a visual representation of the experiment, created using BioRender.

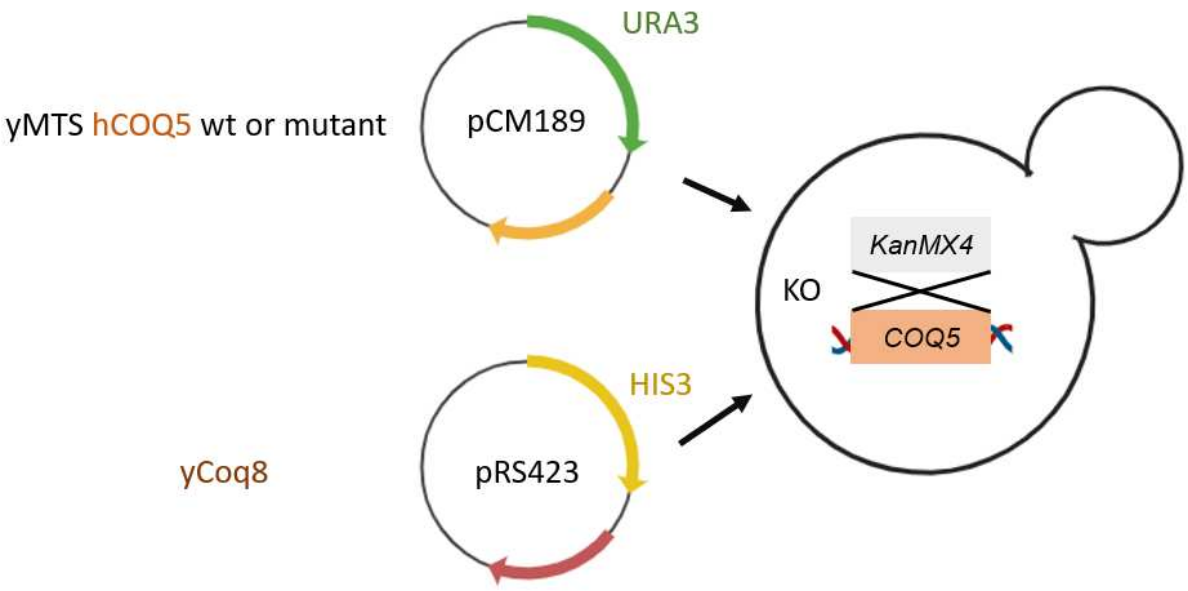

Fig.4.22 Representation of the working model used in this study to obtain a functional yeast-based assay to validate putative h*COQ5* mutations. Image generated using BioRender (BioRender.com)

4.C.2.3 Functional complementation spot test assay

For testing the ability of the different wt and mutant COQ5 proteins to rescue respiratory growth in *coq5*-deleted yeast, the different yeast strains were inoculated in glucose-containing selective liquid medium and grown for 2 days and 2 nights at 30°C.

The concentration of each culture was then adjusted to OD_{600} = 1 (approximately 10^7 cells/mL) in sterile water, after two washes in water to remove glucose medium, and four serial 10-fold dilutions were performed. For each of these dilutions, 5µL were spotted onto YPD, SM Glu (with proper amino acid selection), and YPGly, plate media. Plates were incubated at 30°C and images were taken 5 days after incubation.

4.C.3 Results

4.C.3.1 Patients

Whole exome sequencing revealed two copies of the variant c.352G>A, p.(Gly118Ser) in the *COQ5* gene of the 7-year-old child, who was born to parents who are related from Pakistan. The *COQ5* gene transcript (NM_032314.4) showed a homozygous genotype with consequences involving a missense variant and follows an autosomal recessive inheritance pattern. Although it is classified as a variant of uncertain significance because there is not enough evidence to determine its clinical relevance definitively, several prediction tools suggest that it is likely to be harmful. Polyphen predicts it as "probably damaging," SIFT indicates it as "deleterious," and Mutation Taster suggests it could cause pathology. The variant is associated with a phenotype of Coenzyme Q_{10} deficiency (MIM#619028), which manifests with a complex clinical presentation that includes ataxia, distal action tremor, ponto-cerebellar atrophy, intellectual disability, speech delay, neonatal jaundice and hypoglycaemia (Table 4.11). The intellectual disability (MIM#615516) in this patient is linked to a second homozygous mutation identified in the *HERC2* gene (NM_004667.5), specifically, the c.11398G>C, p.(Asp3800His) variant. This mutation will not be the focus of our further investigation. Segregation analysis of variants in the *COQ5* gene was carried out on the parents. In the mother, the analysis revealed the presence of the c.352G>A p.(Gly118Ser) variant in exon 2 of the *COQ5* gene in a heterozygous state. Similarly, the father exhibited the same result as the mother. To provide a complete overview, it is noteworthy that both parents also carried the identical heterozygous mutation in the HERC2 gene, which the patient had in a homozygous form.

The quantification of Coenzyme Q10 in the muscle biopsy showed a significant decrease in Coenzyme Q levels. This finding is consistent with the patient's clinical symptoms and the detection of the homozygous *COQ5* variant. As depicted in Figure 4.23, Gly118 exhibits a high degree of conservation across COQ5 homologs.

Meanwhile, the second mutation we chose to investigate, using our yeast model, is the Arg123Trp (Table 4.24) variant. This alteration in the human COQ5 protein (NP_115690.3) affects a residue

that is highly conserved, except for *E.coli* and *S.cerevisiae* COQ5 homologs (Fig.4.23). Importantly, this mutation is generally associated with a milder phenotype characterized by symptoms such as muscle weakness and vision problems (Jurkute et al., 2022).

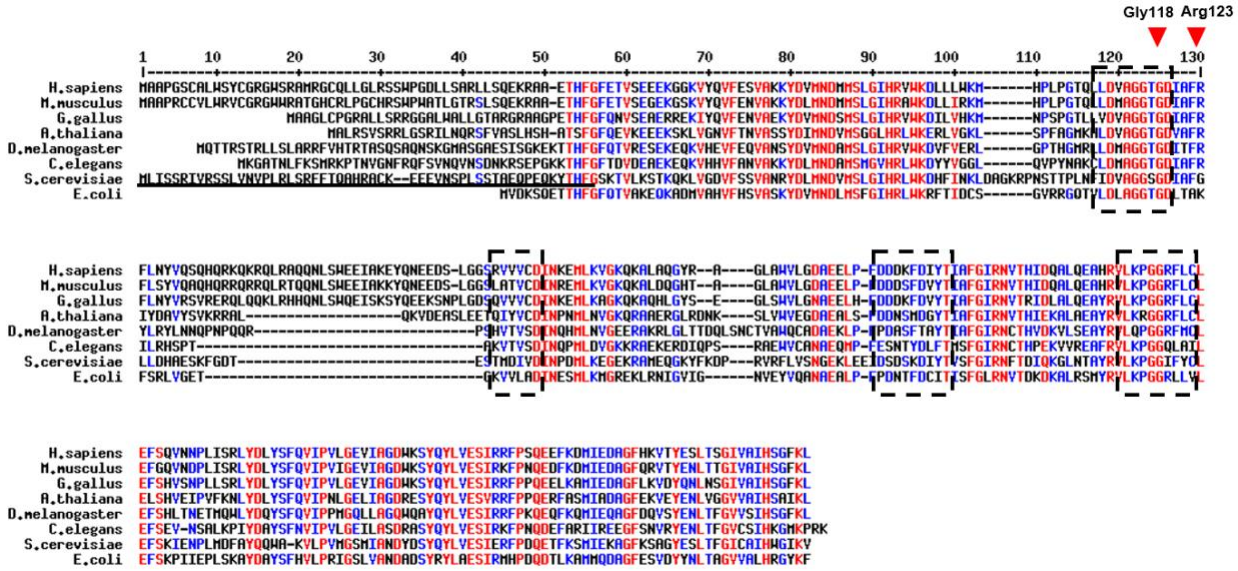

Fig.4.23 The amino acid alignments of COQ5 homologs, as generated by MultAlin and shown in Figure 4.20, highlight two notable features. The positions of two specific residues within the human COQ5 protein sequence (NP_115690.3), namely Gly118 and Arg123, are indicated by red triangles. Gly118 is highly conserved, while Arg123 is well-conserved across these homologues, except for *E.coli* and *S.cerevisiae* COQ5 homologues.

Human Gene name	Protein Human Change	Reference Sequence	Phenotype	Zigosity	Reference
hCOQ5	Gly118Ser	NP_115690.3	ataxia, distal action tremor, ponto-cerebellar atrophy, intellectual disability, speech delay, neonatal jaundice and hypoglycaemia	Homozygous	This work
hCOQ5	Arg123Trp	NP_115690.3	Muscle weakness, followed by vision problems in the dark	Compound heterozygous with a nonsense mutation	Jurkute et al., 2022

Table 4.11 The COQ5 mutations under investigation are Gly118Ser and Arg123Trp, located within the COQ5 protein (NP_115690.3). These mutations are associated with specific phenotypes and zygosities, as outlined in the table.

4.C.3.2 Genotype-phenotype correlation

In previous experiments conducted by Nguyen et al. in 2014, it was observed that the human COQ5 protein was unable to rescue the respiratory deficiency in the yeast Δ*coq5*-null strain. Additionally, it

couldn't restore CoQ biosynthesis or respiration in this yeast strain. These findings clearly indicate that only the yeast Coq5 protein is effective in complementing our yeast model.

The hybrid gene, yMTSh*COQ5*, which combines the mitochondrial targeting sequence of the yeast Coq5 protein (amino acids 1-54) with the conserved C-terminal domain of the human COQ5 protein (amino acids 56–327), was the key factor in complementing the null-strain yeast. It's worth noting that the over-expression of the yeast Coq8 protein was also essential in this process. Coq8 is a putative regulatory kinase known to enhance the levels and assembly of several Coq proteins and complexes (He et al., 2014; Awad et al., 2018).

We conducted a study to assess the impact of COQ5 mutations Gly118Ser and Arg123Trp, in combination with yCoq8, on the growth of yeast strains using a non-fermentable carbon source. As control groups, we established two additional yeast strains: one was a Δ*coq5* yeast expressing the wild type yMTSh*COQ5* along with y*COQ8*, labeled as "WT" in Figure 4.24, and the other was a Δ*coq5* yeast expressing the empty pCM189 vector in combination with y*COQ8* alone, and simply referred to it as "Δ*coq5".* The initial group, labelled as "WT", was predicted to demonstrate growth on respiratory medium, while the latter group was predicted to have a total lack of respiration, leading to no growth on glycerol medium.

The results obtained align with the phenotypes observed in the patients. After 5 days, we noticed slightly stronger growth in the case of the Arg123Trp mutant, which is associated with a milder phenotype related to retinitis pigmentosa. In contrast, the growth of the Gly118Ser mutant, identified in the 7-year-old child and linked to a much more severe phenotype, appeared to be more inhibited (Fig.4.24).

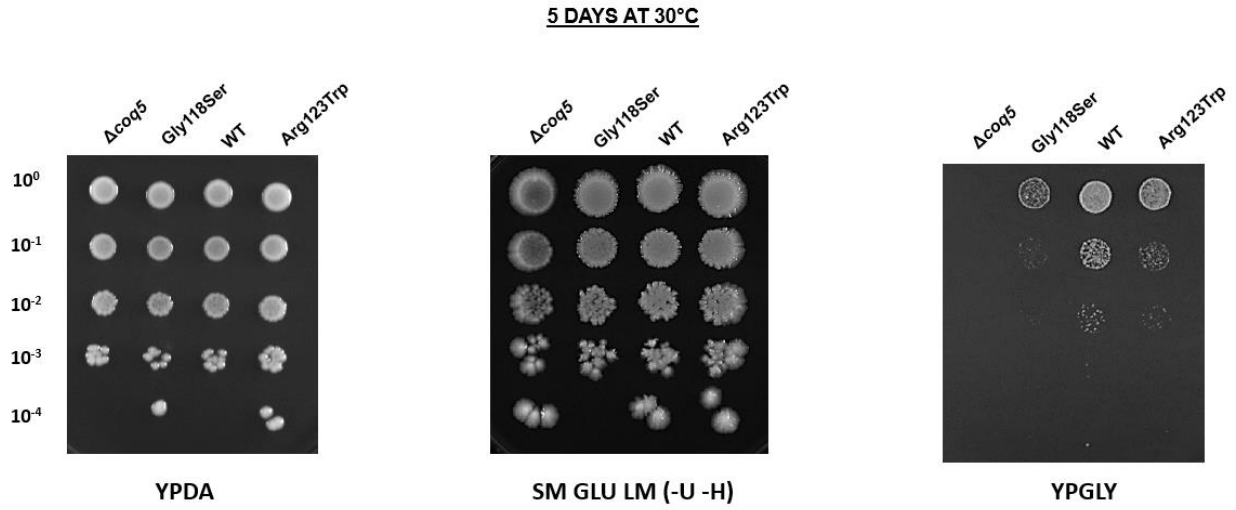

Figure 4.24 Functional complementation assay of yMTSh*COQ5* wt or mutant proteins Gly118Ser and Arg123Trp co-expressed with yCoq8 in *Δcoq5* yeast strain. The Gly118Ser strongly impaired the ability of the wt yMTSh*COQ5* hybrid protein to compensate for the absence of endogenous yCoq5, while the Arg123Trp showed a slightly greater growth. The analysis was conducted via spot test, where cell cultures were serially diluted and spotted onto the different agar media and incubated at 30°C. After 5 days, we observed the following results, from left to right: rich medium (YPD) for the growth of all strains, synthetic minimal medium (except uracil and histidine, which were supplied by the plasmids used for co-transformation) for the growth of transformants, and YPGly medium to test yeast respiration. Each spot test analysis was repeated three times.

4.C.4 Discussion

Once again, we have demonstrated the usefulness of creating a yeast strain with a specific *COQ* gene inactivated as a robust model for studying the effects of mutations in the corresponding human protein. This is especially beneficial when such mutations affect highly conserved amino acids, and the consequences can be evaluated by observing yeast growth on a respiratory substrate.

There is a significant correlation between the severity of the human disease phenotype and the yeast's capacity to grow on a non-fermentable medium, with or without recovery of mitochondrial function. This correlation is primarily due to the common conservation of the Q pathway across eukaryotes, highlighting the similarities between humans and *S.cerevisiae* in this context.

The close relationship between the COQ proteins and the complex they form is intriguing. The overexpression of yCoq8 has a vital role in maintaining yMTShCOQ5 within yeast mitochondria, thus promoting its catalytic function. Moreover, the identification of the yeast N-terminal sequence, responsible for mitochondrial import, has extensively contributed to the development of the application of human proteins in these efficient yeast models.

Therefore, additional studies can be carried out to improve our understanding of the processes occurring within the mitochondria of yeast expressing mutant COQ proteins. Assessing the activity of respiratory complexes and conducting western blot analysis may be needed to confirm COQ5 expression levels. It is intriguing to consider the significant impact on the functionality of the Q precursor due to a mutation in a gene responsible for modifying its head group, resulting in a severe phenotype observed in a 7-year-old patient with the Gly123Ser mutation. This highlights the critical role of CoQ and mitochondrial function. Investigating and understanding the absent stages in Q biosynthesis can unquestionably aid in the advancement of enhanced therapies for individuals with COQ_{10} insufficiency.

PART V

General Conclusions

Saccharomyces cerevisiae, commonly known as yeast, emerges as a versatile and robust unicellular eukaryotic model organism. It boasts a plethora of advantages, including its cellular simplicity, rapid growth, cost-effective maintenance, and ease of genetic manipulation. Particularly striking is the fact that approximately 30% of yeast genes share orthologs with their human counterparts, exhibiting an average amino acid sequence overlap of 32% (Leslie, 2015). This remarkable degree of conservation has firmly established yeast as a fundamental basis in the investigation of human diseases and, notably, in the validation of pathogenic mutations, as exemplified in this thesis.

One widely employed assay for exploring the pathogenicity of variants of uncertain significance (VUS) involves functional complementation of yeast deletion mutants with newly discovered mutant alleles sourced from patients. This approach not only serves to confirm the pathogenic nature of novel genetic variants but also estabilishes a direct connection between a patient's genotype and clinical phenotype (Trevisson, et al., 2009). Recent scientific literature abounds with successful applications of this assay. Within our research group, we have extensively harnessed functional complementation in *S.cerevisiae* to validate mutations identified in patients suffering from various metabolic disorders. The yeast spot test assay assumes a pivotal role in assessing the growth of cells transformed with mutated genes of interest across a spectrum of media. This multifaceted assay greatly facilitates the identification of specific deficiencies in mutant strains.

Yeast offers a multitude of applications in research, facilitating various analyses. In the *STRADA* project (Part I), we assessed the impact on yeast sporulation capacity by utilizing the CRISPR/Cas9 technique to delete the orthologous gene *sps1* or reproduce the human mutation on corresponding yeast sequence. This approach enabled us to correlate the sporulation capacity of the yeast model with the neurological complications observed in humans with the Ser264Arg missense protein alteration.

Another valuable application, discussed in Part II of our study, was employed in the *SGPL1* project. The yeast model provided an opportunity to investigate the pathogenicity of the human missense mutation Gly210Glu, which was identified in the *SGPL1* human gene and causing nephrotic syndrome. To achieve this, we deleted the yeast orthologous gene, *dpl1*, utilizing the conventional approach involving homologous recombination, followed by the specific locus inactivation through

the insertion of an antibiotic cassette (Vetro et al., 2017). This approach enabled us to characterize the phenotype induced by phytosphingosine toxicity directly in the yeast model expressing the human mutant allele. Additionally, it allowed us to investigate the potential mitigation of this toxicity through B6 supplementation in yeast cells.

As previously highlighted, many *COQ* genes were initially characterized in yeast, and the connection between *COQ* gene mutations and specific clinical phenotypes was delineated through yeast complementation studies, as exemplified in this thesis for *PDSS1*, *PDSS2*, *COQ4*, and *COQ5*.

Another valuable model that contributed to my research was *E.coli*. Bacteria, particularly *E.coli*, are frequently utilized for the production of proteins from various organisms for research and functional characterization purposes. This choice is primarily attributed to its rapid growth rate and cost-effectiveness. *E.coli* is known for its swift growth and well-established genetics, making it an ideal choice for protein production. Additionally, it has the capacity to generate substantial quantities of proteins, simplifying experimental procedures. The straightforward nature of bacteria further facilitates the isolation and analysis of foreign proteins. In summary, the *E.coli* expression system offers a practical and efficient approach to gaini insights into protein functions and this helped us to express and purify the human COQ4 protein and will enable us to perform functional studies *in vitro* and further experiments.

In conclusion, yeast strains serve as invaluable tools for a wide range of research applications. They are utilized to detect the biochemical activity of transgenic mutated proteins and to analyze the expression and stability of individual proteins or multiprotein complexes. Common techniques such as Western blotting or Blue Native-PAGE are employed for these purposes. Moreover, yeast models offer the opportunity to study mitochondrial respiration by assessing the activity of respiratory complexes. Furthermore, researchers have leveraged the power of yeast, a unicellular model organism, to investigate how human proteins lacking direct equivalents in yeast can impact diseases or specific cellular processes *Saccharomyces cerevisiae* emerges as a simple eukaryotic model organism with a well-annotated genome, swift generation times, and a vibrant research community that has cultivated a robust toolkit for scientific inquiry. These attributes render yeast an ideal choice for unraveling the functions of genes and mutations implicated in human diseases.

BIBLIOGRAPHY

Acosta Lopez, M. J., Trevisson, E., Canton, M., Vazquez-Fonseca, L., Morbidoni, V., Baschiera, E., Frasson, C., Pelosi, L., Rascalou, B., Desbats, M. A., Alcázar-Fabra, M., Ríos, J. J., Sánchez-Garciá, A., Basso, G., Navas, P., Pierrel, F., Brea-Calvo, G., & Salviati, L. (2019). Vanillic Acid Restores Coenzyme Q Biosynthesis and ATP Production in Human Cells Lacking COQ6. *Oxidative Medicine and Cellular Longevity*, *2019*. https://doi.org/10.1155/2019/3904905

Acosta, M. J., Vazquez Fonseca, L., Desbats, M. A., Cerqua, C., Zordan, R., Trevisson, E., & Salviati, L. (2016). Coenzyme Q biosynthesis in health and disease. *Biochimica et Biophysica Acta - Bioenergetics*, *1857*(8). https://doi.org/10.1016/j.bbabio.2016.03.036

Adzhubei, I., Jordan, D. M., & Sunyaev, S. R. (2013). Predicting functional effect of human missense mutations using PolyPhen-2. *Current Protocols in Human Genetics*, *SUPPL.76*. https://doi.org/10.1002/0471142905.hg0720s76

Aerden, M., Vallaeys, L., Holvoet, M., De Waele, L., Van Den Bogaert, K., & Devriendt, K. (2021). Homozygous missense STRADA mutation in a patient with polyhydramnios, megalencephaly and symptomatic epilepsy syndrome. *Clinical Dysmorphology*, *30*(3), 121–124. https://doi.org/10.1097/mcd.0000000000000368

Alcázar-Fabra, M., Rodríguez-Sánchez, F., Trevisson, E., & Brea-Calvo, G. (2021). Primary Coenzyme Q deficiencies: A literature review and online platform of clinical features to uncover genotype-phenotype correlations. *Free Radical Biology and Medicine*, *167*. https://doi.org/10.1016/j.freeradbiomed.2021.02.046

Alfares, A., Alfadhel, M., Wani, T., Alsahli, S., Alluhaydan, I., Al Mutairi, F., Alothaim, A., Albalwi, M., Al subaie, L., Alturki, S., Al-Twaijri, W., Alrifai, M., Al-Rumayya, A., Alameer, S., Faqeeh, E., Alasmari, A., Alsamman, A., Tashkandia, S., Alghamdi, A., … Zada, A. A. P. (2017). A multicenter clinical exome study in unselected cohorts from a consanguineous population of Saudi Arabia demonstrated a high diagnostic yield. *Molecular Genetics and Metabolism*, *121*(2), 91–95. https://doi.org/10.1016/j.ymgme.2017.04.002

Allan, C. M., Awad, A. M., Johnson, J. S., Shirasaki, D. I., Wang, C., Blaby-Haas, C. E., Merchant, S. S., Loo, J. A., & Clarke, C. F. (2015). Identification of Coq11, a new coenzyme Q biosynthetic protein in the CoQ-synthome in saccharomyces cerevisiae. *Journal of Biological Chemistry*, *290*(12). https://doi.org/10.1074/jbc.M114.633131

Alsaif, H. S., Youssef L Khashab, H. E., Alkuraya, F. S., & Fowzan Alkuraya, C. S. (2020). *Two further cases of polyhydramnios, megalencephaly, and symptomatic epilepsy syndrome, caused by a truncating variant in STRADA*. https://doi.org/10.1002/ajmg.a.61990

Amberg, D. C., Burke, D. J., & Strathern, J. N. (2005). Methods in Yeast Genetics: A Cold Spring Harbor Laboratory Course Manual, 2005 Edition. In *A Cold Spring Harbor Laboratory Course Manual*.

Anderson, C. M., Kazantzis, M., Wang, J., Venkatraman, S., Goncalves, R. L. S., Quinlan, C. L., Ng, R., Jastroch, M., Benjamin, D. I., Nie, B., Herber, C., Van, A. A. N., Park, M. J., Yun, D., Chan, K., Yu, A., Vuong, P., Febbraio, M., Nomura, D. K., … Stahl, A. (2015). Dependence of brown adipose tissue function on CD36-mediated coenzyme Q uptake. *Cell Reports*, *10*(4). https://doi.org/10.1016/j.celrep.2014.12.048

Andreux, P. A., Houtkooper, R. H., & Auwerx, J. (2013). Pharmacological approaches to restore mitochondrial function. In *Nature Reviews Drug Discovery* (Vol. 12, Issue 6). https://doi.org/10.1038/nrd4023

Arenz, C. (2017). Recent advances and novel treatments for sphingolipidoses. In *Future Medicinal Chemistry* (Vol. 9, Issue 14). https://doi.org/10.4155/fmc-2017-0065

Argyropoulos, G., & Harper, M. E. (2002). Invited review: Uncoupling proteins and thermoregulation. In *Journal of Applied Physiology* (Vol. 92, Issue 5). https://doi.org/10.1152/japplphysiol.00994.2001

Arias-Mayenco, I., González-Rodríguez, P., Torres-Torrelo, H., Gao, L., Fernández-Agüera, M. C., Bonilla-Henao, V., Ortega-Sáenz, P., & López-Barneo, J. (2018). Acute O2 Sensing: Role of Coenzyme QH2/Q Ratio and Mitochondrial ROS Compartmentalization. *Cell Metabolism*, *28*(1). https://doi.org/10.1016/j.cmet.2018.05.009

Ashby, M. N., & Edwards, P. A. (1990). Elucidation of the deficiency in two yeast coenzyme Q mutants. Characterization of the structural gene encoding hexaprenyl pyrophosphate synthetase. *Journal of Biological Chemistry*, *265*(22). https://doi.org/10.1016/s0021-9258(19)38280-8

Ashraf, S., Gee, H. Y., Woerner, S., Xie, L. X., Vega-Warner, V., Lovric, S., Fang, H., Song, X., Cattran, D. C., Avila-Casado, C., Paterson, A. D., Nitschké, P., Bole-Feysot, C., Cochat, P., Esteve-Rudd, J., Haberberger, B., Allen, S. J., Zhou, W., Airik, R., … Hildebrandt, F. (2013). ADCK4 mutations promote steroid-Resistant nephrotic syndrome through CoQ10 biosynthesis disruption. *Journal of Clinical Investigation*, *123*(12). https://doi.org/10.1172/JCI69000

Auld, D. S. (2001). Zinc coordination sphere in biochemical zinc sites. In *BioMetals* (Vol. 14, Issues 3–4). https://doi.org/10.1023/A:1012976615056

Awad, A. M., Bradley, M. C., Fernández-del-Río, L., Nag, A., Tsui, H. S., & Clarke, C. F. (2018). Coenzyme Q10 deficiencies: Pathways in yeast and humans. In *Essays in Biochemistry* (Vol. 62, Issue 3). https://doi.org/10.1042/EBC20170106

Bandelt, H. J., Kloss-Brandstätter, A., Richards, M. B., Yao, Y. G., & Logan, I. (2014). The case for the continuing use of the revised Cambridge Reference Sequence (rCRS) and the standardization of notation in human mitochondrial DNA studies. In *Journal of Human Genetics* (Vol. 59, Issue 2). https://doi.org/10.1038/jhg.2013.120

Banh, R. S., Kim, E. S., Spillier, Q., Biancur, D. E., Yamamoto, K., Sohn, A. S. W., Shi, G., Jones, D. R., Kimmelman, A. C., & Pacold, M. E. (2021). The polar oxy-metabolome reveals the 4-hydroxymandelate CoQ10 synthesis pathway. *Nature*, *597*(7876). https://doi.org/10.1038/s41586-021-03865-w

Bao, Z., Xiao, H., Liang, J., Zhang, L., Xiong, X., Sun, N., Si, T., & Zhao, H. (2015). Homology-Integrated CRISPR-Cas (HI-CRISPR) System for One-Step Multigene Disruption in Saccharomyces cerevisiae. *ACS Synthetic Biology*, *4*(5). https://doi.org/10.1021/sb500255k

Baretić, D., & Williams, R. L. (2014). The structural basis for mTOR function. In *Seminars in Cell and Developmental Biology* (Vol. 36). https://doi.org/10.1016/j.semcdb.2014.09.024

Barkovich, R. J., Shtanko, A., Shepherd, J. A., Lee, P. T., Myles, D. C., Tzagoloff, A., & Clarke, C. F. (1997). Characterization of the COQ5 gene from Saccharomyces cerevisiae: Evidence for a C-methyltransferase in ubiquinone biosynthesis. *Journal of Biological Chemistry*, *272*(14). https://doi.org/10.1074/jbc.272.14.9182

Barrangou, R., Fremaux, C., Deveau, H., Richards, M., Boyaval, P., Moineau, S., Romero, D. A., & Horvath, P. (2007). CRISPR provides acquired resistance against viruses in prokaryotes. *Science*, *315*(5819). https://doi.org/10.1126/science.1138140

Baschiera, E., Sorrentino, U., Calderan, C., Desbats, M. A., & Salviati, L. (2021). The multiple roles of coenzyme Q in cellular homeostasis and their relevance for the pathogenesis of coenzyme Q deficiency. In *Free Radical Biology and Medicine* (Vol. 166). https://doi.org/10.1016/j.freeradbiomed.2021.02.039

Baudin, A., Ozier-kalogeropoulos, O., Denouel, A., Lacroute, F., & Cullin, C. (1993). A simple and efficient method for direct gene deletion in Saccharomyces cerevisiae. In *Nucleic Acids Research* (Vol. 21, Issue 14). https://doi.org/10.1093/nar/21.14.3329

Beadle, G. W., & Tatum, E. L. (1941). Genetic Control of Biochemical Reactions in Neurospora. *Proceedings of the National Academy of Sciences*, *27*(11). https://doi.org/10.1073/pnas.27.11.499

Bellí, G., Garí, E., Aldea, M., & Herrero, E. (1998). Functional analysis of yeast essential genes using a promoter-substitution cassette and the tetracycline-regulatable dual expression system. *Yeast*, *14*(12). https://doi.org/10.1002/(sici)1097-0061(19980915)14:12<1127::aid-yea300>3.0.co;2-%23

Bello, R. I., Alcaín, F. J., Gómez-Díaz, C., López-Lluch, G., Navas, P., & Villalba, J. M. (2003). Hydrogen peroxide- and cell-density-regulated expression of NADH-cytochrome b5 reductase in HeLa cells. *Journal of Bioenergetics and Biomembranes*, *35*(2). https://doi.org/10.1023/A:1023702321148

Bellusci, M., García-Silva, M. T., Martínez de Aragón, A., & Martín, M. A. (2021). Distal phalangeal erythema in an infant with biallelic PDSS1 mutations: Expanding the phenotype of primary Coenzyme Q10 deficiency. *JIMD Reports*, *62*(1). https://doi.org/10.1002/jmd2.12216

Belogrudov, G. I., Lee, P. T., Jonassen, T., Hsu, A. Y., Gin, P., & Clarke, C. F. (2001). Yeast COQ4 encodes a mitochondrial protein required for coenzyme Q synthesis. *Archives of Biochemistry and Biophysics*, *392*(1). https://doi.org/10.1006/abbi.2001.2448

Bentinger, M., Tekle, M., & Dallner, G. (2010). Coenzyme Q - Biosynthesis and functions. *Biochemical and Biophysical Research Communications*, *396*(1). https://doi.org/10.1016/j.bbrc.2010.02.147

Berardo, A., & Quinzii, C. M. (2020). Redefining infantile-onset multisystem phenotypes of coenzyme Q10-deficiency in the next-generation sequencing era. In *Journal of Translational Genetics and Genomics* (Vol. 4). https://doi.org/10.20517/jtgg.2020.02

Bersuker, K., Hendricks, J. M., Li, Z., Magtanong, L., Ford, B., Tang, P. H., Roberts, M. A., Tong, B., Maimone, T. J., Zoncu, R., Bassik, M. C., Nomura, D. K., Dixon, S. J., & Olzmann, J. A. (2019). The CoQ oxidoreductase FSP1 acts parallel to GPX4 to inhibit ferroptosis. *Nature*, *575*(7784). https://doi.org/10.1038/s41586-019-1705-2

Bi, W., Glass, I. A., Muzny, D. M., Gibbs, R. A., Eng, C. M., Yang, Y., & Sun, A. (n.d.). *Whole Exome Sequencing Identifies the First STRADA Point Mutation in a Patient with Polyhydramnios, Megalencephaly, and Symptomatic Epilepsy Syndrome (PMSE)*. https://doi.org/10.1002/ajmg.a.37727

Birchwood, C. J., Saba, J. D., Dickson, R. C., & Cunningham, K. W. (2001). Calcium Influx and Signaling in Yeast Stimulated by Intracellular Sphingosine 1-Phosphate Accumulation. *Journal of Biological Chemistry*, *276*(15). https://doi.org/10.1074/jbc.M010221200

Boekema, E. J., & Braun, H. P. (2007). Supramolecular structure of the mitochondrial oxidative phosphorylation system. In *Journal of Biological Chemistry* (Vol. 282, Issue 1). https://doi.org/10.1074/jbc.R600031200

Bosch, A. M., Kamsteeg, E. J., Rodenburg, R. J., van Deutekom, A. W., Buis, D. R., Engelen, M., & Cobben, J. M. (2018). Coenzyme Q10 deficiency due to a COQ4 gene defect causes childhood-onset spinocerebellar ataxia and stroke-like episodes. *Molecular Genetics and Metabolism Reports*, *17*. https://doi.org/10.1016/j.ymgmr.2018.09.002

Bourquin, F., Riezman, H., Capitani, G., & Grütter, M. G. (2010). Structure and function of sphingosine-1-phosphate lyase, a key enzyme of sphingolipid metabolism. *Structure*, *18*(8). https://doi.org/10.1016/j.str.2010.05.011

Brea-Calvo, G., Haack, T. B., Karall, D., Ohtake, A., Invernizzi, F., Carrozzo, R., Kremer, L., Dusi, S., Fauth, C., Scholl-Bürgi, S., Graf, E., Ahting, U., Resta, N., Laforgia, N., Verrigni, D., Okazaki, Y., Kohda, M., Martinelli, D., Freisinger, P., … Ghezzi, D. (2015). COQ4 mutations cause a broad spectrum of mitochondrial disorders associated with CoQ10 deficiency. *American Journal of Human Genetics*, *96*(2). https://doi.org/10.1016/j.ajhg.2014.12.023

Breslow, D. K., Collins, S. R., Bodenmiller, B., Aebersold, R., Simons, K., Shevchenko, A., Ejsing, C. S., & Weissman, J. S. (2010). Orm family proteins mediate sphingolipid homeostasis. *Nature*, *463*(7284). https://doi.org/10.1038/nature08787

Bross, P., Corydon, T. J., Andresen, B. S., Jørgensen, M. M., Bolund, L., & Gregersen, N. (1999). Protein misfolding and degradation in genetic diseases. *Human Mutation*, *14*(3). https://doi.org/10.1002/(SICI)1098-1004(1999)14:3<186::AID-HUMU2>3.0.CO;2-J

Burgess, S. M., Powers, T., & Mell, J. C. (2017). Budding Yeast S accharomyces Cerevisiae as a Model Genetic Organism . In *eLS*. https://doi.org/10.1002/9780470015902.a0000821.pub2

Calvo, S. E., & Mootha, V. K. (2010). The mitochondrial proteome and human disease. In *Annual Review of Genomics and Human Genetics* (Vol. 11). https://doi.org/10.1146/annurev-genom-082509-141720

Casarin, A., Jimenez-Ortega, J. C., Trevisson, E., Pertegato, V., Doimo, M., Ferrero-Gomez, M. L., Abbadi, S., Artuch, R., Quinzii, C., Hirano, M., Basso, G., Ocaña, C. S., Navas, P., & Salviati, L. (2008). Functional characterization of human COQ4, a gene required for Coenzyme Q10 biosynthesis. *Biochemical and Biophysical Research Communications*, *372*(1). https://doi.org/10.1016/j.bbrc.2008.04.172

Cellini, B., Montioli, R., Oppici, E., Astegno, A., & Borri Voltattorni, C. (2014). The chaperone role of the pyridoxal 5'-phosphate and its implications for rare diseases involving B6-dependent enzymes. In *Clinical Biochemistry* (Vol. 47, Issue 3). https://doi.org/10.1016/j.clinbiochem.2013.11.021

Chen, H., & Chan, D. C. (2009). Mitochondrial dynamics-fusion, fission, movement, and mitophagy-in neurodegenerative diseases. *Human Molecular Genetics*, *18*(R2). https://doi.org/10.1093/hmg/ddp326

Chew, W. S., Wang, W., & Herr, D. R. (2016). To fingolimod and beyond: The rich pipeline of drug candidates that target S1P signaling. In *Pharmacological Research* (Vol. 113). https://doi.org/10.1016/j.phrs.2016.09.025

Chung, N., Mao, C., Heitman, J., Hannun, Y. A., & Obeid, L. M. (2001). Phytosphingosine as a Specific Inhibitor of Growth and Nutrient Import in Saccharomyces cerevisiae. *Journal of Biological Chemistry*, *276*(38). https://doi.org/10.1074/jbc.M105653200

Chung, W. K., Martin, K., Jalas, C., Braddock, S. R., Juusola, J., Monaghan, K. G., Warner, B., Franks, S., Yudkoff, M., Lulis, L., Rhodes, R. H., Prasad, V., Torti, E., Cho, M. T., & Shinawi, M. (2015). Mutations in COQ4, an essential component of coenzyme Q biosynthesis, cause

lethal neonatal mitochondrial encephalomyopathy. *Journal of Medical Genetics*, *52*(9). https://doi.org/10.1136/jmedgenet-2015-103140

Clarke, L., & Carbon, J. (1980). Isolation of a yeast centromere and construction of functional small circular chromosomes. *Nature*, *287*(5782). https://doi.org/10.1038/287504a0

Coleman, S. T., Fang, T. K., Rovinsky, S. A., Turano, F. J., & Moye-Rowley, W. S. (2001). Expression of a glutamate decarboxylase homologue is required for normal oxidative stress tolerance in Saccharomyces cerevisiae. *Journal of Biological Chemistry*, *276*(1). https://doi.org/10.1074/jbc.M007103200

Collins, M. D., & Jones, D. (1981). Distribution of isoprenoid quinone structural types in bacteria and their taxonomic implications. In *Microbiological Reviews* (Vol. 45, Issue 2). https://doi.org/10.1128/mmbr.45.2.316-354.1981

Corpet, F. (1988). Multiple sequence alignment with hierarchical clustering. *Nucleic Acids Research*, *16*(22). https://doi.org/10.1093/nar/16.22.10881

Crane, F. L., Hatefi, Y., Lester, R. L., & Widmer, C. (1957). Isolation of a quinone from beef heart mitochondria. *BBA - Biochimica et Biophysica Acta*, *25*(C). https://doi.org/10.1016/0006-3002(57)90457-2

Crino, P. B. (2016). The mTOR signalling cascade: Paving new roads to cure neurological disease. In *Nature Reviews Neurology* (Vol. 12, Issue 7). https://doi.org/10.1038/nrneurol.2016.81

Cui, T. Z., Kaino, T., & Kawamukai, M. (2010). A subunit of decaprenyl diphosphate synthase stabilizes octaprenyl diphosphate synthase in Escherichia coli by forming a high-molecular weight complex. *FEBS Letters*, *584*(4). https://doi.org/10.1016/j.febslet.2009.12.029

Dai, Y. N., Zhou, K., Cao, D. D., Jiang, Y. L., Meng, F., Chi, C. B., Ren, Y. M., Chen, Y., & Zhou, C. Z. (2014). Crystal structures and catalytic mechanism of the C-methyltransferase Coq5 provide insights into a key step of the yeast coenzyme Q synthesis pathway. *Acta Crystallographica Section D: Biological Crystallography*, *70*(8). https://doi.org/10.1107/S1399004714011559

Deltcheva, E., Chylinski, K., Sharma, C. M., Gonzales, K., Chao, Y., Pirzada, Z. A., Eckert, M. R., Vogel, J., & Charpentier, E. (2011). CRISPR RNA maturation by trans-encoded small RNA and host factor RNase III. *Nature*, *471*(7340). https://doi.org/10.1038/nature09886

Desbats, M. A., Lunardi, G., Doimo, M., Trevisson, E., & Salviati, L. (2015). Genetic bases and clinical manifestations of coenzyme Q10 (CoQ10) deficiency. *Journal of Inherited Metabolic Disease*, *38*(1). https://doi.org/10.1007/s10545-014-9749-9

Desbats, M. A., Morbidoni, V., Silic-Benussi, M., Doimo, M., Ciminale, V., Cassina, M., Sacconi, S., Hirano, M., Basso, G., Pierrel, F., Navas, P., Salviati, L., & Trevisson, E. (2016). The COQ2 genotype predicts the severity of Coenzyme Q10 deficiency. *Human Molecular Genetics*, *25*(19). https://doi.org/10.1093/hmg/ddw257

Dicarlo, J. E., Norville, J. E., Mali, P., Rios, X., Aach, J., & Church, G. M. (2013). Genome engineering in Saccharomyces cerevisiae using CRISPR-Cas systems. *Nucleic Acids Research*, *41*(7). https://doi.org/10.1093/nar/gkt135

Dimauro, S. (2004). Mitochondrial medicine. *Biochimica et Biophysica Acta - Bioenergetics*, *1659*(2–3). https://doi.org/10.1016/j.bbabio.2004.08.003

DiMauro, S., & Schon, E. A. (2003). Mitochondrial Respiratory-Chain Diseases. *New England Journal of Medicine*, *348*(26). https://doi.org/10.1056/nejmra022567

DiMauro, S., Schon, E. A., Carelli, V., & Hirano, M. (2013). The clinical maze of mitochondrial neurology. In *Nature Reviews Neurology* (Vol. 9, Issue 8). https://doi.org/10.1038/nrneurol.2013.126

Dimmer, K. S., & Rapaport, D. (2017). Mitochondrial contact sites as platforms for phospholipid exchange. In *Biochimica et Biophysica Acta - Molecular and Cell Biology of Lipids* (Vol. 1862, Issue 1). https://doi.org/10.1016/j.bbalip.2016.07.010

Dixon, S. J., Lemberg, K. M., Lamprecht, M. R., Skouta, R., Zaitsev, E. M., Gleason, C. E., Patel, D. N., Bauer, A. J., Cantley, A. M., Yang, W. S., Morrison, B., & Stockwell, B. R. (2012). Ferroptosis: An iron-dependent form of nonapoptotic cell death. *Cell*, *149*(5). https://doi.org/10.1016/j.cell.2012.03.042

Doimo, M., Desbats, M. A., Cerqua, C., Cassina, M., Trevisson, E., & Salviati, L. (2014). Genetics of coenzyme Q10 deficiency. *Molecular Syndromology*, *5*(3–4). https://doi.org/10.1159/000362826

Dolezal, P., Likic, V., Tachezy, J., & Lithgow, T. (2006). Evolution of the molecular machines for protein import into mitochondria. In *Science* (Vol. 313, Issue 5785). https://doi.org/10.1126/science.1127895

Dolinski, K., & Botstein, D. (2007). Orthology and functional conservation in eukaryotes. In *Annual Review of Genetics* (Vol. 41). https://doi.org/10.1146/annurev.genet.40.110405.090439

Doll, S., Freitas, F. P., Shah, R., Aldrovandi, M., da Silva, M. C., Ingold, I., Grocin, A. G., Xavier da Silva, T. N., Panzilius, E., Scheel, C. H., Mourão, A., Buday, K., Sato, M., Wanninger, J., Vignane, T., Mohana, V., Rehberg, M., Flatley, A., Schepers, A., … Conrad, M. (2019). FSP1 is a glutathione-independent ferroptosis suppressor. *Nature*, *575*(7784). https://doi.org/10.1038/s41586-019-1707-0

Doudna, J. A., & Charpentier, E. (2014). The new frontier of genome engineering with CRISPR-Cas9. In *Science* (Vol. 346, Issue 6213). https://doi.org/10.1126/science.1258096

Du, X., Yang, Y., Zhan, X., Huang, Y., Fu, Y., Zhang, Z., Liu, H., Zhang, L., Li, Y., Wen, Q., Zhou, X., Zuo, D., Zhou, C., Li, L., Hu, S., & Ma, L. (2020). Vitamin B6 prevents excessive inflammation by reducing accumulation of sphingosine-1-phosphate in a sphingosine-1-phosphate lyase–dependent manner. *Journal of Cellular and Molecular Medicine*, *24*(22). https://doi.org/10.1111/jcmm.15917

Dudkina, N. V., Kudryashev, M., Stahlberg, H., & Boekema, E. J. (2011). Interaction of complexes I, III, and IV within the bovine respirasome by single particle cryoelectron tomography. *Proceedings of the National Academy of Sciences of the United States of America*, *108*(37). https://doi.org/10.1073/pnas.1107819108

Echtay, K. S., Winkler, E., Frischmuth, K., & Klingenberg, M. (2001). Uncoupling proteins 2 and 3 are highly active H+ transporters and highly nucleotide sensitive when activated by coenzyme Q (ubiquinone). *Proceedings of the National Academy of Sciences of the United States of America*, *98*(4). https://doi.org/10.1073/pnas.98.4.1416

Echtay, K. S., Winkler, E., & Klingenberg, M. (2000). Coenzyme Q is an obligatory cofactor for uncoupling protein function. *Nature*, *408*(6812). https://doi.org/10.1038/35046114

Epinat, J. C., Amould, S., Chames, P., Rochaix, P., Desfontaines, D., Puzin, C., Patin, A., Zanghellini, A., Pâques, F., & Lacroix, E. (2003). A novel engineered meganuclease induces homologous recombination in yeast and mammalian cells. *Nucleic Acids Research*, *31*(11). https://doi.org/10.1093/nar/gkg375

Ernster, L., Ikkos, D., & Luft, R. (1959). Enzymic activities of human skeletal muscle mitochondria: A tool in clinical cetabolic research. *Nature*, *184*(4702). https://doi.org/10.1038/1841851a0

Espinosa-Cantú, A., Cruz-Bonilla, E., Noda-Garcia, L., & DeLuna, A. (2020). Multiple Forms of Multifunctional Proteins in Health and Disease. In *Frontiers in Cell and Developmental Biology* (Vol. 8). https://doi.org/10.3389/fcell.2020.00451

Esteves, T. C., Echtay, K. S., Jonassen, T., Clarke, C. F., & Brand, M. D. (2004). Ubiquinone is not required for proton conductance by uncoupling protein 1 in yeast mitochondria. *Biochemical Journal*, *379*(2). https://doi.org/10.1042/BJ20031682

Evers, C., Staufner, C., Granzow, M., Paramasivam, N., Hinderhofer, K., Kaufmann, L., Fischer, C., Thiel, C., Opladen, T., Kotzaeridou, U., Wiemann, S., Schlesner, M., Eils, R., Kölker, S., Bartram, C. R., Hoffmann, G. F., & Moog, U. (2017). Impact of clinical exomes in neurodevelopmental and neurometabolic disorders. *Molecular Genetics and Metabolism*, *121*(4), 297–307. https://doi.org/10.1016/j.ymgme.2017.06.014

Feng, Z., Zhang, B., Ding, W., Liu, X., Yang, D. L., Wei, P., Cao, F., Zhu, S., Zhang, F., Mao, Y., & Zhu, J. K. (2013). Efficient genome editing in plants using a CRISPR/Cas system. In *Cell Research* (Vol. 23, Issue 10). https://doi.org/10.1038/cr.2013.114

Fernández-Ayala, D. J. M., Brea-Calvo, G., López-Lluch, G., & Navas, P. (2005). Coenzyme Q distribution in HL-60 human cells depends on the endomembrane system. *Biochimica et Biophysica Acta - Biomembranes*, *1713*(2). https://doi.org/10.1016/j.bbamem.2005.05.010

Fernández-del-Río, L., Kelly, M. E., Contreras, J., Bradley, M. C., James, A. M., Murphy, M. P., Payne, G. S., & Clarke, C. F. (2020). Genes and lipids that impact uptake and assimilation of exogenous coenzyme Q in Saccharomyces cerevisiae. *Free Radical Biology and Medicine*, *154*. https://doi.org/10.1016/j.freeradbiomed.2020.04.029

Fishbein, J. D., Dobrowsky, R. T., Bielawska, A., Garrett, S., & Hannun, Y. A. (1993). Ceramide-mediated growth inhibition and CAPP are conserved in Saccharomyces cerevisiae. *Journal of Biological Chemistry*, *268*(13). https://doi.org/10.1016/s0021-9258(18)98343-2

Floyd, B. J., Wilkerson, E. M., Veling, M. T., Minogue, C. E., Xia, C., Beebe, E. T., Wrobel, R. L., Cho, H., Kremer, L. S., Alston, C. L., Gromek, K. A., Dolan, B. K., Ulbrich, A., Stefely, J. A., Bohl, S. L., Werner, K. M., Jochem, A., Westphall, M. S., Rensvold, J. W., … Pagliarini, D. J. (2016). Mitochondrial Protein Interaction Mapping Identifies Regulators of Respiratory Chain Function. *Molecular Cell*, *63*(4). https://doi.org/10.1016/j.molcel.2016.06.033

Fox, T. D. (2012). Mitochondrial protein synthesis, import, and assembly. *Genetics*, *192*(4). https://doi.org/10.1534/genetics.112.141267

Freyer, C., Stranneheim, H., Naess, K., Mourier, A., Felser, A., Maffezzini, C., Lesko, N., Bruhn, H., Engvall, M., Wibom, R., Barbaro, M., Hinze, Y., Magnusson, M., Andeer, R., Zetterström, R. H., Von Döbeln, U., Wredenberg, A., & Wedell, A. (2015). Rescue of primary ubiquinone deficiency due to a novel COQ7 defect using 2,4-dihydroxybensoic acid. *Journal of Medical Genetics*, *52*(11). https://doi.org/10.1136/jmedgenet-2015-102986

Galluzzi, L., Kepp, O., & Kroemer, G. (2012). Mitochondria: Master regulators of danger signalling. In *Nature Reviews Molecular Cell Biology* (Vol. 13, Issue 12). https://doi.org/10.1038/nrm3479

Garí, E., Piedrafita, L., Aldea, M., & Herrero, E. (1997). A set of vectors with a tetracycline-regulatable promoter system for modulated gene expression in Saccharomyces cervisiae. *Yeast*, *13*(9). https://doi.org/10.1002/(SICI)1097-0061(199707)13:9<837::AID-YEA145>3.0.CO;2-T

Gault, C. R., Obeid, L. M., & Hannun, Y. A. (2010). An overview of sphingolipid metabolism: From synthesis to breakdown. In *Advances in Experimental Medicine and Biology* (Vol. 688). https://doi.org/10.1007/978-1-4419-6741-1_1

Gennero, I., Fauvel, J., Niéto, M., Cariven, C., Gaits, F., Briand-Mésange, F., Chap, H., & Salles, J. P. (2002). Apoptotic effect of sphingosine 1-phosphate and increased sphingosine 1-phosphate hydrolysis on mesangial cells cultured at low cell density. *Journal of Biological Chemistry*, *277*(15). https://doi.org/10.1074/jbc.M108933200

Gietz, R. D., & Woods, R. A. (2006). Yeast transformation by the LiAc/SS Carrier DNA/PEG method. *Methods in Molecular Biology (Clifton, N.J.)*, *313*. https://doi.org/10.1385/1-59259-958-3:107

Gille, L., & Nohl, H. (2000). The existence of a lysosomal redox chain and the role of ubiquinone. *Archives of Biochemistry and Biophysics*, *375*(2). https://doi.org/10.1006/abbi.1999.1649

Gin, P., & Clarke, C. F. (2005). Genetic evidence for a multi-subunit complex in coenzyme Q biosynthesis in yeast and the role of the Coq1 hexaprenyl diphosphate synthase. *Journal of Biological Chemistry*, *280*(4). https://doi.org/10.1074/jbc.M411527200

Gnügge, R., & Rudolf, F. (2017). Saccharomyces cerevisiae Shuttle vectors. In *Yeast* (Vol. 34, Issue 5). https://doi.org/10.1002/yea.3228

González-Ramos, D., Van Den Broek, M., Van Maris, A. J. A., Pronk, J. T., & Daran, J. M. G. (2013). Genome-scale analyses of butanol tolerance in Saccharomyces cerevisiae reveal an essential role of protein degradation. *Biotechnology for Biofuels*, *6*(1). https://doi.org/10.1186/1754-6834-6-48

Gottlieb, D., Heideman, W., & Saba, J. D. (1999). The DPL1 gene is involved in mediating the response to nutrient deprivation in saccharomyces cerevisiae. *Molecular Cell Biology Research Communications*, *1*(1). https://doi.org/10.1006/mcbr.1999.0109

Gratz, S. J., Cummings, A. M., Nguyen, J. N., Hamm, D. C., Donohue, L. K., Harrison, M. M., Wildonger, J., & O'connor-Giles, K. M. (2013). Genome engineering of Drosophila with the CRISPR RNA-guided Cas9 nuclease. In *Genetics* (Vol. 194, Issue 4). https://doi.org/10.1534/genetics.113.152710

Gray, M. W. (2014). The pre-endosymbiont hypothesis: A new perspective on the origin and evolution of mitochondria. *Cold Spring Harbor Perspectives in Biology*, *6*(3). https://doi.org/10.1101/cshperspect.a016097

Guerra, R. M., & Pagliarini, D. J. (2023). Coenzyme Q biochemistry and biosynthesis. In *Trends in Biochemical Sciences* (Vol. 48, Issue 5). https://doi.org/10.1016/j.tibs.2022.12.006

Guo, R. T., Kuo, C. J., Chou, C. C., Ko, T. P., Shr, H. L., Liang, P. H., & Wang, A. H. J. (2004). Crystal Structure of Octaprenyl Pyrophosphate Synthase from Hyperthermophilic Thermotoga maritima and Mechanism of Product Chain Length Determination. *Journal of Biological Chemistry*, *279*(6). https://doi.org/10.1074/jbc.M310161200

Haak, D., Gable, K., Beeler, T., & Dunn, T. (1997). Hydroxylation of Saccharomyces cerevisiae ceramides requires Sur2p and Scs7p. *Journal of Biological Chemistry*, *272*(47). https://doi.org/10.1074/jbc.272.47.29704

Hannun, Y. A., & Obeid, L. M. (2008). Principles of bioactive lipid signalling: Lessons from sphingolipids. In *Nature Reviews Molecular Cell Biology* (Vol. 9, Issue 2). https://doi.org/10.1038/nrm2329

Harbauer, A. B., Zahedi, R. P., Sickmann, A., Pfanner, N., & Meisinger, C. (2014). The protein import machinery of mitochondria - A regulatory hub in metabolism, stress, and disease. In *Cell Metabolism* (Vol. 19, Issue 3). https://doi.org/10.1016/j.cmet.2014.01.010

Hayashi, K., Ogiyama, Y., Yokomi, K., Nakagawa, T., Kaino, T., & Kawamukai, M. (2014). Functional conservation of coenzyme Q biosynthetic genes among yeasts, plants, and humans. *PLoS ONE*, *9*(6). https://doi.org/10.1371/journal.pone.0099038

He, C. H., Xie, L. X., Allan, C. M., Tran, U. C., & Clarke, C. F. (2014). Coenzyme Q supplementation or over-expression of the yeast Coq8 putative kinase stabilizes multi-subunit Coq polypeptide complexes in yeast coq null mutants. *Biochimica et Biophysica Acta - Molecular and Cell Biology of Lipids*, *1841*(4). https://doi.org/10.1016/j.bbalip.2013.12.017

Heaton, R. A., Heales, S., Rahman, K., Sexton, D. W., & Hargreaves, I. (2020). The effect of cellular coenzyme q10 deficiency on lysosomal acidification. *Journal of Clinical Medicine*, *9*(6). https://doi.org/10.3390/jcm9061923

Heeringa, S. F., Chernin, G., Chaki, M., Zhou, W., Sloan, A. J., Ji, Z., Xie, L. X., Salviati, L., Hurd, T. W., Vega-Warner, V., Killen, P. D., Raphael, Y., Ashraf, S., Ovunc, B., Schoeb, D. S., McLaughlin, H. M., Airik, R., Vlangos, C. N., Gbadegesin, R., … Hildebrandt, F. (2011). COQ6 mutations in human patients produce nephrotic syndrome with sensorineural deafness. *Journal of Clinical Investigation*, *121*(5). https://doi.org/10.1172/JCI45693

Hermann, G. J., & Shaw, J. M. (1998). Mitochondrial dynamics in yeast. In *Annual Review of Cell and Developmental Biology* (Vol. 14). https://doi.org/10.1146/annurev.cellbio.14.1.265

Horvath, S. E., & Daum, G. (2013). Lipids of mitochondria. In *Progress in Lipid Research* (Vol. 52, Issue 4). https://doi.org/10.1016/j.plipres.2013.07.002

Hsieh, E. J., Gin, P., Gulmezian, M., Tran, U. P. C., Saiki, R., Marbois, B. N., & Clarke, C. F. (2007). Saccharomyces cerevisiae Coq9 polypeptide is a subunit of the mitochondrial coenzyme Q biosynthetic complex. *Archives of Biochemistry and Biophysics*, *463*(1). https://doi.org/10.1016/j.abb.2007.02.016

Hsu, P. D., Lander, E. S., & Zhang, F. (2014). Development and applications of CRISPR-Cas9 for genome engineering. In *Cell* (Vol. 157, Issue 6). https://doi.org/10.1016/j.cell.2014.05.010

Hughes, B. G., Harrison, P. M., & Hekimi, S. (2017). Estimating the occurrence of primary ubiquinone deficiency by analysis of large-scale sequencing data. *Scientific Reports*, *7*(1). https://doi.org/10.1038/s41598-017-17564-y

Huwiler, A., Bourquin, F., Kotelevets, N., Pastukhov, O., Capitani, G., Grütter, M. G., & Zangemeister-Wittke, U. (2011). A prokaryotic S1P lyase degrades extracellular S1P in vitro and in vivo: Implication for treating hyperproliferative disorders. *PLoS ONE*, *6*(8). https://doi.org/10.1371/journal.pone.0022436

Hwang, W. Y., Fu, Y., Reyon, D., Maeder, M. L., Tsai, S. Q., Sander, J. D., Peterson, R. T., Yeh, J. R. J., & Joung, J. K. (2013). Efficient genome editing in zebrafish using a CRISPR-Cas system. *Nature Biotechnology*, *31*(3). https://doi.org/10.1038/nbt.2501

Iványi, B., Rácz, G. Z., Gál, P., Brinyiczki, K., Bódi, I., Kalmár, T., Maróti, Z., & Bereczki, C. (2018). Diffuse mesangial sclerosis in a PDSS2 mutation-induced coenzyme Q10 deficiency. *Pediatric Nephrology*, *33*(3). https://doi.org/10.1007/s00467-017-3814-1

Iwamoto, M. A., Fairclough, S. R., Rudge, S. A., & Engebrecht, J. A. (2005). Saccharomyces cerevisiae Sps1p regulates trafficking of enzymes required for spore wall synthesis. *Eukaryotic Cell*, *4*(3). https://doi.org/10.1128/EC.4.3.536-544.2005

Janecke, A. R., Xu, R., Steichen-Gersdorf, E., Waldegger, S., Entenmann, A., Giner, T., Krainer, I., Huber, L. A., Hess, M. W., Frishberg, Y., Barash, H., Tzur, S., Schreyer-Shafir, N., Sukenik–Halevy, R., Zehavi, T., Raas-Rothschild, A., Mao, C., & Müller, T. (2017). Deficiency of the sphingosine-1-phosphate lyase SGPL1 is associated with congenital nephrotic syndrome and congenital adrenal calcifications. *Human Mutation*, *38*(4). https://doi.org/10.1002/humu.23192

Jiang, X., Stockwell, B. R., & Conrad, M. (2021). Ferroptosis: mechanisms, biology and role in disease. In *Nature Reviews Molecular Cell Biology* (Vol. 22, Issue 4). https://doi.org/10.1038/s41580-020-00324-8

Jinek, M., Chylinski, K., Fonfara, I., Hauer, M., Doudna, J. A., & Charpentier, E. (2012). A programmable dual-RNA-guided DNA endonuclease in adaptive bacterial immunity. *Science*, *337*(6096). https://doi.org/10.1126/science.1225829

Jonassen, T., Davis, D. E., Larsen, P. L., & Clarke, C. F. (2003). Reproductive Fitness and Quinone Content of Caenorhabditis elegans clk-1 Mutants Fed Coenzyme Q Isoforms of Varying Length. *Journal of Biological Chemistry*, *278*(51). https://doi.org/10.1074/jbc.M308760200

Joung, J. K., & Sander, J. D. (2013). TALENs: A widely applicable technology for targeted genome editing. In *Nature Reviews Molecular Cell Biology* (Vol. 14, Issue 1). https://doi.org/10.1038/nrm3486

Katz, S. S., Gimble, F. S., & Storici, F. (2014). To nick or not to nick: Comparison of I-SceI single-And double-strand break-induced recombination in yeast and human cells. *PLoS ONE*, *9*(2). https://doi.org/10.1371/journal.pone.0088840

Kawamukai, M. (2009). Biosynthesis and bioproduction of coenzyme Q 10 by yeasts and other organisms . *Biotechnology and Applied Biochemistry*, *53*(4). https://doi.org/10.1042/ba20090035

Kawamukai, M. (2016). Biosynthesis of coenzyme Q in eukaryotes. In *Bioscience, Biotechnology and Biochemistry* (Vol. 80, Issue 1). https://doi.org/10.1080/09168451.2015.1065172

Kawamukai, M. (2018). Biosynthesis and applications of prenylquinones. *Bioscience, Biotechnology and Biochemistry*, *82*(6). https://doi.org/10.1080/09168451.2018.1433020

Kemmerer, Z. A., Robinson, K. P., Schmitz, J. M., Manicki, M., Paulson, B. R., Jochem, A., Hutchins, P. D., Coon, J. J., & Pagliarini, D. J. (2021). UbiB proteins regulate cellular CoQ distribution in Saccharomyces cerevisiae. *Nature Communications*, *12*(1). https://doi.org/10.1038/s41467-021-25084-7

Kerr, D. S. (2010). Treatment of mitochondrial electron transport chain disorders: A review of clinical trials over the past decade. In *Molecular Genetics and Metabolism* (Vol. 99, Issue 3). https://doi.org/10.1016/j.ymgme.2009.11.005

Kerr, D. S. (2013). Review of Clinical Trials for Mitochondrial Disorders: 1997-2012. In *Neurotherapeutics* (Vol. 10, Issue 2). https://doi.org/10.1007/s13311-013-0176-7

Kido, Y., Shiba, T., Inaoka, D. K., Sakamoto, K., Nara, T., Aoki, T., Honma, T., Tanaka, A., Inoue, M., Matsuoka, S., Moore, A., Harada, S., & Kita, K. (2010). Crystallization and preliminary crystallographic analysis of cyanide-insensitive alternative oxidase from Trypanosoma brucei brucei. *Acta Crystallographica Section F: Structural Biology and Crystallization Communications*, *66*(3). https://doi.org/10.1107/S1744309109054062

Kim, S., Fyrst, H., & Saba, J. (2000). Accumulation of phosphorylated sphingoid long chain bases results in cell growth inhibition in Saccharomyces cerevisiae. *Genetics*, *156*(4). https://doi.org/10.1093/genetics/156.4.1519

Koike-Takeshita, A., Koyama, T., Obata, S., & Ogura, K. (1995). Molecular cloning and nucleotide sequences of the genes for two essential proteins constituting a novel enzyme system for heptaprenyl diphosphate synthesis. *Journal of Biological Chemistry*, *270*(31). https://doi.org/10.1074/jbc.270.31.18396

Koyama, T. (1999). Molecular analysis of prenyl chain elongating enzymes. *Bioscience, Biotechnology and Biochemistry*, *63*(10). https://doi.org/10.1271/bbb.63.1671

Lapuente-Brun, E., Moreno-Loshuertos, R., Aciń-Pérez, R., Latorre-Pellicer, A., Colaś, C., Balsa, E., Perales-Clemente, E., Quirós, P. M., Calvo, E., Rodríguez-Hernández, M. A., Navas, P., Cruz, R., Carracedo, Á., Loṕez-Otín, C., Peŕez-Martos, A., Fernańdez-Silva, P., Fernańdez-Vizarra, E., & Enríquez, J. A. (2013). Supercomplex assembly determines electron flux in the mitochondrial electron transport chain. *Science*, *340*(6140). https://doi.org/10.1126/science.1230381

Laurent, J. M., Young, J. H., Kachroo, A. H., & Marcotte, E. M. (2016). Efforts to make and apply humanized yeast. *Briefings in Functional Genomics*, *15*(2). https://doi.org/10.1093/bfgp/elv041

Leslie, M. (2015). Yeast can live with human genes. *Science*. https://doi.org/10.1126/science.aac4634

LESTER, R. L., & CRANE, F. L. (1959). The natural occurrence of coenzyme Q and related compounds. *The Journal of Biological Chemistry*, *234*(8). https://doi.org/10.1016/s0021-9258(18)69886-2

Liang, J., Han, Q., Tan, Y., Ding, H., & Li, J. (2019). Current advances on structure-function relationships of pyridoxal 5'-phosphate-dependent enzymes. In *Frontiers in Molecular Biosciences* (Vol. 6, Issue MAR). https://doi.org/10.3389/fmolb.2019.00004

Liang, P. H., Ko, T. P., & Wang, A. H. J. (2002). Structure, mechanism and function of prenyltransferases. In *European Journal of Biochemistry* (Vol. 269, Issue 14). https://doi.org/10.1046/j.1432-1033.2002.03014.x

Lill, R., Hoffmann, B., Molik, S., Pierik, A. J., Rietzschel, N., Stehling, O., Uzarska, M. A., Webert, H., Wilbrecht, C., & Mühlenhoff, U. (2012). The role of mitochondria in cellular iron-sulfur protein biogenesis and iron metabolism. In *Biochimica et Biophysica Acta - Molecular Cell Research* (Vol. 1823, Issue 9). https://doi.org/10.1016/j.bbamcr.2012.05.009

López, L. C., Schuelke, M., Quinzii, C. M., Kanki, T., Rodenburg, R. J. T., Naini, A., DiMauro, S., & Hirano, M. (2006). Leigh syndrome with nephropathy and CoQ10 deficiency due to decaprenyl diphosphote synthase subunit 2 (PDSS2) mutations. *American Journal of Human Genetics*, *79*(6). https://doi.org/10.1086/510023

Lorenz, E. C., Lieske, J. C., Seide, B. M., Meek, A. M., Olson, J. B., Bergstralh, E. J., & Milliner, D. S. (2014). Sustained pyridoxine response in primary hyperoxaluria type 1 recipients of kidney alone transplant. *American Journal of Transplantation*, *14*(6). https://doi.org/10.1111/ajt.12706

Lorenz, M. C., Muir, R. S., Lim, E., McElver, J., Weber, S. C., & Heitman, J. (1995). Gene disruption with PCR products in Saccharomyces cerevisiae. *Gene*, *158*(1). https://doi.org/10.1016/0378-1119(95)00144-U

Lovric, S., Goncalves, S., Gee, H. Y., Oskouian, B., Srinivas, H., Choi, W. Il, Shril, S., Ashraf, S., Tan, W., Rao, J., Airik, M., Schapiro, D., Braun, D. A., Sadowski, C. E., Widmeier, E., Jobst-Schwan, T., Schmidt, J. M., Girik, V., Capitani, G., … Hildebrandt, F. (2017). Mutations in sphingosine-1-phosphate lyase cause nephrosis with ichthyosis and adrenal insufficiency. *Journal of Clinical Investigation*, *127*(3). https://doi.org/10.1172/JCI89626

Lu, T. Te, Lee, S. J., Apfel, U. P., & Lippard, S. J. (2013). Aging-associated enzyme human clock-1: Substrate-mediated reduction of the diiron center for 5-demethoxyubiquinone hydroxylation. *Biochemistry*, *52*(13). https://doi.org/10.1021/bi301674p

Lucito, R., Healy, J., Alexander, J., Reiner, A., Esposito, D., Chi, M., Rodgers, L., Brady, A., Sebat, J., Troge, J., West, J. A., Rostan, S., Nguyen, K. C. Q., Powers, S., Ye, K. Q., Olshen, A., Venkatraman, E., Norton, L., & Wigler, M. (2003). Representational oligonucleotide microarray analysis: A high-resolution method to detect genome copy number variation. *Genome Research*, *13*(10). https://doi.org/10.1101/gr.1349003

Luna-Sánchez, M., Díaz-Casado, E., Barca, E., Tejada, M. Á., Montilla-García, Á., Cobos, E. J., Escames, G., Acuña-Castroviejo, D., Quinzii, C. M., & López, L. C. (2015). The clinical heterogeneity of coenzyme Q 10 deficiency results from genotypic differences in the Coq9 gene . *EMBO Molecular Medicine*, *7*(5). https://doi.org/10.15252/emmm.201404632

Maceyka, M., Harikumar, K. B., Milstien, S., & Spiegel, S. (2012). Sphingosine-1-phosphate signaling and its role in disease. In *Trends in Cell Biology* (Vol. 22, Issue 1). https://doi.org/10.1016/j.tcb.2011.09.003

Maharaj, A., Williams, J., Bradshaw, T., Güran, T., Braslavsky, D., Casas, J., Chan, L. F., Metherell, L. A., & Prasad, R. (2020). Sphingosine-1-phosphate lyase (SGPL1) deficiency is associated with mitochondrial dysfunction. *Journal of Steroid Biochemistry and Molecular Biology*, *202*. https://doi.org/10.1016/j.jsbmb.2020.105730

Malicdan, M. C. V., Vilboux, T., Ben-Zeev, B., Guo, J., Eliyahu, A., Pode-Shakked, B., Dori, A., Kakani, S., Chandrasekharappa, S. C., Ferreira, C. R., Shelestovich, N., Marek-Yagel, D., Pri-Chen, H., Blatt, I., Niederhuber, J. E., He, L., Toro, C., Taylor, R. W., Deeken, J., … Anikster, Y. (2018). A novel inborn error of the coenzyme Q10 biosynthesis pathway: cerebellar ataxia and static encephalomyopathy due to COQ5 C-methyltransferase deficiency. *Human Mutation*, *39*(1). https://doi.org/10.1002/humu.23345

Malina, C., Yu, R., Bjorkeroth, J., Kerkhoven, E. J., & Nielsen, J. (2021). Adaptations in metabolism and protein translation give rise to the Crabtree effect in yeast. *Proceedings of the National Academy of Sciences of the United States of America*, *118*(51). https://doi.org/10.1073/pnas.2112836118

Mandala, S. M., Thornton, R., Tu, Z., Kurtz, M. B., Nickels, J., Broach, J., Menzeleev, R., & Spiegel, S. (1998). Sphingoid base 1-phosphate phosphatase: A key regulator of sphingolipid metabolism and stress response. *Proceedings of the National Academy of Sciences of the United States of America*, *95*(1). https://doi.org/10.1073/pnas.95.1.150

Manicki, M., Aydin, H., Abriata, L. A., Overmyer, K. A., Guerra, R. M., Coon, J. J., Dal Peraro, M., Frost, A., & Pagliarini, D. J. (2022). Structure and functionality of a multimeric human COQ7:COQ9 complex. *Molecular Cell*, *82*(22). https://doi.org/10.1016/j.molcel.2022.10.003

Mans, R., van Rossum, H. M., Wijsman, M., Backx, A., Kuijpers, N. G. A., van den Broek, M., Daran-Lapujade, P., Pronk, J. T., van Maris, A. J. A., & Daran, J. M. G. (2015). CRISPR/Cas9: A molecular Swiss army knife for simultaneous introduction of multiple genetic modifications in Saccharomyces cerevisiae. *FEMS Yeast Research*, *15*(2). https://doi.org/10.1093/femsyr/fov004

Mao, C., Wadleigh, M., Jenkins, G. M., Hannun, Y. A., & Obeid, L. M. (1997). Identification and characterization of Saccharomyces cerevisiae dihydrosphingosine-1-phosphate phosphatase. *Journal of Biological Chemistry*, *272*(45). https://doi.org/10.1074/jbc.272.45.28690

Marbois, B., Gin, P., Faull, K. F., Poon, W. W., Lee, P. T., Strahan, J., Shepherd, J. N., & Clarke, C. F. (2005). Coq3 and Coq4 define a polypeptide complex in yeast mitochondria for the biosynthesis of coenzyme Q. *Journal of Biological Chemistry*, *280*(21). https://doi.org/10.1074/jbc.M501315200

Marbois, B., Gin, P., Gulmezian, M., & Clarke, C. F. (2009). The yeast Coq4 polypeptide organizes a mitochondrial protein complex essential for coenzyme Q biosynthesis. *Biochimica et Biophysica Acta - Molecular and Cell Biology of Lipids*, *1791*(1). https://doi.org/10.1016/j.bbalip.2008.10.006

Mardis, E. R. (2013). Next-generation sequencing platforms. *Annual Review of Analytical Chemistry*, *6*. https://doi.org/10.1146/annurev-anchem-062012-092628

Marrero, P. F., Poulter, C. D., & Edwards, P. A. (1992). Effects of site-directed mutagenesis of the highly conserved aspartate residues in domain II of farnesyl diphosphate synthase activity. *Journal of Biological Chemistry*, *267*(30). https://doi.org/10.1016/s0021-9258(19)36693-1

Martínez-Reyes, I., Cardona, L. R., Kong, H., Vasan, K., McElroy, G. S., Werner, M., Kihshen, H., Reczek, C. R., Weinberg, S. E., Gao, P., Steinert, E. M., Piseaux, R., Budinger, G. R. S., & Chandel, N. S. (2020). Mitochondrial ubiquinol oxidation is necessary for tumour growth. *Nature*, *585*(7824). https://doi.org/10.1038/s41586-020-2475-6

Matmati, N., & Hannun, Y. A. (2008). ISC1 (inositol phosphosphingolipid-phospholipase C), the yeast homologue of neutral sphingomyelinases. *Journal of Lipid Research*, *49*(5). https://doi.org/10.1194/jlr.R800004-JLR200

McIlwain, H. (1964). A Treatise on the Chemical Constitution of the Brain . J. L. W. Thudichum . *Isis*, *55*(2). https://doi.org/10.1086/349859

Mero, S., Timonen, S., Lääveri, T., Løfberg, S., Kirveskari, J., Ursing, J., Rombo, L., Kofoed, P. E., & Kantele, A. (2021). Prevalence of diarrhoeal pathogens among children under five years of age with and without diarrhoea in guinea-bissau. *PLoS Neglected Tropical Diseases*, *15*(9). https://doi.org/10.1371/journal.pntd.0009709

Mezzar, S., De Schryver, E., & Van Veldhoven, P. P. (2014). RP-HPLC-fluorescence analysis of aliphatic aldehydes: Application to aldehyde-generating enzymes HACL1 and SGPL1. *Journal of Lipid Research*, *55*(3). https://doi.org/10.1194/jlr.D044230

Mitić, N., Smith, S. J., Neves, A., Guddat, L. W., Gahan, L. R., & Schenk, G. (2006). The catalytic mechanisms of binuclear metallohydrolases. In *Chemical Reviews* (Vol. 106, Issue 8). https://doi.org/10.1021/cr050318f

Mollet, J., Giurgea, I., Schlemmer, D., Dallner, G., Chretien, D., Delahodde, A., Bacq, D., De Lonlay, P., Munnich, A., & Rötig, A. (2007). Prenyldiphosphate synthase, subunit 1 (PDSS1) and OH-benzoate polyprenyltransferase (COQ2) mutations in ubiquinone deficiency and oxidative phosphorylation disorders. *Journal of Clinical Investigation*, *117*(3). https://doi.org/10.1172/JCI29089

Momose, K., & Rudney, H. (1972). 3-Polyprenyl-4-hydroxybenzoate synthesis in the inner membrane of mitochondria from p-hydroxybenzoate and isopentenylpyrophosphate. A demonstration of isoprenoid synthesis in rat liver mitochondria. *Journal of Biological Chemistry*, *247*(12).

Montini, G., Malaventura, C., & Salviati, L. (2008). Early Coenzyme Q10 Supplementation in Primary Coenzyme Q10 Deficiency. *New England Journal of Medicine*, *358*(26). https://doi.org/10.1056/nejmc0800582

Morton, R. A. (1958). Ubiquinone. *Nature*, *182*(4652). https://doi.org/10.1038/1821764a0

Mu, F. S., Luo, M., Fu, Y. J., Zhang, X., Yu, P., & Zu, Y. G. (2011). Synthesis of the key intermediate of coenzyme Q10. *Molecules*, *16*(5). https://doi.org/10.3390/molecules16054097

Mukhopadhyay, D., Howell, K. S., Riezman, H., & Capitani, G. (2008). Identifying key residues of sphinganine-1-phosphate lyase for function in vivo and in vitro. *Journal of Biological Chemistry*, *283*(29). https://doi.org/10.1074/jbc.M709753200

Murphy, M. P., & Chouchani, E. T. (2022). Why succinate? Physiological regulation by a mitochondrial coenzyme Q sentinel. In *Nature Chemical Biology* (Vol. 18, Issue 5). https://doi.org/10.1038/s41589-022-01004-8

Murray, J. A. (1987). Bending the rules: the 2-mu plasmid of yeast. *Molecular Microbiology*, *1*(1).

Nagiec, M. M., Skrzypek, M., Nagiec, E. E., Lester, R. L., & Dickson, R. C. (1998). The LCB4 (YOR171c) and LCB5 (YLR260w) genes of Saccharomyces encode sphingoid long chain base kinases. *Journal of Biological Chemistry*, *273*(31). https://doi.org/10.1074/jbc.273.31.19437

Nardecchia, F., De Giorgi, A., Palombo, F., Fiorini, C., De Negri, A. M., Carelli, V., Caporali, L., & Leuzzi, V. (2021). Missense PDSS1 mutations in CoenzymeQ10 synthesis cause optic atrophy and sensorineural deafness. *Annals of Clinical and Translational Neurology*, *8*(1). https://doi.org/10.1002/acn3.51232

Navas, P., Villalba, J. M., & de Cabo, R. (2007). The importance of plasma membrane coenzyme Q in aging and stress responses. *Mitochondrion*, *7*(SUPPL.). https://doi.org/10.1016/j.mito.2007.02.010

Nelson, K., Jackman, C., Bell, J., Shih, C. S., Payne, K., Dlouhy, S., & Walsh, L. (2018). Novel Homozygous Deletion in STRADA Gene Associated With Polyhydramnios, Megalencephaly, and Epilepsy in 2 Siblings: Implications for Diagnosis and Treatment. *Journal of Child Neurology*, *33*(14), 925–929. https://doi.org/10.1177/0883073818802724

Neupert, W., & Herrmann, J. M. (2007). Translocation of proteins into mitochondria. In *Annual Review of Biochemistry* (Vol. 76). https://doi.org/10.1146/annurev.biochem.76.052705.163409

Ng, P. C., & Henikoff, S. (2003). SIFT: Predicting amino acid changes that affect protein function. *Nucleic Acids Research*, *31*(13). https://doi.org/10.1093/nar/gkg509

Nguyen, T. P. T., Casarin, A., Desbats, M. A., Doimo, M., Trevisson, E., Santos-Ocaña, C., Navas, P., Clarke, C. F., & Salviati, L. (2014). Molecular characterization of the human COQ5 C-methyltransferase in coenzyme Q10 biosynthesis. *Biochimica et Biophysica Acta - Molecular and Cell Biology of Lipids*, *1841*(11). https://doi.org/10.1016/j.bbalip.2014.08.007

Nurk, S., Koren, S., Rhie, A., Rautiainen, M., Bzikadze, A. V., Mikheenko, A., Vollger, M. R., Altemose, N., Uralsky, L., Gershman, A., Aganezov, S., Hoyt, S. J., Diekhans, M., Logsdon, G. A., Alonge, M., Antonarakis, S. E., Borchers, M., Bouffard, G. G., Brooks, S. Y., … Phillippy, A. M. (2022). The complete sequence of a human genome. *Science*, *376*(6588). https://doi.org/10.1126/science.abj6987

Okada, K., Kainou, T., Tanaka, K., Nakagawa, T., Matsuda, H., & Kawamukai, M. (1998). Molecular cloning and mutational analysis of the ddsA gene encoding decaprenyl diphosphate synthase from Gluconobacter suboxydans. *European Journal of Biochemistry*, *255*(1). https://doi.org/10.1046/j.1432-1327.1998.2550052.x

Okada, K., Kamiya, Y., Zhu, X., Suzuki, K., Tanaka, K., Nakagawa, T., Matsuda, H., & Kawamukai, M. (1997). Cloning of the sdsA gene encoding solanesyl diphosphate synthase from Rhodobacter capsulatus and its functional expression in Escherichia coli and Saccharomyces cerevisiae. *Journal of Bacteriology*, *179*(19). https://doi.org/10.1128/jb.179.19.5992-5998.1997

Okada, K., Minehira, M., Zhu, X., Suzuki, K., Nakagawa, T., Matsuda, H., & Kawamukai, M. (1997). The ispB gene encoding octaprenyl diphosphate synthase is essential for growth of Escherichia coli. *Journal of Bacteriology*, *179*(9). https://doi.org/10.1128/jb.179.9.3058-3060.1997

Okada, K., Ohara, K., Yazaki, K., Nozaki, K., Uchida, N., Kawamukai, M., Nojiri, H., & Yamane, H. (2004). The AtPPT1 gene encoding 4-hydroxybenzoate polyprenyl diphosphate transferase in ubiquinone biosynthesis is required for embryo development in Arabidopsis thaliana. *Plant Molecular Biology*, *55*(4). https://doi.org/10.1007/s11103-004-1298-4

Okada, K., Suzuki, K., Kamiya, Y., Zhu, X. F., Fujisaki, S., Nishimura, Y., Nishino, T., Nakagawa, T., Kawamukai, M., & Matsuda, H. (1996). Polyprenyl diphosphate synthase essentially defines the length of the side chain of ubiquinone. *Biochimica et Biophysica Acta - Lipids and Lipid Metabolism*, *1302*(3). https://doi.org/10.1016/0005-2760(96)00064-1

Ozbay, T., Rowan, A., Leon, A., Patel, P., & Sewer, M. B. (2006). Cyclic adenosine 5′-monophosphate-dependent sphingosine-1-phosphate biosynthesis induces human CYP17 gene transcription by activating cleavage of sterol regulatory element binding protein 1. *Endocrinology*, *147*(3). https://doi.org/10.1210/en.2005-1091

Ozeir, M., Mühlenhoff, U., Webert, H., Lill, R., Fontecave, M., & Pierrel, F. (2011). Coenzyme Q biosynthesis: Coq6 is required for the C5-hydroxylation reaction and substrate analogs rescue Coq6 deficiency. *Chemistry and Biology*, *18*(9). https://doi.org/10.1016/j.chembiol.2011.07.008

Ozeir, M., Pelosi, L., Ismail, A., Mellot-Draznieks, C., Fontecave, M., & Pierrel, F. (2015). Coq6 is responsible for the C4-deamination reaction in coenzyme Q biosynthesis in Saccharomyces cerevisiae. *Journal of Biological Chemistry*, *290*(40). https://doi.org/10.1074/jbc.M115.675744

Pareek, V., Sha, Z., He, J., Wingreen, N. S., & Benkovic, S. J. (2021). Metabolic channeling: predictions, deductions, and evidence. In *Molecular Cell* (Vol. 81, Issue 18). https://doi.org/10.1016/j.molcel.2021.08.030

Paret, C., Ostermann, K., Krause-Buchholz, U., Rentzsch, A., & Rödel, G. (1999). Human members of the SCO1 gene family: Complementation analysis in yeast and intracellular localization. *FEBS Letters*, *447*(1). https://doi.org/10.1016/S0014-5793(99)00266-5

Park, Y. C., Kim, S. J., Choi, J. H., Lee, W. H., Park, K. M., Kawamukai, M., Ryu, Y. W., & Seo, J. H. (2005). Batch and fed-batch production of coenzyme Q10 in recombinant Escherichia coli containing the decaprenyl diphosphate synthase gene from Gluconobacter suboxydans. *Applied Microbiology and Biotechnology*, *67*(2). https://doi.org/10.1007/s00253-004-1743-y

Parker, W. E., Orlova, K. A., Parker, W. H., Birnbaum, J. F., Krymskaya, V. P., Goncharov, D. A., Baybis, M., Helfferich, J., Okochi, K., Strauss, K. A., & Crino, P. B. (2013a). Rapamycin prevents seizures after depletion of STRADA in a rare neurodevelopmental disorder. *Science Translational Medicine*, *5*(182). https://doi.org/10.1126/scitranslmed.3005271

Parker, W. E., Orlova, K. A., Parker, W. H., Birnbaum, J. F., Krymskaya, V. P., Goncharov, D. A., Baybis, M., Helfferich, J., Okochi, K., Strauss, K. A., & Crino, P. B. (2013b). Rapamycin prevents seizures after depletion of STRADA in a rare neurodevelopmental disorder. *Science Translational Medicine*, *5*(182). https://doi.org/10.1126/scitranslmed.3005271

Paulissen, S. M., & Huang, L. S. (2016). Efficient sporulation of Saccharomyces cerevisiae in a 96 multiwell format. *Journal of Visualized Experiments*, *2016*(115). https://doi.org/10.3791/54584

Paulissen, S. M., Slubowski, C. J., Roesner, J. M., & Huang, L. S. (2016). Timely closure of the prospore membrane requires SPS1 and SPo77 in Saccharomyces cerevisiae. *Genetics*, *203*(3). https://doi.org/10.1534/genetics.115.183939

Peng, M., Falk, M. J., Haase, V. H., King, R., Polyak, E., Selak, M., Yudkoff, M., Hancock, W. W., Meade, R., Saiki, R., Lunceford, A. L., Clarke, C. F., & Gasser, D. L. (2008). Primary coenzyme Q deficiency in Pdss2 mutant mice causes isolated renal disease. *PLoS Genetics*, *4*(4). https://doi.org/10.1371/journal.pgen.1000061

Perli, T., Wronska, A. K., Ortiz-Merino, R. A., Pronk, J. T., & Daran, J. M. (2020). Vitamin requirements and biosynthesis in Saccharomyces cerevisiae. *Yeast*, *37*(4). https://doi.org/10.1002/yea.3461

Petrossian, T. C., & Clarke, S. G. (2011). Uncovering the human methyltransferasome. *Molecular and Cellular Proteomics*, *10*(1). https://doi.org/10.1074/mcp.M110.000976

Petrossian, T., & Clarke, S. (2009). Bioinformatic identification of novel methyltransferases. *Epigenomics*, *1*(1). https://doi.org/10.2217/epi.09.3

Pfeiffer, T., & Morley, A. (2014). An evolutionary perspective on the Crabtree effect. *Frontiers in Molecular Biosciences*, *1*(OCT). https://doi.org/10.3389/fmolb.2014.00017

Prasad, R., Hadjidemetriou, I., Maharaj, A., Meimaridou, E., Buonocore, F., Saleem, M., Hurcombe, J., Bierzynska, A., Barbagelata, E., Bergadá, I., Cassinelli, H., Das, U., Sgene, G., Krone, R., Hacihamdioglu, B., Sari, E., Yesilkaya, E., Storr, H. L., Clemente, M., … Metherell, L. A. (2017). Sphingosine-1-phosphate lyase mutations cause primary adrenal insufficiency and steroid-resistant nephrotic syndrome. *Journal of Clinical Investigation*, *127*(3). https://doi.org/10.1172/JCI90171

Pray, L. (2008). Eukaryotic Genome Complexity. *Nature Education*, *1*(2008).

Puffenberger, E. G., Strauss, K. A., Ramsey, K. E., Craig, D. W., Stephan, D. A., Robinson, D. L., Hendrickson, C. L., Gottlieb, S., Ramsay, D. A., Siu, V. M., Heuer, G. G., Crino, P. B., & Morton, D. H. (2007). Polyhydramnios, megalencephaly and symptomatic epilepsy caused by a homozygous 7-kilobase deletion in LYK5. *Brain*, *130*(7), 1929–1941. https://doi.org/10.1093/brain/awm100

Qie, L., Nagiec, M. M., Baltisberger, J. A., Lester, R. L., & Dickson, R. C. (1997). Identification of a Saccharomyces gene, LCB3, necessary for incorporation of exogenous long chain bases into sphingolipids. *Journal of Biological Chemistry*, *272*(26). https://doi.org/10.1074/jbc.272.26.16110

Quinzii, C. M., López, L. C., Von-Moltke, J., Naini, A., Krishna, S., Schuelke, M., Salviati, L., Navas, P., DiMauro, S., & Hirano, M. (2008). Respiratory chain dysfunction and oxidative stress correlate with severity of primary CoQ 10 deficiency . *The FASEB Journal*, *22*(6). https://doi.org/10.1096/fj.07-100149

Rampelt, H., Zerbes, R. M., van der Laan, M., & Pfanner, N. (2017). Role of the mitochondrial contact site and cristae organizing system in membrane architecture and dynamics. In *Biochimica et Biophysica Acta - Molecular Cell Research* (Vol. 1864, Issue 4). https://doi.org/10.1016/j.bbamcr.2016.05.020

Romanos, M. A., Scorer, C. A., & Clare, J. J. (1992). Foreign gene expression in yeast: a review. *Yeast*, *8*(6). https://doi.org/10.1002/yea.320080602

Ross, D., & Siegel, D. (2017). Functions of NQO1 in cellular protection and CoQ10 metabolism and its potential role as a redox sensitive molecular switch. In *Frontiers in Physiology* (Vol. 8, Issue AUG). https://doi.org/10.3389/fphys.2017.00595

Rötig, A., Appelkvist, E. L., Geromel, V., Chretien, D., Kadhom, N., Edery, P., Lebideau, M., Dallner, G., Munnich, A., Ernster, L., & Rustin, P. (2000). Quinone-responsive multiple respiratory-chain dysfunction due to widespread coenzyme Q10 deficiency. *Lancet*, *356*(9227). https://doi.org/10.1016/S0140-6736(00)02531-9

Saba, J. D. (2019). Fifty years of lyase and a moment of truth: Sphingosine phosphate lyase from discovery to disease. *Journal of Lipid Research*, *60*(3). https://doi.org/10.1194/jlr.S091181

Saba, J. D., Nara, F., Bielawska, A., Garrett, S., & Hannun, Y. A. (1997). The BST1 gene of Saccharomyces cerevisiae is the sphingosine-1-phosphate lyase. *Journal of Biological Chemistry*, *272*(42). https://doi.org/10.1074/jbc.272.42.26087

Sacconi, S., Trevisson, E., Pistollato, F., Baldoin, M. C., Rezzonico, R., Bourget, I., Desnuelle, C., Tenconi, R., Basso, G., DiMauro, S., & Salviati, L. (2005). hCOX18 and hCOX19: Two human genes involved in cytochrome c oxidase assembly. *Biochemical and Biophysical Research Communications*, *337*(3). https://doi.org/10.1016/j.bbrc.2005.09.127

Sadowski, C. E., Lovric, S., Ashraf, S., Pabst, W. L., Gee, H. Y., Kohl, S., Engelmann, S., Vega-Warner, V., Fang, H., Halbritter, J., Somers, M. J., Tan, W., Shril, S., Fessi, I., Lifton, R. P., Bockenhauer, D., El-Desoky, S., Kari, J. A., Zenker, M., … Zolotnistskaya, A. (2015). A single-gene cause in 29.5% of cases of steroid-resistant nephrotic syndrome. *Journal of the American Society of Nephrology*, *26*(6). https://doi.org/10.1681/ASN.2014050489

Saiki, R., Lunceford, A. L., Shi, Y., Marbois, B., King, R., Pachuski, J., Kawamukai, M., Gasser, D. L., & Clarke, C. F. (2008). Coenzyme Q10 supplementation rescues renal disease in Pdss2 kd/kd mice with mutations in prenyl diphosphate synthase subunit 2. *American Journal of Physiology - Renal Physiology*, *295*(5). https://doi.org/10.1152/ajprenal.90445.2008

Saiki, R., Nagata, A., Kainou, T., Matsuda, H., & Kawamukai, M. (2005). Characterization of solanesyl and decaprenyl diphosphate synthases in mice and humans. *FEBS Journal*, *272*(21). https://doi.org/10.1111/j.1742-4658.2005.04956.x

Salviati, L., Sacconi, S., Murer, L., Zacchello, G., Franceschini, L., Laverda, A. M., Basso, G., Quinzii, C., Angelini, C., Hirano, M., Naini, A. B., Navas, P., DiMauro, S., & Montini, G. (2005). Infantile encephalomyopathy and nephropathy with CoQ10 deficiency: A CoQ10-responsive condition. *Neurology*, *65*(4). https://doi.org/10.1212/01.wnl.0000172859.55579.a7

Salviati, L., Trevisson, E., Hernandez, M. A. R., Casarin, A., Pertegato, V., Doimo, M., Cassina, M., Agosto, C., Desbats, M. A., Sartori, G., Sacconi, S., Memo, L., Zuffardi, O., Artuch, R., Quinzii, C., DiMauro, S., Hirano, M., Santos-Ocaña, C., & Navas, P. (2012). Haploinsufficiency of COQ4 causes coenzyme Q10 deficiency. *Journal of Medical Genetics*, *49*(3). https://doi.org/10.1136/jmedgenet-2011-100394

Saraste, M. (1999). Oxidative phosphorylation at the fin de siecle. In *Science* (Vol. 283, Issue 5407). https://doi.org/10.1126/science.283.5407.1488

Savić, N., & Schwank, G. (2016). Advances in therapeutic CRISPR/Cas9 genome editing. In *Translational Research* (Vol. 168). https://doi.org/10.1016/j.trsl.2015.09.008

Schenk, G., Mitić, N., Gahan, L. R., Ollis, D. L., McGeary, R. P., & Guddat, L. W. (2012). Binuclear metallohydrolases: Complex mechanistic strategies for a simple chemical reaction. In *Accounts of Chemical Research* (Vol. 45, Issue 9). https://doi.org/10.1021/ar300067g

Skladal, D., Halliday, J., & Thorburn, D. R. (2003). Minimum birth prevalence of mitochondrial respiratory chain disorders in children. *Brain*, *126*(8). https://doi.org/10.1093/brain/awg170

Slubowski, C. J., Paulissen, S. M., & Huang, L. S. (2014). The GCKIII kinase Sps1 and the 14-3-3 isoforms, Bmh1 and Bmh2, cooperate to ensure proper sporulation in Saccharomyces cerevisiae. *PloS One*, *9*(11). https://doi.org/10.1371/JOURNAL.PONE.0113528

Smith, M. G., & Snyder, M. (2006). Yeast as a model for human disease. In *Current protocols in human genetics / editorial board, Jonathan L. Haines ... [et al.]: Vol. Chapter 15*. https://doi.org/10.1002/0471142905.hg1506s48

Sondheimer, N., Hewson, S., Cameron, J. M., Somers, G. R., Broadbent, J. D., Ziosi, M., Quinzii, C. M., & Naini, A. B. (2017). Novel recessive mutations in COQ4 cause severe infantile cardiomyopathy and encephalopathy associated with CoQ10 deficiency. *Molecular Genetics and Metabolism Reports*, *12*. https://doi.org/10.1016/j.ymgmr.2017.05.001

Song, L., & Poulter, C. D. (1994). Yeast farnesyl-diphosphate synthase: Site-directed mutagenesis of residues in highly conserved prenyltransferase domains I and II. *Proceedings of the National Academy of Sciences of the United States of America*, *91*(8). https://doi.org/10.1073/pnas.91.8.3044

Spinelli, J. B., Rosen, P. C., Sprenger, H. G., Puszynska, A. M., Mann, J. L., Roessler, J. M., Cangelosi, A. L., Henne, A., Condon, K. J., Zhang, T., Kunchok, T., Lewis, C. A., Chandel, N. S., & Sabatini, D. M. (2021). Fumarate is a terminal electron acceptor in the mammalian electron transport chain. *Science*, *374*(6572). https://doi.org/10.1126/science.abi7495

Srere, P. A. (1985). The metabolon. In *Trends in Biochemical Sciences* (Vol. 10, Issue 3). https://doi.org/10.1016/0968-0004(85)90266-X

Stefely, J. A., & Pagliarini, D. J. (2017). Biochemistry of Mitochondrial Coenzyme Q Biosynthesis. In *Trends in Biochemical Sciences* (Vol. 42, Issue 10). https://doi.org/10.1016/j.tibs.2017.06.008

Stewart, J. B., & Chinnery, P. F. (2015). The dynamics of mitochondrial DNA heteroplasmy: Implications for human health and disease. In *Nature Reviews Genetics* (Vol. 16, Issue 9). https://doi.org/10.1038/nrg3966

Stoffel, W., Lekim, D., & Sticht, G. (1969). Distribution and Properties of Dihydrosphingosine-1-phosphate Aldolase (Sphinganine-1-phosphate alkanal-lyase). *Hoppe-Seyler's Zeitschrift Fur Physiologische Chemie*, *350*(2). https://doi.org/10.1515/bchm2.1969.350.2.1233

Storici, F., & Resnick, M. A. (2003). Delitto perfetto targeted mutagenesis in yeast with oligonucleotides. In *Genetic engineering* (Vol. 25). https://doi.org/10.1007/978-1-4615-0073-5_9

Subramanian, K., Jochem, A., Le Vasseur, M., Lewis, S., Paulson, B. R., Reddy, T. R., Russell, J. D., Coon, J. J., Pagliarini, D. J., & Nunnari, J. (2019). Coenzyme Q biosynthetic proteins assemble in a substrate-dependent manner into domains at ER–mitochondria contacts. *Journal of Cell Biology*, *218*(4). https://doi.org/10.1083/jcb.201808044

Sun, F., Huo, X., Zhai, Y., Wang, A., Xu, J., Su, D., Bartlam, M., & Rao, Z. (2005). Crystal structure of mitochondrial respiratory membrane protein Complex II. *Cell*, *121*(7). https://doi.org/10.1016/j.cell.2005.05.025

Suzuki, A., & Rothstein, S. (1997). Structure and regulation of ferredoxin-dependent glutamase synthase from Arabidopsis thaliana. Cloning of cDNA, expression in different tissues of wild-type and gltS mutant strains, and light induction. *European Journal of Biochemistry*, *243*(3). https://doi.org/10.1111/j.1432-1033.1997.00708.x

Takahashi, M., Kinoshita, T., Maruyama, K., & Suzuki, T. (2022). CYP7A1, NPC1L1, ABCB1, and CD36 Polymorphisms Associated with Coenzyme Q10 Availability Affect the Subjective Quality of Life Score (SF-36) after Long-Term CoQ10 Supplementation in Women. *Nutrients*, *14*(13). https://doi.org/10.3390/nu14132579

Takahashi, M., Nagata, M., Kinoshita, T., Kaneko, T., & Suzuki, T. (2021). Cyp7a1, npc1l1, abcb1, and cd36 polymorphisms are associated with increased serum coenzyme q10 after long-term supplementation in women. *Antioxidants*, *10*(3). https://doi.org/10.3390/antiox10030431

Tarshis, L. C., Sacchettini, J. C., Yan, M., & Poulter, C. D. (1994). Crystal Structure of Recombinant Farnesyl Diphosphate Synthase at 2.6-Å Resolution. *Biochemistry*, *33*(36). https://doi.org/10.1021/bi00202a004

Thon, G., Maki, T., Haber, J. E., & Iwasaki, H. (2019). Mating-type switching by homology-directed recombinational repair: a matter of choice. In *Current Genetics* (Vol. 65, Issue 2, pp. 351–362). Springer Verlag. https://doi.org/10.1007/s00294-018-0900-2

Tiainen, M., Vaahtomeri, K., Ylikorkala, A., & Mäkelä, T. P. (2002). Growth arrest by the LKB1 tumor suppressor: Induction of p21WAF1/CIP1. *Human Molecular Genetics*, *11*(13). https://doi.org/10.1093/hmg/11.13.1497

Trevisson, E., Burlina, A., Doimo, M., Pertegato, V., Casarin, A., Cesaro, L., Navas, P., Basso, G., Sartori, G., & Salviati, L. (2009). Functional complementation in yeast allows molecular characterization of missense argininosuccinate lyase mutations. *Journal of Biological Chemistry*, *284*(42). https://doi.org/10.1074/jbc.M109.050195

Trevisson, E., Dimauro, S., Navas, P., & Salviati, L. (2011). Coenzyme Q deficiency in muscle. In *Current Opinion in Neurology* (Vol. 24, Issue 5). https://doi.org/10.1097/WCO.0b013e32834ab528

Tsui, H. S., Pham, N. V. B., Amer, B. R., Bradley, M. C., Gosschalk, J. E., Gallagher-Jones, M., Ibarra, H., Clubb, R. T., Blaby-Haas, C. E., & Clarke, C. F. (2019). Human COQ10A and COQ10B are distinct lipid-binding START domain proteins required for coenzyme Q function. *Journal of Lipid Research*, *60*(7). https://doi.org/10.1194/jlr.M093534

Tzagoloff, A., & Dieckmann, C. L. (1990). PET genes of Saccharomyces cerevisiae. *Microbiological Reviews*, *54*(3). https://doi.org/10.1128/mr.54.3.211-225.1990

Urnov, F. D., Rebar, E. J., Holmes, M. C., Zhang, H. S., & Gregory, P. D. (2010). Genome editing with engineered zinc finger nucleases. In *Nature Reviews Genetics* (Vol. 11, Issue 9). https://doi.org/10.1038/nrg2842

Vafai, S. B., & Mootha, V. K. (2012). Mitochondrial disorders as windows into an ancient organelle. In *Nature* (Vol. 491, Issue 7424). https://doi.org/10.1038/nature11707

Vafai, S. B., & Mootha, V. K. (2013). A common pathway for a rare disease? In *Science* (Vol. 342, Issue 6165). https://doi.org/10.1126/science.1248449

Vallee, B. L., & Auld, D. S. (1989). Short and long spacer sequences and other structural features of zinc binding sites in zinc enzymes. *FEBS Letters*, *257*(1). https://doi.org/10.1016/0014-5793(89)81805-8

Vallee, B. L., & Auld, D. S. (1993). Cocatalytic zinc motifs in enzyme catalysis. *Proceedings of the National Academy of Sciences of the United States of America*, *90*(7). https://doi.org/10.1073/pnas.90.7.2715

Vasta, V., Merritt, J. L., Saneto, R. P., & Hahn, S. H. (2012). Next-generation sequencing for mitochondrial diseases: A wide diagnostic spectrum. *Pediatrics International*, *54*(5). https://doi.org/10.1111/j.1442-200X.2012.03644.x

Vetro, A., Savasta, S., Russo Raucci, A., Cerqua, C., Sartori, G., Limongelli, I., Forlino, A., Maruelli, S., Perucca, P., Vergani, D., Mazzini, G., Mattevi, A., Stivala, L. A., Salviati, L., & Zuffardi, O. (2017). MCM5: A new actor in the link between DNA replication and Meier-Gorlin syndrome. *European Journal of Human Genetics*, *25*(5). https://doi.org/10.1038/ejhg.2017.5

Villalba, J. M., Navarro, F., Gómez-Díaz, C., Arroyo, A., Bello, R. I., & Navas, P. (1997). Role of cytochrome b5, reductase on the antioxidant function of coenzyme Q in the plasma membrane. *Molecular Aspects of Medicine*, *18*(SUPPL.). https://doi.org/10.1016/S0098-2997(97)00015-0

Visser, W., van Spronsen, E. A., Nanninga, N., Pronk, J. T., Kuenen, J. G., & van Dijken, J. P. (1995). Effects of growth conditions on mitochondrial morphology in Saccharomyces cerevisiae. *Antonie van Leeuwenhoek*, *67*(3). https://doi.org/10.1007/BF00873688

Wallace, D. C. (2010). Mitochondrial DNA mutations in disease and aging. In *Environmental and Molecular Mutagenesis* (Vol. 51, Issue 5). https://doi.org/10.1002/em.20586

Wang, Y., & Hekimi, S. (2013). Mitochondrial respiration without ubiquinone biosynthesis. *Human Molecular Genetics*, *22*(23). https://doi.org/10.1093/hmg/ddt330

Wang, Y., & Hekimi, S. (2016). Understanding Ubiquinone. In *Trends in Cell Biology* (Vol. 26, Issue 5). https://doi.org/10.1016/j.tcb.2015.12.007

Weiler, S., Braendlin, N., Beerli, C., Bergsdorf, C., Schubart, A., Srinivas, H., Oberhauser, B., & Billich, A. (2014). Orally active 7-substituted (4-benzylphthalazin-1-yl)-2-methylpiperazin-1-yl]nicotinonitriles as active-site inhibitors of sphingosine 1-phosphate lyase for the treatment of multiple sclerosis. *Journal of Medicinal Chemistry*, *57*(12). https://doi.org/10.1021/jm500338n

Westermann, B. (2010). Mitochondrial fusion and fission in cell life and death. In *Nature Reviews Molecular Cell Biology* (Vol. 11, Issue 12). https://doi.org/10.1038/nrm3013

Winge, D. R. (2012). Sealing the Mitochondrial Respirasome. *Molecular and Cellular Biology*, *32*(14). https://doi.org/10.1128/mcb.00573-12

Wittig, I., & Schägger, H. (2009). Supramolecular organization of ATP synthase and respiratory chain in mitochondrial membranes. *Biochimica et Biophysica Acta - Bioenergetics*, *1787*(6). https://doi.org/10.1016/j.bbabio.2008.12.016

Xie, L. X., Hsieh, E. J., Watanabe, S., Allan, C. M., Chen, J. Y., Tran, U. C., & Clarke, C. F. (2011). Expression of the human atypical kinase ADCK3 rescues coenzyme Q biosynthesis and phosphorylation of Coq polypeptides in yeast coq8 mutants. *Biochimica et Biophysica Acta - Molecular and Cell Biology of Lipids*, *1811*(5). https://doi.org/10.1016/j.bbalip.2011.01.009

Xie, L. X., Ozeir, M., Tang, J. Y., Chen, J. Y., Jaquinod, S. K., Fontecave, M., Clarke, C. F., & Pierrel, F. (2012). Overexpression of the Coq8 kinase in Saccharomyces cerevisiae coq null mutants allows for accumulation of diagnostic intermediates of the coenzyme Q6 biosynthetic pathway. *Journal of Biological Chemistry*, *287*(28). https://doi.org/10.1074/jbc.M112.360354

Yaffe, M. P. (1999). The machinery of mitochondrial inheritance and behavior. In *Science* (Vol. 283, Issue 5407). https://doi.org/10.1126/science.283.5407.1493

Yang, W. S., Sriramaratnam, R., Welsch, M. E., Shimada, K., Skouta, R., Viswanathan, V. S., Cheah, J. H., Clemons, P. A., Shamji, A. F., Clish, C. B., Brown, L. M., Girotti, A. W., Cornish, V. W., Schreiber, S. L., & Stockwell, B. R. (2014). Regulation of ferroptotic cancer cell death by GPX4. *Cell*, *156*(1–2). https://doi.org/10.1016/j.cell.2013.12.010

Yen, H. C., Yeh, W. Y., Lee, S. H., Feng, Y. H., & Yang, S. L. (2020). Characterization of human mitochondrial PDSS and COQ proteins and their roles in maintaining coenzyme Q10 levels and each other's stability. *Biochimica et Biophysica Acta - Bioenergetics*, *1861*(7). https://doi.org/10.1016/j.bbabio.2020.148192

Yu, M. H. C., Tsang, M. H. Y., Lai, S., Ho, M. S. P., Tse, D. M. L., Willis, B., Kwong, A. K. Y., Chou, Y. Y., Lin, S. P., Quinzii, C. M., Hwu, W. L., Chien, Y. H., Kuo, P. L., Chan, V. C. M., Tsoi, C., Chong, S. C., Rodenburg, R. J. T., Smeitink, J., Mak, C. C. Y., … Chung, B. H. Y. (2019). Primary coenzyme Q10 deficiency-7: expanded phenotypic spectrum and a founder mutation in southern Chinese. *Npj Genomic Medicine*, *4*(1). https://doi.org/10.1038/s41525-019-0091-x

Zeqiraj, E., Filippi, B. M., Deak, M., Alessi, D. R., & Van Aalten, D. M. F. (2009). Structure of the LKB1-STRAD-MO25 complex reveals an allosteric mechanism of kinase activation. *Science*, *326*(5960). https://doi.org/10.1126/science.1178377

Zhang, M., Luo, J., Ogiyama, Y., Saiki, R., & Kawamukai, M. (2008). Heteromer formation of a long-chain prenyl diphosphate synthase from fission yeast Dps1 and budding yeast Coq1. *FEBS Journal*, *275*(14). https://doi.org/10.1111/j.1742-4658.2008.06510.x

Zhao, P., Liu, I. D., Hodgin, J. B., Benke, P. I., Selva, J., Torta, F., Wenk, M. R., Endrizzi, J. A., West, O., Ou, W., Tang, E., Goh, D. L. M., Tay, S. K. H., Yap, H. K., Loh, A., Weaver, N., Sullivan, B., Larson, A., Cooper, M. A., … Saba, J. D. (2020). Responsiveness of sphingosine

phosphate lyase insufficiency syndrome to vitamin B6 cofactor supplementation. *Journal of Inherited Metabolic Disease*, *43*(5). https://doi.org/10.1002/jimd.12238

Zhu, X. F., Suzuki, K., Okada, K., Tanaka, K., Nakagawa, T., Kawamukai, M., & Matsuda, H. (1997). Cloning and functional expression of a novel geranylgeranyl pyrophosphate synthase gene from Arabidopsis thaliana in Escherichia coli. *Plant and Cell Physiology*, *38*(3). https://doi.org/10.1093/oxfordjournals.pcp.a029174